Carbon materials synthesis by Hydrothermal Carbonization of olive stones : Process and Product Characterization

Asma Jeder

THÈSE

Pour l'obtention du double titre de :

DOCTEUR de L'UNIVERSITÉ DE LORRAINE

Spécialité: Chimie

Et

DOCTEUR du L'ÉCOLE NATIONALE D'INGÉNIEURS DE GABES

Spécialité: Génie Chimique et procédés

Présentée par :

Asma JEDER

Matériaux carbonés par voie hydrothermale à partir de noyaux d'olive: étude du procédé, caractérisation des produits et applications

Thèse soutenue publiquement le 14 décembre 2017 à Gabés devant le jury composé de :

M Mehrez ROMDHANE	Professeur de l'Ecole Nationale d'Ingénieur de Gabés	Examinateur
M. Hamza EL FIL	Professeur de Centre de Recherche et des Technologies des Eauxde Borj-Cédria	Rapporteur
M. Jean-Michel LEBAN	Directeur de Recherches, Inra, Xylologist	Rapporteur
Mme Andreea PASC	Maître de conférencesNANO Group, HDR, MC	Examinatrice
Mme Vanessa FIERRO	Directeur de Recherches au CNRS, HDR, IJL	Directrice de thèse
M. Abdelmottaleb OUEDERNI	Professeur de l'Ecole Nationale d'Ingénieur de Gabés	Directeur de thèse

Institut Jean Lamour –UMR 7198- Département N2EV – Equipe 402
ENSTIB - CS 60036- 88026 EPINAL Cedex
Université de Lorraine – Pôle M4 - Collegium Sciences et Technologie
Ecole Nationale d'Ingénieurs de Gabès, Université de Gabès, Rue Omar Ibn Elkhattab, 6029 Gabès, Tunisie

ABSTRACT

Asma JEDER

Matériaux carbonés par voie hydrothermale à partir de noyaux d'olive: étude du procédé, caractérisation des produits et applications

Encadré par: Abdelmottaleb Ouederni and Vanessa Fierro

La carbonisation hydrothermale transforme les déchets municipaux (copeaux de bois, boues d'épuration, bagasse, feuilles…) en un produit solide appelé bio-charbon. Le produit hydrothermal connu sous le nom hydrochar est fréquemment utilisé comme carburant ou engrais, mais aussi il pourrait être converti en un produit à haute valeur ajoutée, à savoir le charbon actif.

L'objectif principal de cette thèse est d'étudier la transformation de grignon d'olive, précurseur lignocellulosique largement disponible en Tunisie et en pays méditerranéen, en hydrochar et en charbon actif.

Dans cette étude, un réacteur discontinu de laboratoire a été conçu et construit. Les grignons d'olive transformés en hydrochar ont été préparés à différentes sévérités et avec addition de sels, acide et ammoniac. Les hydrochars ont été caractérisés par plusieurs méthodes d'analyse. L'eau de traitement de la carbonisation hydrothermale a été analysée et les résultats montrent qu'elle contient des composants à haute valeur ajoutée comme le furfural et le 5-HMF.

Les charbons actifs ont été préparés à partir du hydrochar suivant des voies d'activation physique (à l'aide de l'agent d'activation CO_2) et voies d'activation chimique (par l'agent d'activation KOH). Les matériaux obtenus ont une surface spécifique élevée (1400 m^2g^{-1}) et aussi une chimie de surface riche en groupe fonctionnel. Les performances de ces charbons actifs dans l'adsorption de molécules pharmaceutiques en phase liquide et de l'hydrogène en phase gazeuse ont été examinées. Des capacités intéressantes ont été relevées pour les deux applications.

Mots-clés : Carbonisation hydrothermale, charbon actif, biomasse lignocellulosique, adsorption de molécules pharmaceutiques, adsorption d'hydrogène.

ABSTRACT

Carbon materials synthesis by Hydrothermal Carbonization of olive stones: Process and Product Characterization

Asma JEDER

Advisors: Abdelmottaleb Ouederni and Vanessa Fierro

Hydrothermal carbonization process uses green waste from municipalities (Wood chips, sewage sludge, bagasse, leaves …) to produce solid bio-coal. The solid HTC product known as hydrochar commonly used as a fuel or fertilizer but it could be converted also into high-value products like activated carbon. The principal purpose of this thesis is to study the conversion of olive stones, widely available lignocellulosic biomass in Tunisia and Mediterranean country, into hydrochar and then activated carbon.

In this study, a laboratory scale batch reactor has been designed and built. The hydrothermally carbonized olive stones were prepared at different reaction severity and with addition of salts, acid or ammonia. All prepared hydrochar are characterized by different analysis methods. The HTC water was also analyzed and the results show that HTC-liquid contains high added value components such as furfural and 5-HMF.

The hydrothermally carbonized olive stones were activated by both physical activation, using CO_2 and chemical activation, using KOH. The materials had high surface area (as high as 1400 m^2 g^{-1}) and rich surface chemistry. The potential for pharmaceuticals (Ibuprofen and Metronidazole) and hydrogen adsorption were assessed for HTC-activated carbon and they showed good performance in both application.

Keywords: Hydrothermal Carbonization, Carbon materials, olive stones, Pharmaceutical Adsorption, Hydrogen Adsorption

Acknowledgement

I would like to thank my supervisors Pr. Abdelmottaleb Ouederni and Dr. Vanessa Fierro for providing interesting research subject to work on it. In addition, I would like to thank them for their professional help to the realization of this thesis.

I am also grateful to Pr Alain Cerlzard for accepting me on their group and to Dr Vanessa Fierro for giving me the opportunity to receive a scholarship from Lorraine University.

I would like also to thank the member of jury: Mr Mehrez Romdhane, Mr Hamza El Fil, Mr Jean-Michel LEBAN and Mrs Andrea PASC

Special thanks to Philippe Gadonneix for being patient and for performing some analysis during my work in the Tunisian laboratory.

Thanks to my friends in ENIG Ines, Hanen, Marwa, Manel, Abir, Besma, Souhir, Zohour, Amina, Mouzaina, Fatma, khaoula, Ameni we spent a good time and I have been lucky to work with you, Asma and Hayet for their patient despite my numerous questions.

And my colleagues in ENSTIB Flavia, Luda, Andrejz, Guiseppe, Antonio, Taher, Clara, Jimena, Sébestian, Marie and angela, it was pleasure to meet you.

Special thanks to Elmouwahidi abdelhaim and Sihem amirou for their moral support in my most difficult time.

I would like to thank also Eric Masson for his collaboration in Project Title: Understanding hydrothermal Carbonization mechanisms

Great thanks to my parents, brothers Chokri and Chawki, my sister Leila, my little nephew Hassen and my step-sister Maria-Olympia for their support and encouragement; you are the most precious person in my life.

Table of contents

Abbreviation

C	Thickness of the boundary layer	mg/g
Ce	solute concentration at equilibrium	mg/L
K_F	Freundlich model parameters	L/g
K_L	equilibrium constant of adsorption	l/mg
Kp	intraparticle diffusion constant	$mg/(g.min^{0.5})$
K1	rate constant of the pseudo-first-order	min^{-1}
K2	pseudo second-order constant	g/(mg.min)
n	Freundlich model parameters	
qe	the amount of solute adsorbed	Mg/l
qm	The maximum adsorption capacity	Mg/l
qt	amount adsorbed at time t	Mg/l
R	gas constant	$J\ mol^{-1}\ K^{-1}$
T	Temperature	°C
t	time	min
Z	compressibility factor	

Symbols

AC	Activated carbon
AC-HTC-180	Activated Carbon from hydrochar at180°C
AC-HTC-240	Activated Carbon from hydrochar at240°C
AC-HTC-180-O3	Activated Carbon from hydrochar at180°C modified by ozone
AC-HTC-240-O3	Activated Carbon from hydrochar at240°C modified by ozone
N-CO2-2h	Activated Carbon from hydrochar modified by ammonia
AC-KOH-Dir	Activated carbon from olive stones
HTC	Hydrothermal carbonization
NLDFT	The Non-Local Density Functional Theory
PSD	Pore size distribution
S_{NLDFT}	NLDFT specific surface area
Vmes	Mesopore volume
Vmic	Micropore volume
Vsupmic	Supermicropores Volumes
Vumic	ultramicropores

List of figures

List of Tables

Résumé de la thèse

Ce travail s‘inscrit dans un contexte de la recherche d‘une voie facile à faible coût, respectueuse de l'environnement, et non toxique pour la production de nouveaux matériaux carbonés. La demande croissante de matériaux adsorbants pour des procédés de protection de l‘environnement suscite une recherche profonde dans la fabrication des charbons actifs à partir de matières premières d‘origine végétale. La synthèse des charbons actifs (CA) par des procédés simples à partir de biomasse lignocellulosique, l‘un des précurseurs du CA et considéré comme une ressource abondante et renouvelable, est très intéressante du point de vue économique.

En outre les matériaux carbonés ont vu un développement très rapide vu les besoins dans diverses applications exigeant des caractéristiques texturales, physiques et chimiques très variés. Ces matériaux répondent bien au potentiel important de divers champs d‘utilisation du fait de la souplesse dans la maitrise et l‘adaptation de leur architecture. Les caractéristiques des charbons actifs dépendent étroitement du précurseur, du procédé et des conditions opératoires de fabrication. Dans le présent travail, le procédé choisi est la voie hydrothermale. Ce dernier est considéré une innovation dans l'industrie chimique, surtout que les techniques classiques sont énergivores et nécessitent souvent l'utilisation de précurseurs nuisibles.

Cette thèse a pour objectif d‘étudier la carbonisation hydrothermale (HTC), comme alternative potentielle, pour la synthèse de matériaux peu coûteux et facilement disponibles selon une voie simple qui nécessite uniquement de l'eau comme solvant. Même si le procédé HTC a suscité plusieurs travaux de recherche, il reste beaucoup à faire en particulier son application avec certains précurseurs tels que les noyaux d‘olive.

Ce travail a été réalisé en collaboration entre laboratoire de « Génie de Procédés et Système Industriels » à l‘Ecole Nationale d‘Ingénieurs de Gabés – Université de Gabès et l‘équipe 402 « Matériaux Biosourcés » et l‘Institut Jean Lamour (IJL – UMR CNRS 7198), hébergée dans les locaux de l‘Ecole Nationale Supérieure des Techniques et Industries du Bois (ENSTIB), à l‘Université de Lorraine.

Chapitre I: Etat de l'art

La première partie de la thèse a été consacrée à la recherche bibliographique afin de construire une base d'information à partir de laquelle il sera possible d'élaborer les lignes directrices pour ce travail.

Dans ce but, une description détaillée de matériaux lignocellulosique est présenté, ces matériaux sont riche en carbone et disponible en grande quantité. Elle est constituée principalement de trois polymères : Lignine, Cellulose et hémicellulose (figure 1), leurs proportions sont variables d'un précurseur lignocellulosique à un autre mais généralement la fraction de cellulose varie entre 30-50%, hémicellulose 20- 40% et lignine 10- 30%.

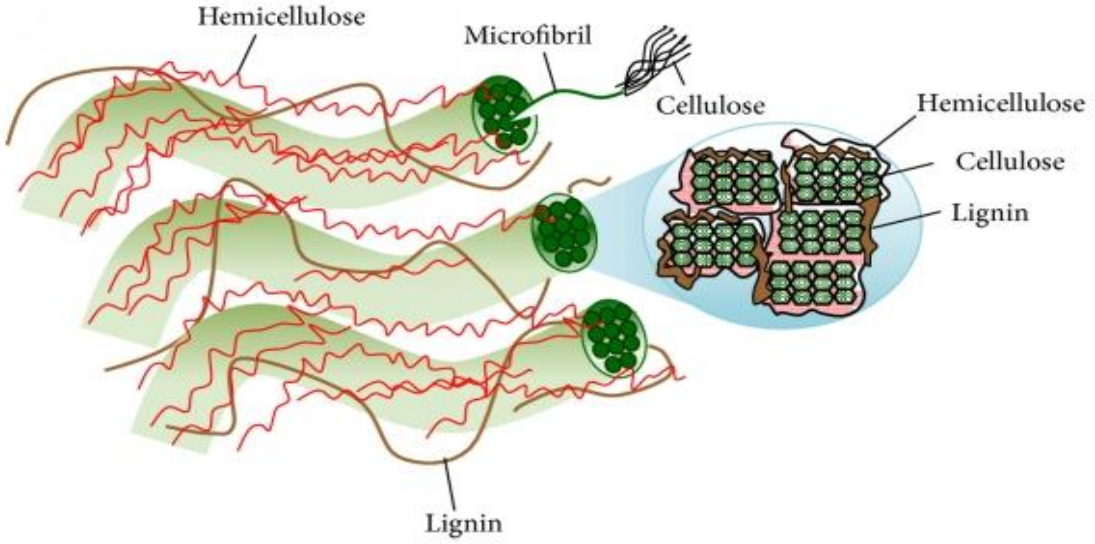

Figure 1 : Structure de paroi cellulaire et une coupe transversale des microfibres

A l'heure actuelle, différentes voies de conversion de la biomasse lignocellulosique ont été étudiées vu leur importance dans le domaine énergétique et environnementale, parmi ces voies, la carbonisation hydrothermaleest un procédé thermochimique développé par Friedrich Bergius (1913). La carbonisation hydrothermale (HTC) permet de convertir la biomasse à basse température (130 à 250°C) sous pression et en phase aqueuse.

Le processus réactionnel du HTC de précurseurs ayant une structure simple (par exemple, les monosaccharides) a été rapporté par la littérature, par contre ce processus n'est pas encore détaillé surtout pour les précurseurs complexes comme la matière lignocellulosique.

Cependant on sait qu‘il est contrôlé généralement par des réactions de déshydrations, polymérisation ou condensations et aromatisations.

La carbonisation hydrothermale transforme la biomasse en liquide riche en composés organiques (furfural, 5-HMF, phénol…), des traces de gaz et un produit solide (hydrochar).L‘hydrochar est fréquemment utilisé comme carburant ou engrais mais il peut être transformé aussi en matériaux à haute valeur ajoutée, comme le charbon actif par un traitement thermique additionnel (activation chimique, physique ou combinée).

En effet, les charbons actifs sont des matériaux poreux caractérisés par leurs surfaces spécifiques élevées, volume poreux, taille et forme des pores. Les pores sont classifiés en trois catégories (figure 2) selon leurs tailles (micropores, mesopores et macropore).

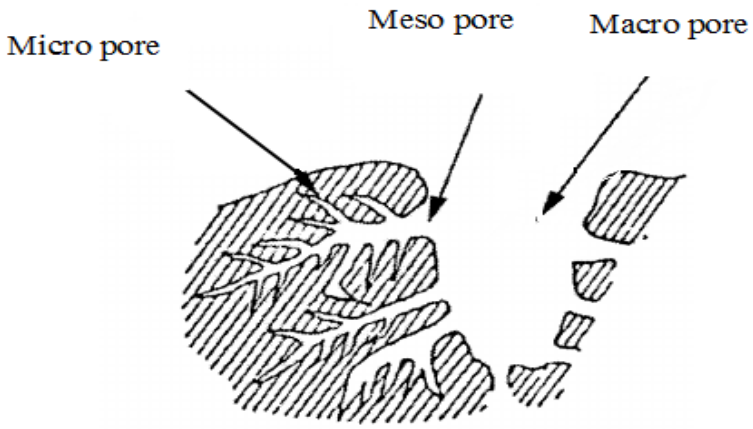

Figure 2 : La structure poreuse d‘un charbon actif granulé.

Les charbons actifs sont largement utilisés à l‘échelle industrielle comme matériau adsorbant des polluants. Les molécules pharmaceutiques sont parmi les substances qui peuvent être éliminés par ces matériaux. En outre, ces polluants font parti des composés actuellement retrouvées dans divers systèmes aquatiques tels que les eaux usées, les eaux souterraines ainsi que les eaux de surfaces. Ces substances entrainent des effets néfastes sur l‘environnement et l‘être humain.

Plusieurs études et recherches ont été menées pour tester l‘efficacité des charbons actifs dans l‘adsorption d‘hydrogène et différents résultats ont été obtenus, une comparaison de ces résultats avec d‘autre matériaux adsorbants est présentée par le figure 3.

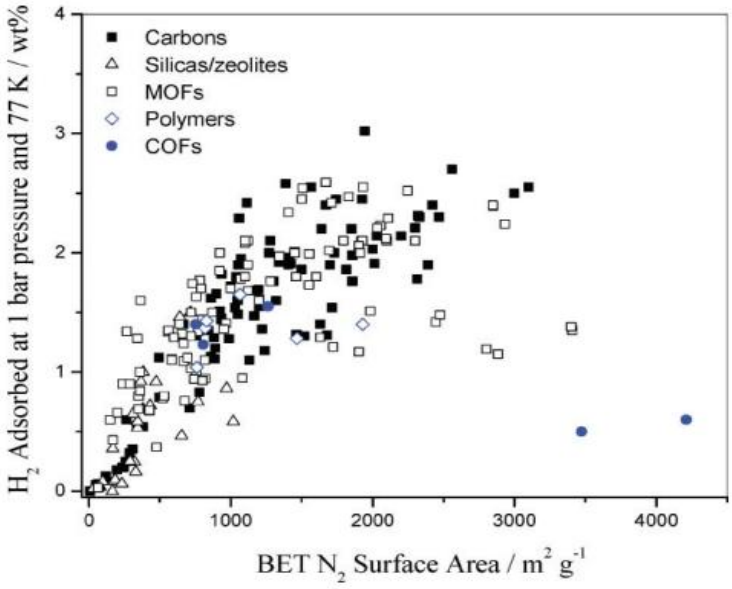

Figure 3 : L'adsorption d'hydrogène à 1 bar et 77K en fonction de la surface BET de matériaux poreux (Thomas 2009).

Chapitre II: Carbonisation hydrothermale des noyaux d'olive

Dans ce chapitre, les noyaux d'olive (figure 4) sont sélectionnés comme précurseur lignocellulosique de la carbonisation hydrothermale. Les analyses, élémentaire et des fibres, sont présentés dans le tableau 1. Un tel précurseur est notamment riche en lignine : environ 30%.

Tableau 1: Analyse élémentaire et de fibre de noyaux d'olive

Elemental analysis		Compositions Biopolymer (wt %)	
Carbon	50.10	Cellulose	40.53
Oxygen	43.50	Hemicellulose	21.68
Hydrogen	6.22	Lignine	29.88
Nitrogen	0.15	Extractible	7.9
Sulphur	0.04		

Figure 4 : Noyaux d'olive.

Les expériences de carbonisation hydrothermale ont été menées tout en faisant varier la température entre 160 et 240°C et le temps de réaction entre 3 et 48 heures (figure 5). Ces expériences ont pour but de comprendre l'effet de la température et du temps de séjour sur les produits solides obtenus. Une autre série d'expériences consiste à modifier le pH : 1, 2 et 3 et ajouter de sels : chlorure de sodium, chlorure de potassium, chlorure de lithium, nitrate de sodium et Sodium sulfate. L'objectif est de mener une investigation sur l'effet de la température, temps de réaction, pH et des sels sur l'hydrochar obtenu et les modifications du processus de carbonisation hydrothermale.

On a produit des hydrochars à basse température et en milieu liquide, les hydrochars sont chimiquement très complexes. La variation de trois paramètres importants (température, temps et nature du milieu) aboutit à des solides ayant des propriétés différentes.

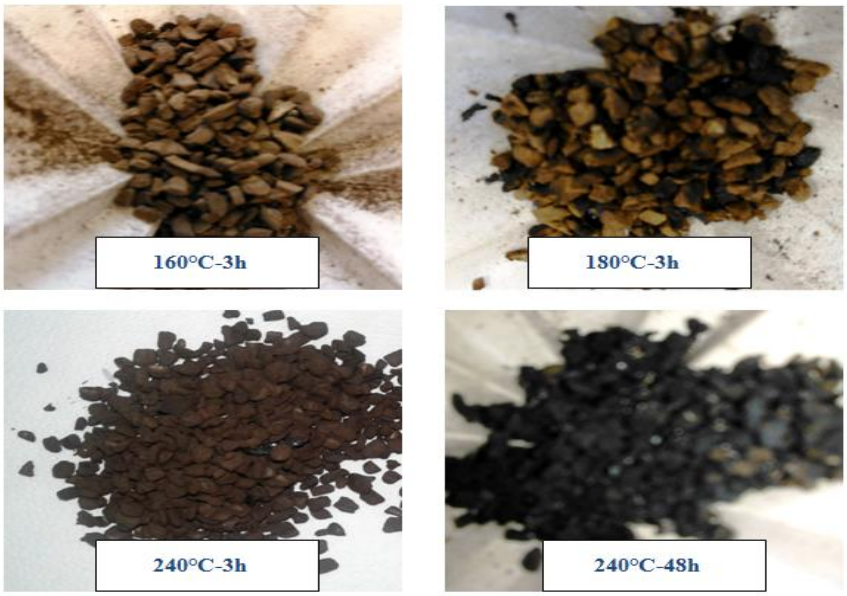

Figure 5 : Hydrochar préparés à différentes température et temps de réaction.

Les matériaux obtenus sont caractérisés par différentes techniques d'analyse (Analyse élémentaire et analyse thermogravimétrique).En utilisant les résultats de l'analyse élémentaire, on a tracé le diagramme de van Krevelen représentant les rapports atomique H/C en fonction de O/C, à partir de ce diagramme on a constaté que la carbonisation hydrothermale a transformé les grignons d'olive (H/C=1.49 et O/C=0.65) à un solide riche en carbone avec un rapport atomique (H/C=0.88 et O/C=0.27) similaire à celui du lignite.

Les courbes thermogravimétriques montrent une altération importante au niveau de la structure des matériaux, en effet le pic caractéristique de l'hémicellulose n'est pas détecté

même pour les hydrochars traités à faible sévérité (figure 5 a). On note aussi une modification remarquable de pic de cellulose à une température élevée (figure 5 b).

a) b)

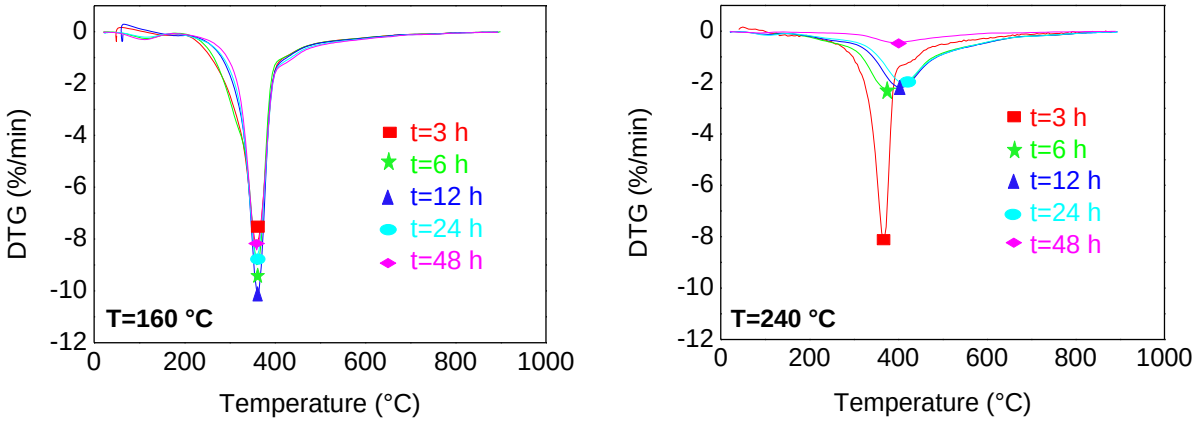

Figure 6 : Courbes DTG hydrochar préparé à 160 °C (a) et 240°C (b)

La déconvolution des courbes thermogravimétriques, en utilisant Origin® lab, nous a permis d'identifier cinq intervalles de température correspondant à la dégradation de la lignine, la cellulose et l'hémicellulose. L'aire de chaque pic correspondant à un intervalle de température bien déterminé est divisé par l'aire totale des pics obtenus de chaque courbe et tracé en fonction de sévérité de réaction (figure 6).

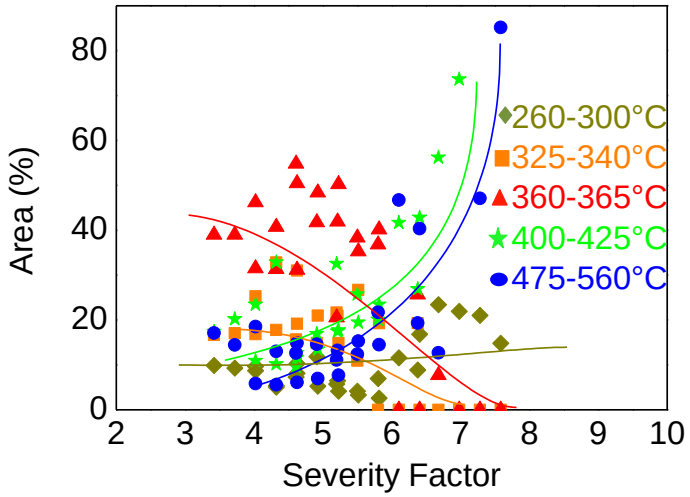

Figure 7 : L'aire de pic (%) en fonction de facteur de sévérité.

On a trouvé que l'hémicellulose commence à se dégrader dans conditions moins sévères que la cellulose. La lignine, étant le composant le plus complexe, sa dégradation commence à faible sévérité inférieur à 3 (160°C-3h) mais elle résiste aux conditions sévères et la structure finale des hydrochars préparés à de sévérités supérieures à 6 sont constitués principalement par la lignine (figure 6).

D‘autre part, la modification de pH du milieu réactionnel n‘a pas d‘effet significatif sur la structure poreuse des hydrochars carbonisés à 900þC mais l‘addition d‘un acide peut accélérer le processus hydrothermale, par contre l‘ajout de sels dans le milieu réactionnel hydrothermale peut bloquer les pores des hydrochar carbonisés.

Chapitre III: Synthèse de charbons actifs à partir d’hydrochar

Ce chapitre porte sur la synthèse de charbons actifs à partir de l‘hydrochar. Les charbons actifs ont été préparés suivant des voies d‘activation physique (à l‘aide de l‘agent d‘activation CO_2) et voies d‘activation chimique (par l‘agent d‘activation KOH). Les charbons actifs synthétisés à partir des hydrochars à 180°C et 240°C (AC-HTC-180 et AC-HTC-240) ont été soumis à une modification par l‘ozone en phase aqueuse. Les propriétés texturales et chimique ont été analysés.

Généralement, les charbons actifs issus des hydrochars présentent des surfaces spécifiques et volume de pores plus élevé que ceux de matériaux préparés par les grignons d‘olive (AC-KOH-Dir).Il faut signaler aussi que l‘activation des hydrochars préparés à basse température (AC-HTC-180) a montré des propriétés texturales intéressante par rapport à ceux qui ont été synthétisés à température élevée AC-HTC-240. En effet, les hydrochars HTC-240, constitués principalement de la lignine, ont tendance à développer de matériaux microporeux. D‘autre part, lorsqu‘ils sont activés par l‘agent chimique KOH, il est probable qu‘une quantité importante de potassium K restait attachée dans la structure poreuse du charbon et par conséquent elle induit une occlusion dans la structure de matrice carbonée. Par conséquent il est indispensable de sélectionner les conditions de traitement hydrothermal selon le type de précurseurs utilisé et les résultats souhaités.

L‘ozonation de CA en phase liquide pendant 2h a abouti à une amélioration importante de la texture des pores, telle que l‘augmentation significative de la surfaces spécifique de (S_{NLDFT}= 536 m^2g^{-1}et S_{BET}= 400 m^2g^{-1}) à (S_{NLDFT}= 1242 m^2g^{-1}et S_{BET}= 987 m^2g^{-1}) et du volume de pores de 0.23 cm^3g^{-1} à 0.44 cm^3g^{-1} des AC-KOH-240. Une observation similaire pour les matériaux AC-KOH-180, la surface spécifique a augmenté d‘une façon importante de (S_{NLDFT}= 1217 m^2g^{-1}et S_{BET}= 981 m^2g^{-1}) à (S_{NLDFT}= 1478 m^2g^{-1}et S_{BET}= 1245 m^2g^{-1}) et volume de pores de 0.43 cm^3g^{-1} à 0.53 cm^3g^{-1}, (figures 8 et 9).

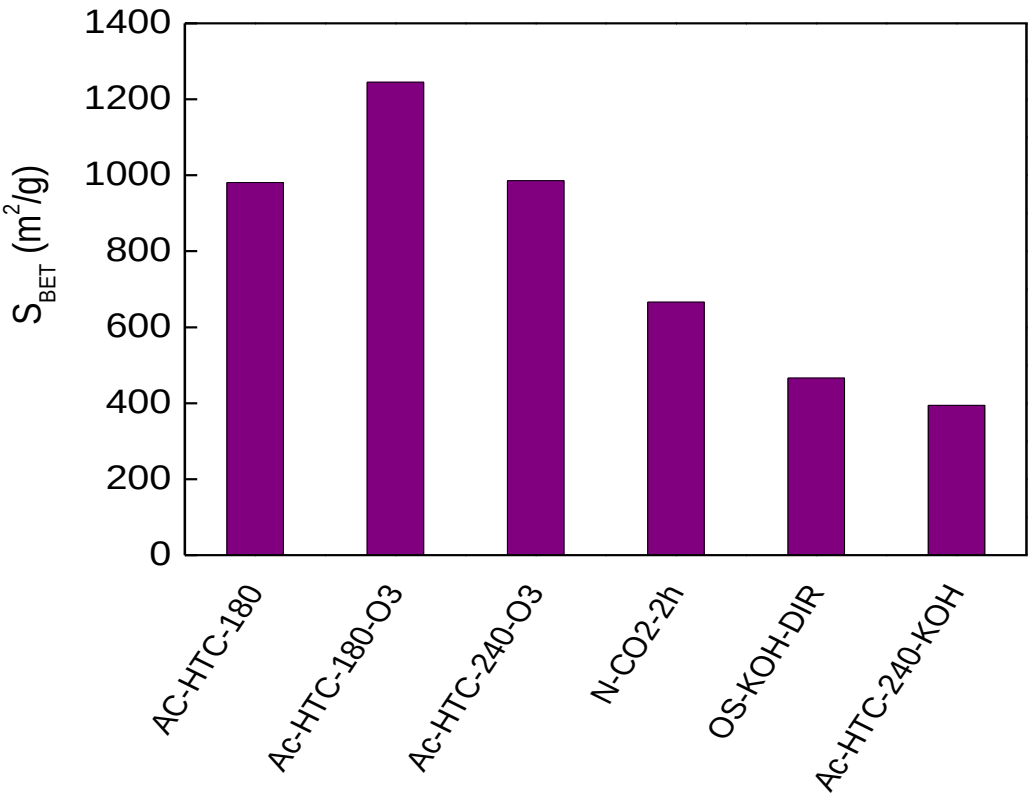

Figure 8 : Surface spécifique BET de charbon actif

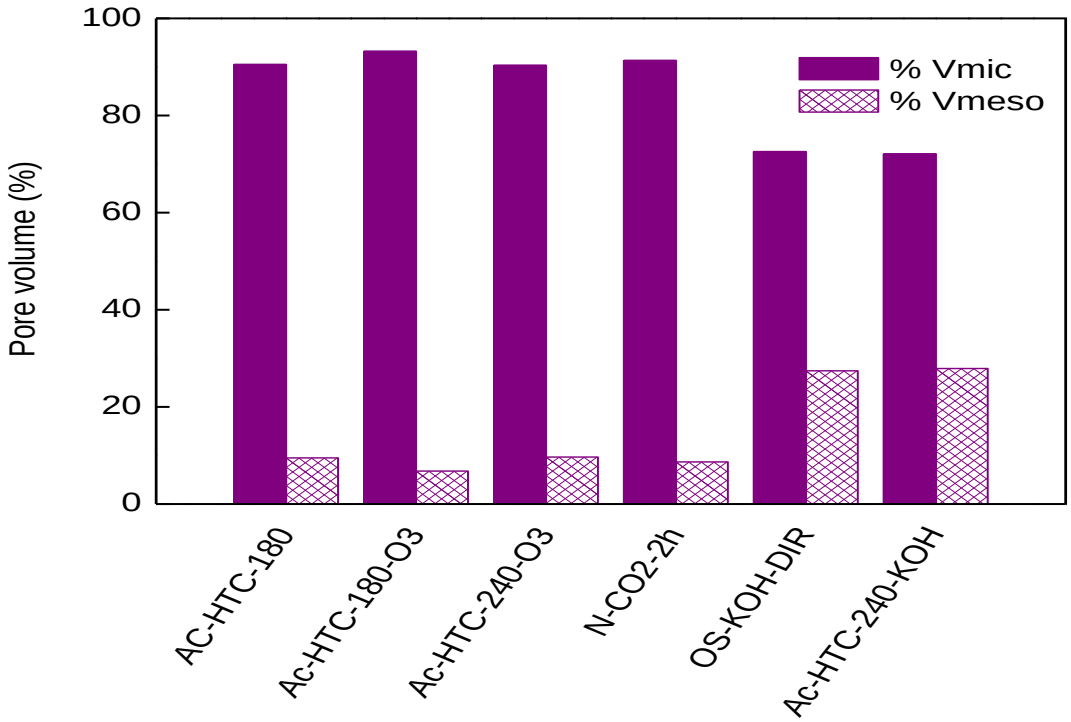

Figure 9 : Volume de pore de charbon actif

La nature chimique de la surface des charbons actifs a été analysée par la méthode de Boehm et pHpzc, les résultats sont présentés dans les tableaux 2 et 3, respectivement. La chimie de surface à un rôle important dans la sélectivité du CA dans les processus d'adsorption.

Les OS-KOH-DIR possèdent la quantité de groupement acide la plus faible, ceci est cohérent avec les valeurs mesurées de pHpzc (pHpzc = 10.25) (tableau 3). Les fonctions de surfaces d'AC-KOH-180 et AC-KOH-240 ont majoritairement un caractère basique, il faut noter aussi que les AC-KOH-180 ont une surface riche en groupements fonctionnels et présentent aussi une quantité des groupements acides la plus élevée, cela est dû à l'effet du traitement hydrothermal à basse température qui augmente la teneur des groupements fonctionnels acide.

Comme c'était attendu, l'ozonation du CA a abouti à une amélioration importante de teneur de groupements acide et basique, en effet la quantité de phénol d'AC-HTC-240 a augmenté de 0.09 à 0.18 meq/g et la quantité carboxylique de 0.015 à 0.12 meq/g (tableau 2).

Tableau 2: Chimie de surface des charbons actifs (meq.g-1)

	Carboxyle	**Lactone**	**Phénol**	**Total basique**	**Total acide**
AC-KOH-180	0.015	0	0.23	0.5	0.245
AC-KOH-240	0	0	0.09	0.4	0.09
AC-KOH-180-O3	0.12	0.03	0.03	**0.12**	0.18
AC-KOH-240-O3	0.0575	0.0125	0.18	0.37	0.25
OS-KOH-DIR	0	0	0	0.47	0

Tableau 3: les valeurs du pHPZC du Charbons Actifs

	AC-KOH-180	AC-KOH-240	AC-KOH-180-O3	AC-KOH-240-O3	OS-KOH-DIR
pH pzc	9.2	9.8	7.23	8.5	10.25

Les isothermes d'adsorption de l'eau et les coefficients d'affinité ont été déterminés, on a trouvé que le processus d'adsorption dépend fortement de la distribution de taille de pores et de groupements fonctionnels (fig. 10). Les matériaux préparés par activation chimique sont

caractérisés par leurs surfaces hydrophile d'où les valeurs élevées de leur coefficients d'affinité. Les isothermes d'AC-KOH-180 et OS-KOH-DIR est de type II, correspondent en général à l'adsorption multicouche, AC-HTC-180-O3 et AC-HTC-240-O3 sont de type IV, ce type résulte de la combinaison d'une isotherme de type I (adsorption forte, mais limitée) et de type V, est le cas de l'eau sur les charbons actifs riches en oxygène.

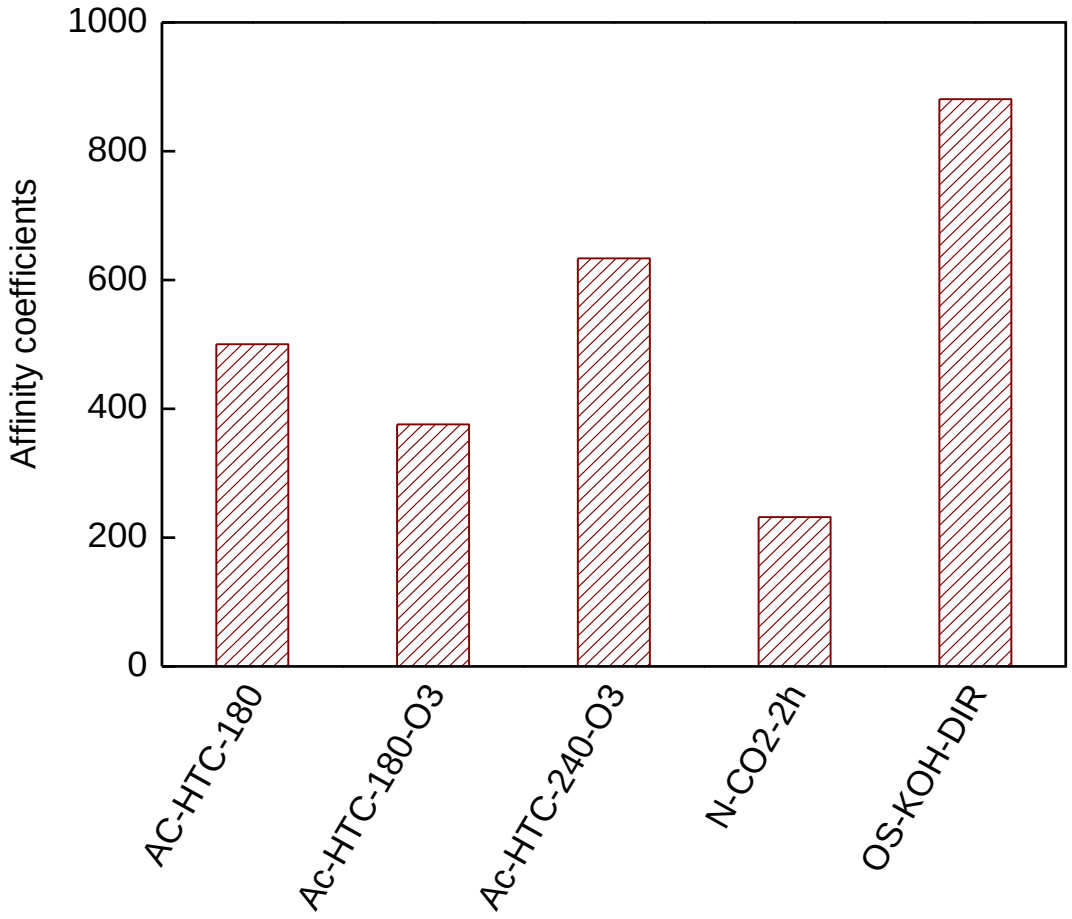

Figure 10 : Les coefficients d'affinités

Finalement, il est possible de conclure que les AC issus des hydrochars préparés à une faible sévérité (sévérité inférieure à 5) sont susceptibles de développer des surfaces spécifiques élevées de l'ordre de 1215 m^2g^{-1}, une distribution de taille de pore étroite et une surface riche en groupement fonctionnels.

D'autre part, le traitement des CA par l'ozone tend à augmenter les surfaces spécifiques et la quantité de groupement acide à la surface.

Chapitre IV: Application de HTC- Charbon actifs (Adsorption)

Ce chapitre est divisé en deux parties, la première partie est consacrée à l'étude des performances des matériaux élaborés dans l'adsorption des molécules pharmaceutiques (ibuprofène et métronidazole). Une investigation profonde des cinétiques et des isothermes d'adsorption, a été faite dans différentes conditions (température et concentration). Ces résultats expérimentaux sont lissés par différents modèles thermodynamiques et cinétiques. La meilleure capacité d'adsorption d'ibuprofène mesurée est de 288 mg/g sur les CA AC-HTC-240 et de 258 mg/g de métronidazole sur AC-HTC-180-O3, ces capacités sont parmi les plus élevées jamais rapportées par la bibliographie pour des charbons actifs.

Ces excellentes performances ont été attribuées aux propriétés chimiques et texturales de ces matériaux. Les AC-HTC-240 ont une fraction de mésopores élevée de l'ordre de 27%, ceci permet aux molécules d'ibuprofènes de pénétrer facilement dans les pores des canaux, par contre les AC-HTC-180 ont un caractère hydrophiles ce qui augmente la compétitivité de l'eau par rapport aux molécules d'ibuprofène, par conséquence leur performance diminue.

Par contre, une quantité importante de métronidazole a été éliminée par les AC-HTC-180 et AC-HTC-180-O3, ceci peut être expliqué par le fait que ces matériaux possèdent non seulement une grande surface spécifique et un volume de pores important, mais ils sont aussi caractérisés par leur surface riche en groupements acides notamment en phénol, ces groupes fonctionnels de surface favorisent l'adsorption des composés aromatiques tel que la métronidazole. L'adsorption est possible grâce aux interactions dispersives de l'électron π de noyau aromatique de composés pharmaceutique et l'électron des plans basaux du charbon actif.

Les résultats de modélisation montrent que la cinétique d'adsorption des deux molécules pharmaceutiques obéit à une cinétique de pseudo-second ordre. Le modèle de diffusion intra particulaire montre deux zones :

- Une zone importante qui décrirait l'adsorption graduelle avec la diffusion intraparticulaire comme étape limitante.
- une deuxième zone attribuée à l'étape d'adsorption lente où la diffusion intraparticulaire

Le modèle de Freundlich se trouve être les plus adéquat pour décrire les isothermes d'adsorption de l'ibuprofène et métronidazole sur les deux charbons actifs AC-HTC-180 et AC-HTC-240. La variation de la température 20 à 50þC n'a pas un effet significatif sur le processus de l'adsorption.

La deuxième partie de ce chapitre est dédiée à l'étude de performance des matériaux élaborés dans l'adsorption d'hydrogène.

Tableau 4: Comparaison des capacités d'adsorption d'hydrogène

Materials	S_{BET} ($m^2.g^{-1}$)	Vmicropore ($cm^3.g^{-1}$)	H2 asorbé (wt %)
AC-HTC-180	1217	0.39	0.34
N-CO2	932	0.26	0.35
OS-KOH-DIR	655	0.19	0.21
AC-HTC-240	536	0.16	0.23
AC-HTC-240-O3	1242	0.39	0.32

Les résultats d'adsorption d'hydrogène à 298K sont présentés dans le tableau 4.Les quantités adsorbées varient d'un charbon actif à un autre dans l'ordre décroissant suivant :

N-CO_2-2h ≈ AC-180-KOH 〉 AC-240-KOH-O3 〉 AC-HTC-240-KOH 〉 OS-KOH-Dir

La quantité maximale est adsorbé par N-CO_2-2h, par contre ces matériaux ne présentent pas une grande surface spécifique, cela confirme que la surface spécifique n'est pas le seul paramètre qui contrôle l'adsorption d'hydrogène. Une large investigation montre que la chimie de surface joue un rôle important, en effet la teneur élevée en azote de N-CO_2-2h a amélioré la capacité d'adsorption. Aussi les groupements acides contribuent à une augmentation significative de quantité d'hydrogène adsorbée.

Introduction

The Green Chemistry is the next revolutionary concept that will set aside the entire world‘s variance; it is about design and application of renewable raw materials to mitigate the environmental issues as well as the energy demand, in fact Green Chemistry is attempts to develop innovative technology to produce high added-value product without use and generation of hazardous chemical compound. In this context, hydrothermal carbonization (HTC) is modern technology start to growing from small grassroots research to industrial project based on conversion of renewable and inexpensive material ―Biomass" into sustainable carbon rich product using water as reaction medium and under soft condition (low temperature and self generated pressure). The solid products of HTC called hydrochar were submitted to several investigations to evaluate its physical and chemical properties, and then assess its efficiency for numerous applications such as soil amendments in agriculture, carbon dioxide sorption and sequestration and many others applications related mainly to energy and environment. In this study, we prepare hydrochar through hydrothermal carbonization of olive stones which is a lignocellulosic biomass extensively produced in Mediterranean countries (Greece, Spain, Italy and Tunisia), and then we tried in second steps to evaluate the efficiency of olive stones derived hydrochar in production of sustainable porous activated carbon materials.

Hydrochar have been characterized by their functional groups rich on oxygen content on their surface and the fact that hydrochar prepared at low temperature it could be easy to incorporate their functional groups with heteroatom such as Nitrogen, Fluor or sulphur, subsequently HTC offers the opportunity to overcome the lack of control of chemical structure, surface functionality and the porosity of activated carbon. This properties has a fundamental effect on activated carbon efficiency on different application especially adsorption and storage as there are the most common applications of activated carbon.

Therefore, our main motivation is to highlights the aforementioned advantage of HTC as green route to produce advanced carbon materials based on hydrochar derived olive stone and prove its effectiveness in medicines adsorption and hydrogen storage.

This thesis is divided into four chapters as detailed bellow:

Chapter 1: State of the art

This chapter provides the necessary background on the key topics of this research, the first part focus on the description of lignocellulosic biomass structure and olive stones as example, the second part present an overview of hydrothermal carbonization process, from its infancy to industrial applications and final part it deduced to the activated carbon materials and its applications especially adsorption

Chapter 2: Hydrothermal carbonization of olive stones

In this section a systematic investigation of HTC of olive stone and deep studies on thermogravimetric behavior of hydrochar prepared at different severities reactions and then on textural properties of carbonized hydrochar. In the same way we will explore the effect of salts and acid addition on the thermal behavior of hydrochar and its carbonized textural properties.

Chapter 3: Synthesis of activated carbon from hydrochar

This chapter examines the possibility to use hydrochar prepared at three different conditions as started materials for activated carbon production. Different activated carbon materials were obtained by physical and chemical activation with different chemical structure and textural properties. In a further step, a post-preparative modification has been performed by ozone treatment. The main objective of this study is to produce and characterize the hydrochar derived activated carbon and compare its properties with activated carbon prepared directly from olive stones.

Chapter 4: Application of HTC- Activated Carbon: Adsorption

This chapter is dedicated to the application of HTC activated carbon materials in one of the most old and common area field which adsorption. The purpose is to evaluate the efficiency of these materials on adsorption of medicines (ibuprofen and metronidazole) and then assess its efficiency in hydrogen adsorption.

Finally, a conclusion resumes the main achievement of this thesis and perspectives of future works are also presented at the end.

Chapter 1: State of the art

I.1 Lignocellulosic biomass

Biomass has recognized an important attention since the last decades because of its high availability (Kumar et al. 2009) which made it a low-cost renewable alternative for many applications and also because it is the only sustainable route for fuels production and therefore satisfies future energy demands. Lignocellulosic biomass is not only potential feedstock for fuel but also it has been considered as powerful precursors for chemicals, polymers and bio-based materials. Numerous researches have been published to prove the efficiency of biomass in the aforementioned fields, depending on treatment process lignocellulosic biomass could be able to produce over 200 value-added compounds (Isikgor and Becer 2015). The annual world production of biomass is about 200 billion tonnes per year of which over 90% are lignocelluloses (De Jong and Van Ommen 2014). The lignocellulosic biomass includes all of agriculture residues and crops (e.g., olive stones, coconut shell, sugarcane bagasse and crop straws …) forest residue (hardwood and softwood).

Lignocellulosic, as its name indicates, is mainly composed by three carbohydrate polymers lignin, cellulose and hemicelluloses (figure 1). It has a complex three-dimensional, the three polymers are highly interconnected with each other and strongly bonded in a hetero-matrix to different degrees and varying relative composition depending on the species, type, and even origin of the biomass. Generally the cellulose amount vary between 30 and 50, hemicelluloses 20 - 40 % and lignin 10 - 30% (table 1) (Jung and Kim 2014).

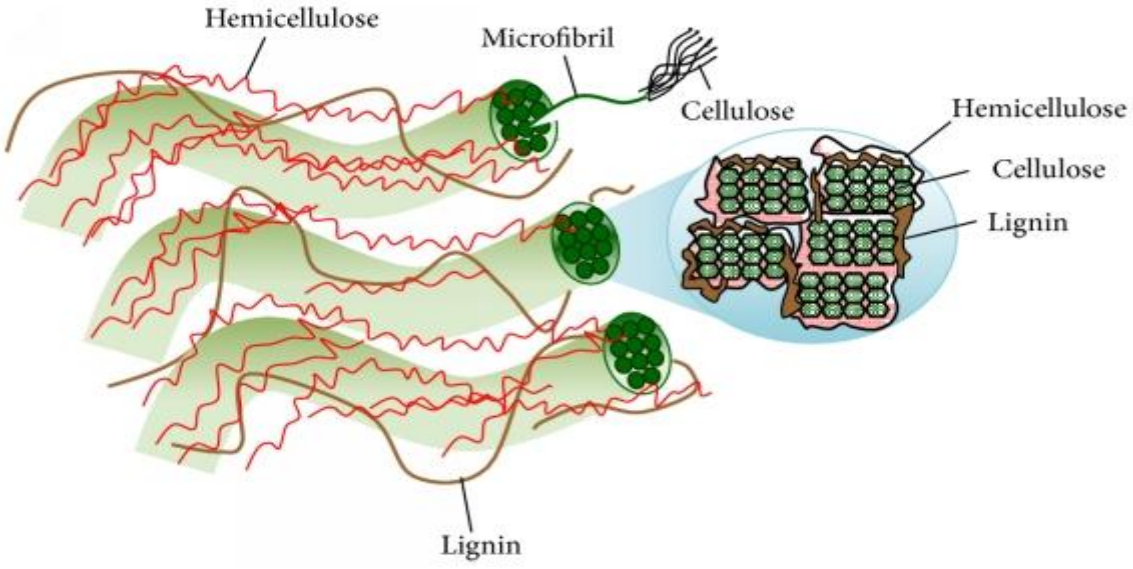

Figure 1: Plant cell wall structure and microfibril cross-section (Lee et al. 2014)

Table 1: Chemical composition of different type of biomass

Biomass	Cellulose (%)	Hemicellulose (%)	Lignin (%)
Hardwood	40-55	24-40	18-25
Softwood	45 -50	25-35	25-35
Switchgrass	45	31.4	12
Corn cobs	45	35	15
Wheat straw	30	15	15
Nut shells	25- 30	25-30	30-40

I.1.1 Cellulose

Cellulose is the most abundant polymer, consist of D-glucose subunits, linked by beta-1,4 glycosidic bonds, the long chain of cellulose are tightly attached by hydrogen bonding and van der waals forces, the beta-linkage chains in the cellulose are a considerably stabile and resistance to chemical treatments due to the presence of intra and intermolecular H-bonding besides to the strong hydrogen bonding which made polymer extremely resistant to biological treatment and insoluble in the most common solvent, in addition cellulose present in biomass generally in highly crystalline forms which result an important resist to hot water treatment.

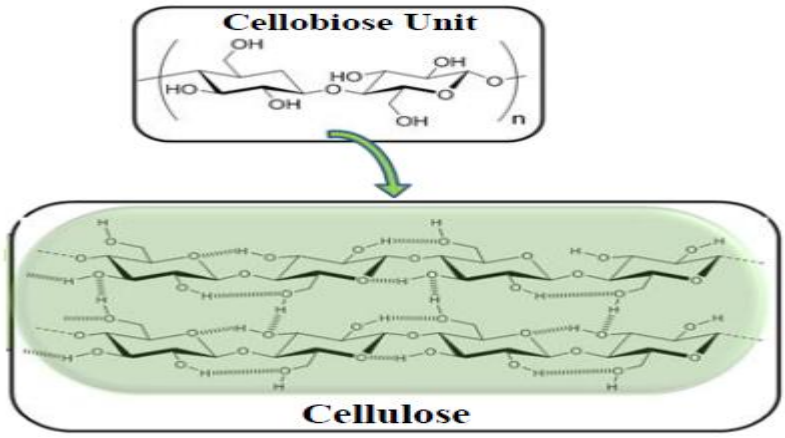

Figure 2: Structure of cellulose (Isikgor and Becer 2015)

I.1.2 Hemicellulose

Hemicelluloses are heterogeneous polymers, containing several monomers pentoses (xylose, rhamnose and galactose), hexoses (glucose, mannose and galactose) and uronic acids (e.g., D-glucuronic and D-galactouronic acids), although the real structure of hemicelluloses still unknown until know, but it is a much more complicated and linkage than cellulose, hemicelluloses present amorphous forms and low molecular weight therefore it is extremely hydrolysable and its thermal degradation generally occurs in temperature range between 200 – 300°C (Harmsen et al. 2010).

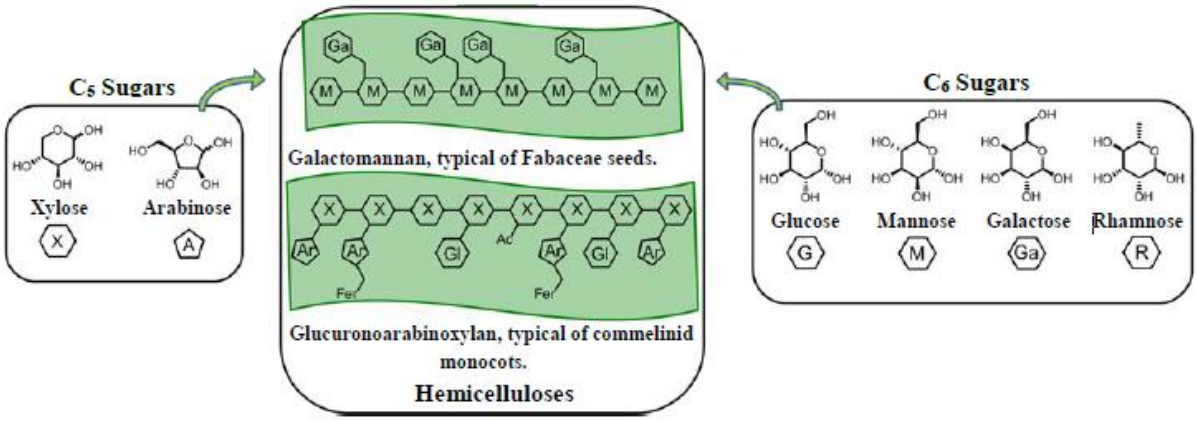

Figure 3: Hemicelluloses and its compounds structure (Isikgor and Becer 2015)

I.2.3 Lignin

Lignin has the most complex polymers three-dimensional structure; it is widely abundant in the nature, lignin composed by phenyl propane units, more particularly sinapyl alcohol, p-coumaryl alcohol and coniferyl alcohol. Lignin hold together cellulose and hemicelluloses fibers by tightly bonded physical and chemical interactions, this structure give support, resistance and impermeability to the lignocellulosic materials, the amorphous heteropolymer is non-water soluble and optically inactive(Hendriks and Zeeman 2009), its decomposition at around 600°C in case of thermal treatment under atmospheric conditions (Kambo 2014), therefore lignin is the most thermally stable polymers, its treatment depends strongly on water density and environment conditions such as acidic or alkaline medium. Lignin can be converted to produce important phenol-derived chemicals used in various chemical industries, its structure is shown in figure 4.

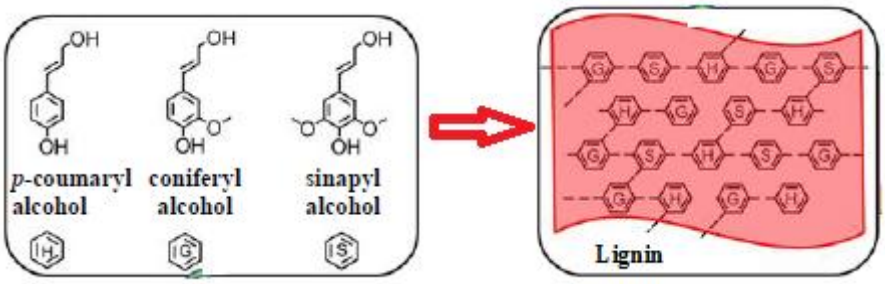

Figure 4: Lignin structure (Jung and Kim 2014)

I.1.4 Olive stones

Recently olive by-product has gained increasing attention in Mediterranean countries, especially Tunisia; it is the second largest producer of olive after Spain and it has reached around 340 Kt of olive oil annual production in 2014/ 2015, therefore olive stones, olive by-product, are of important interest from both economical and environmental point of view. Three different types of solid residues are generally produced depending on the oil-extraction process (Rodríguez et al. 2008):

- Crude olive cake: the first intact solid from the first oil extraction process, has a high moisture content and small amount of oil
- Exhausted olive cake: the solid from the solvent extraction (usually hexane) of the crude olive cake results homogeneous clean brown granular material
- Partly destines olive cake: solid from the partial separation of the stone from the pulp.

The residues compositions depend to the extraction technologies, there are three extraction systems: the traditional discontinuous pressing process, the two-phase continuous extraction and the 3-phase continuous extraction. The olive stones are lignocellulosic materials, recovered by filtration of solid residue; lignin, cellulose and hemicelluloses are its main compounds.

The olive stones by product are extensively used for different industries such as an abrasive, a plastic filled, in cosmetic, furfural production and activated carbon synthesis, table 2 present the polymers compositions ranges of olive stones.

Table 2: Polymers fraction of various variety of olive stones (Rodríguez et al. 2008)

Compounds	Compositions (%)
Cellulose	29.79 -34.35
Hemicellulose	21.45 -27.64
Lignin	20.63 -25.11
Ash	0.01 -0.68

I.2 Hydrothermal carbonisation

A hydrothermal treatment is a quiet new versatile thermo-chemical process, the final products: solid, liquid and gaseous depend strongly on the arrangement of treatment conditions (temperature, pressure, residence time and catalyst). This technique is initiated in the beginning of the 20th century by German Nobel owner Friedrich Bergius (F.B) (1931). It aimed to produce hydrogen via coal oxidation using water as medium reaction under high pressure 200 bars and temperature below 600°C avoiding carbon dioxide CO_2 formation (Titirici et al. 2015). An important observation was found during the experiments when peat is used as carbon material for the reaction, an large amount of CO is released and the solid residues of the process has elemental composition close to that natural coal. Through this discovery F.B continues his research exposing biomass mixed water to mild temperature condition (180-250°C) and high pressure the precursor transform to solid without gases emission.

Later, a number of researchers varied type of precursor (Berl and Schmidt 1928) and investigate the effect of pH in order to understand the decomposition mechanisms (Schumacher, Huntjens and van Krevelen) but the hydrothermal process has been omitted for a while and rediscovered again to produce carbon spheres using glucose or sugar under low temperature (200°C) by (Wang et al. 2001).

Hydrothermal carbonization usually occurs under temperature range between (130-250°C) for reaction experiment above this temperature range hydrothermal treatment can be classified to hydrothermal liquefaction and hydrothermal gasification (figure 5).

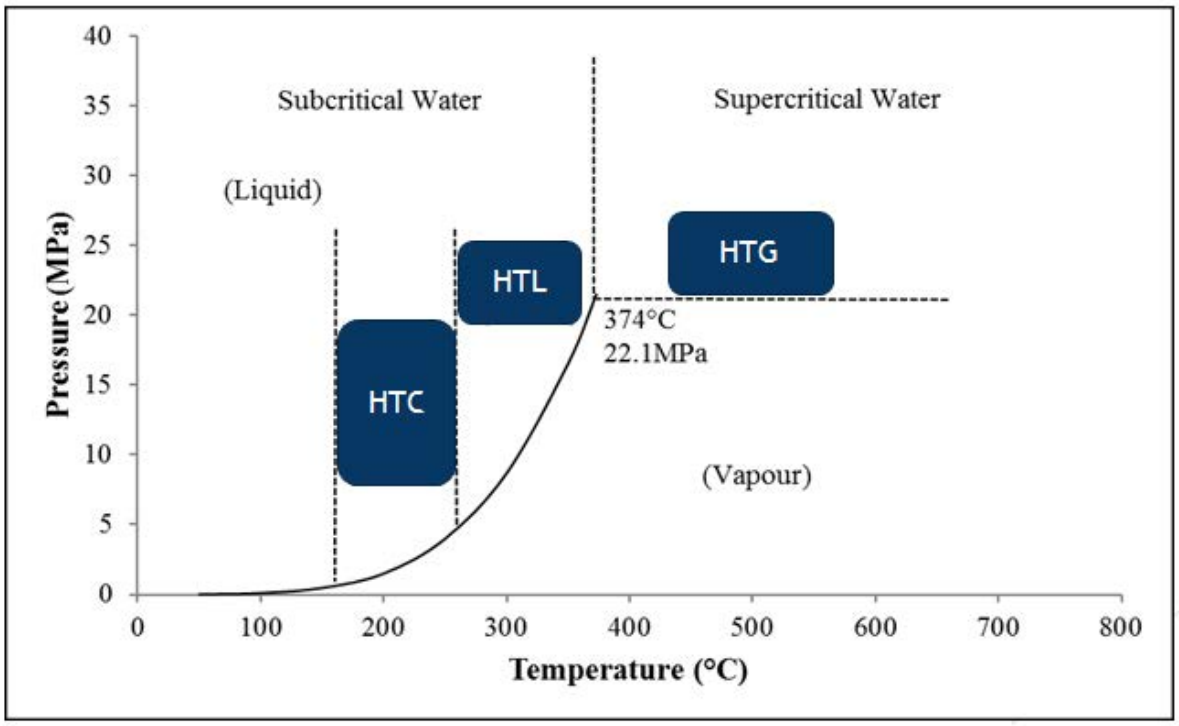

Figure 5: Classification of hydrothermal treatment

Hydrothermal liquefaction takes place at temperature between (260 and 350°C), during this process a significant amount of liquid fuel is produced, called crude oil or bio-crude, it is a deoxygenated and viscous product similar to petroleum crude (Jin 2014). It contains acids, alcohols, cyclic ketones, phenols, and other condensed structures, like naphthols and benzofuran s(Elliott et al. 2015).

Enhancing temperature above 374°C, hydrothermal gasification (HTG) or Hydrothermal vaporization (HTV) occurs and the water is on its supercritical conditions. At very high temperature of around 600 °C biomass is converted mainly to H_2 and CO_2, otherwise at temperature around 400°C, generally a metal catalyst is necessary to inhibit char formation and promotes CH_4 at the expense of H_2 (Kopetzki 2011).
Hydrothermal process overcome the limits of traditional conversion process and use varied type of renewable feedstock even with high moisture content: wet animal manures (Toufiq Reza et al. 2016), human waste (Berge et al. 2011) and lignocellulosic biomass.

The hydrothermal carbonization (HTC) has gained recently a special interest, the remaining products of this control are hydrochar (solid product), liquid or bio-oil in water and gases mainly CO_2 and some traces of H_2 and CO, the proprieties of hydrochar and bio-oil strongly depend on type of precursor, temperature, residence time and catalyst.

Hydrochar are significantly different from biochar (solid product of pyrolysis), depending on HTC conditions, usually hydrochar has a lower H/C and O/C ratio than the initial biomass.

A several studies of HTC of different type of precursor have been developed in order to assess the effect HTC conditions on precursor, commonly using simple saccharides e.g xylose, maltose, fructose and glucose and complex feedstock such as lignocellulosic biomass e,g wheat straw, walnut shell and rice husk , sewage sludge and animals waste. The composition and surface functional groups of solid product depend on feedstock and operating conditions, a spherical carbon shape is obtained in case of carbohydrate based materials and generally hydrochar are more hydrophobic than the original biomass. The HTC products consist approximately about 10% of the original biomass gases mainly CO_2, solid content between 41–90% and HTC-liquid content essentially sugars, acetic acid, and other organic compounds 5-HMF, levunic acid and furfural (Jin et al. 2007; Borrero-López et al. 2016). According to the type of biomass used in the treatment 60-90% of carbon can be obtained in the final solid product.

I.2.1 HTC mechanism

The detailed HTC mechanism still ambiguous especially for the complex feedstock, numerous publications deal with it in order to find a satisfying answer. Series, simultaneous or parallel reactions take place. Only simple carbohydrate precursors (e.g., monosaccharide) made the exception, such as glucose and fructose ($C_6H_{12}O_6$), and they are frequently chosen as model to study HTC-mechanism. According to Titrici et al., hydrothermal reactions pathway of glucose started at temperature above160°C, 5-hydroxymethylfurfural (HMF) is formed through the dehydration of glucose via Lobry de Bruyn-Alberta van Ekstein rearrangement at the initial phase of HTC, HMF is decomposed to levulinic acid, dihydrohyacetone, acetic acid and formic acid, ulterior polymerization and condensation reaction contribute to result polyfaruranic type compounds, after a cascade of chemical reaction the nucleation process takes place and aromatic network carbon particles could be attained with different final diameter size and spherical morphology.

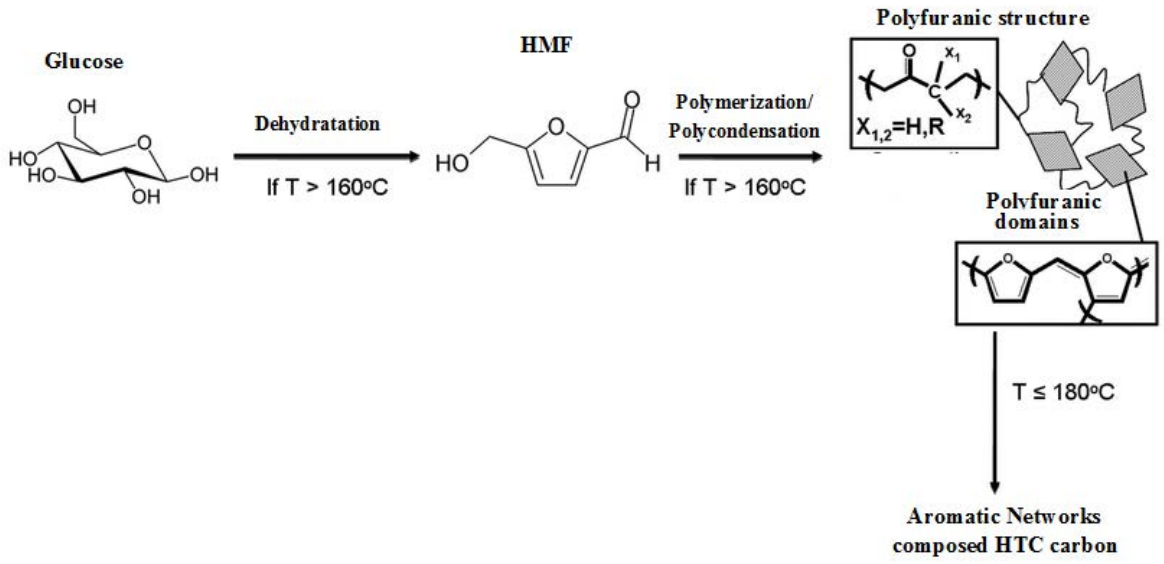

Figure 6: Decomposition mechanism of cellulose under HTC treatment updated (Falco et al. 2011)

In case of macromolecular carbohydrates (e.g,cellulose) different reaction mechanisms were proposed. Usually cellulose remains intact for HTC temperature less than 220°C (Sevilla and Fuertes 2009) but rearrangement on its structure can be occurred at 180°C (Falco et al. 2011). A possible pathway for decomposition of cellulose is described in figure 6. In both cases cellulose disintegration under HTC treatment shows a higher resistance than glucose, its stability is promoted by its macromolecular structure, crystallinity and the hydrogen bonds that hold the polymeric chains together (Bobleter 1994). The first step is its degradation under hydrolysis reaction into monomers which decompose later through dehydration reaction to produce HMF. Sevilla and Fuertes 2009 suggest the following possible degradation steps:

1. Hydrolysis of cellulose chains at temperature above 220°C.
2. Dehydration and fragmentation into soluble products of the monomers that come from the hydrolysis of cellulose.
3. Polymerization or condensation of the soluble products.
4. Aromatization of the polymers thus formed,
5. Appearance of a short burst of nucleation
6. Finally growth of the nuclei so formed by diffusion and linkage of species from the solution to the surface of the nuclei

Many attempts to investigate HTC mechanism of heterogeneous precursors, such as lignocellulosic biomass, the presence of its ternary compounds modify strongly the decomposition pathway, but its reaction process steps still unknown that is due to its complex

structure, a careful understand of reaction mechanism of HTC- biomass is required since it allows the control of the final product structure. Under HTC treatment the decomposition of lignin and hemicelluloses two polymers of lignocellulosic compounds is much easier than cellulose and it started at earlier hydrothermal stage. Hemicellulose is quickly hydrolyses to several organic acid and furfural at temperature around 180 °C but there is no significant alteration on lignocellulosic structure occurred under this temperature. Also lignin starts to decompose to phenolic and alcohol groups above 150°C and 200°C and the remained solid in the solution is mainly rich on lignin.

I.2.2 Water properties

Water has an important role in HTC treatment as the temperature is varied from 100 to 250 °C water is in subcritical condition. The pressure is high a enough inside the autoclave to keep water under liquid form, besides its function as reaction medium, hot compressed water can serve as catalyst that because owing to its properties such as ion product, density, dielectric constant and hydrogen bonding. As shown in figure 7, the polarity of water (or dielectric constant) decreases as the temperature and pressure increase which enhance the hydrolysis of the usual water insoluble lignin and breaks down the cellulose bonds, water can be useful as acid or base catalysis depending on its high degree of ionization into H^+ and OH^- which can affect the kinetic process of some organic reaction (hydrolysis and decarboxylation) because it decreases their activation energy (Jin 2014). Water made hydrothermal treatment advantageous process to treat all type of biomass even with high moisture content therefore biomass could be directly used and the drying pretreatment step could be avoided.

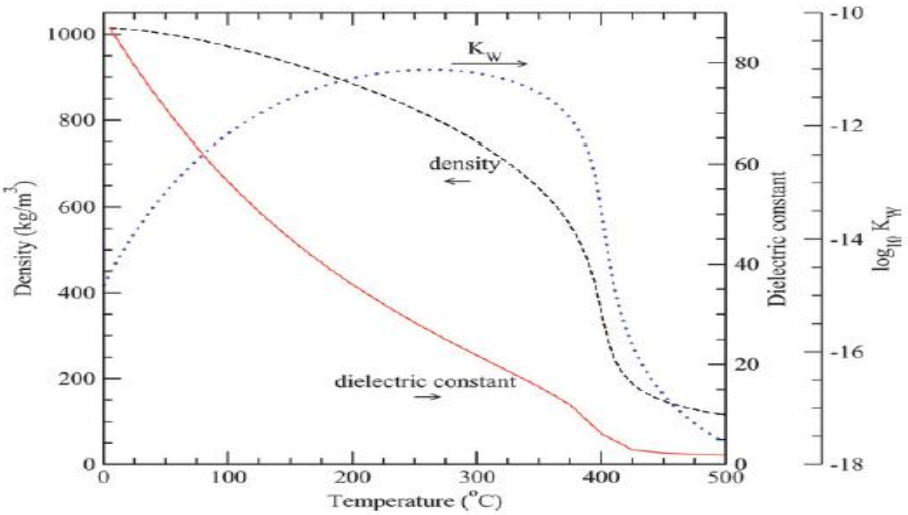

Figure 7: Density, static dielectric constant and ion dissociation constant of water at 30 MPa as a function of temperature. (Peterson et al. 2008)

I.2.3 HTC-liquid properties

Recently, aqueous co-product of hydrothermal carbonization which is known in the literature as bio-oil in water, bio crude and liquid fuel, has gained an important attention due to its interesting uses in the industries of bio-refinery and some chemicals compounds. HTC liquid products characteristics depends basically on type of precursor, temperature, time and catalysis, usually it is pH value is between 3.0 and 3.5 in case of lignocellulosic feedstock and it is rich in organic acid (e.g levunic acid, acetic acid and formic acid), phenolic compounds and furan derivatives.

A substantial attention on producing HMF and levunic acid from HTC-liquid phase, recently many scientist groups are carrying out studies and experiments on the synthesis and application of HMF. It is considered as an attractive area of investment for industry, 5-HMF is a versatile chemical compound which has a potential access to various industrial application across a wide range of industries, 5 -HMF could replace petroleum-based monomers for the synthesis of fine chemicals and plastics, it has unique and spatial proprieties made of it a key compounds in biochemistry. HMF and its derivatives levunic acid are classified as one of the 12 high value added chemicals from biomass according to the US Department of Energy.

The biofine process occurs in to different steps of process, the first step of control is the reduction of 5-hydroxymethylfurfural (HMF) and the second steps consist of the production of levunic acid. The production of these two compounds in hydrothermal treatment depends significantly on the process conditions temperature, time, type of biomass, the amount and type of used acid. Usually a high amount addition of acid can rehydrate HMF to levunic and formic acid. HMF production from lignocellulosic biomass under HTC related only to cellulose content (Borrero-López et al. 2016).

Furfural, ―the sleeping beauty bio-renewable chemical" could be possibly be obtained by hydrothermal carbonization of biomass based on hemicelluloses content of lignocellulosic precursor, furfural is one of the top value added chemicals and it is considered as a potential chemical used in large range of applications. Furfural and its derivatives have been widely used as solvent such as dihydropyran, methyltetrahydrofuran, tetrahydro-furan, methylfuranfurfuryl alcohol, tetrahydrofurfuryl alcohol and furoic acid, as transportation fuel, gasoline additive, lubricant, resin and decolorizing agent, as fungicides and nematicides, drugs, insecticides, bio-plastics, flavor enhancers for food and drinks.

I.2.4 Catalysis: acid and salt effect

The hydrothermal treatment aims to break-up macromolecule bonding networks and destabilized the complex three-dimensional structure of lignocellulosic biomass to make it more accessible for thermal and chemical post treatments, therefore in additional chemicals additives such as inorganic salts may catalyze HTC- treatment and therefore overcome limitations of biomass conversion. The effect of alkaline salt is extensively investigated in numerous conversion processes but in less extent in hydrothermal carbonization treatments. The role of inorganic salt such as ca salts (Calcium chloride and Calcium lactate), as well Mg acetate were studied (Lynam et al. 2012; Kambo 2014)in HTC of loblolly pine and it has been found that salts promoted the reactions occurring, consequently the resulting solid had increased the higher heating value and decrease pretreatment pressure which may have great advantage for industrial scale. On other hand, Kamboo et al found unusual trend on mass yield after using different amount of calcium chloride ($CaCl_2$) that because addition of high salt amount may bended with precursor and increase hydrochar mass yield and generally chloride ion strongly effect the decomposition of hydrogen bonding and subsequently the polymers of biomass, in additions depending of type of salts some HTC-product may be selectively enhanced (Mishima and Matsuyama).

Various acids such as sulfuric acid, para-toluensulfonic acid (pTSA), acetic acid and acrylic acid can be added in hydrothermal carbonization processes to catalyze or promote the selectivity of some reactions, recently acid used in hydrothermal conversion of cellulose to enhance the production of HMF compound and increase its yield (Wang et al. 2014), generally under acidic conditions the hydrochar yield reduce and hemicelluloses easily hydrolyzed releasing monomoric sugars and soluble oligomers from the cell wall matrix (Chaturvedi and Verma 2013) whereas lignin remained unaffected.

I.2.5 Nitrogen-doped carbon material

Doping heteroatoms into carbon network is considered as a powerful strategy to promote the efficiency of carbon materials in several applications. Hydrothermal carbonization is an easy and straightforward technique to stabilize heteroatom in carbon matrix at low temperature. In case of nitrogen doping via HTC, the method is simple, it consists to use started materials with high nitrogen content such as glucosamine, chitosan, peanuts, and cane or beet molasses; water can be also replaced by ammonia, amine or urine. The N-doped strategies has a strong effect on electrochemical performances of carbon materials, it promotes the electronic

properties, increase the active sites, promote the interaction bonding between carbon and adsorbents and improves the electronic conductivity. These properties have a particular impact in electrochemistry application as super capacitors, batteries and cells (Yan et al. 2017).

In addition, the novel carbon materials show a remarkable result in both gas and liquid adsorption. The nitrogen addition leads to give a basic character to the surface which made carbon suitable for CO_2 adsorption, that because of the interaction between N-containing basic functional group and acidic CO_2 gas increases (Xing et al. 2012), the same properties influence the adsorption process in liquid phase, Parmar et al. 2014 demonstrate that adsorption of copper was increase from 13.12 mg/g to 29.11 mg/g as the nitrogen content increase from 1.28% to 7.37% this mainly attributed to the low hydrophobicity and high basicity of modified carbon materials.

I.2.6 Applications of HTC

The HTC laboratory results were sufficiently favorable to encourage its further application on a large industrial scale. AVA CO_2, one of the world‘s first industries, has a capacity to process 8 000 tones of biomass to produce clean coal, a CO_2-neutral source of energy in a limited time. A newly potential of this plant, in 2019 it will start production of 5-Hydroxymethylfurfural (5-HMF). INGELIA, established in Spain, uses a various type of organic residues sewage sludge, onion peel and sugar cane bagasse to produce solid biofuel with high calorific value and without CO_2 emissions for further use as an energy source. SunCoal Industries and carbon solution has been made in Germany, working in the same field with high capacity of production (Parmar et al. 2014).

The carbonaceous end-products have been investigated as effective sol additives, that because it hold functional group (–OH, –COOH, -OOH) which enhance cation exchange capacity of soil to improve soil fertility, however a post treatment of hydrochar a strongly recommended to prevent plant yield depressions.

Recently, several research project aim to infix HTC as a new technology to modernize toilet system and dairy farms using animal manure and sewage sludge as feedstock. Cow Power Nevada project found that the bio-carbon pellets result from HTC-cow manure has characteristic of a good fuel similar to lignite, according to professor Coronella (coronella 2014) this dairy firm could generate twice the electricity it consumes in a year by converting manure to power.

Reinvent the Toilet Challenge (RTTC) is another innovative project aim for the developing of new toilet system using autothermic, hydrothermal carbonizing process to convert human waste to carbon-rich solid for further use as soil conditioner or fuel (Danso-Boateng et al. 2013).

I.3 Activated carbon

Activated carbon is set of a solid matrix characterized by highly tunable porosity and specific surface area. Its uses extended so far back in time, the first recorded date 3750 BC, back to the Egyptian and Sumerians, it was firstly used for reduction of metal in the fabrication of bronze, it was employed later in medicinal application in Greece than in different applications such remove bad taste and odor, prevent several diseases, water treatment and its first large application in gas-phase application started in the mid of 19th century.

Activated carbon prepared generally from precursor rich on carbon content such as hard and soft wood, coconut shell, olive stones, coal and peat, sugarcane bagasse, cherry stones and lignite. It is manufactured in countries rich in Biomass such as Asian country (Indonesia, Malaysia, china and Philippines), European (France and Italy). The global activated carbon consumption is expected to increase about 5.5% approximately from 1.437 million tons in 2014 and expected to hit 1.733 million tons in 2017 (Leimkuehler 2010).

United state and Japan are the largest activated carbon consuming country, which together consume two to four times more active carbon than others Europeans and Asian countries. Practically 80% of activated carbon is used for liquid phase applications and 20% for gas phase applications. The per capita consumption per year is 0.5 Kg in Japan 0.4 KG in U.S and 0.2 in Europe and 0.03 Kg in the rest of the word that may be because that the Asian countries didn‘t start to use activated carbon for water and air purification yet (Leimkuehler 2010).

Due to its unique and versatile properties activated carbon still one of the most important materials or ―Cinderella of the carbon family" as affirmed professor Harry Marsh (Reinoso et al. 1997) that because is used in very wide range of applications especially liquid adsorption, gas adsorption, catalysis and energy production and storage.

I.3.1 Structural properties and morphologies of activated carbon

Activated carbon usually present a large surface around 3000 $m^2 .g^{-1}$, its pores volume varied from 0.2 to 1.2 $cm^3.g^{-1}$ and its density from 0.2 to 0.6 $g.cm^{-3}$ (Radovic 2004). Activated

carbons contains a small amount of heteroatoms, average elemental composition of activated carbon is 88 % Carbon, 0.5% Hydrogen, 0.5% Nitrogen, 1.0% Sulfur and 6-7% (Hao 2014) and variable amount of mineral matter depending on the nature of raw materials (Bandosz 2006). Therefore, activated carbon could be considered as amphoteric solid but it has microcrystalline structures differs from that of graphite with interlayer spacing of 0.34-0.35 nm, the orientation of microcrystalline layers depends on the embedded heteroatom, also the surface chemistry of activated carbon depends on the non carbon elements and its amount, especially oxygen surface groups, owing to the influence of wettability, polarity, acidity and other physic-chemical properties.

The structure of activated carbon is determined as function of rearrangement of graphite interlayer. The imperfect structure and the disordered layers of carbon atoms result networks of porosity of activated carbons, the International Union of Pure and Applied Chemistry proposed the following classification of pores by their internal pore with (Burress 2009):

- Macropore: pores with size greater than 50 nm and their volume varied from 0.2 to 0.8cm^3/g.

- Mesopore: pore of internal with between 2 and 50 nm and volume of 0.1 to 0.5 cm3/g

- Micro pore: pore of internal with less than 2 nm, among microporous, those pores with size less than 0,7 nm are classified as ultra micropores and pores with size ringing from 0,7 and 2 nm turned as super micropores.

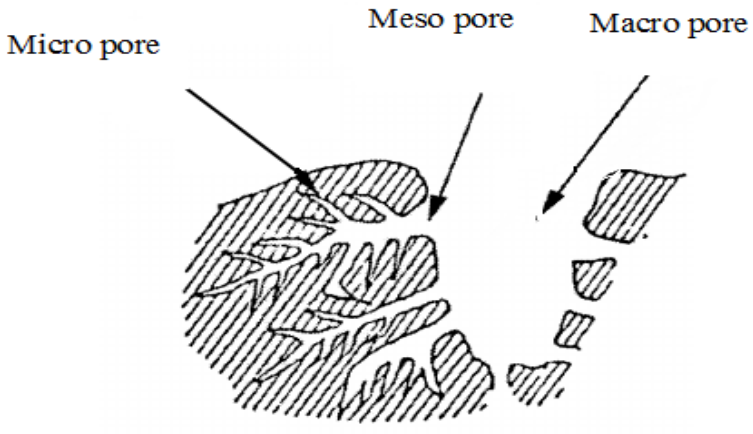

Figure 8: Schematic representation of the pore network of carbon material (Burress 2009)

This classification was attributed in relation with nitrogen adsorption at its normal boiling point 77 K(Kral et al. 1988). Gas adsorption has a great importance to characterize porous solid materials, this technique is essential and definitely the most popular and widely method to determine the aforementioned type of pores, pore volume also pore size distribution and surface area. The sorption behavior is dependent on the size of the pore. Macropores are large they could be considered almost as flat surface (Çeçen and Aktas 2011) and they act as transport pores to the meso and micropores (J. 2012). On the other hand, ultramicropores (size less than 0.7 nm) can accommodate only single molecules and the adsorption is enhanced by the overlap of the opposite pore walls, otherwise in case of super micropores (0.7-2 nm), the adsorption is mainly enhanced by the interactions between adsorbed molecules, generally the adsorption in case of micropores is referred as pores filling. The adsorption mechanism of mesopores is more enhanced by the interaction between fluid molecules theses leads the capillary condensation and multilayer adsorption (Burress 2009; Hendriks and Zeeman 2009).

N_2 and CO_2 are the most common used gaseous probe molecules in porous solids characterization, CO_2 adsorption isotherms at 273.15 K has been recognized to be used in case of ultramicroporous carbon materials, for the range of ultamicorpores (pores widhs<0.7 nm), that is because the bilayer thickness of the N_2 molecules are close to the pores widths therefore the pre-adsorbed N_2 molecules near the entry of an ultramicroporous may block further adsorption. On the other hand, N_2 is adsorbed at 77 K and relative pressure of 10^{-7} to 10^{-5}may be problematic for characterising very narrow micropores because diffusion of nitrogen is quite slow at such low temperature. As a consequence, the analyses are not only extremely long but, most of the time, are erroneous (Rodriguez-Reinoso et al. 1989; Silvestre-Albero et al. 2012). $CO_2$is therefore recommended as a suitable mean for the complete determination of textural parameters of porous solids (Eddaoudi 2005) because it allows assessing of pores narrower than 1 nm and leads to higher diffusion rate and faster achievement of equilibrium time comparing to nitrogen adsorption. Nitrogen adsorption could be useful to characterize the range of supermicropores (0.7-1 nm < pore width < 2 nm) and mesopores (2nm < pore width < 50 nm), both gas adsorption N_2 and CO_2 could be combined for full assessment of the different pore-size ranges. An interpretation of a possible adsorption experiments results, in case of adsorbed nitrogen volume (V_{N2}) is equal to that of CO_2 the material is microporous and its pore size distribution is relatively narrow, for V_{N2} superior than V_{CO2} the materials has a broad pore size distribution and may be present mesopores the

last case where V_{N2} less than V_{CO2} the materials are mostly narrow micropores and not accessible to N_2(Falco 2012).

Brunauer, Emmet and Teller BET model is commonly used to fit the experiments gas adsorption isotherm, the BET theory is based on the following assumptions (McMillan and Teller 1951):

- There are a fixed number of sites on which gas adsorption may occur,
- Allows for multilayer sorption, with the number of layer approaching infinity at saturation pressure,
- Surface is energetically homogenous,
- Allows for absorbent-adsorbate interactions as well as adsorbate-adsorbate interactions perpendicular to the surface.

The BET model gives satisfied results in case of the nonporous, mesoporous, and macroporous materials, but practically in the case of very narrow pores, the real surface is underestimated because only one gas monolayer can fit between two very near pore walls and the occurrence of micropore filling instead of multilayer adsorption. Despite these limitations the BET is useful to compare materials surface area with literature and as reference for materials properties. Recently Non-Local Density Function Theory (NLDFT, 1993) also known as smoothed density approximation (SDA) provides a much more versatile approach to determine the pore structure parameters and accurate description of a fluid confined to narrow pores, the NLDFT model based on the assumption that the slit ship-shaped pores have smooth and homogenous graphitic walls.

I.3.2 Adsorption-desorption isotherms

The isotherm curves derived from the adsorption-desorption measurement of gases (usually N_2) are illustrated by relation of the adsorbed amount of gases (cm^3/g) versus the equilibrium relative pressure (P/P°). The international union of pure and applied chemistry (IUPAC) recommends a classification based on six types of isotherms (Figure 9).

- Type I: Isotherm types I is rise very steeply and is concave to the P/P° axis, this indicative of sample have predominantly small micropores. A type I isotherm don‘t display any hysteresis in the adsorption desorption branches.
- Type II: This type of sorption isotherms describe the adsorption of non-porous or macropours solid.

- Type III: This type is not common, it characterize adsorption into macroporous or non porous materials where adsorbate-adsorbate interactions play an important role and the interaction adsorbent-adsorbate is weak.
- Type IV and V: These isotherms occur for sorption in mesoporeous materials, they are generally display a hysteresis loop between the adsorption-desorption branches which is associated with occurrence of pore condensation
- The type VI: represent stepwise multilayer adsorption on uniform, non porous surface.

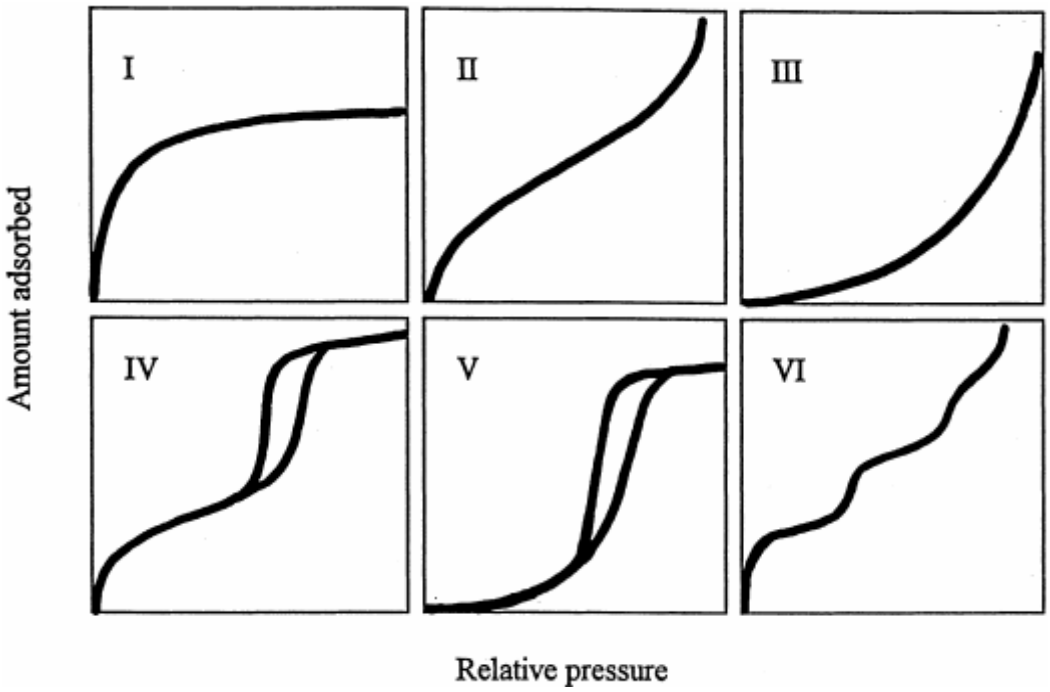

Figure 9: Physisorption isotherms according to IUPAC (Sing 1982)

I.3.3 Surface chemistry

The surface chemistry plays an important role in carbon materials applications such as adsorption and catalysis. Activated carbon has been recognized to include a huge variety of surface functional groups due to the existence of heteroatoms mainly oxygen, hydrogen, nitrogen, sulfur, phosphorous and halogens, which is depend mainly on precursor type, activation process, activation agent and post-treatment. The functional groups and the delocalized electrons of carbon structure confer acid, base or neutral character to the carbon surface.

Oxygen functional groups or acidic surface groups, shown in figure 10, commonly exist in the form of carboxylic acid, phenolic hydroxyl, quinine carbonyl and lactone. They had a

significant impact on activated carbon properties such as surface reactivity, hydrophobicity and adsorption capacity.

Nitrogen functional groups (figure 11) generally confer basic property which promotes the interaction between porous carbon and acidic molecules such as H-bonding, dipole-dipole and covalent bonding. The nitrogen-containg groups could be incorporated to the carbonaceous network through reaction with nitrogen containing reagents or activation of precursor with high nitrogen content. The nitrogen functionalities groups include amide, lactame, pyrrolic and pyridinic.

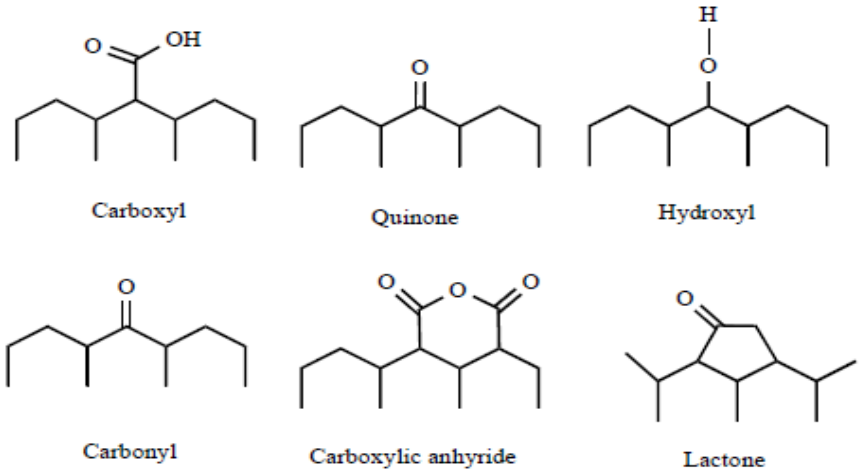

Figure 10: A simplified possible structure of some acidic groups bonded to of activated carbon surface (Shen et al. 2008)

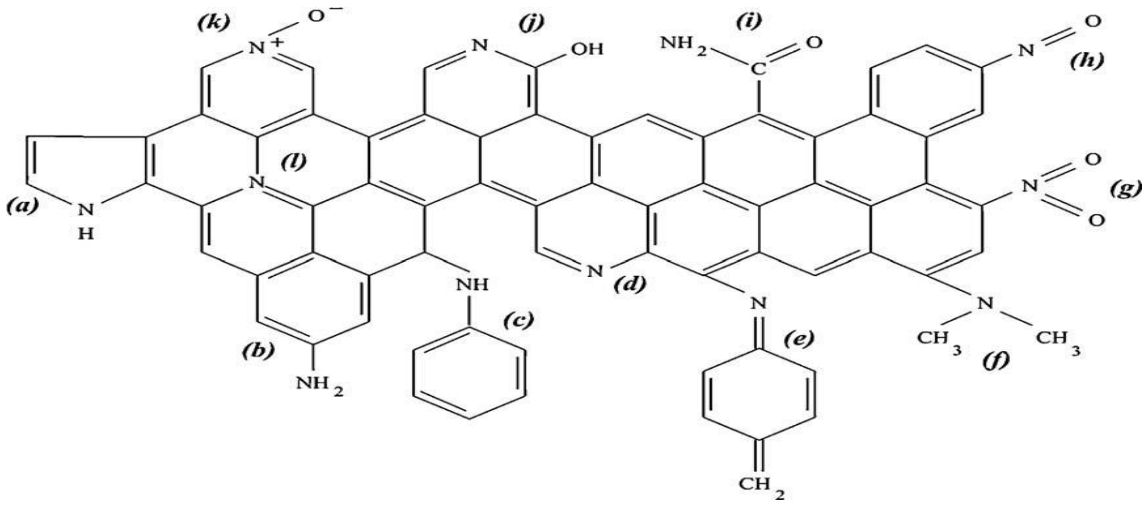

Figure 11: Type of Nitrogen surface functional groups attached to carbon aromatic structure: (a) pyrrole, (b) primary amine, (c) secondary amine, (d) pyridine, (e) imine,(f) teriary amine, (g) nitro, (h) nitroso,(i) amide, (j) pyridine, (k) pyridine-N-oxide, (l) quaternary nitrogen (Shafeeyan et al. 2010).

I.3.4 Activation process

Activated carbons can be produced in many different ways, which could be classified into two main types: physical activation and chemical activation. These types are described below.

I.3.4.1 Physical activation

The physical process usually involves two steps in serial: carbonization (pyrolysis) and activation. The lignocellulosic precursor is heated under inert atmosphere usually at temperatures between 400 and 800°C. During the carbonization step, the total or partial devotilization of raw material take place leads to removal of an important part of non-carbon atoms such nitrogen, oxygen and hydrogen and the micropore structure starts to develop but at limited extend (a specific surface area of about $10m^2/g$) (Braghiroli 2014). The objective of this thermal treatment aims to improve the final properties of the solid product (char), pore structure, carbon content, density, mechanical and electrical strength (Bandosz 2006). The activation is pivotal step to produce a well developed microporous materials, among this treatment a large fraction of undesirable by-products such as tarry matter and hydrocarbons released in the previous carbonization step and blocked the internally microporous are removed in order to make the porous volume in the materials more accessible. The activation process occurs under oxidizing atmosphere (steam, air or carbon dioxide) and temperature range between 700 and 1000°C.

I.3.4.2 Chemical activation

The chemical activation process involves a previous impregnation of the raw materials with activating agent (KOH, $ZnCl_2$, H_3PO_4, H_2SO_4, K_2CO_3 and NaOH) and a carbonization stage under inert atmosphere, usually nitrogen flow, at 400 to 900°C and residence time from 0.5 to 4 hours. The ratio of oxidizing agent to precursor is an important parameter may have a significant impact on the final activated carbon properties. Usually chemical activation develops higher porosity comparing to the physical process and it has as advantages of suppressing tar formation and reduce the pyrolysis temperature. It is for a major interest to mention that the carbonization steps could be substituted by hydrothermal carbonization treatment and hydrochar could be used as precursor for chemical activation, recently the hydrothermal carbonization appears to be a low-cost and environment friendly route for the production of activated carbon. Table 3 shows the characteristic of hydrochar derived activated carbon of some previous results.

Table 3: Major characteristic of activated carbon prepared from hydrochar

Precursor	HTC conditions	Activation Agent	Sp. area (m^2/g)	Pore volume (cm^3/g)	Applications	Author
Switch grass	T=300°C t= 0.5 h	KOH	726	–	Metal Adsorption	(Regmi et al. 2012)
Eucalyptus sawdust	T=250°C t= 2h	KOH	2252	Vmic=0.96	Supercapacitors CO_2 capture	(Titirici et al. 2012)
Glucose	T=240°C t=24 h	KOH	2210	Vmic=1.21	CO_2 CH_4 Storage	(Falco 2012)
Olive stone	T=220 °C t=20 °C	CO_2	438	Vmic=0.231 Vmes=0.006	–	(Román et al. 2013)
Grass cutting	T=180- 230 °C t= 5 – 6 h	CO_2	841	V mic 0.281	CO_2separation Water treatment	(Hao 2014)
Pulp paper sludge	T=160 200 240 °C t= 12 h	$ZnCl_2$	550	V_p=0.25	Metal and Dyes Adsorption	(Alatalo et al. 2013)
Cocnut shells	T=275°C t= 20 min	$ZnCl_2$	1652	Vp=1.29 Vmes=0.768	Li-ion capacitors	(Jain et al. 2015)
Sunflower stem	T=220°C t=20h	Air	213	Vmic=0.105 Vmes=0.052	–	(Román et al. 2013)
Rye straw	T=240 °C t= 24 h	KOH	2200	Vmic=1.11	CO_2 CH_4 Storage	(Falco 2012)
Banana pseudo stem coconut fiber	T=200 °C t=24 h	H_3PO_4	2500	Vp=1	–	(Romero-Anaya et al. 2011)
Sucrose	T=180°C t=24 h	KOH	2217	Vp=0.776	Desulfurization Adsorbents	(Shi et al. 2015)
Acrocomia aculeata	T=220°C t=5 h	KOH	803	–	–	(Correa et al. 2014)
Coconut shells	T=315 °C t=20 min	$ZnCl_2$	1877	Vp= 1.306	Phenol adsorption	(Jain et al. 2015)

I.3.4.3 Application of HTC-Activated carbon

Additional thermal treatment of hydrochar might promote its properties and made it suitable for many other applications for chemical energy storage and pollution control.

Adsorption onto activated carbon is one of its oldest applications which classified by US Environment Protection Agency as one of the best available environmental control technologies. Adsorption in aqueous phase is widely used to remove organic and inorganic pollutant from drinking water, municipal and industrial waste water. Using carbon material prepared from HTC seems to be efficient on this kind of application (Kambo 2014) Hydrochar has been tested to remove heavy metals from water and showed high adsorption capacity of copper than char prepared by pyrolysis. This finding is related to the fact that hydrochar surface chemistry rich on oxygenate functionalities such as COOH and OH groups at mild temperature (Jain et al. 2016). Liu et al. 2010 found that HTC treatment increased to 95% total oxygen-containing groups (carboxylic, lactone and phenolic group) comparing to raw biomass. Carbon materials prepared from hydrochar had been investigated also as adsorbent of 2-methylisoborneol and geosmin in drinking water in Japon (Ishibashi et al. 2014) and it shows a high adsorption capacity than commercial activated carbon.

I.4 Removal of pharmaceutical Substances

Pharmaceuticals substances are ~~–u~~nusual" synthetic or natural chemicals. Nowadays due to the advances in analytical technology, drugs are detected in surface waters, wastewater, groundwater and drinking-water, that because an important amount of unused drug is not returned to the pharmacy but it is discharged via toilets or via domestic refuse as well hospital waste water is an important source of pharmaceuticals which most of them are directly connected to the municipal sewer system and without further treatment (Kümmerer 2004; Gómez et al. 2007). The amount of pharmaceuticals waste is varied from country to another in Switzerland the collected amount is very high 237 tonnes/million capita and in the other states it's generally varied between 10 to 100 tonnes/million capita (Kümmerer 2004).

The presence of drugs in water increases concerns that because concentrations of pharmaceuticals in drinking-water are generally more than 1000-fold below the minimum therapeutic dose (MTD). MTD was used by some researchers to assess potential risks to human health from exposure to pharmaceuticals but it is difficult to identify the risk specially in terms of ecological exposure according to Daughton an environmental chemist from the Environmental Protection Agency (EPA) (Daughton 2001) .

Recently removal of pharmaceuticals is increasing attention and many researchers have endeavored to eliminate some medicine pollutant that to avert its harmful and chronic effects caused by their presences in water.

Metronidazole (2-methyl-5-nitroimidazole-1- ethanol) is an antibiotic, commonly used 15.5 t/annum in UK (Jones et al. 2001) to treat infectious diseases caused by anaerobic and protozoa bacteria, it is in the World Health Organization's List of Essential Medicines, it is also used for treatment of protozoal infection in dogs, cats, and other pets. MNZ is gaining interest because it is frequently detected in the industrials effluent 7850 (ng/l) (Lin et al. 2008), besides its high solubility in water and low biodegrability MNZ suspected carcinogen and mutagenic therefore its removal is of pivotal importance for human health and terrestrial organisms.

Ibuprofen, a propionic acid derivative, is a prototypical nonsteroidal anti-inflammatory agent with analgesic and antipyretic properties, extensively used all over the word to treat rheumatic disorders, pain and fever. It is the third-most popular medicine in the world. IBU has been detected in hospital waste waters, in surface (rivers, lakes) and ground water. A study carried out in 2011,(Jones et al. 2001) estimate 203 tonnes/a were produced in France an important amount of it (between 53-101.5 tonnes/a) were rejected as household waste.

Numerous health specialists consider that ibuprofen can cause kidney, cardiovascular, gastrointestinal and brain conditions. The main characteristic of IBU and MNZ are present in Table I.4.

Table 4: Ibuprofen and Metronidazole properties

Molecules	**Ibuprofen**	**Metronidazole**
Molecular formula	$C_{13}H_{18}O_2$	$C_6H_9N_3O_3$
Molecular Weight (g mol^{-1})	206.29	171.2
pKa	4.54	2.58
Structure	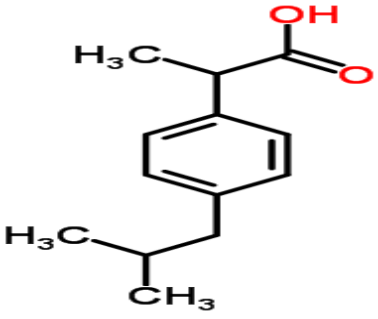	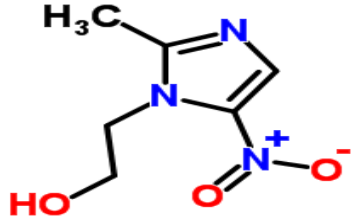

Nowadays, there is no specific treatment process designed especially to eliminate pharmaceuticals from water. Nevertheless there is a wide range of techniques may help to reduce or completely remove pharmaceuticals substances.

Biological remove process is one of these techniques, it has been shown to be effective, unfortunately is very expensive and it is very difficult to implant it in the most treatment facilities. Many researchers found that coagulation is largely inefficient for pharmaceuticals removal in pilot and full-scale investigations. Ozonation, ultraviolet radiation (UV) and membrane processes (reverse osmosis and nanofiltration) can achieve high removal level of ibuprofen from wastewater (Rivera-Utrilla et al. 2012). However, using some techniques such as ozonation may result harmful product for human health.

Adsorption in liquid phase is widely used treatment processes, it has proven its effectiveness and promises result for pharmaceutical removal in bench-scale, pilot-scale and full-scale applications, but to achieve the target level of removal, adsorption is strongly depend on physical and chemical properties of pharmaceuticals substances and treatment process conditions (pH, temperature and contact time). The common adsorbents used are zeolites, resins and activated carbon. Previous results of IBU and MDZ removal are shown in table 5 and 6 respectively.

Recently activated carbon derived from hydrochars shows that the two-step technology produces super activated carbons with tailored morphologies and micropore size distribution (MPSD), that because HTC step gives the possibility of controlling the pores size distribution, consequently a remarkable adsorption capacities of distinct pharmaceutical compounds (Mestre et al. 2015).

Table 5: Adsorption results of previous studies of Ibuprofen

Adsorbent	Temperature (°C)	Adsorbent Dose (g)	Initial Concentration (mg/L)	Adsorbed amount (mg/g)	References
Activated carbon prepared from K_2CO_3 activation of cork powder	30	0.01	60	85.5	(Mestre et al. 2007)
Commercial activated carbon cloths	30	0.01	100	150	(Mestre et al. 2009)
Activated carbon cloth	25	0.01	82	123	(Guedidi et al. 2017)
Clay	25	0.025	50	36	(Khazri et al. 2016)
Activated carbon prepared from H_3PO_4 activation of olive stone	25	0.3	10.04	9.083	(Baccar et al. 2012)
Graphene oxide nanoplatelets	35	1	10	9.165	(Banerjee et al. 2016)
Activated carbon prepared from co2 activation olive stone	25	0.03	100	126	(Mansouri et al. 2015)

Table 6: Metronidazole adsorption results of previous

Adsorbent	Temperature (°C)	Adsorbent Dose (g)	Initial Concentration (mg/L)	Adsorption Capacities (mg/g)	References
Commercial Activated carbon(NORIT)	25	0.01	20	138.5	(Çalışkan and Göktürk 2010)
Fe-modified sepiolite	30	0.3	30	2.737	(Ding and Bian 2015)
Activaed carbon prepared from Siris seed pods	30	0.5	100	169.38	(Ahmed and Theydan 2013)
Activated carbon	37	0.23	100	200	(O. 2011)

I.4.1 Adsorption models

Adsorption isotherm describes the equilibrium relationship between the concentration of adsorbate per unit of mass of adsorbent and its degree of accumulation on the adsorbent surface at constant temperature.

In the literature, the adsorption isotherms are simulated using conventional models determined through a physical formalism; Langmuir and Freundlich are commonly used for the phenomenological description of adsorption isotherms.

I.4.1.1 Langmuir Model

Langmuir is the most commonly used model to describe the adsorption of numerous fluid-solid system, it is based on various assumptions such as:

1. The adsorption is a monolayer,
2. Adsorption occurs in homogenous surface,
3. Once a molecule occupies a site, no further sorption takes place,
4. The binding sites have uniform energies,
5. There is no interaction between the adsorbent molecules.

The linear forms of Langmuir model is giving by the following equation.

$$\frac{C_e}{q_e} = \frac{C_e}{q_m} + \frac{1}{q_m \times K_L} \qquad (1)$$

Where: q_e (mg/g):is the amount of solute adsorbed

C_e(mg/l): is the solute concentration at equilibrium

q_m(mg/g): is the maximum adsorption capacity associated with complete monolayer coverage

K_L (l/mg): K_L is the equilibrium constant of adsorption

I.4.1.2 Freundlich model

Freundlich model was appropriate to fit adsorption experimental data for varied fluid-solid system, is based on the following assumptions

1. The adsorption occurs on heterogenic surface by uniform energy distribution,
2. Suggest the formation of multilayer adsorption,
3. The interaction between adsorbed molecules is not neglected ,
4. Reversible adsorption.

The Freundlich equation is given by the equation (2) and the linearized form by equation (3)

$$q_e = K_F \times C_e^{\frac{1}{n}} \qquad (2)$$

$$\log q_e = \frac{1}{n}\log C_e + \log K_F \qquad (3)$$

Where: K_F (L/g) and _n' are Freundlich model parameters.

K_F represents the affinity of the solute for the adsorbent and n indicates the capacitance of the adsorbent. The n value could be interpreted as following:

$n = 1$: The adsorption is linear therefore the adsorption sites are homogeneous and no interaction between adsorbed molecules

$\frac{1}{n} \langle 1$: The adsorption is favorable

$\frac{1}{n} \rangle 1$: The adsorption is not favorable

I.4.2 Adsorption Mechanisms

The adsorption mechanism could be described according to the following serial steps:

Step1: External transport

Step 2: Transport within the particle (intra-particle diffusion)

Step 3: Adsorption of molecules onto internal surface site of the particle

The adsorption kinetic modeling is developed to assess the adsorption rates of the controlling steps. There are different kinetics models including: pseudo first order, pseudo second order and the intraparticle diffusion model.

I.4.3 Adsorption Kinetics

I.4.3.1 Pseudo first order

The first pseudo order describes the adsorption phenomena occur in the first minute of the process. The linearized form of the first order model is identified as following:

$$Ln(q_e - q_t) = \ln q_e - K_1 t \qquad (4)$$

Where qe and qt are respectively the adsorbed amounts at equilibrium and at time t (mg/g), and k_1 is the rate constant of the pseudo-first-order adsorption (min^{-1}).

I.4.3.2 Pseudo second order

The linear expression (5) describes the pseudo second order is:

$$\frac{t}{q_t} = \frac{1}{K_2 q_e^2} + \frac{1}{q_e} t \qquad (5)$$

Where q_e and q_t (mg/g) present respectively the adsorption capacity at equilibrium and at time t and k_2 (g/(mg.min)) is the pseudo second-order constant.

I.4.3.3 Intra particle diffusion

The intra particle diffusion model describes the sorption kinetic and allowing to identify the controlling step or the combinations of steps. The intra particle diffusion equation (6)is:

$$q_t = K_P t^{1/2} + C \qquad (6)$$

Where: q_t (mg/g) is the amount adsorbed at time t (min), K_p (mg/(g.min$^{0.5}$)) is the intraparticle diffusion constant, and C (mg/g) is a constant related to the thickness of the boundary layer.

I.5 Hydrogen adsorption

Today humans are not facing a shortage of energy but facing a technical challenge in capturing and delivering of energy to consumers. In this framework, hydrogen storage is expected to guarantee mankind‘s core requirements for energy, hydrogen is the third commonest element on the Earth‘s surface and it is an attractive, sustainable energy vector, it will play an important role in future, low-carbon diversified energy resources. The hydrogen does not naturally exist in its elemental form on Earth but it is rarely found in free state and almost contained in chemical compounds, actually, total hydrogen production is 48% from natural gas, 30% from oil, 18% from coal and 4% from water electrolysis (figure 12)(Ministry of New and Renewable Energy Government of India[60]).

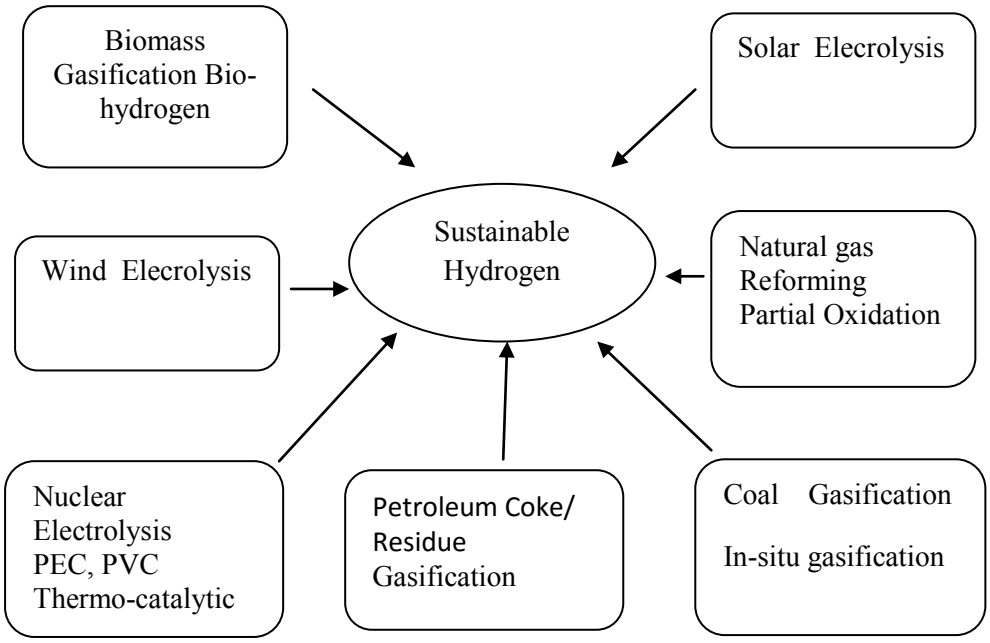

Figure 12: Hydrogen production sources (Ramaprabhu et al. 2012)

Hydrogen has an efficient and reliable ability to be used in various applications such as:

- Fuel of choice in mobile applications especially that hydrogen is a light gas and combustible.
- Transport light- and heavy-duty vehicles, Buses, Trains, Boats and ships Aerospace, without gas emission only water as waste product.
- Stationary application, hydrogen could be converted to electricity, heat or kinetic energy.
- Industry applications by using it as a chemical compound.

Hydrogen could satisfy three essential concerns; security, environment issues and energy demand, but the major challenge for hydrogen uses as renewable energy production is storage technologies. Currently, there are numerous of techniques that has been extensively studied since a long period of time, at the moment there are two main methodologies to store hydrogen, first one is by liquefy hydrogen at cryogenic temperature which incredibly difficult to achieve and maintain or the second technique by compressing hydrogen at high pressure (350-700 bar) tanks (Zhao 2012), which is faced with problems of safety and management .Recently, completely different vision of hydrogen storage has been investigated by several researches; which attempt to store hydrogen at porous solids by adsorption or within solids by absorption. But the storage ways has to overcome several problems such as high pressure, long refueling times of hydrogen and the cost of the storage systems, so to improve storage technologies, many researches are focusing to develop and ameliorate materials capacity for hydrogen capture. The most promising materials are metal-organic frameworks (MOFs), zeolite, porous polymers and activated carbon; the following figure 13 resumes the efficiency of these materials on hydrogen adsorption as function of their surface area.

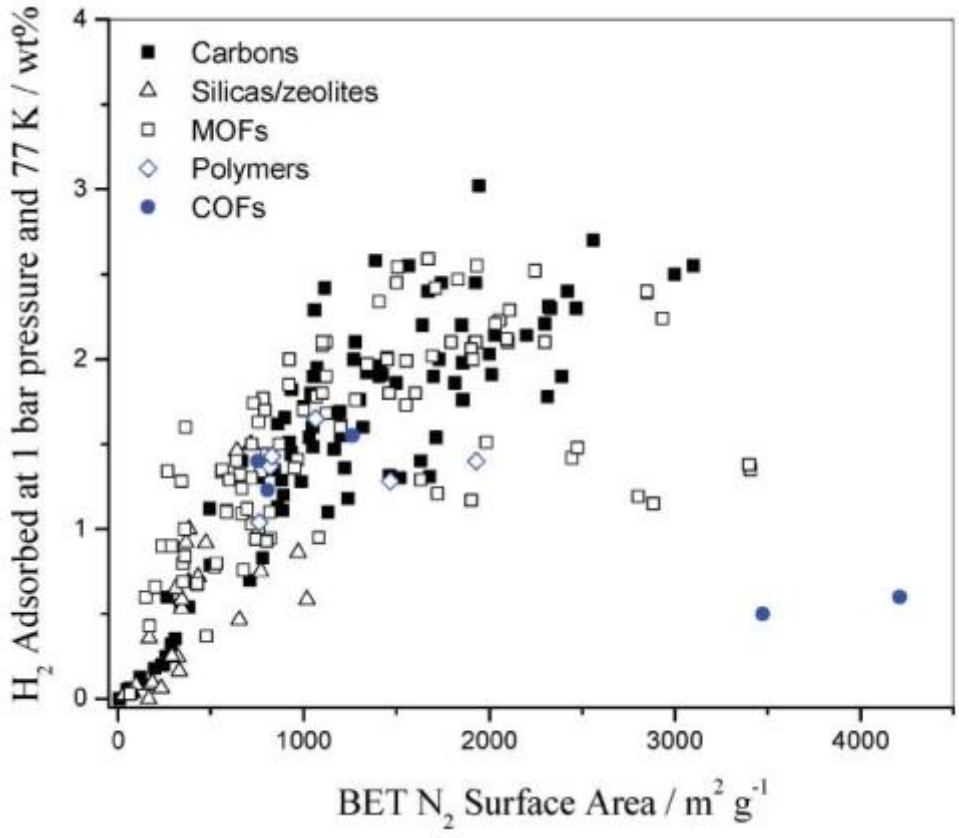

Figure 13: The variation of hydrogen uptake at 1 bar and 77K as function of BET surface of selective porous materials (Thomas 2009)

Carbonaceous material has been recognizing to be one of the most attractive materials for hydrogen adsorption, this materials has a high capability in hydrogen storage (Thomas 2009), a fallow weight and a fast adsorption/ desorption kinetics.

Adsorption into activated carbon could be classified as physical or chemical adsorption, depending to the types of forces involved in adsorption mechanism: the phenomenon of physical adsorption or physisorption is described as the accumulation of undissociated hydrogen molecule in the surface of carbon materials, it involves Van Der Waals interactions which relatively weak forces. Chemical adsorption or chemisorptions consist of interactions and ion exchange, leads to the formation of strong covalent bonds and therefore resulting in a true chemical reaction. The difference between the two types of adsorption is basically difference in the interactions involved in the adsorption process, besides to high chemisorptions enthalpy another important point should be highlighted that during chemisorptions the molecule are linked on the surface of solid by valence bond that can occupy certain site adsorption and therefore one layer could be formed in contrast whereas it could be multilayer in case of physisorption.

There are several factors that should be taken in account when selecting an activated carbon as hydrogen adsorbent. The hydrogen adsorption capacity is strongly related to the properties of activated carbon, numerous researches shows that there are a linear relationship between activated carbon specific surface area and pores size distribution with adsorption capacity, so materials has two or three times diameters of hydrogen molecule selected as good adsorbent and high specific surface area also may leads to high hydrogen uptake (Valtchev et al. 2009).

There are extensive investigations on the efficiency of activated carbon on hydrogen storage, hydrogen uptake on coconut-shell activated by potassium hydroxide with surface area 2800 m^2g^{-1}show capacity of 0.85wt. % at 100 bars and 298K (Lim et al. 2010), a maximum hydrogen adsorption of 0.44wt% at 298 K and 50°C for activated carbon prepared from waste agricultural waste corncob with high surface area 3012 m^2g^{-1} and 1.7 cm^3g^{-1}(Rajalakshmi et al. 2015) and 3.34 % were obtained by olive stones physically activated by CO_2 at 900°C for 8 h (Moussa et al. 2017)

Activated carbons derived from hydrochar are excellent and versatile materials in a range of gas adsorption and gas storage processes. Recently Sevilla et al, tested hydrochar precursor prepared from different raw materials such as furfural, glucose, starch, cellulose and eucalyptus sawdust on hydrogen adsorption, the HTC-derived activated carbon shows a high surface area up to 2700 m^2g^{-1} and exhibit a high hydrogen uptake up to 6.4 wt%, these results provided by materials with pore size less than 1 nm where the interaction between carbon materials and hydrogen is extremely strong. Similar result obtain by Wantana Sangchoom and Robert Mokaya, using lignin-derived hydrochar as precursor for chemical activation with KOH, materials shows high surface area 3235 $m^2\ g^{-1}$ and pore volume 1.77 $cm^3\ g^{-1}$, the hydrogen adsorption capacity was 6.4 at -196°C and 20 bar.

The hydrogen adsorption capacity could be enhanced by incorporation heteroatoms and transition metal or modification of activated carbon structure, which can be easily performed through the hydrothermal treatment as it occurs at low temperature (Huang et al. 2010). Huang et al demonstrate that the adsorption capacity of activated carbon after modification with palladium or acidic oxidation increase enhanced from 0.41 and 0.32 wt.% to 0.53 and 0.45 wt.%, respectively. Similar result shown in case of activated carbon modified with nickel metal the stored capacity increase from 0.1% to 0.53% at 30 bars (Zieâlisld et al.). Studies using different activated carbon in hydrogen adsorption are represented in table 7.

Table 7: Experimental Hydrogen adsorption of different activated carbons

Precursor	HTC/Activation conditions	Adsorption conditions	Adsorption capacity (wt.%)	Authors
Sucrose	HTC: T= 453 K t= 24h KOH activation	T=298 K P= 10 MPa	0.59	(Schaefer et al. 2016)
Lignin	HTC:T= 300°C KOH activation T=900 °C t=1h	T=−196 °C P= 20 bar	6.2	(Sangchoom and Mokaya 2015)
Cellulose	HTC: T= 250°C t= 2h Activation KOH T=700ºC t=1h	T=-196ºC P= 20 bar	6.4	(Sevilla et al. 2011)
Olive stones	Activation CO_2 T=900°C t=8h	T= -196ºC P=25 bar	3.34	(Moussa et al. 2017)
Olive stone	Activation KOH T=850°C t=3h	T=-196 °C P= 25 bar	3	(Bader et al. 2017)
Coconut-shell	Activation KOH T= 1073 K t=2h	T=298 K P= 100 bars	0.85	(Jin et al. 2007)
Litchi trunk	KOH activation T=823 K t= 2 h	T=77 K P= 0.1 MPa	2.89	(Huang et al. 2010)
Coffee bean	KOH activation T=850 °C t= 2 h	T=298 K P= 10 bar	0.6	(Akasaka et al. 2011)
Rice hull	NaOH activation T=800°C t=1h	T=77 K P=1.2 MPa	7.7	(Chen et al. 2012)
Malaleuca	KOH activation T= 1023 K t= 1 h	T= 77 K P= 10 bar	4.08	(Xiao et al. 2014)
Sawdust	KOH activation T=780°C t=1.5 h	T= -196 °C P= 10 bar	5.05	(Cheng et al. 2008)
waste corncob	NaOH activation T= 450°C t= 4h	T= 298 K P= 5 MPa	0.44	(Sun and Webley 2010)

I.1 Conclusion

In this thesis, a deep investigation in chapter I on the solid fraction recovered after HTC of olive stones, the experiments occur on large range of time and temperature (3, 6, 12, 24, 48 h) and (160, 180, 200, 220 and 240°C), these two parameters could be combined on severity factor which allowed an ample understanding on the physicochemical characteristics of the hydrochars. Moreover, in order to get helpful insight on the transformation of lignocellulosic biomass, a profound investigation on differential thermogravemetric curves of each hydrochar prepared at specific temperature and time. The curves were deconvoluted using Gaussian functions with the Origin® software, and each area corresponding to ranges of temperature was divided by the total area of the peaks. The value of each area normalised by the total area was then plotted as function of the severity factor. Detailed information of this method presented inthe same chapter.

Chapter 3 presents the characterization of HTC-Activated carbon prepared from hydrochar (240°C and 6 h), (180°C and 6h) and (180°C, 6 h and using ammonia as reaction medium).

Finally, in chapter 4, in depth investigation of the efficiency of hydrochar modified with nitrogen and physically activated, hydrochar chemically activated with KOH and activated carbon oxidized with ozone on hydrogen adsorption at 298 K and 10 MPa, and on pharmaceuticals adsorption at different conditions.

Chapter II: Hydrothermal Carbonization of olive stones

II.1 Experimental methods

II.1.1 Raw materials: olive stones

The precursor in hydrothermal treatment has an important role and depends strongly on ulterior uses of liquid or solid product. Usually simple monosaccharide and oligosaccharides are commonly used as stared materials. In this thesis project, olive stones had been chosen as precursor, olive stones are extensively used for pyrolysis (Blanco López et al. 2002), alkaline treatment, combustion, liquefaction and steam explosion (Rodríguez et al. 2008) but barely exploited in hydrothermal treatment, actually using olive stone as raw materials could be considered as challenge for HTC that because of high degree of heterogeneity and complexity structure of olive stones. Olive stones used in the following experiments were produced via two-phase continuous extraction in Gabes south of Tunisia, the olive stone were washed with hot distilled water and then left to dry naturally. The fiber analysis of alpha cellulose and lignin content of OS were determined according to T203 and T222 Tappis standards respectively, hemicelluloses were determent by difference.

II.1.2 Hydrochar and carbon synthesis

The experiments were carried out in a 100 ml Teflon®-lined autoclave using 2 g of OS mixed with 16 ml of distilled water, then the autoclave were putted in preheated oven at a defined temperature (160, 180, 200, 220 and 240 °C) and for each defined temperature the experiments were repeated at several time (3, 6, 12, 24 and 48 h). The hydrochar samples were dried for 8 h at 80°C before analysis.

All prepared hydrochar were then carbonized at 900°C (1°C min^{-1}) for 3 h under nitrogen flow (80 cm^3 min^{-1}) and in a quartz tube installed in a tubular furnace.

II.1.3 Characterization

The hydrochars (solid product of hydrothermal of olive stone) and carbonized hydrochar were subsequently characterized by several techniques such as:

The elemental analysis of carbon (C), hydrogen (H), nitrogen (N), sulphur (S) were performed using in an Elementar EL Cube apparatus and oxygen content was determined by difference.

The thermogravimetric analysis of hydrochar was deeply investigated using a STA 449F1 apparatus (Netzsch, Germany), the analyses experiments were carried out under argon flow of 20 ml min^{-1} and heated rate of 10°C min^{-1}.

The textural properties of carbonized hydrochar (pore volume, pore size distribution and specific surface area) were studied by physical adsorption of gas (CO_2 at 0°C and N_2 at -196°C). The analyses were performed using an ASAP 2020 automatic manometric analyser (Micromeritics, USA). The samples were priory degassed at 250°C for 24 h.

The GC/MS analysis was performed on liquid product of HT treatment for a few selected samples, a Clarus 500 GC gas chromatograph (Perkin-Elmer Inc., USA) coupled to a Clarus 500 MS quadrupole mass spectrometer (Perkin-Elmer Inc., USA). The samples were submitted to liquid-liquid extraction by adding 5 ml of dichloromethane to 1 ml of hydrothermal liquid. The remains solutions were stirred vigorously and then dichloromethane was removed before analysis

II.2 Results and discussion

II.2.1 Olive stone characterization

II.2.1.1 Elemental and fiber analysis

The elemental and fiber analysis of raw material are given in table 8. Olive stones are rich in cellulose (40%) and lignin (30%) therefore it was very attractive to numerous conversion processes, the compositions shown in tale 8 are consistent with values reported in the literature of olive stones containing 35 to 50 % of lignin, and usually the cellulose amount is higher than that of hemicelluloses (Nefzaoui 1991; Blanco López et al. 2002).

Table 8: Elemental and fiber composition dry basis

Elemental analysis		Biopolymer compositions (wt %)	
Carbon	50.10	Cellulose	40.53
Oxygen	43.50	Hemicellulose	21.68
Hydrogen	6.22	Lignin	29.88
Nitrogen	0.15	Extractible	7.9
Sulphur	0.04		

Figure 14: olive stone after washes

II.2.1.2 Thermo-gravimetric analysis

The Thermal degradation of (Cellulose, Holocellulose and Lignin) is shown in figure (15) and (16) in order to extrapolate the thermal degradation of the original biomass (olive stones) and its individual compounds.

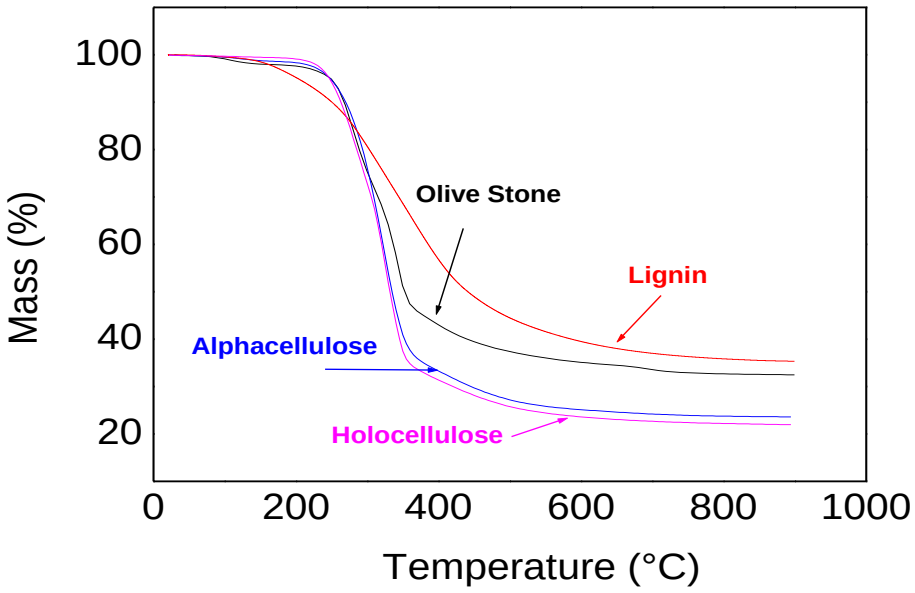

Figure 15: TGA thermogram of Olive stones and its compounds

Three major weight losses were noted: for temperature range less than 160°C, the weight loss is associated to the removal of moisture and some extractive compounds, the second at temperature range between 215 and 310°C, and a third maximum weight loss of 48% occurred one between 310 and 360°C. At temperatures higher than 360°C, a constant weight loss about 35 % was showed until temperature up to 800°C (Figure 15) that could be associated to the very progressive carbonisation of the biomass. In the interest to get close idea and exact interpretation for these thermo-gravimetric results, alpha-cellulose, holocellulose and lignin were separated from the olive stones and studied separately, their differential DTG curves are shown in Figure 16 (b), (c) and (d), respectively. The alpha-cellulose degradation figure 16 (b) has been initiated at 200°C and finished at 400°C with a maximum at 320°C. Figure 16(c) shows the thermal decomposition of holocellulose, with a maximum at 320°C and a shoulder at 270°C.Since holocellulose is a combination of cellulose and hemicellulose, the lowest temperature was referred to the decomposition of hemicelluloses. Eventually, lignin decomposes at large temperature between 200 to 800°C Figure 16 (d), Similarly results reported by other authors (Fierro et al. 2005).Therefore, the

long decomposition tail observed up to 800°C was probably due to lignin, which represents 29.88 wt. % of OS. It is possibly to identify the 2nd and 3rd the aforementioned weight losses on DTG curves of OS which are mainly the decomposition of hemicellulose and alpha-cellulose, respectively.

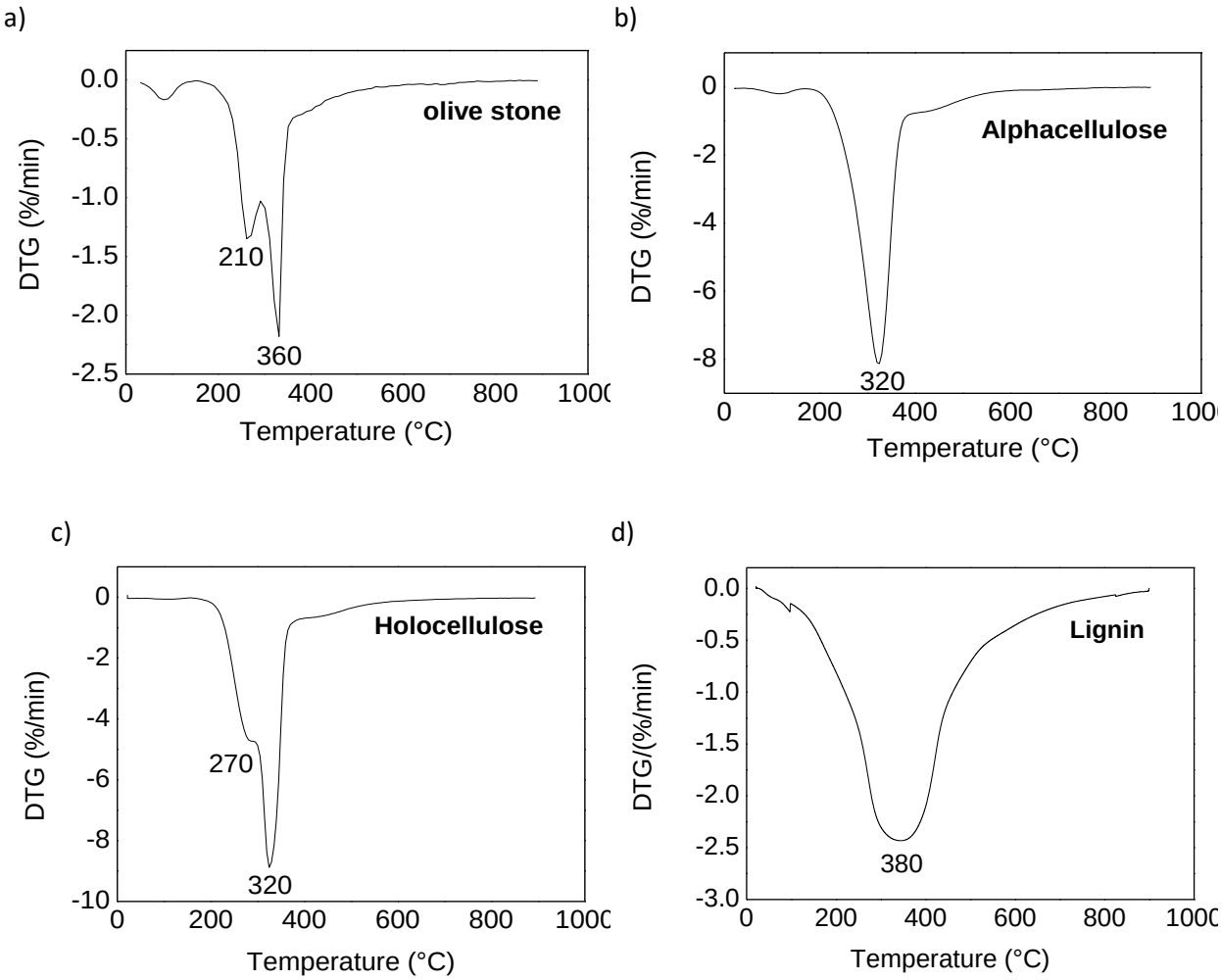

Figure 16: DTG curves of: a) olive stone, and of its three polymers: b) alpha-cellulose, c) holocellulose, and d) lignin

II.2.3 characterisation of hydrochar

The HTC yields are defined as the amount of recoverd solid product as percentage of the initial weight of olive stones.

$$HTC\ \ yield\,(\%) = \frac{mass\ of\ hydrochar}{mass\ of\ olive\ stones} * 100 \quad \text{(II.1)}$$

Temperature and time are the most important parameters of hydrothermal treatment and generraly in hot liquid water process, in order to appropriately assess their effect on hydrochar, severity factor will be introduced as reaction ordinate, R_0, it is based on the combination of temperature, T (°C), and residence time, t (min), this parameter ($R_{0)}$ was first defined by (Overend et al. 1987) to describe the impact of liquid hot water treatments on lignocellulosic components:

$$R_0 = t \cdot \exp\left(\frac{T-100}{14.75}\right) \text{(II.2)}$$

In Eq. (II.2), 14.75 are the activation energy (kJ/mol) based on the assumptions that the reaction is hydrolytic and the overall conversion is first-order.

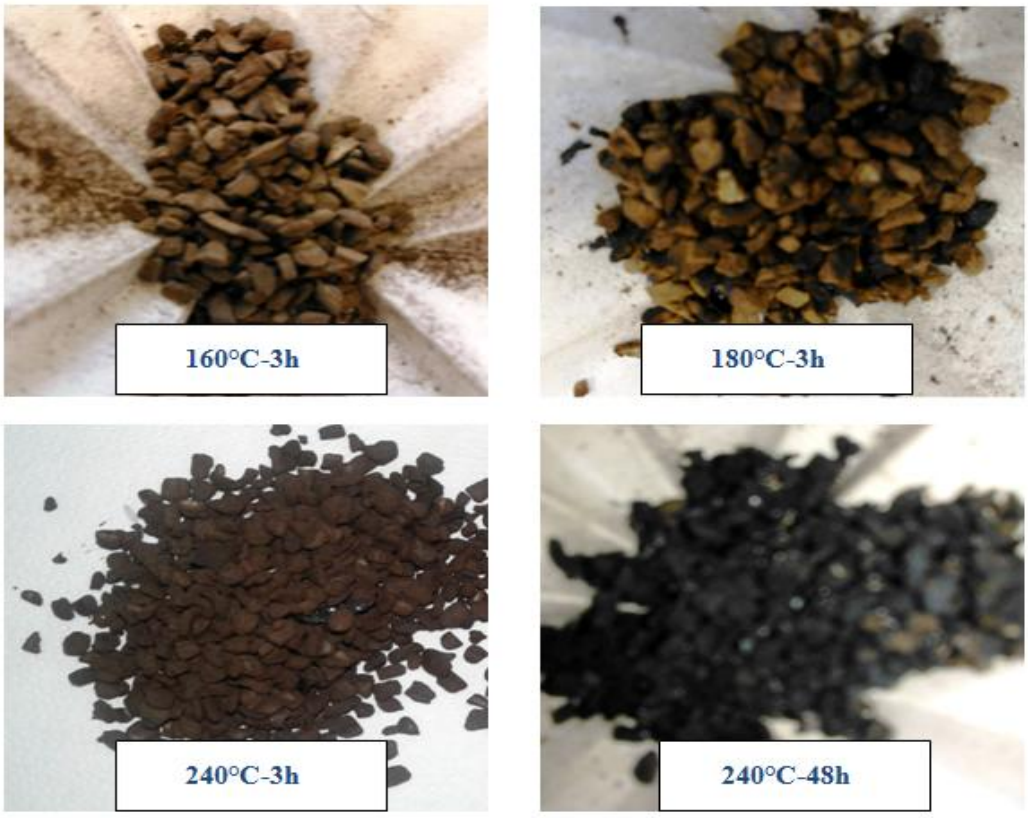

Figure 17: Hydrochar prepared at different temperature and time

Hydro char prepared at different severities are shown in the Figure 17; the hydrochar colour is modified from light brown to dark black as the severity of reaction increase.

II.2.3.1 HTC yield analysis

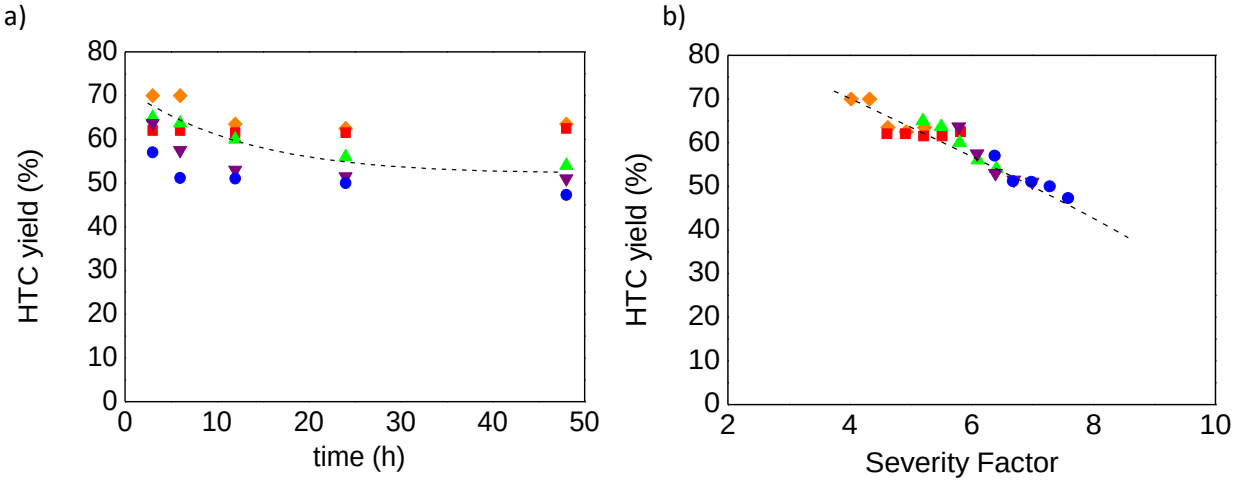

Figure 18: Hydrochar yield as function time (a) and severity factor (b)

The HTC yield is represented as function of time and severity factor as seen in figure 18. Temperature and time have a significant effect on HTC yield, the mass yield percentage decreases from 65% (200°C,3h) to 51 % (220°C, 48h). To have an accurate idea about their combined impact, it could be notice in the figure 18.a that the discontinuous lines are dropped from 70% to 47 % as the severity factor increase from 4.2 to 7.5.

According to the literature lignocelluosic precursors are sensitive to hot liquid water treatment at low reaction severity due to the presence of hemicellulose and xylose-based polysaccharides (Falco et al), in contrast precursors with prevailing lignin content are less sensitive at high severity, Joan G. Lynam (lyman 2014) found that mass yield decreases to 57% in case of Loblolly pine (lignin content (30%) and to 27% for switch grass (low lignin content 5.6 %) at severity factor of 5.4.

II.2.3.2 Elemental composition analysis

Figure 19 shows clearly that the increase of carbon content accompanied with a decrease in the molar fraction of Hydrogen and Oxygen as the severity of reaction ranging from 4 to 7.5, but the Nitrogen and sulphur contents are almost stable at the same severity factor range. In fact, loss in oxygen and hydrogen content in hydrochars from (6% and 40%) to (5 and 25%) is principally due to the hydrolysis of cellulose and hemicellulose during HT which followed by an significant exceed in carbon content to over than 70% (Parshetti et al.

2013). As seen in figure 19.b, The van krevelen diagram was obtained from the data of elemental composition; the diagram relates the (H/C) to (O/C) atomic ratio, The H/C and O/C atomic ratios of feedstock are given as a reference (drawn in black hexagon symbol in the Figure 19.b), and are equal to 1.49 and 0.65, respectively. The HT process is mainly governed by dehydration (release of H_2O) and decarboxylation (release of CO_2) reactions, they remarkably effect the elemental composition of OS-derived hydrochars (Wiedner et al. 2013). At severity around 4, the composition of the hydrocharis (H/C = 1.48; O/C =0.60) which is very close to that of olive stones. At the highest severity 7.6, the atomic ratios were decreased to (H/C = 0.87; O/C = 0.27) and these values are similar to lignite coals molar ratio (H/C = 0.9; O/C = 0.2) (Benavente et al. 2015). Obviously the H/C atomic ratio is more sensible to HT therefore it could be concluding that the main reaction seems to carry out is the dehydration of olive stone, these results are in accordance with those obtained by (Funke and Ziegler 2010; Basso 2016)

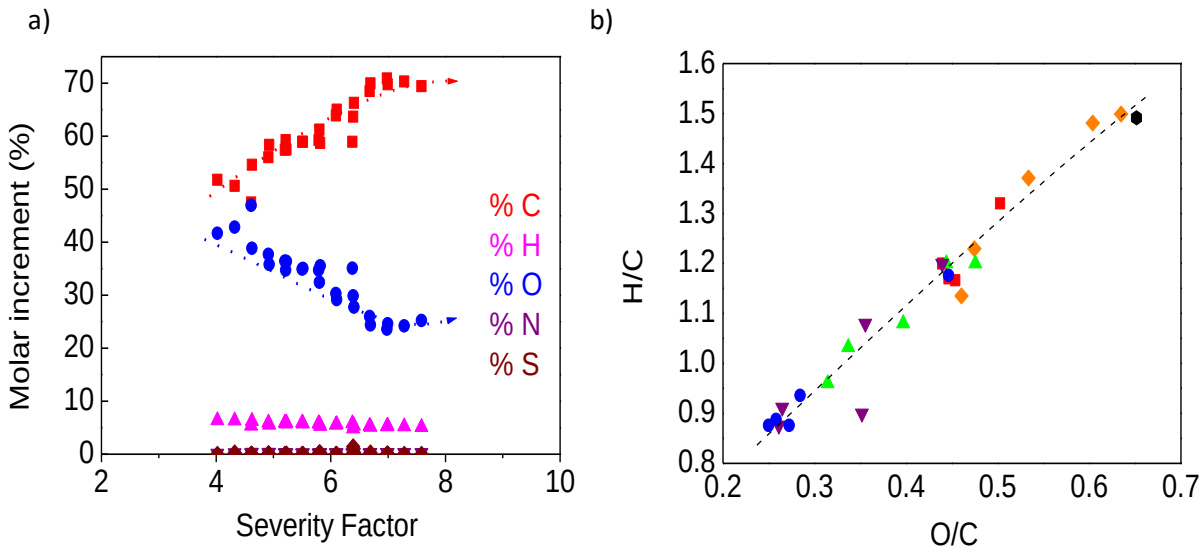

Figure 19: Elemental analysis (a) and Kerevelen diagram (b)

II.2.3.3 Thermo-gravimetric analysis

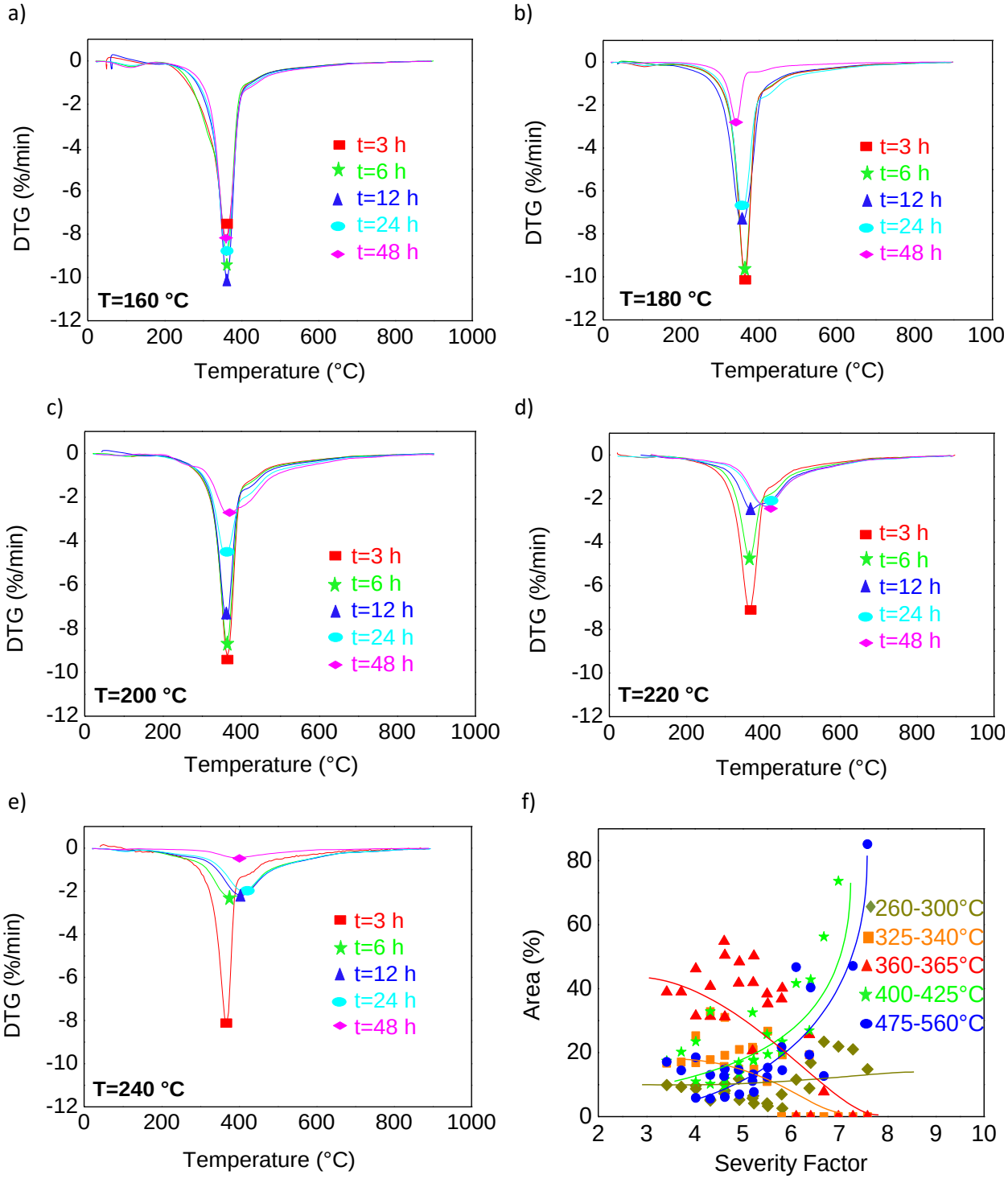

Figure 20: DTG curves of hydrochars prepared at temperatures varied from 180 to 240°C and at reactions times ranging from 6 to 48h (a) to (e); (f) fraction of peak areas as a function of severity factor

It has been shown in the previous studies of HTC treatment of lignocellulosic biomass that is very tough to insert a perspicuous explanation of the progress of the reactions and its impact on the complex structure of such precursor; therefore to get close insight into the mechanisms occurred during hydrothermal process, all the resultant hydrochar prepared at various temperature and time were submitted to thermo-gravimetric analysis. The thermal behaviour of olive stones during HT is extremely depending on the treatment conditions (temperature and time). As shown in figure 20 all thermo gravimetric curves of hydrochar were characterised by the absence of hemicelluloses peak (peak appeared at 210°C in figure 16 (a) or at 270°C in figure 16 (c)), that because hemicelluloses was already hydrolysed during HT even when it occurs at low reaction severity R= 4.02 (T=160°C, t=3h). (Peterson et al. 2008) found that hemicellulose could be readily dissolved in water at temperatures above 180°C; in addition the auto-generated pressure of the current system improves the hemicellulose dissolution and hydrolysis. (Mok and Antal Jr 1993) found that it is possible to release an average of 95% of hemicellulose as monomeric sugars at. 200-230°C within a few minutes only.(Reza 2011) reported that most of hemicellulose is extracted, and likely hydrolysed to monosaccharides at 200°C in 5 min.

The modification in DTG curves started to be strongly remarkable at temperature 180°C, as seen in figure20.b the peak appearing at 380°C disappeared progressively when the HT time ranging from 3 to 48h. The peak appeared at high HTC residence time is shifted to the right as the hydrothermal temperature increase from 180 to 240 °C and it is attributed to lignin compound, which is the most stable of the three considered biopolymers and according to some authors is an inert compound and not affected by HTC process (Reza 2011). But, it is possibly to alter the three-dimensional structure of lignin by increasing the severity of reaction. (Jin 2014) reported that biomass processing can be governed by water density, which reflects water changes at the molecular level such as solvation effect, hydrogen bonding, polarity, dielectric strength, molecular diffusivity and viscosity. (Kanetake et al. 2007) indicates that the decomposition of lignin was improved by increasing water density.

During HT treatment of lignocellulosic biomass, several parallels, simultaneous and sequential reactions take place and the structure of precursor is quiet complex therefore it is extremely difficult to draw any conclusion about the exact effect of such treatment on olive stones. A five temperature ranges were identified in all hydrochar curves in which maxima of weight loss appeared: T1 (260-300°C), T2 (325-340°C), T3 (360-365°C), T4 (400-425°C), and T5

(475-560°C).

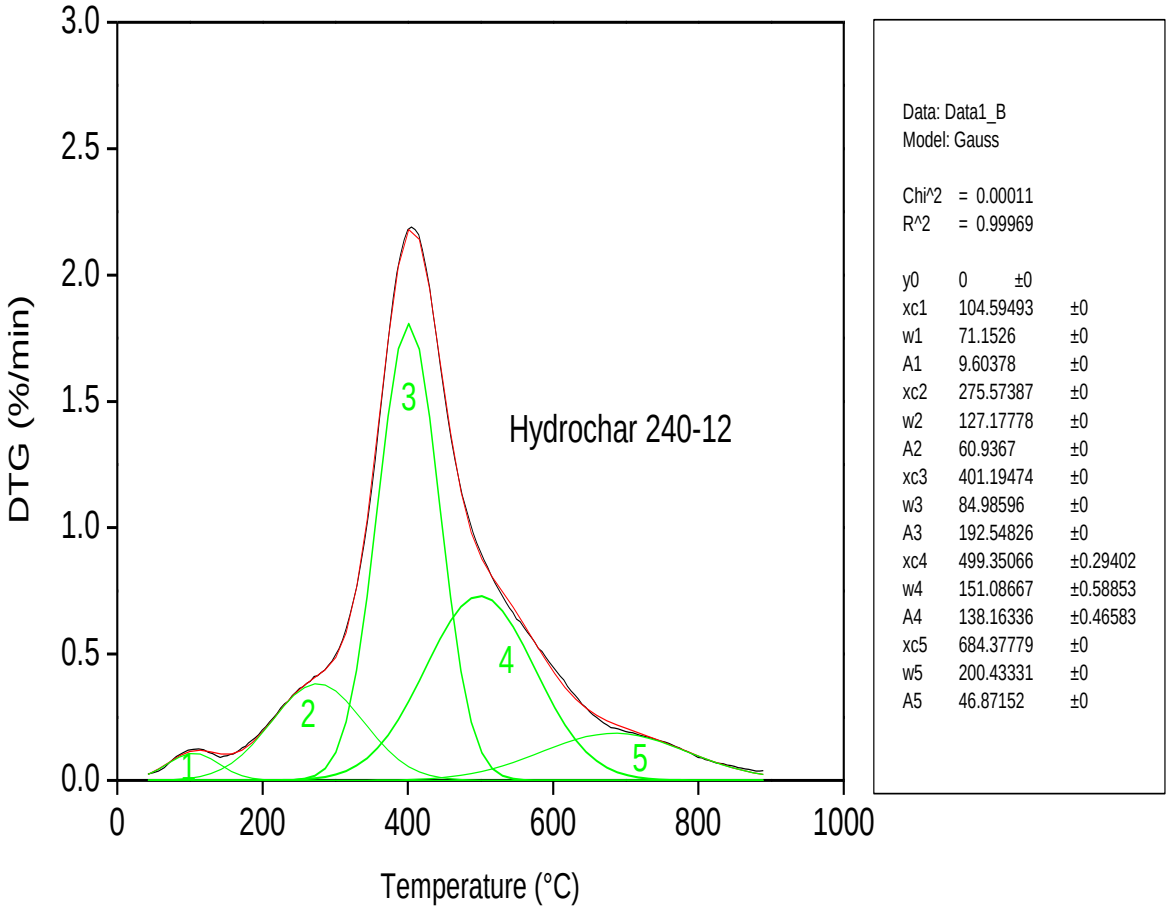

Figure 21: An example of deconvolution of DTG curve of hyrocar prepared at 240°C and 12h

Each differential TGA curve was then deconvoluted using Gaussian functions with the Origin® software (Figure 21shows an example of deconvolution DTG of hydrochar prepared at 240°C for 12 h), and each area corresponding to the aforementioned ranges of temperature was divided by the total area of the peaks. The value of each normalised area was then plotted as function of hydrothermal residence time; the results are given in figure 22. Figure 20(f) shows the ratio of peak area, of each temperature range as a function of the severity factor.

The goal of this method is to follow the effect of hydrothermal treatment conditions (temperatures and time) on the three main compounds of olive stone hemicelluloses, cellulose and lignin through the evolution of area of temperature peak.

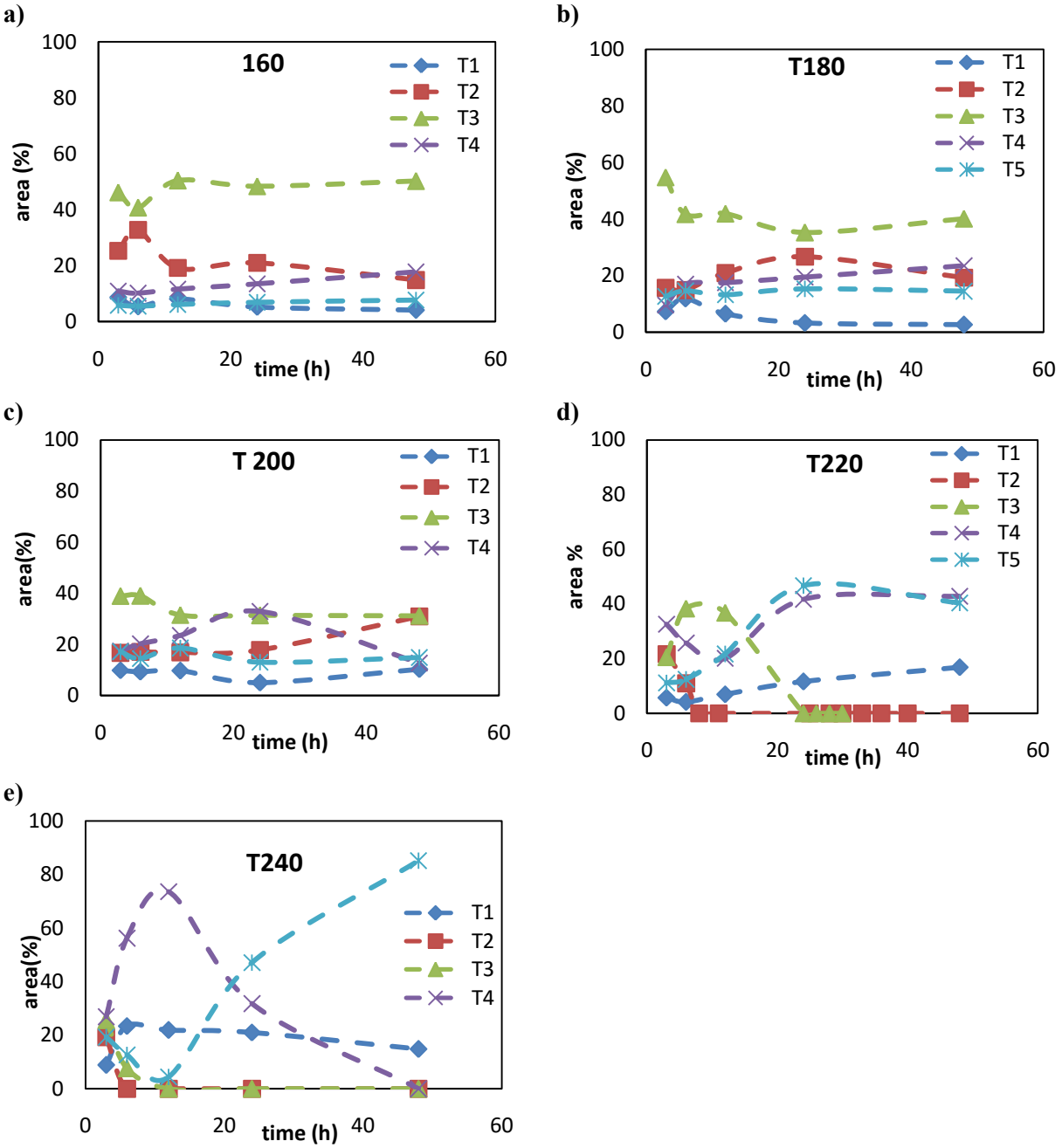

Figure 22: Area (%) of five temperature ranges as function of HTC residence time

The area corresponding to the temperature range 260-300°C (T1) exhibit the lowest value at low severity, but it continue to show up even at severity as high as 7,5. The contributions of both the second (325-340°C) and the third (360-365°C) temperature ranges almost disappeared at severity factors higher than 6, this might prove the total conversion of cellulose. This results is confirmed by previous studies carried out on rye straw, where (Titirici 2013) admit the existence of a temperature threshold in which fibrous networks of cellulose destabilized when submitted to hydrothermal treatment.(Kumagai and Hirajima

2014) reported that hydrolysis was significantly improved at temperatures close to 250°C because hot compressed water has an ion product (Kw) about three orders of magnitude higher than that of ambient liquid water; in this condition, water acts as an acid–base catalyst precursor (Kruse and Dinjus 2007).

Thermal degradation at the two final temperature ranges (400-425°C and 475-560°C) was particularly important at severity factors higher than 6 (220°C and 24 h), and obviously attributed to the fraction of lignin that kept intact under hydrothermal treatment.

II.2.4 Characteristics of carbon materials

The next challenging step is to assess the effectiveness of hydrothermal process using olive stone as precursor to produce carbon materials; consequently all the previous hydrochar samples were carbonized at 900°C under nitrogen atmosphere and their main characteristics were examined in order to evaluate their potential applications.

II.2.4.1 Carbon yield and elemental composition

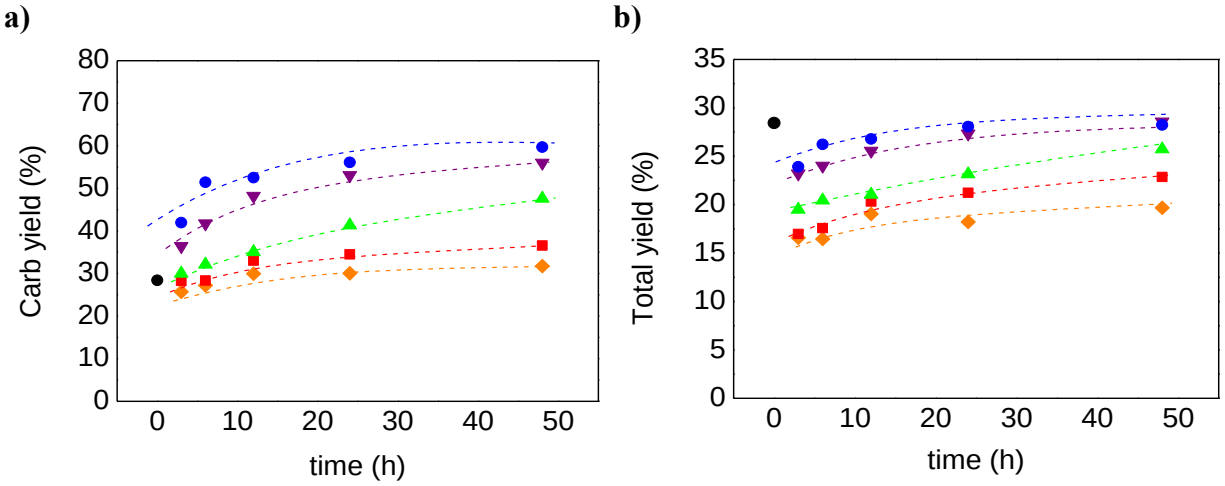

Figure 23: a) Carbonisation and b) total yield of hydrochars as a function of HT time

The carbonization yield and total yield represent the yield after both hydrothermal and carbonization steps (given by eq. II.3 and 4) are shown in figure 23. The carbonization and total yield show a different trend than of those obtained after hydrothermal step, the carbonization yield gradually increase from 25 to 60 %, moreover the total yield of carbon materials varied from 15 to 30 %, it should be pointed that the hydrochar prepared at high severity conditions result a high carbonisation and total yield this finding may be explained by the enhanced evolution of oxidising gases, particularly CO_2 and H_2O.

$$Cab\ yield\ (\%) = \frac{mass\ of\ carbonized\ hydrochar}{mass\ of\ hydrochar} \times 100 \qquad \text{(II.3)}$$

$$Tot\ yield\ (\%) = \frac{mass\ of\ hyrochar \bullet mass\ carbonized\ hydrochar}{100} \qquad \text{(II.4)}$$

These gases can efficiently oxidise and gasify carbon during carbonisation, thereby reducing the carbon yield. In addition, hydrochars exhibit highly aromatic and stable structure when severity factor increase. OS directly pyrolysed for the sake of comparison present a carbonisation yield of 28%.

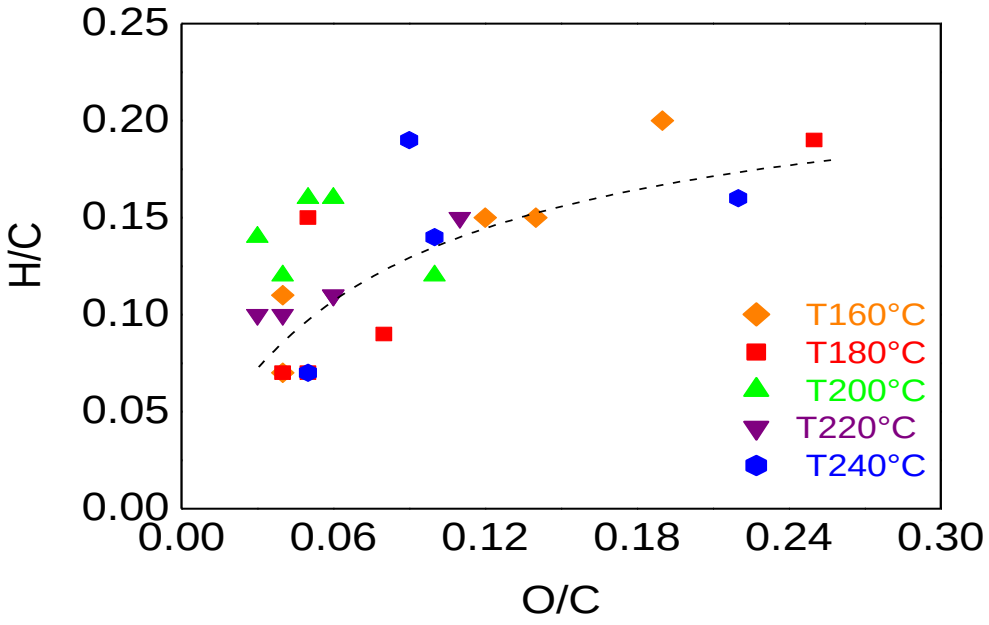

Figure 24: Van Krevelen diagram of carbonised hydrochars

The van krevelen diagram of carbonized hydrochar (figure 24) shows a different trend to than that of hydrochar, there is no more linear relationship between H/C and O/C ratio the line is shift from right down to upper left that because the carbonisation process is mainly controlled by decarboxylation reactions (Jagiello and Olivier 2013)rather than dehydrataion process as have been see in case of HT.

II.2.4.2 Porous characterization

Gas adsorption into carbon materials is the most common straightforward technique to obtain a maximum amount of information about the physical properties of surface (i.e, surface area and pore volume). There are numerous gas adsorptive used to characterize porous materials such as: carbon dioxide (CO_2), nitrogen (N_2), argon (Ar) and helium (He) (Do et al. 2010). Nitrogen is the most commonly used as probe gas that because it has the ability to cover wide range of relative pressure from 10^{-8} to 1. But unfortunately, in case of material exhibit very

narrow micropores, using N_2 is not suitable as the adsorption experiments performed at low temperature -196 °C, the diffusion of the gas will be quiet slow and subsequently an extremely long measurement time which usually leads to an erroneous results, therefore using CO_2 is extremely recommended to assess materials with pores size less than 1 nm that to avoid diffusion problems and to achieve the experiment at much more faster time than N_2, But in this studies the CO_2 adsorption into the selected hydrochar derived carbon materials persisted more than 7 days, suggesting an extremely narrow microporosity. The isotherm data were interpreted by BET and NLDFT methods and all carbonized hydrochar are analyzed by CO_2 and only six samples were chosen to analyze by both CO_2 and N_2 gas.

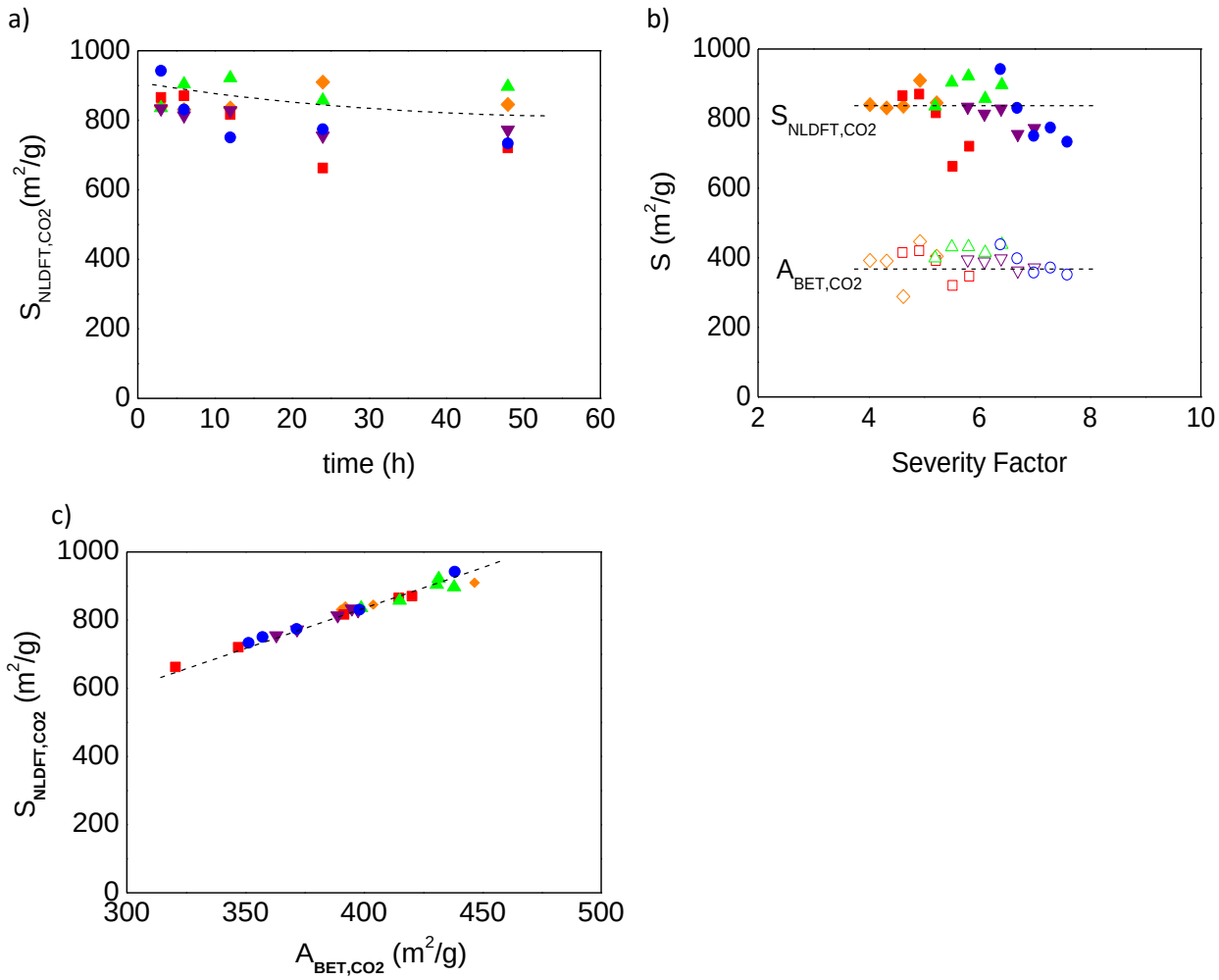

Figure 25: Surface areas of carbons materials: (a) S_{NLDFT}, CO_2 as a function of HT time ;(b) S_{NLDFT}, CO_2 and A_{BET}, CO_2 as a function of severity. (c)S_{NLDFT}, CO_2 as a function of S_{BET,CO_2}

Additional thermal treatment of hydrochar at 900°C improves its surface physical properties by releasing more volatile matter and creating more avoid thereby increasing surface are and pore volume. The NLDFT surface area ringing from 662 to 942 $m^2g^{-1}$and BET area from 320 to 446 m^2g^{-1}, these results are much more higher than those of activated carbon prepared from OS derived hydrochar at 220°C for 20 hours physically activated by air (S_{BET}= 204 m^2g^{-1}) and quiet similar to those materials activated by CO_2 (S_{BET}=438 m^2g^{-1}) (Román et al. 2013). According to figure 25b and c the S_{NLDFT} is to twice higher than $S_{BET,}$ one explanation of this finding that actually BET method considers that a monolayer of CO_2 is adsorbed on pore walls and uses the cross-sectional area of CO_2 for measuring the surface area or in case of narrow pore particularly case of this study the materials show an extremely narrow porosity, the exact surface is underestimated (divided by a factor 2) because only one CO_2 monolayer can fit between two very near pore walls (Do et al. 2010).

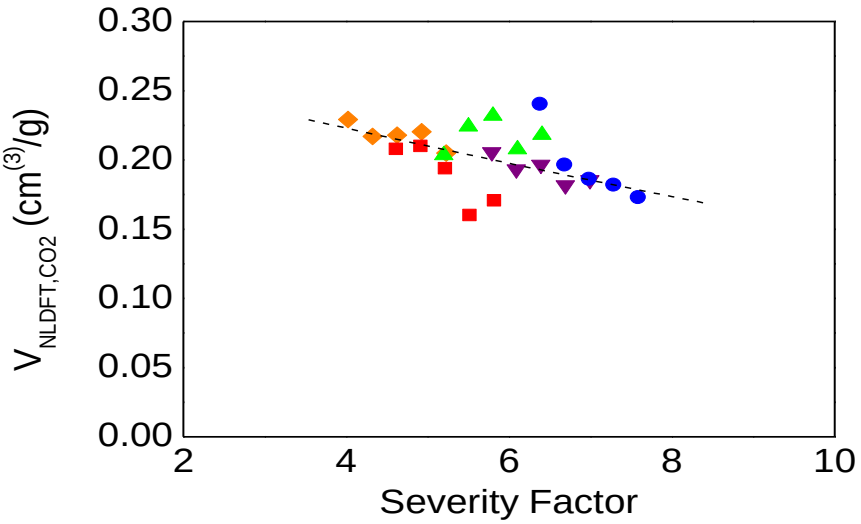

Figure 26: Pore volume $V_{NLDFT,CO2}$ as a function of severity factor

T=160°C T=180°C T=200°C T= 220°C T= 240°C

The volumes of narrow pores determined by CO_2 are decreased with increasing severity. These results could be related to the fact that at severity higher than 6 he pore start widening also at this severity condition lignin degraded progressively during HTC as have been discussed in the section above (figure 26).

In order to have a satisfying overview carbonised hydrochar six samples were chosen to analyse its textural properties by both CO_2 and N_2 gas, the pore size distribution of materials prepared at severities 4.3, 6.1 and 7.3 were measured following NLDFT model, as shown in figure 27) there PSDs obtained from CO_2 isotherm didn‘t change significantly, on other hand PSDs obtained by N2 measurement substantially vary.

HT treatment at low severity ($logR_0$ =4.3) the PSDs obtained by CO_2 adsorption shows a sharper curve than the one obtained by N_2 that because CO_2 is more efficient to enter into the extremely narrow pores as mentioned in the graphs the maximum of the PSD was centred on 0.6 nm except for the harshest conditions ($logR_0$ =7.3) the maximum is shifted to 0.7 nm and the PSD was broader (Figure 27.C). Regarding the of S_{NLDFT} as function of HT severity, it could be observe that S_{NLDFT} increasing from 800 to 1270 m^2g^{-1} as severities ranging from 4.3 to 4.9, respectively, actually the lowest surface (800 m^2g^{-1}) attribute to the highest and lowest severity, otherwise the maximum of surface area (1200 m^2g^{-1}) was reached at intermediate HT severities that because this treatment condition characterized by degradation of cellulose compound and consequently surface area of the resultant carbon were higher, for treatment severities above 6.5 lignin, whose pyrolysis fundamentally produces microporous carbons (Suhas et al. 2007), start to react and may release more gases evolved during pyrolysis, producing the broadening of the PSD and, therefore, the S_{NLDFT} decreased.

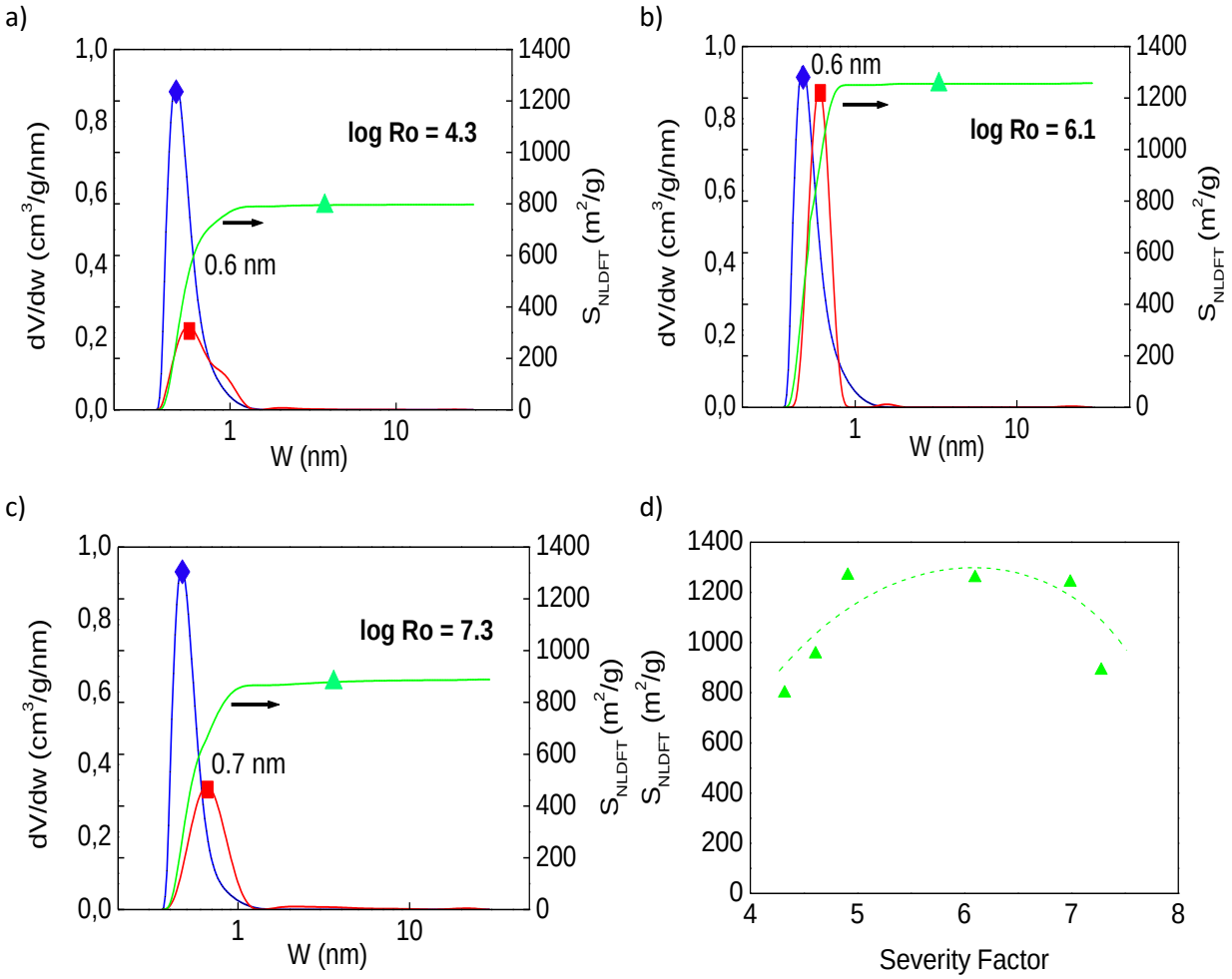

Figure 27: NLDFT pore size distributions, CO_2 (◆) and N_2 (■), and S_{NLDFT} (▲) of carbons derived from hydrochar prepared at severity of: (a) 4.3 (160°C, 6h); (b) 6.1 (200°C, 24h); and (c) 7.3 (240°C, 24h); d) S_{NLDFT} (▲) as function of severity

II.3 Effect of addition of salt on HTC

II.3.1 Experimental set-up

The experiments were realised as have been describe in the first section. The salts effect were investigated using, Potassium chloride (KCl) , Lithium chloride (LiCl), Sodium chloride (NaCl), Sodium nitrate ($NaNO_3$) and Sodium sulphate (Na_2SO_4). All salts were supplied by Sigma Aldrich®, 99% purity.

A defined amount of each salt were introduced in a beaker of 1000 ml of distilled water and stirred for a sufficient time in order to obtain a homogenous solution of 1M, only KCl salt was tested at varied concentrations 0.5 M, 1 M and 2M. Then, a 16 ml of each solution were added to 2 g of olive stones and heated at 180°C for 3, 6, 12, 24 and 48 h.

The solid product (hydrochar) is recovered by filtration, and the mass weight was measured after drying inside a vacuum oven for 8 h at 80°C.

The carbonization of hydrochar was carried out as similar in first section II.2, and the characterization of solid product was performed by the same equipments.

II.3.2 Effect of addition of salt on mass yield and elemental composition of hyrochar

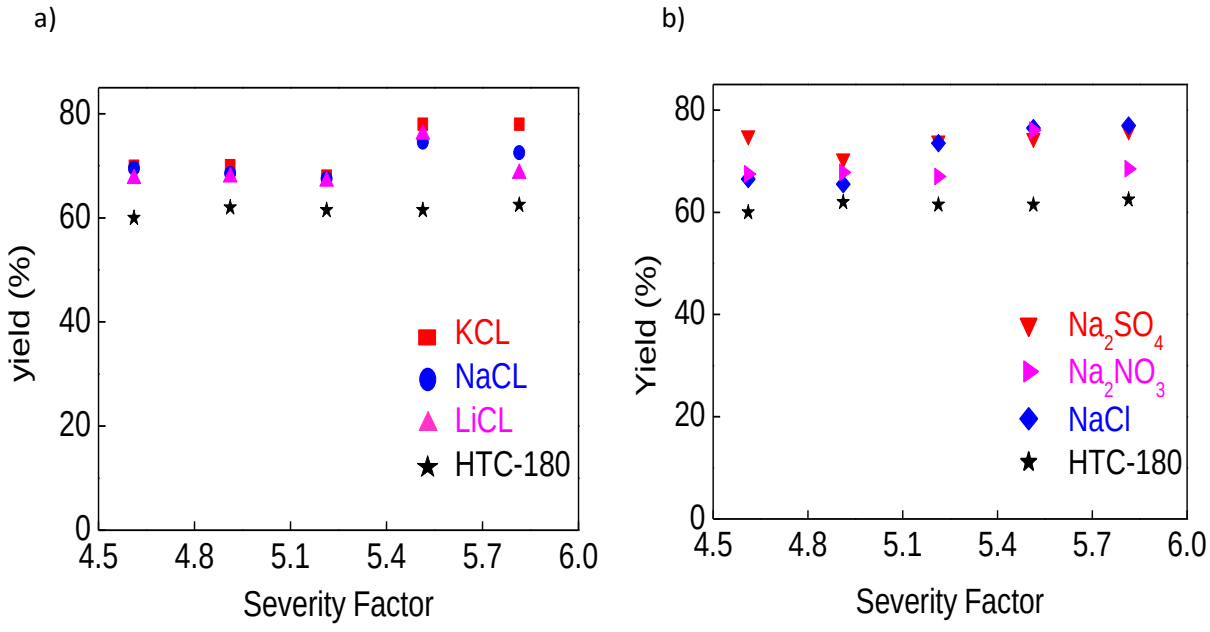

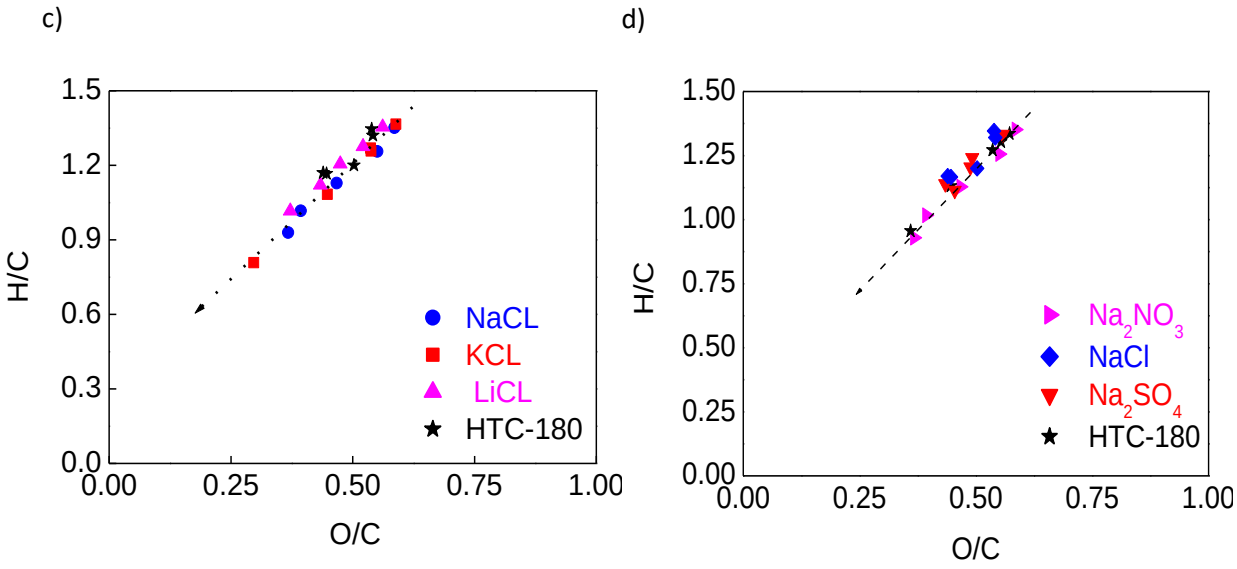

Figure 28: Hydrothermal yield and Kerevelen diagram of chlorid salt (a,c) and sodium salt (c,d)

The adittion of salts leads to unusal trend in the mass yield of hydrochar as seen in figure 28. a and b both sodium salt (Na_2SO_4, $NaNO_3$ and NaCl) and chlorine salts (LiCl, KCl and NaCl) result a particularly high yield comparing to hydrochar without salt addition (HTC-180°C). the mass yield varied from 69 % to 72 % in case of LiCl and from 66 to 77 % in case of $NaNO_3$ salt added. Similar experiments were carried out using $CaCl_2$ at 190°C, (kambo, 2014) was found that a high salt concentration (1g/l) leads to the precipitation of salt and therefore an increase in mass yield from around 82 % to 92 %. Similarly, (Genzeb Belsie Nge 2014) found in increment by 5% of mass yield in case of KCL added salt. The remaining HTC- liquid of HTC of OS with salts added has strong acid character than liquid of HTC of pure OS at 180°C (figure 29). The lowest pH value 2.46 is attributed to OS treated with LiCl, it has been already observed that LiCl catalyze hydrothermal reaction and reduce HTC pressure (Lynam et al. 2012; Genzeb Belsie Nge 2014). In general chlorine salts show minimum pH value than sodium salts, a possible explanation for this finding is that the existence of chlorine ions enhance the degradation of crystalline structure of cellulose by disturbing the hydrogen bonding between different layers of the polymers which consequently promote ion H^+ activity and dramatically reduce pH of the final HTC medium (Kambo 2014). In case of non-chloride salt both yield and pH figure shown a more or less similar result of hydrothermal process at 180°C without salt.

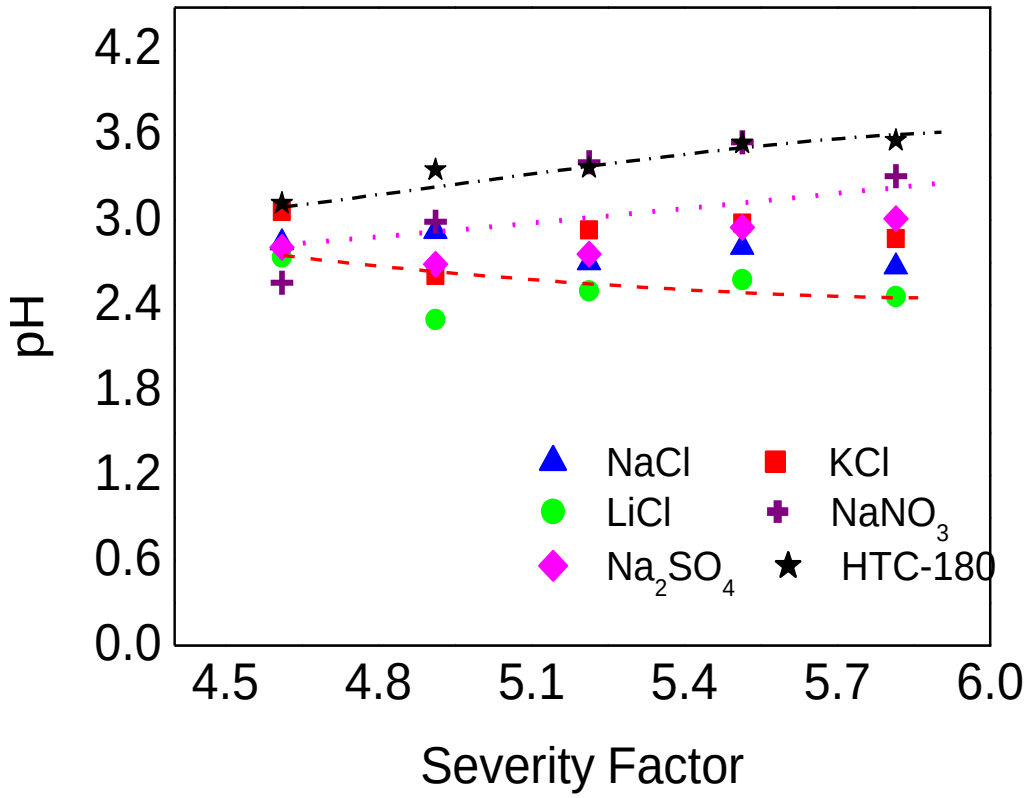

Figure 29: Effect of salt in final HTC-liquid pH

The van kervelen diagram (figure 28 (c), (d)) drawn an approach about elemental composition changes occurs on OS treated by HTC at different reaction severity. At severity factor less than 5.8 there is no noticeable difference in the elemental composition of hydrochar for both salt and pure samples, for severity factor above than 5.8, OS treated with chlorine salts exhibit a remarkable increase of carbon ratio, the elemental ratio H/C and O/C decrease from (O/C:0.45; H/C:1.08/ HTC-180°C) to (O/C :0.36; H/C :0.92) case of modified medium with NaCl. A substantial improvement of carbon yield manifest at high severity for hydrochar treated with chloride salts which have atomic ratio similar to that of lignite. The atomic ratio H/C and O/C follow a line straight in a downward direction according to van kerevelen diagram the conversion of olive stone was predominantly governed by dehydratation reaction processes (loss of water molecules).

II.3.3 Effect of salt concentration

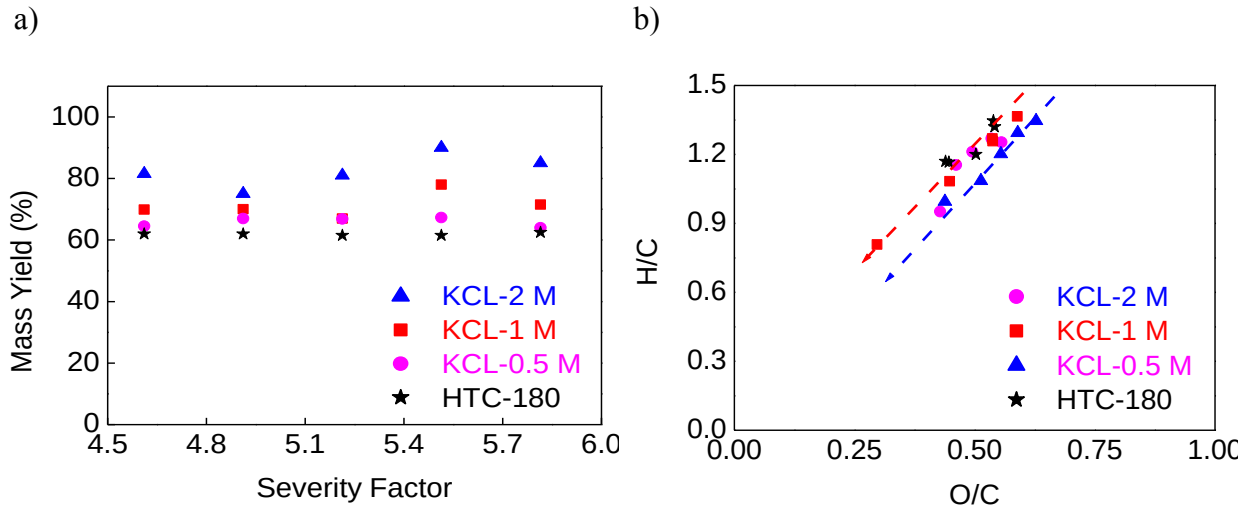

Figure 30: Effect of salt concentration

An increase of KCl concentration to 2 M displayed higher mass yield, indicating an increase of precipitation of salts in the result solid and a lower concentration of salt 0.5 M showed almost the same trend as no salt added control (figure 30), as a possible consequence of HT performed with a high concentration of salt, the part of additive didn‘t react like catalyst might penetrate inside hydrochar pore or forming a complex matrix with char, and these would have a negative effect for further use of hydrochar as fuel or activated carbon.

A slight decrease in H/C ratio of resulting hydrochar prepared in high saline solution concentration suggest more enhancement of dehydratation reaction but generally no significant effect to the chemical and structural properties of HTC-solid product was observed.

II.3.4 Thermogravimetric effect

Thermogravimetric analysis were performed on hydrochar prepared at 180°C for 3 and 48h in salts solution. Generally, the five added salts have an effect on hydrochar thermal behavior but in less extent in case of sodium salts as seen Na_2SO_4 at high HT temperature (figure 31.a) has similar thermogravemetric curve of hydrochar treated on pure water. The weight loss (TGA figure 31 b and d) at low resistance time are 27.58 %, 33 % and 36.8 % for hydrochar treated in pure water, KCl and LiCl salts solution respectively, Generally it seems that salt addition has a slight impact at low residence time as seen in figure 31.a, the curves are shifted to left (lower temperature) this suggessed that salt is remained in the final structure of hydrochar and act as catalysisof the pyrolysis of hydrochar .

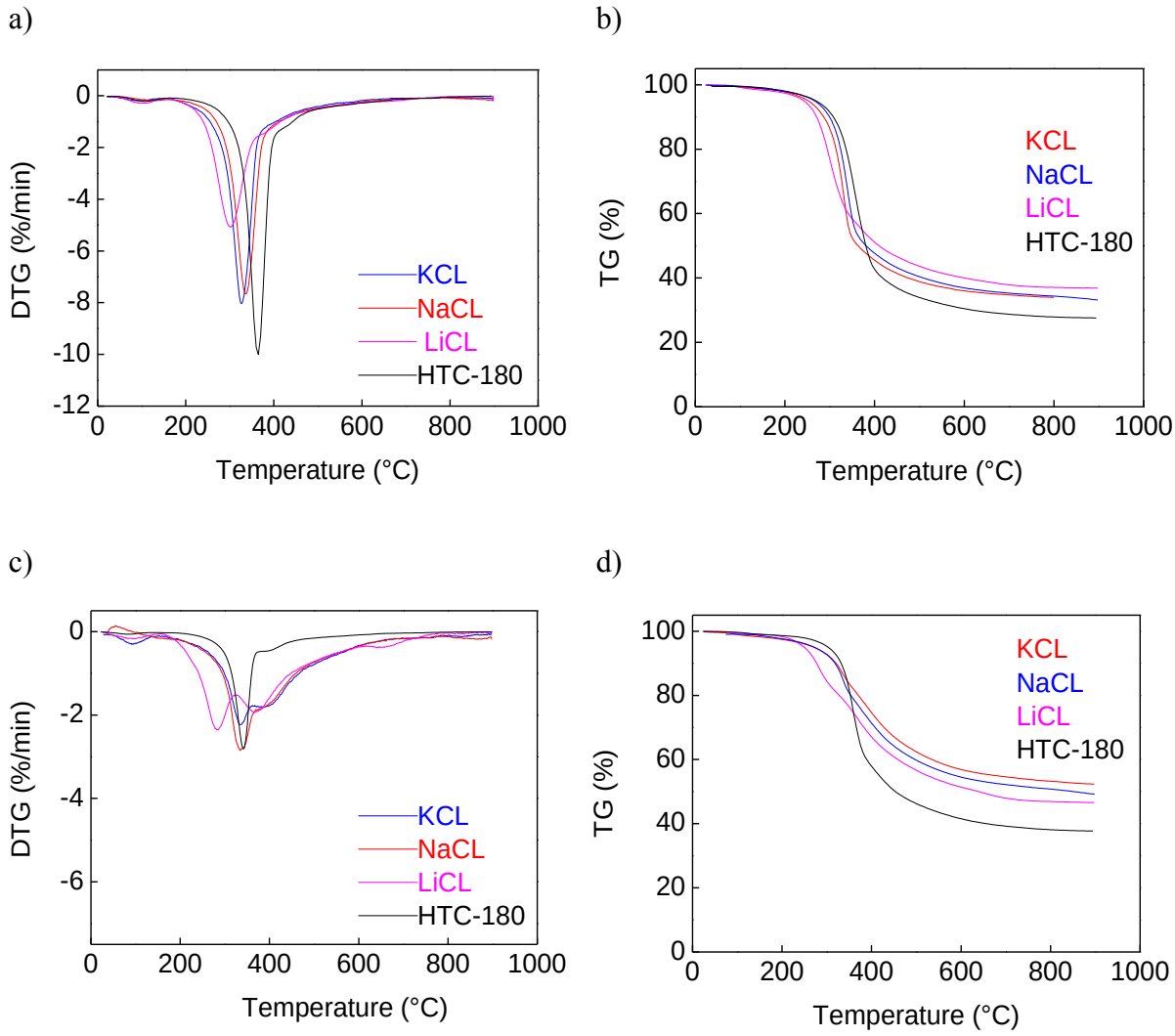

Figure 31: DTG and ATG curves of NaCl, LiCl and KCl at 180°C and 3h (a,b) and 48 h(c,d)

An otherwise the derivative TG curves (figure 31a and 31d) for experiments carried out at 48 h showed a different shape, NaCl, LiCl and KCl has the most remarkable results subsequently has the imprtant catalyst effect, specially lithium chloride which wiedly investigated on the liturature as catalyst for HT process,(Funke and Ziegler 2010; Basso 2016) found that LiCl enhance the reactions occurring and reduce reactor pressure.

The DTG curves of HTC-180°C showed a peak at 360°Cand 340°C at treatment for 3 h and 48 h respectively. This first peak is shifted to less tempreture (304°C and 288°C) and presents a low intensity in case of LiCl treatment at 3 and 48 h, this confirm that LiCl salt still remains wihin hydrochar matrix and effect the pyrolysis too by lowering pyrolysis temperature.

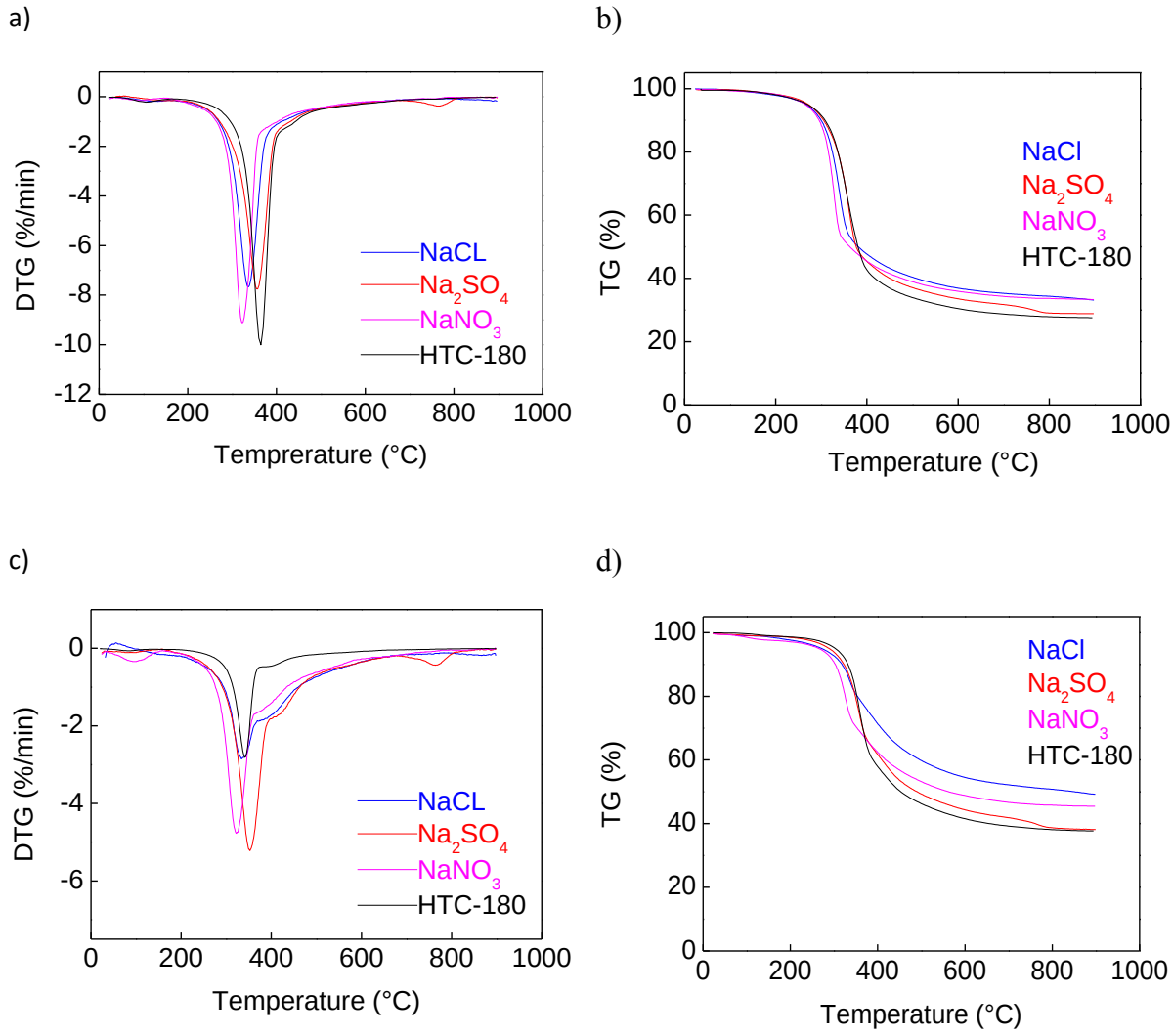

Figure 32: DTG and ATG curves of NaCl, Na2SO4 and NaNO3 at 180°C and 3h (a,b) and 48 h(c,d)

At high residence time (48 h) almost all hydrochar DTG curves showed a second large peak with a less intensity at high temperature 400°C testifying the presence of new compound.

When salt added to water its dielectric constant is reduced, this phenomenon called dielectric decrement (Gavish and Promislow 2016) and it influence the hydrogen bond network and it decrease the water molarities as the ionic concentration increases, which made the impact of HT reaction on the polymers more effective. An another hand, chlorine ions have a strong effect on hydrogen network between the macromolecule chains promoting the decomposition of polymers (Lynam et al. 2012; Kambo 2014) and this could explain the high capability of chlorine salt to catalyze HT reaction rather than sodium salt, Patwardhan et al. 2010 have reported that the influence of salt depends on its ionic nature, Lewis acidity, basicity and/ or

ability to form complexes that stabilize particular reaction intermediates and these finding might justify also the gap between the results obtain from two groups of salts,

Moreover, Lynam et al. 2011; Genzeb Belsie Nge 2014 reported that lithium chloride has been used to reduce the crystalline structure of cellulose by disrupting the strong hydrogen bonding, this explain the drastic changes on the thermo-gravimetric behavior of hydrochar.

Besides the effect of chlorine salts (especially LiCl and KCl) on cellulose, (Wang et al. 2015) reported that salts could improve also the carbonization reactions of lignin and contribute to higher char yield but to a less extent than cellulose.

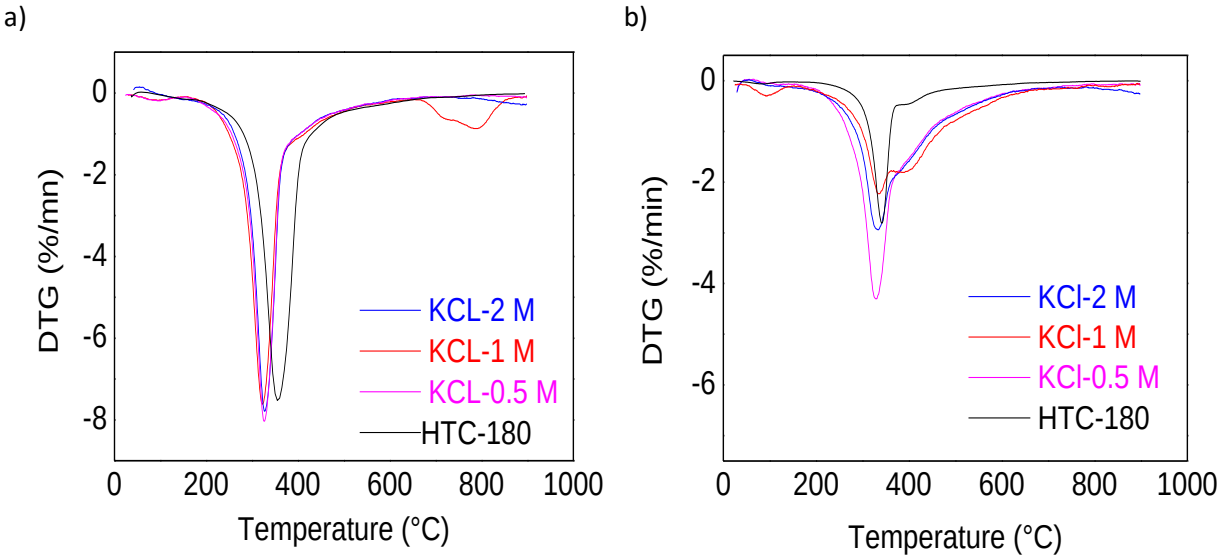

Figure 33: DTG and ATG curves of KCl 2M, 1M and 0.5M at 180°C and 3h (a) and 48 h(b)

Only slight effect have been noted when KCl concentration ranging from 1M to 2M (figure 33). A slight peak appears at temperature higher than 600°C in case of LiCl and Na_2SO_4 salt treatment, these may be attributed to the presence of small amount of sulfur on treated hydrochar (Nowicki and Ledakowicz 2014).

II.3.5 Effect of carbonisation on mass yield

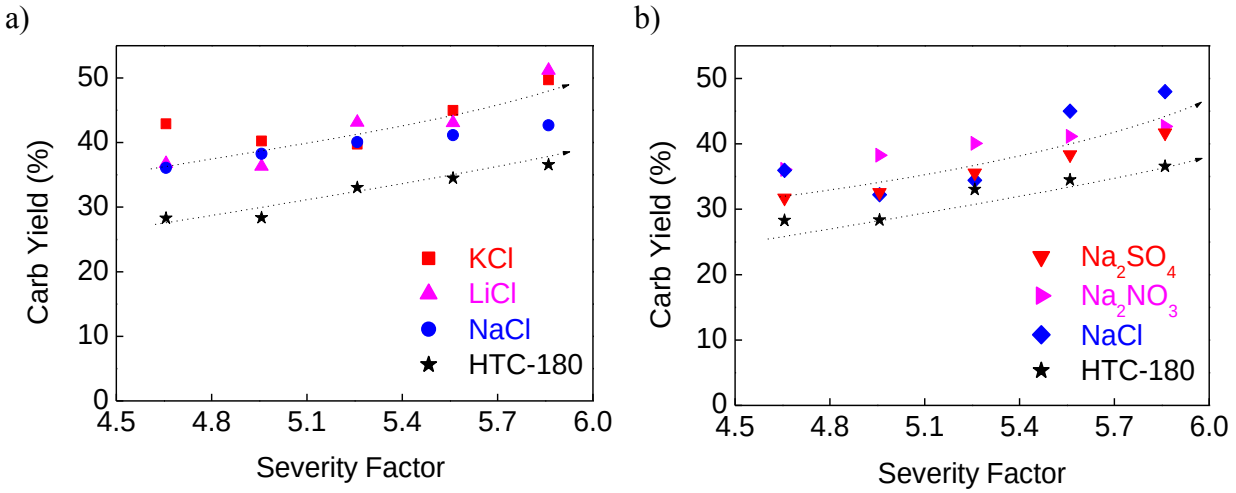

Figure 34: Carbonisation yield of Cl salts (a) and Na salts (a) as function of severity factor

The carbonisation experiments were performed in order to investigate the characteristic of carbon materials derived from hydrochar modified with salts. The mass yield is varied from 28 % and 36% for treatment without salt at severity 4.6 and 5.8, under the same treatment conditions and with addition of LiCl the carbonisation yield increased from 36 % to 50% . The addition of sodium salts (Figure 34 b) leads to an increase of carbonisation yield also but in lower rate than chlorine sals (figure 34. a), this suggest that the salts enhance the repolymerisation reaction and leads to an increase on the yield and may leads to the production of new insoluble compound, Khelfa et. al, found that alkaline salts such sodium and potassium had a significat effect espacially on lignin.

II.3.5.1 Porous texture

The textural properties of the obtained carbon materials were characterized by gas adsorption techniques. CO_2 was selected as probe gas to perform the adsorption experiments; it was not possible to use N_2 at 77 K, that because the experiment could lasted more than 10 days, it was extremely tough to carry out the experiment using nitrogen and even more complicated than the case of carbon materials derived HTC-180.

The maximum BET surface for HTC-180 was 420m^2g^{-1} and for precursor treated with $NaNO_3$ 502 m^2g^{-1} a severity factor 4.9. Previous work (Khezami) claimed that pyrolysis char surface area never exceeds 300m^2g^{-1} but it seems that HT steps promote the surface area.

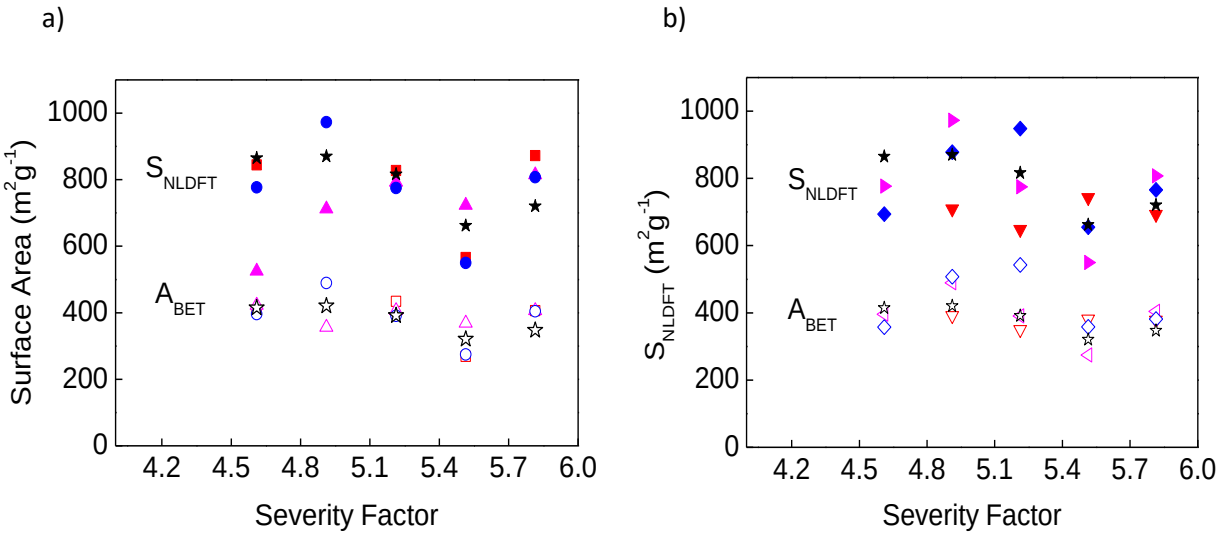

Figure 35: S_{NLDFT} and S_{BET} of Chloride salts (a) and Sodium salts (b) as function of severity factor

The carbon materials treated with both Na salts and Cl salts didn‘t exhibit a remarkable difference comparing to carbon materials derived from hydrochar prepared in pure water. Moreover these materials didn‘t show a clear trend and almost both types of salts had similar results, but it is worthy to report that the maximum surface area for almost all samples had been obtained for carbon prepared from hydrochar at severity factor between 4.9 and 5.2, the previous thermo gravimetric results showed that the fibrous network of cellulose was disrupted and strongly affected by HT at this severity condition.

All carbon materials present micro porosity of about 0.5 nm except carbon derived from hydro char treated with LiCl at low severity which has pore diameter of 1 nm. The pore size distributions were determined using NLDFT models. Actually the choice of CO_2 gas adsorption and NLDFT were discussed in the previous section.

As seen in figure 36, the salts addition seems to have an important impact on pore volume rather than surface area, carbon prepared from sodium salts shows similar PSD than HTC-180°C, and the highest pore volume is attributed to carbon materials derived from hydrochar treated with KCl (pore volume 0.3 cm^3g^{-1}), this finding were similar to previous studies in the effect of NaCl on pyrolysis of cotton stalk at 550°C, the results showed that sodium chloride has moderate impact on the BET surface area but an significant increase on the amount of micropores. Many authors (Garlapalli et al. 2016; Li et al. 2016) indicate that salts

promote the char formation under pyrolysis process and hydrochar yield in case of HT treatment as the severity of reaction increase, this catalytic effect leads to produce high amount of black carbon and enhance the secondary cracking of volatile molecules which decrease the pore volume by block the access of CO_2 gas to active sites (Khelfa 2009; Ming et al. 2013; Reza et al. 2014) this founding justify the decrease of pore volume shown in figure 36:(e) and (f).

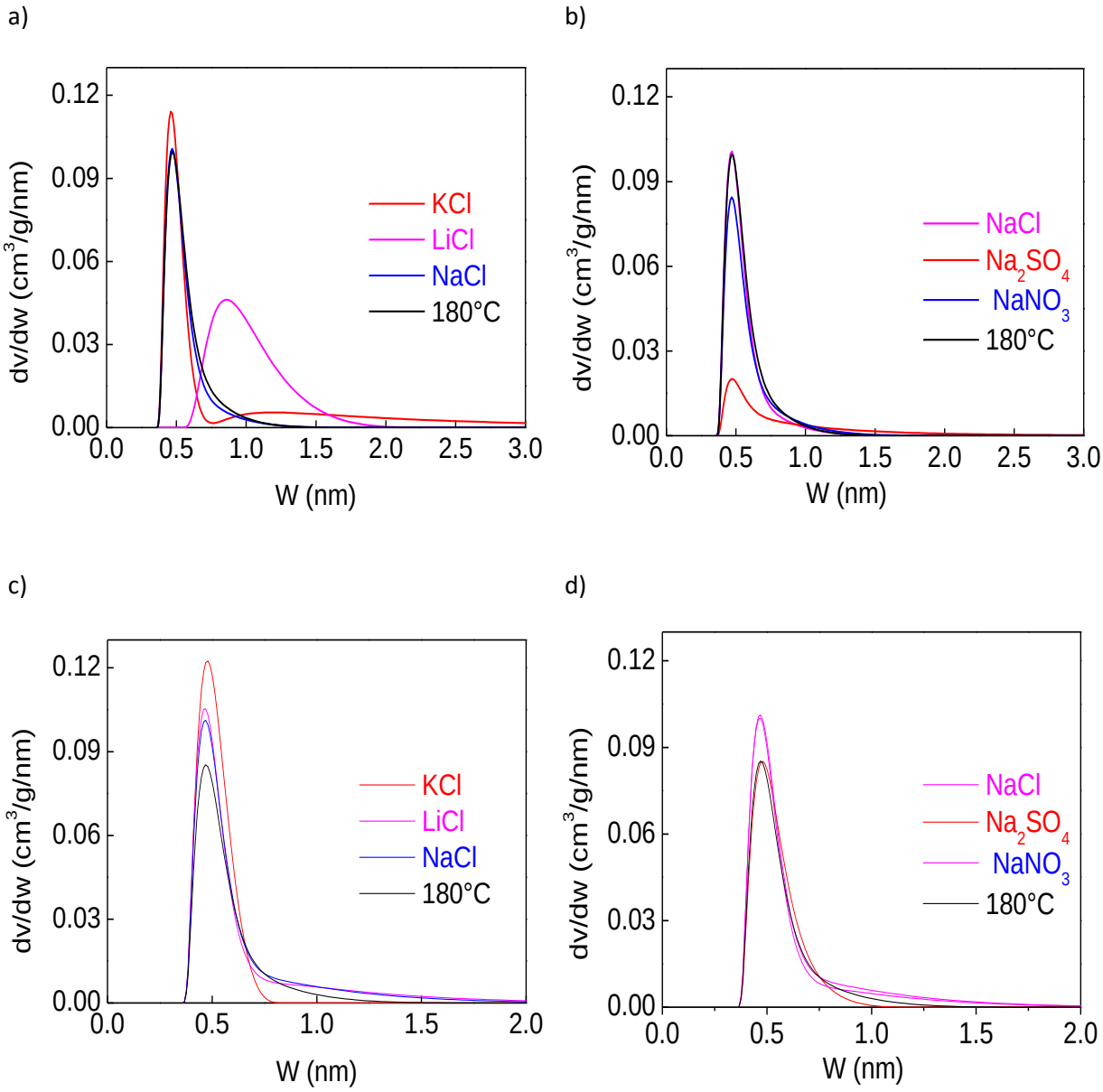

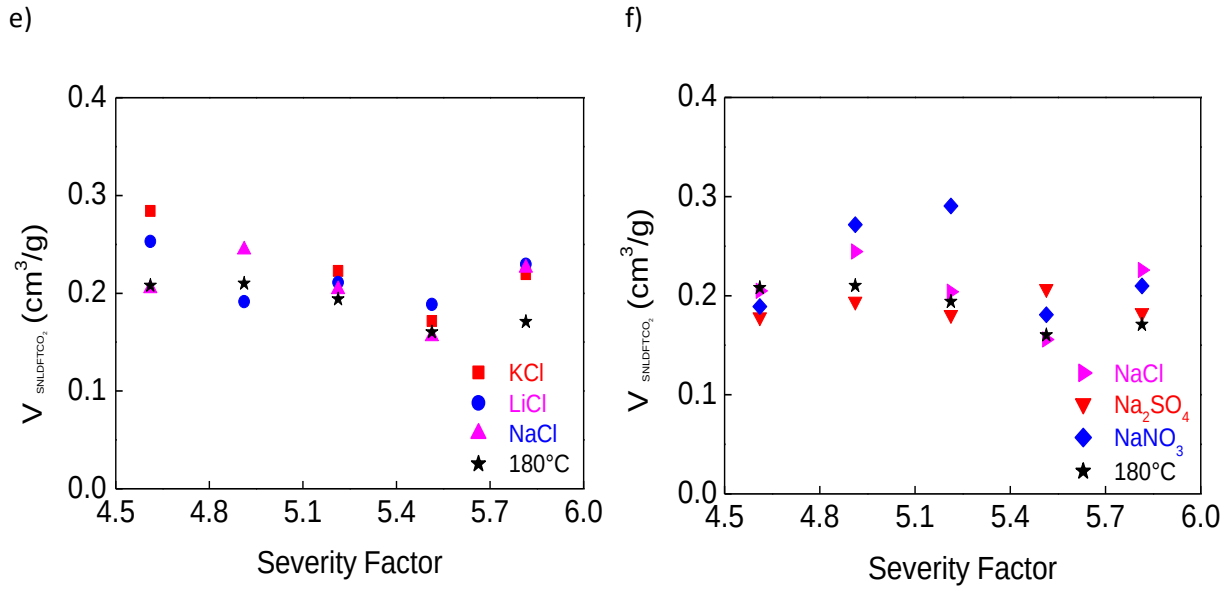

Figure 36: Chloride salts and sodium salts pore size distribution at 3h (a, b), at 48 h (c,d) and pore volume as function of severity factor (e,f)

II.4 Effects of addition of acid

II.4.1 Experimental set-up

The initial pH modification of olive stones solutions were determined using paratoluenesulfonicacid (pTSA), a defined amount of solid acid were added in order to decrease pH to 3, 2 and1. The experiment were performed similar as explained in section II.1 and II.2 and only two temperature levels (180°C and 240°C) have been selected.

II.4.2 Effects of acid on mass yield of hydrochar and carbonized samples

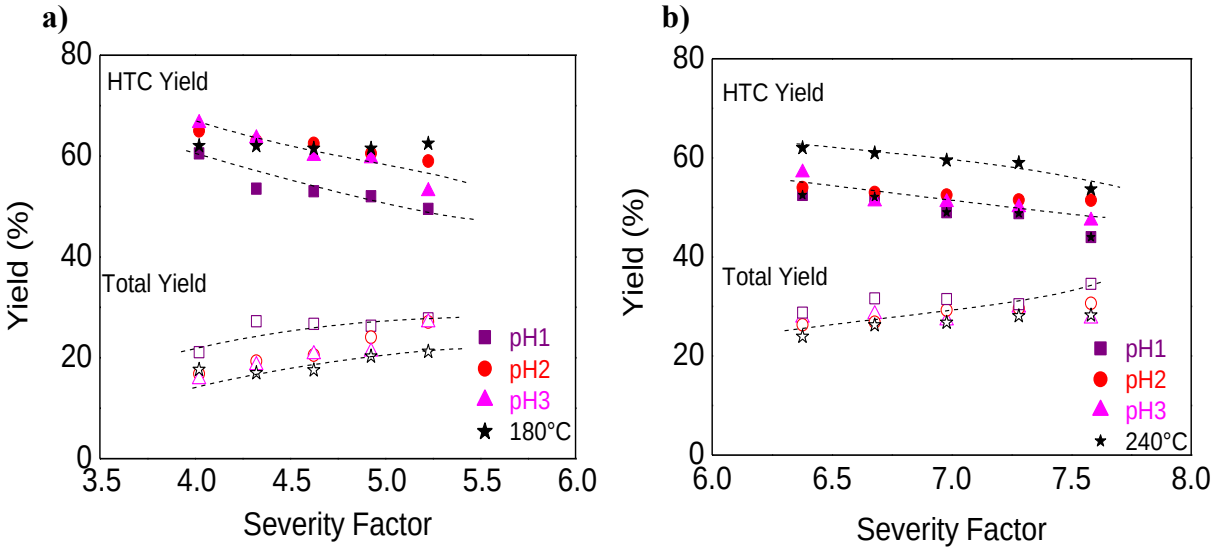

Figure 37: Hydrothermal and carbonization yield of hydrochar at 180°C (a) and 240°C (b) as function of severity factor

The role of acid has not been fully investigated in hydrothermal carbonization despite its importance in lignocellulosic biomass treatments. The paratoluenesulfonic acid (pTSA) was used to decrease the pH value of initial mixture of olive stone and water to 3, 2 and 1. The final solid product were labeled as HTC-T (T: experiments temperature) for unmodified medium and HTC-T-pH for experiment with adjusted initial pH.

The mass yield of hydrochar and carbonized hydrochar at 900°C were reported in figure 36. The major effect of acid on mass yield observed for treatment at 180°C and low pH, the recovered mass of (without acid treatment) HTC-180 and HTC-240 were reduced about 13% and 4% when pH value of initial aqueous solution decrease to 1. At high hydrothermal temperature, increasing acid amount probably has the same effect as seen figure 36.b the mass yield was stable. It seems that strong acid medium effect hydrochar yield on the same way as increasing temperature level; mass yield of HTC-180-pH1 is close to that of HTC-240. By contrast, adjacent acid level (pH 3 and 2) didn‘t show a serious impact at low temperature, on another hand acid addition shows same effect at high temperature, the inconsistency of such effect has been explained by the fact that the acid dissociation constant is reduced and therefore hydrolysis reactions are limited (Funke and Ziegler 2010; Kambo 2014).

It has been proved that is crucial to carefully select acid type and amount in HT that because it has a significant impact on reactions mechanism (Titirici et al. 2012), acetic acid were added in miscanthus HT and quiet similar result to this studies has been found the mass yield were decreased to 9% at 190°C and 6% at 225°C, respectively (Kambo 2014).

II.4.3 Effect of acid treatment on elemental analysis

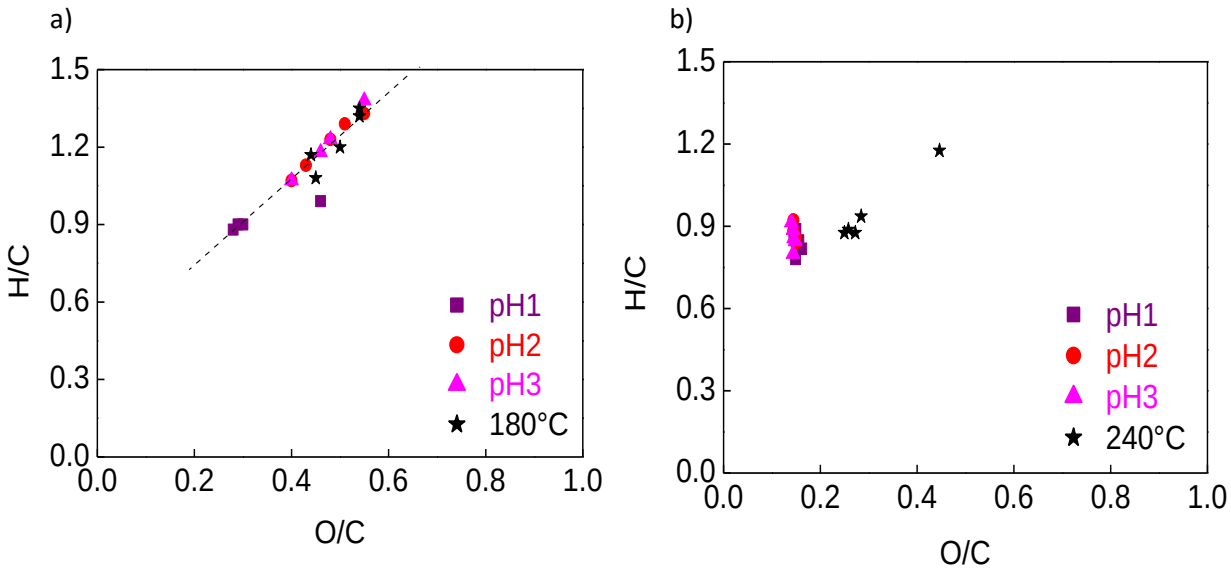

Figure 38: Van Krevelen diagram of hydrochar at 180°C (a) and 240°C (b)

In order to shed more light on the hydrochar structure and on the HT reaction mechanism, the van kerevelen diagram were plotted using elemental analysis of hydrochar prepared at 180 °C and 240°C without and with acid addition. According to the kerevelen diagram the linear trend from upper right to left down it is referred to dehydratation reactions and the trend of right down to upper left means that decarboxylation mechanism control the HT process, figure 38 follows the first interpretation, the mechanism reaction without acid and with acid addition is governed by dehydration reaction, the (H/C, O/C) atomic ratio decrease from 1.35 and 0.54 in case without acid and with pH value of 2 and 3 treatment at 180 °C and 3 h to 0.88 and 0.14 for treatment at 240°C and 3 h within a strong acid environment (pH1). A high acid level at low HT temperature supping the dehydratation reaction and this funding confirm the previous result of the effect of acid addition on hydrochar yield. Otherwise, intensify the severity conditions and initial pH could completely inflect HT mechanism as mentioned on figure 38.b, it is obvious that HT pathway is controlled by decarboxylation reaction; according to this studies, it could be confirmed that acid treatment plays a significant catalytic role on dehydratation process but at this level of temperature it is difficult to draw any conclusion about its effect on decarboxylation reaction therefore a treatment in acidic medium and higher severity (high temperature 260°C as an example or high residence time) is highly recommended. Accordingly to this all finding, a plenty of organic materials and an important amount of water have been released from OS to result solid product with rich aromatic structure subsequently a high hydrophobicity.

II.4.4 Thermo gravimetric analysis

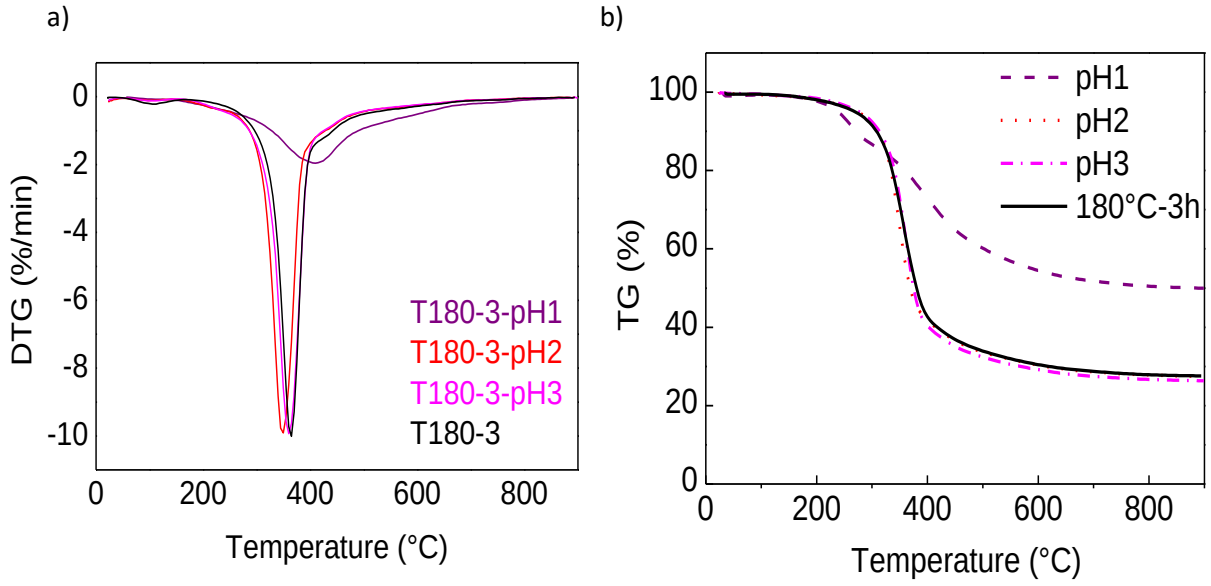

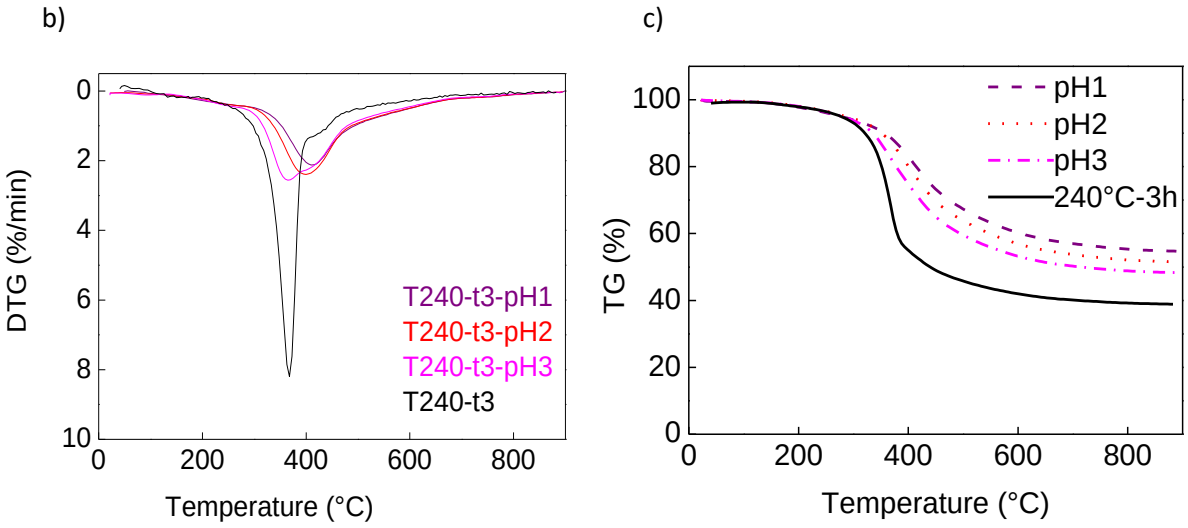

Figure 39: DTG and ATG curves of modified hydrochar at 3 h and 180°C (a and b) and 240°C (c and d)

The thermogravimetric analyses were performed for experiment at high and low severity and pH 3, 2 and 1. For treatment at (180°C, 3h) and pH 2 and 3 the DTG curves sparsely shifted to lower temperature due to the slight catalytic effect of acid, contrary to treatment at pH1 the shape of DTG curve completely modified and the mass loss were dropped to 27% and 50% for HTC-180 and HTC-180-pH1 respectively, that because an important fraction of hydrochar have been released in liquid phase. It is clearly that acid improved the overall rate of HT, the greater impact of acid were observed on cellulose peak, which is progressively reduced at low HT temperature within acidic medium (Figure 39.a) and completely altered on the rest of experiments. A remarkable thermal behavior of treatment of hydrochar prepared at strong acid medium, independently to temperature and residence time, almost all DTG curves of pH1 hydrochar shows similar shape, it seems that acid effect on hydrothermal carbonization of OS is limited at this level; otherwise the effect of acid don‘t significantly affect lignin during HT at high temperature this finding may be due the reduction of dissociation constant of acid at high temperature as have been explained previously and subsequently its effect would be restricted.

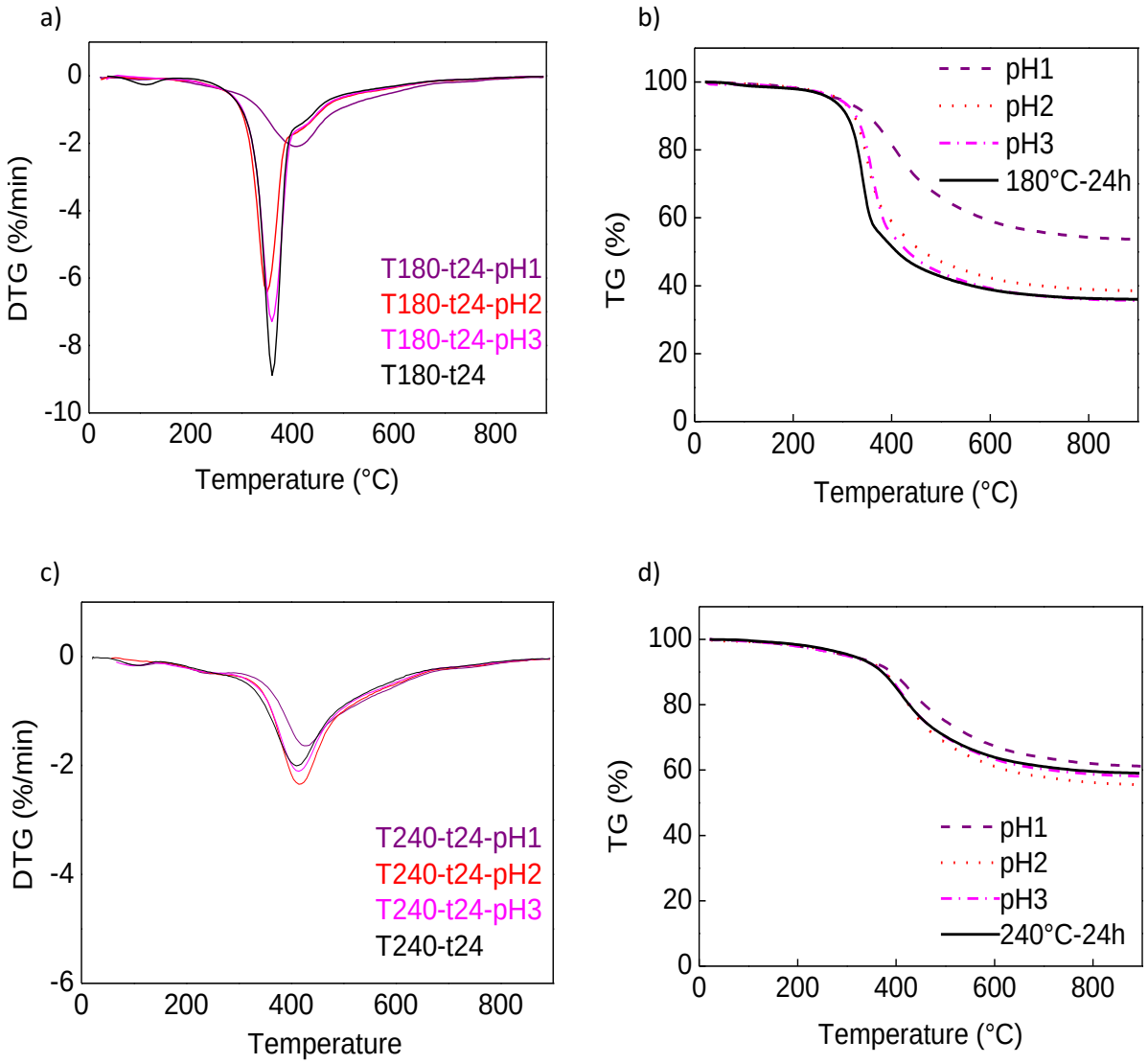

Figure 40: DTG and ATG curves of modified hydrochar at 24 h and 180°C (a,b) and 240°C (c,d)

II.4.5 Textural characterization

Previously the studies of textural characterization of carbonized hydorchar, it has been shown that is impossible to carry out the measurement of N_2 adsorption at 77K on this kind of materials and that is necessary to use CO_2 which is more accessible to very narrow microporosity and efficient to speedily reach the equilibrium. Then the isotherm data of CO_2 physisorption were collected to measure the porosity and surface area according to evaluation methods NLDFT and BET.

The specific surface area of carbonized hydrochar prepared at different severity and within acidic medium were showed in figure 41, the result of surface area of hydrochar without acid addition were presented in the same graph (full black star symbol) for the sake of comparison.

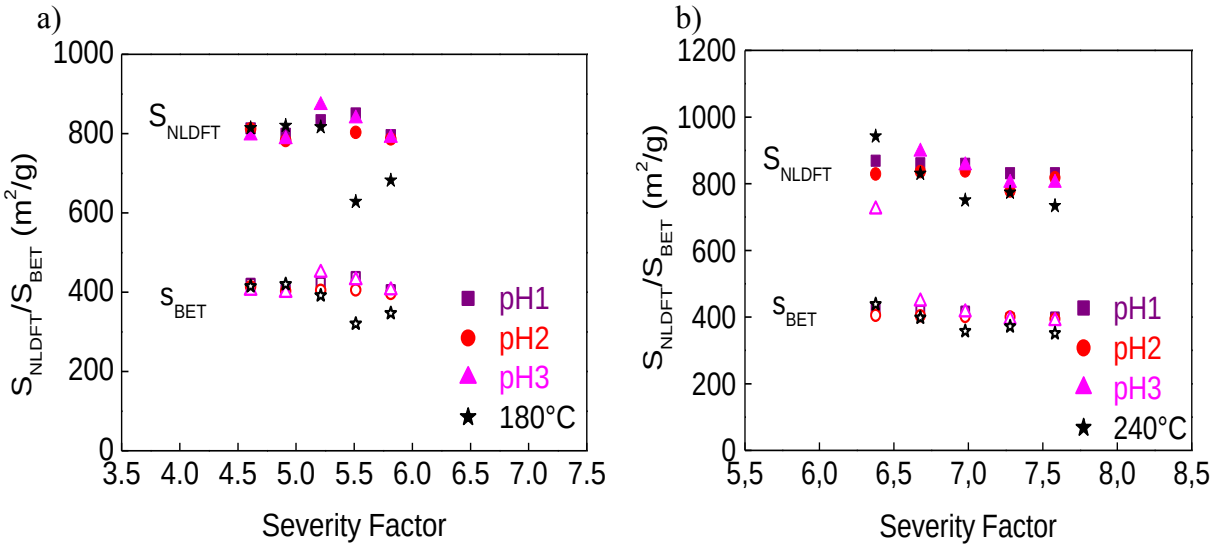

Figure 41: NLDFT and BET surface area for hydrochar prepared at 180°C (a) and (b) 240°C

Basically, reduce initial pH solution didn‘t affect pore size distribution; the maximum for both micropore size distribution is at around 0.6 nm (Figure 42c and d) and generally there is no significant effect of acid addition on surface area, increasing severity factor from 6.4 to 7.5 slightly decrease NLDFT surface area from 868 m^2 g^{-1} to 831 m^2 g^{-1} and BET from 424 m^2 g^{-1} to 398 m^2 g^{-1} (figure 41.a and b) at strong acid environment. The maximum surface area and pore volume (around 0. 24 cm^3/g) were obtained at severity factor between 5 and 6 (Figure 42.a and b).

It could be concluded that the modification of initial pH of hydrothermal reaction may catalyze process mechanism but didn‘t significantly affect textural porosity.

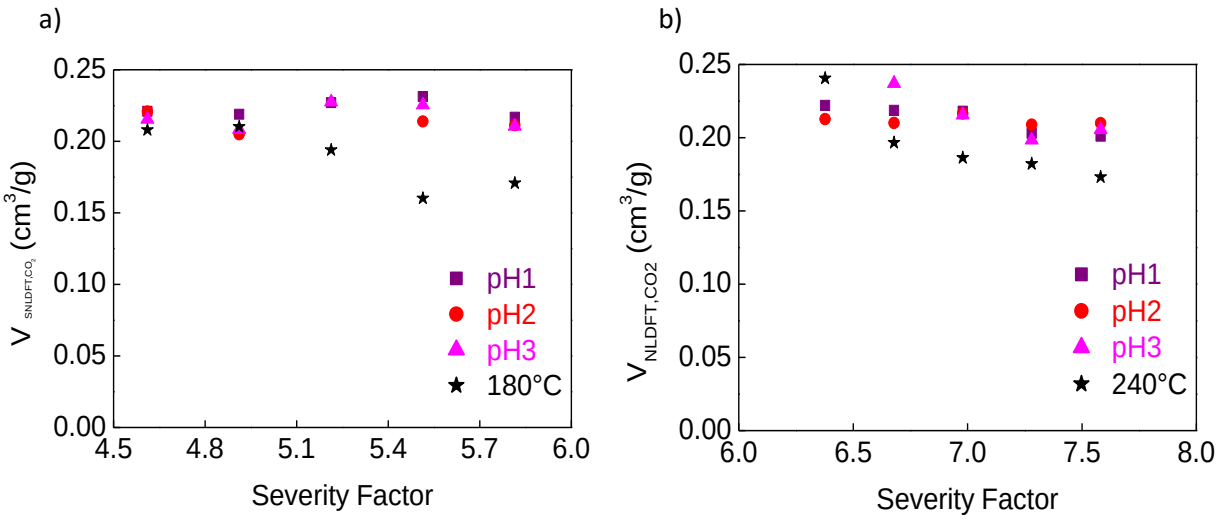

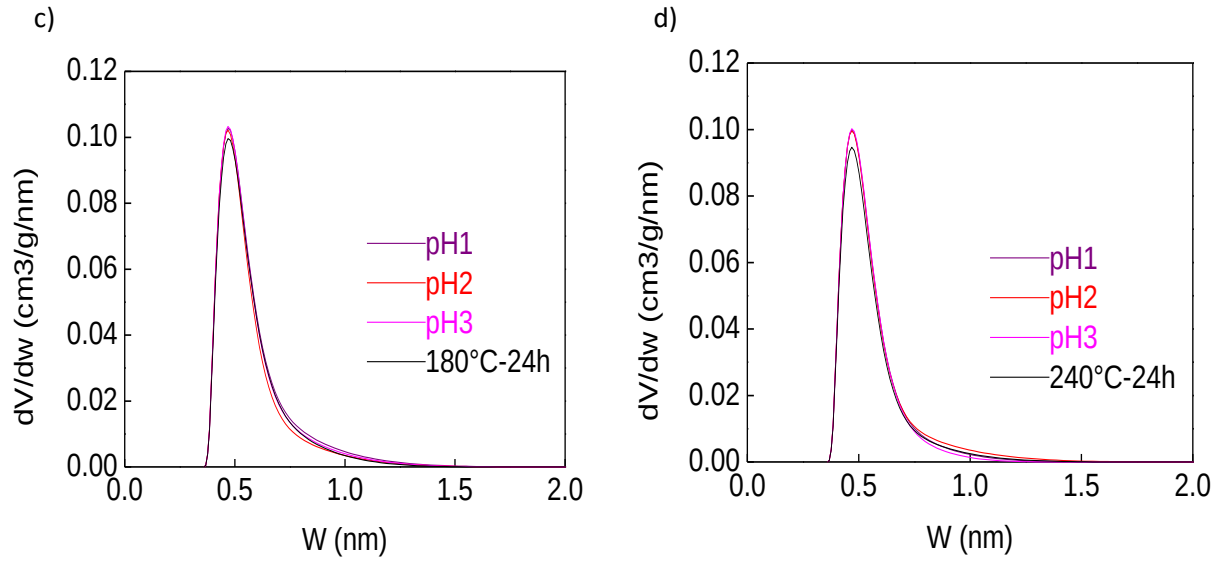

Figure 42: Pore volume as function of severity factor and pore size distribution at 180°C (a,c) and 240°C (b,d)

II.5 HTC-Liquid analysis

II.5.1 HTC liquid analysis of hydrochar without modification

The GC-MS analysis were performed for two liquid fractions obtained at severities of 4.6 (Figure 43. a**)** and 6.4 (Figure 43. b**)**, respectively. The liquid fraction recovered after HTC of OS was rich in valuable organic molecules such as FU, 5-HMF and organic acids.

a)

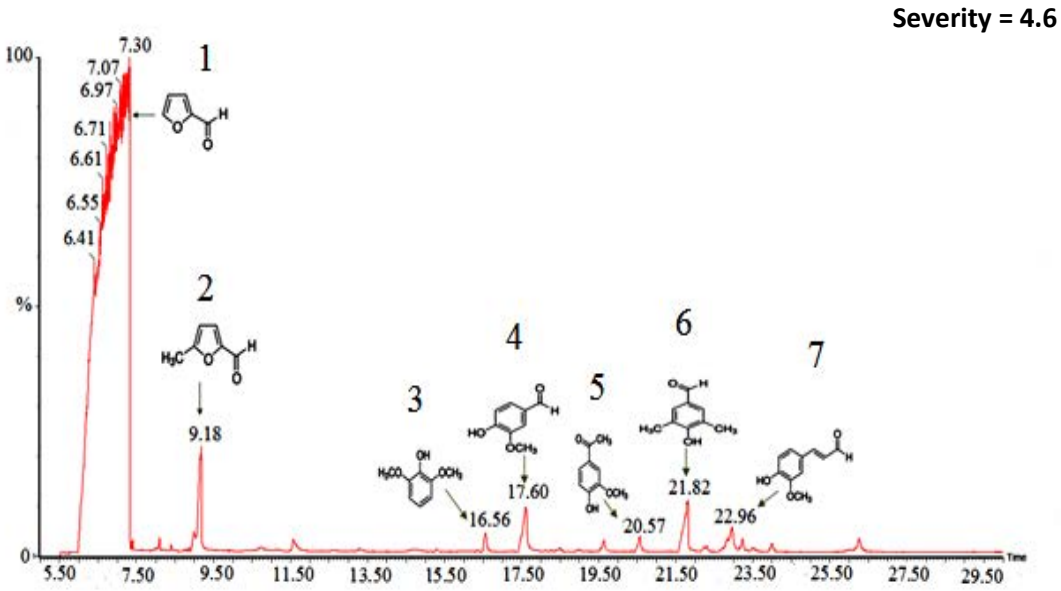

b)

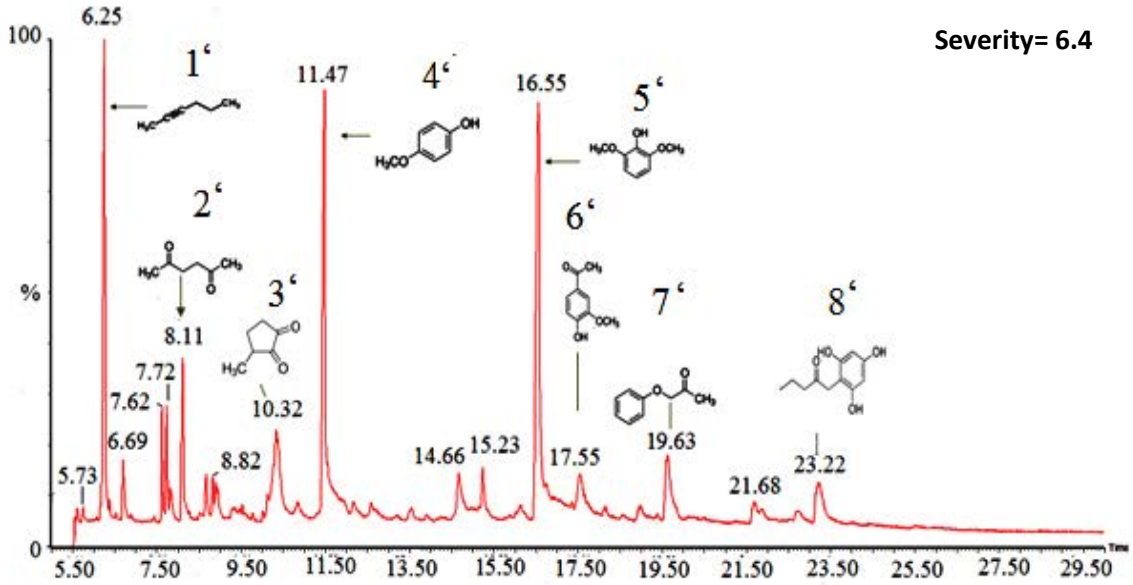

Figure 43: GC-MS analyses of liquid fractions recovered afterHTGC-MS analyses of liquid fractions recovered after HT: (a) at severity 4.6 (180°C, 3h): Furfural (1), 5-HMF (2), 2,6-dimethoxyphenol (3),vanillin (4), 1-(4-hydroxy-3-methoxyphenyl)- ethanone (5),syringaldehyde (6), and4-hydroxy-3-methoxycinamaldehyde (7); and (b)at severity 6.4 (200°C, 48h): 2-hexyne (1‘), 2,5-Hexanedione (2‘), 3-Methyl-1,2-cyclopentanedione (3‘), Mequinol (4‘), 2,6-dimethoxyphenol (5‘), vanillin (6‘), 1-(4-hydroxy-3-methoxyphenyl)-2-propanone (7‘), and 1-(2,4,6-Trihydrixypenyl)-2-pentanone (8‘)

At severity 4.6, FU (7.30 min) and HMF (9.12 min) were the major compounds. FU is the result of hemicelluloses degradation and is classified as one of the top added-value chemicals (Anthonia et al. 2015) as it can be used as selective solvent in the refining of lubricating oils, as gasoline additive, oras decolourising agent. FU production from OS was optimised in a former study, leading to a maximum of 19.9 % based on hemicellulose content of OS (Borrero-López et al. 2016). The liquid fraction also contained 5-HMF, which is mainly formed by the decomposition of cellulose. 5-HMF is also a versatile, multifunctional product that can be used as an intermediate in the synthesis of polymers (Yang et al. 2011). For instance, 5-HMF is used in the production of bioplastics, which are potential substitutes to petroleum-derived plastics commonly used in beverage bottles. Even at a severity of 4.2, aldehydes were observed, such as vanillin (17.60 min) and 4-hydroxy-3-methoxycinamaldehyde (22.96 min), coming from the decomposition of lignin. FU and 5-HMF remained present in the liquid fraction until a severity of 6.10.

Figure 43.bshows the organic molecules present in the liquid fraction at a severity of 6.40 (T=200°C, t=48h): FU and 5-HMF totally disappeared. This result confirms the former

TGA conclusions, according to which cellulose degradation submitted to HTC starts at low severity and is completed at 6.69. The GC-MS studies primarily showed organic molecules derived from lignin degradation such as vanillin (17.55 min), 1-(4-hydroxy-3-methoxyphenyl)-2-propanone (19.63 min) and 1-(2,4,6-Trihydrixypenyl)-2-pentanone (23.22 min). These compounds are of significant importance for producing a broad range of fine chemicals, particularly aromatic compounds, as well as fuel additives (Zhang et al. 2008).

II.5.2 HTC liquid analysis of hydrochar modified with acid

HTC liquid analysis offers an opportunity to understand how acid addition effect the principal ingredients of olive stones during hydrothermal carbonization, the majority of compounds are identified through library of search matches. Figure 44 a, b and c shown the analysis of recovered liquid fraction of HT experiments carried out at severity equal to 4.9 (180°C and 6 h) for pH 1, 2 and 3.

a)

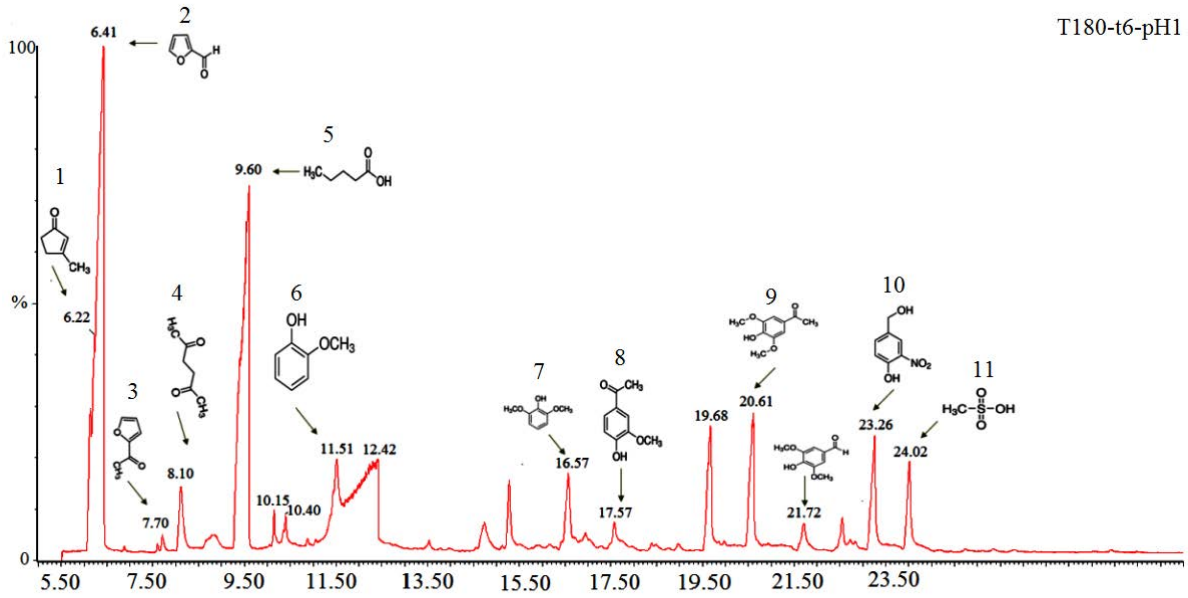

1)2-cyclopenten-1-one,3-methyl **2)** furfural **3)** ethanone,1-(2-furfral) **4)** 5,5-hexanedione **5)** pentanoic acid, 4-oxo, methyl ester **6)** guaiacol **7)** phenol,2,6 dimethoxy **8)** vanillin **9)** ethanone,1-(4-hydroxy-3-methoxyphenyl) **10)** benzaldehyde,4,hydroxyl-3,5-dimethoxy **11)** 4-hydroxy-3-nitrobenzyl alcohol **12)** methansulfanic

b)

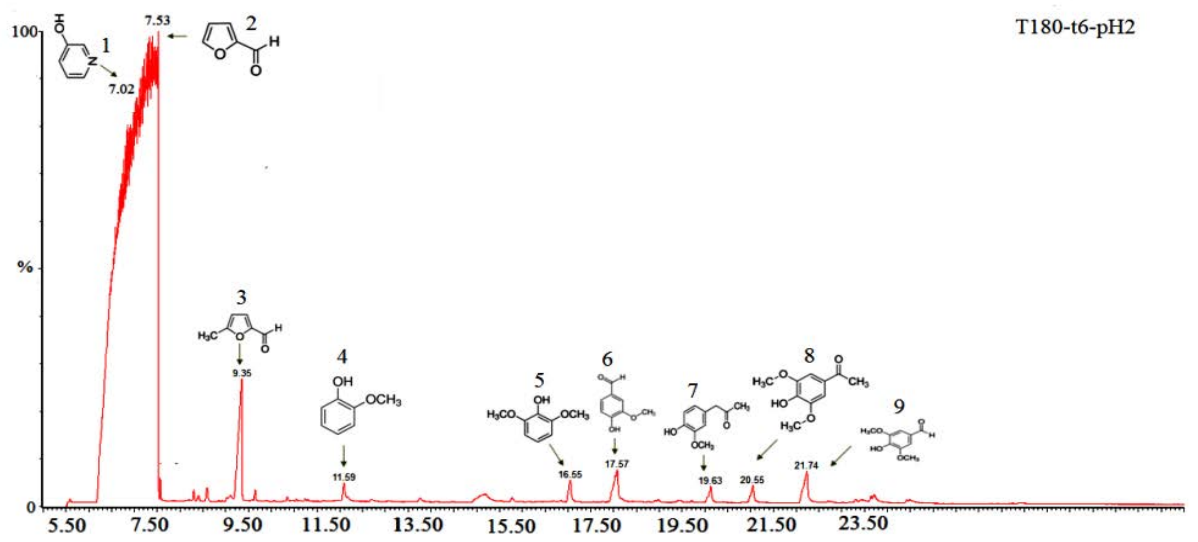

1)3-pyridinol **2)** furfural **3)** 2-furancarboxaldehyde,5-methyl) **4)** guaiacol **5)** phenol,2,6 dimethoxy **6)** vanillin **7)** 2-propane,1-(4-hydroxy-3-methoxyphenyl) **8)** ethanone,1-(4-hydroxy-3-methoxyphenyl **9)** benzaldehyde,4,hydroxyl-3,5-dimethoxy

c)

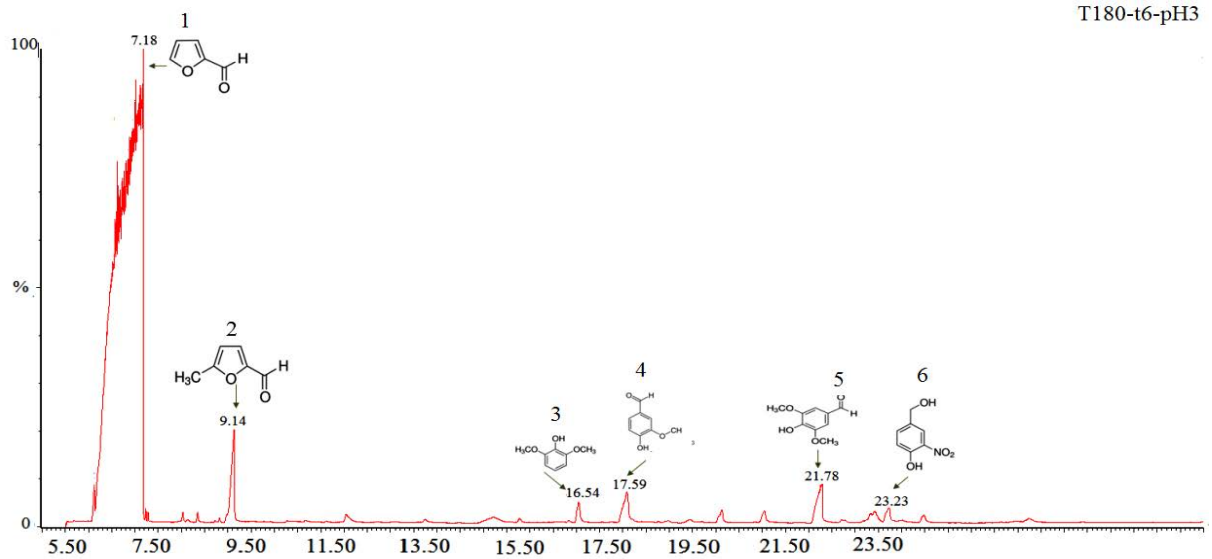

1) furfural **2)** 2-furancarboxaldehyde,5-methyl) **3)** phenol,2,6 dimethoxy **4)** vanillin **5)** benzaldehyde,4,hydroxyl-3,5-dimethoxy **6)** 4-hydroxy-3-nitrobenzyl alcohol

Figure 44: GC/MS analysis of hydrochar prepared at 180°C pH1 (a), pH2 (b) and pH3 (c)

The GC/MS results are coherent with previous thermo gravimetric and elemental analysis as shown in figure 44.b and c the characteristic peak of furfural is significantly intense for pH 2

and 3 but in less extent in case of treatment at pH 1 that because furfural in not stable under acidic conditions (Vanoye et al. 2009) and could be easily transformed to another compounds. The HTC liquid contain several organic compounds such as phenol, acid, furans, aldehyde and alcohol, Some of this compounds are recognized to be classified as one of the potential top 30 value-added chemicals (Broch et al. 2013) like furfural retained at 6.41 min, 7.53 min and 7.18 min observed in figure 44a, b and c respectively, 5-HMF shown at 9.26 min and 9.14 min in figure44.b and c and Guaiacol at 11.51 min and 11.50 min shown in figure44.a and b. The liquid analysis of experiments performed at strong acid medium is particularly rich in organic molecules released from lignin decomposition such as vanillin at (17.58 min), benzaldehyde, 4, hydroxyl-3,5-dimethoxy a (21.72 min) and guaiacol (11.51 min), on another hand it could be observe that lignin derivative compound get decreased as pH value ranging from 2 to 3, that is obviously due to the catalytic effect of acid which is remarkably improve the decomposition of OS ingredients. These results are in agreement with those obtained by (Borrero-López et al. 2016) where found that during HT of OS at severity close to 5 and pH 2, a maximum of 5-HMF were recovered while it was completely transformed at pH1 contrarily to lignin derivative such as vanillin and syringaldehyde where their concentration sharply increased.

II.5.3 HTC liquid analysis of hydrochar modified with salt

a)

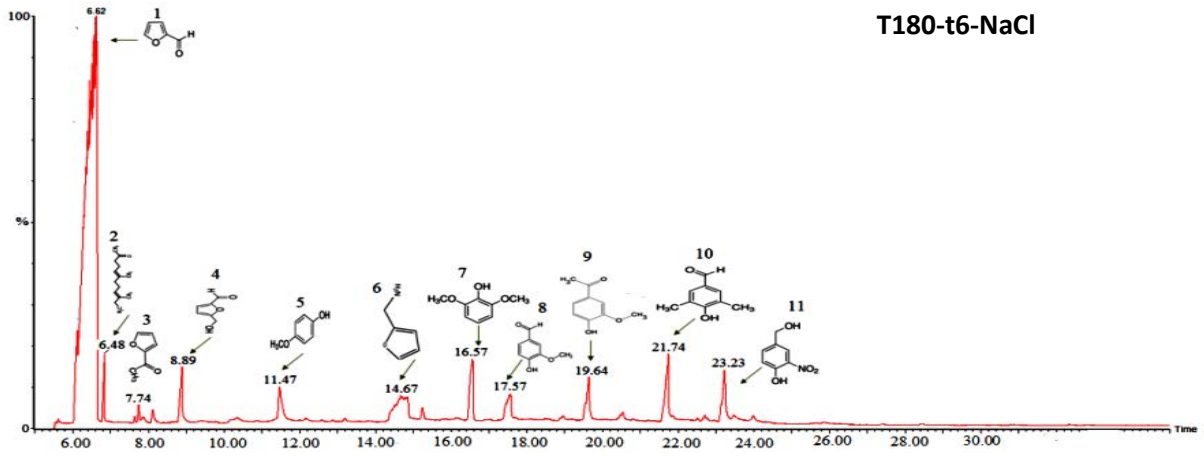

1) furfural **2)** 1,5,9-Undecatrien-1-ol, 2,6,9-trimethyl-3)Ethanone,1-(2-Furanyl)-**4)** 2-furancarboxaldehyde,5-methyl) **5)** guaiacol **6)** 2-Furanmethamine **7)** phenol,2,6 dimethoxy **8)** vanillin **9)** 2-propane,1-(4-hydroxy-3-methoxyphenyl) **10)** benzaldehyde,4,hydroxyl-3,5-dimethoxy **11)** 4-hydroxy-3-nitrobenzyl alcohol

b)

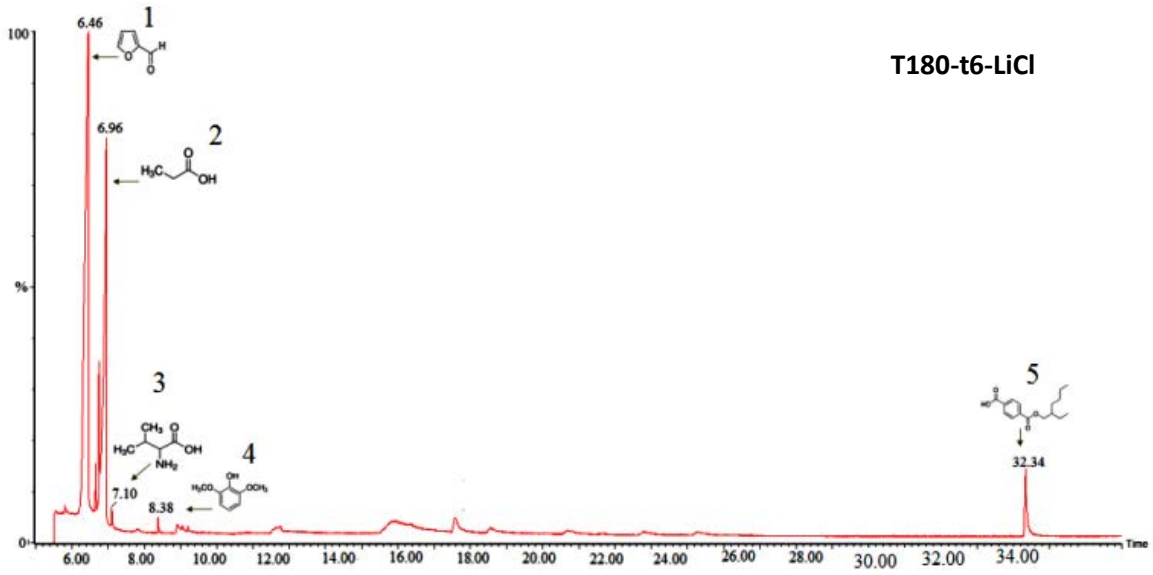

1) Furfural 2**)** propanoic acid **3)** vanillin **4)** phenol, 2,6 dimethoxy**5)** benzenedicarboxylic acid, mono (2-ethylhexyl)

c)

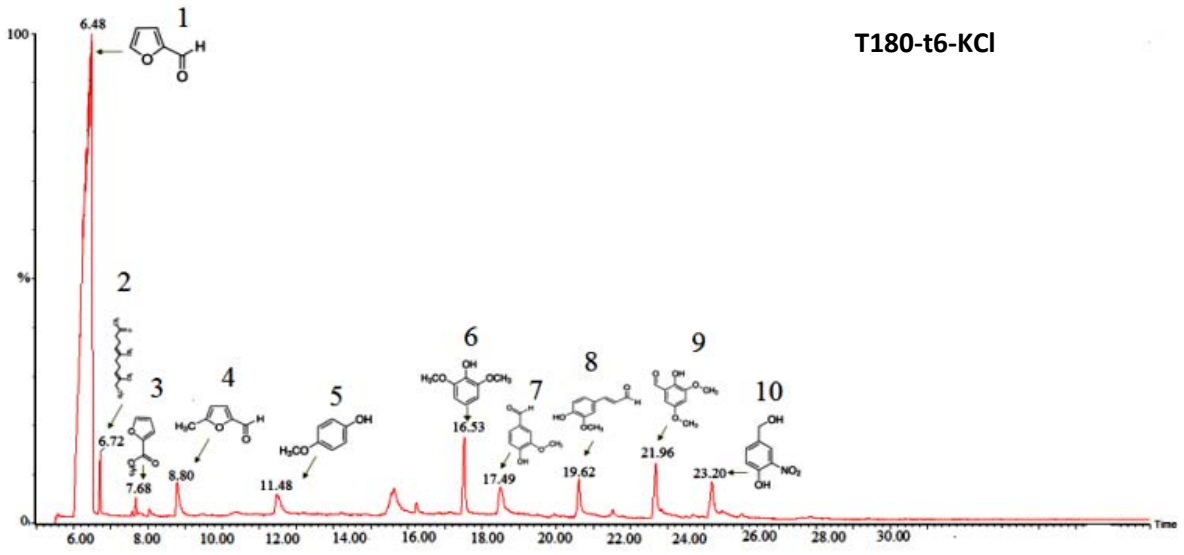

1) Furfural 2)1,5,9-Undecatrien-1-ol, 2,6,9-trimethyl-**3)**Ethanone,1-(2-Furanyl)-**4)** 2-furancarboxaldehyde,5-methyl **5)** guaiacol **6)** phenol,2,6 dimethoxy**7)** vanillin **8)** 2-propane,1-(4-hydroxy-3-methoxyphenyl) **9)**benzaldehyde,4,hydroxyl-3,5-dimethoxy **10)** 4-hydroxy-3-nitrobenzyl alcohol

Figure 45: GC/MS analysis of hydrochar prepared at 180°C modified with NaCl (a), LiCl (b) and KCl (c)

The GC/MS analysis of liquid fraction of hydrochar modified with salts (NaCl, LiCl and KCl) at 180°C and 6h are shown in figure 45, a remarkable effect of salt on the released compounds in the liquid phase, actually, it is an effect on hydrothermal carbonization mechanism, that because for the same experiment conditions (temperature, time) the liquid analysis shows a different result from using salt to another, KCl and NaCl show almost similar effect on HTC-liquid, as shown in figure 45 (a) and (c) both liquid has the same composition and both of them have a remarkable effect on lignin, indeed their liquid is significantly rich in compound released from lignin decomposition such as benzaldehyde,4,hydroxyl-3,5-dimethoxy, phenol,2,6 dimethoxy and guaiacol.

Otherwise LiCl added salt (figure 45 (b)), didn‘t have a strong effect on lignin, although it seems to have an important effect on cellulose that because the characteristic compound of cellulose degradation 2-furancarboxaldehyde,5-methyl) is didn‘t appear in the analysis of liquid fraction, the results are completely consistent with the aforementioned studies of thermo gravimetric and elemental composition analysis.

II.1 Conclusion

In this chapter, a systematic investigation on the mechanism of hydrothermal carbonization of olive stones and its main compounds (Hemicellulose, Cellulose and Lignin) has been performed. It seems that HTC an efficient technique for upgrading olive stone and its conversion into high-value products: solid (hydrochar) and liquid (5-HMF and furfural). Acid and salts addition have an important impact on HT of OS, they catalyse the hydrolysis reactions and destabilize the complex structure of olive stone. The severity index (factor combined time and temperature) was useful to assess the effect of reactions intensity on OS and its compounds. It was found that at severity higher than 6.4, cellulose is completely reacted and lignin degradation started at earlier stage (severity less than 4.2). Once hydrochar are carbonized at 900°C, the resultant carbon materials had high surface areas, as high as 1200 m^2g^{-1}, and narrow pore size distributions centered on 0.5 nm, suggesting their potential use as cheap carbon molecular sieves.

Chapter III: Activated Carbon Synthesis

III.1 Experimental set up

III.1.1 Hydrochar synthesis

HTC autoclave used in the following work was designed and constructed in our Laboratory of Research, the autoclave was equipped by thermocouple and pressure gauge, the pressure maintained autogenic and depended only to water temperature and the thermocouple was connected to a Proportional-Integral-Derivative PID temperature controller, the pressure release valve was introduced for safety reasons. The stainless steel autoclave was filled of less than third of its capacity and submitted to several preliminary tests Schematic diagram of the autoclave reactor is shown in the figure 46.

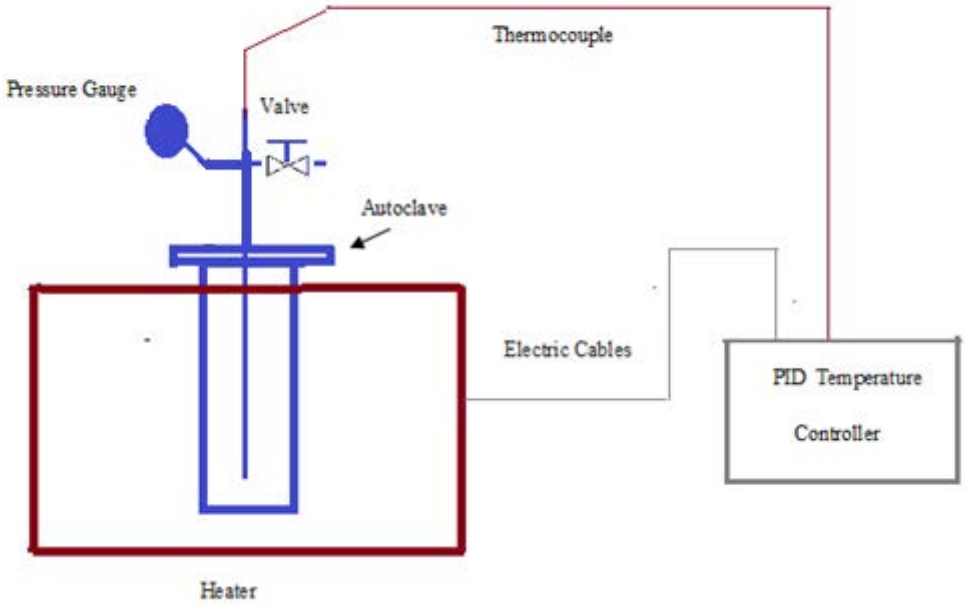

Figure 46: Experimental setup of hydrothermal treatment

The hydrochar used as started materials for activated carbon were prepared according to the following conditions:

- HTC-180: In a typical experiment the amount of OS used is 6 g mixed with 32 ml of distiller water then the mixture were introduced into the autoclave and heated at 180°C for 6 h.
- HTC-240: These experiments typically follow the same procedure of HTC-180 except the temperatures were increased to 240°C.

- HTC-N: The distiller water was replaced by 28% ammonia solution the mixture of OS and ammonia were submitted to HT treatment at 180°C for 6h.

All hydrochar were rigorously washed and dried in vacuum oven at 80°C for 8h. The hydrochar characterizations are given in the following table:

Table 9: Elemental and yield analyses results

	%C	%O	%H	%N	%S	HTC yield (%)
HTC-180	47.48	46.95	5.34	0.24	0.032	58.9
HTC-240	68.48	25.96	5.33	0.23	0	51.15
HTC-N	48.79	43.39	6.59	1.215	0	56.12

III.1.2 Activated carbon synthesis

III.1.2.1 Chemical activation

In this section HTC-180 and HTC-240 were chosen to be a precursor for activated carbon, both hydrochar were chemically activated using KOH, besides OS were directly activated in order to compare the two step procedure with the traditional activation methodology. The hydrochar/ olive stones and KOH were mixed and 20 ml of distiller water were added in order to dissolve the solid, the mixture was first of all heated at 80°C for more than 24 h for drying and then was placed in horizontal electric furnace at 900°C for to 2h under nitrogen flow, the temperature was controlled using a thermocouple installed inside the reactor. The KOH/Hydrochar weight ratio of 2 were selected, according to the literature weight ratio of 2 is suitable to obtain high surface area and to prevent the destruction of micro porosities of carbon matrix by the alkali metal (Ubago-Pérez et al. 2006; Elmouwahidi et al. 2012, 2017). The resulted solid was harshly washed with hot distiller water until the pH of the water remains stable. The activated carbon was dried at 105°C for 24 h and labeled as AC-HTC-180, AC-HTC-240 and KOH-DIR.

III.1.2.2 Physical activation

The hydrochar HTC-N was physically activated using CO_2, the hydrochar was placed into a crucible and then heated into quartz tube of a tubular furnace heated at 5°Cmin^{-1} up to 900 °C under nitrogen flow (80 ml min^{-1}), N_2 flow maintained 1 hour and then replaced by carbon dioxide flow, the activation time were varied between 30 and 120 min, the activated carbon surface area are depicted in the following figure:

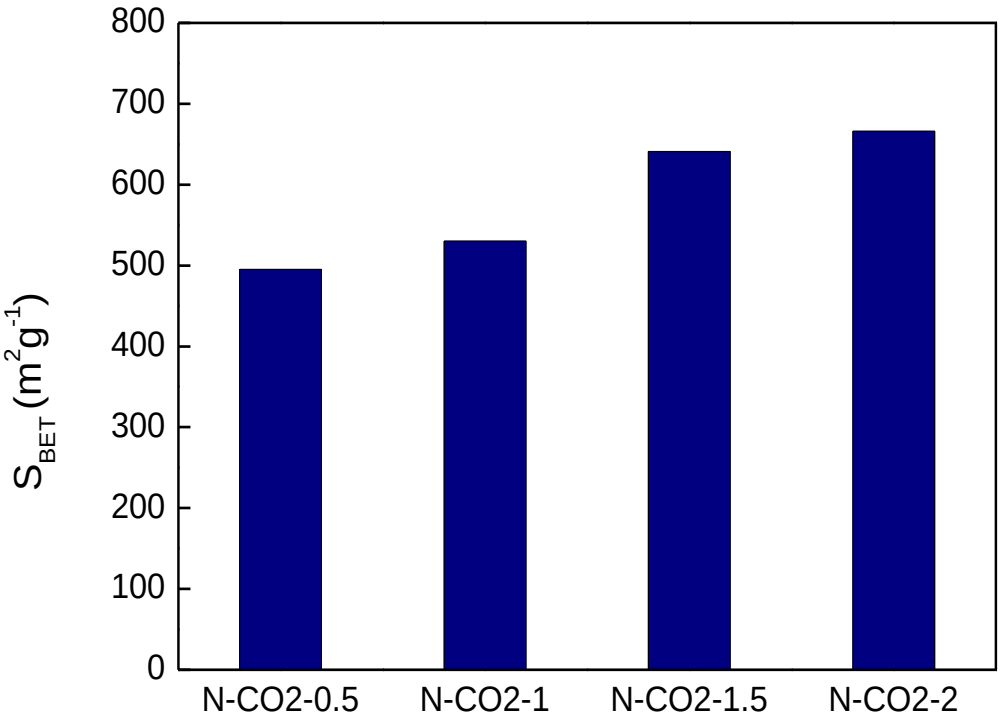

Figure 47: BET surface area as function of activation time

The highest BET surface area 667 $m^2g^{-1}$was obtained for hydrchar activated for 2h; therefore N-CO2-2 will be selected to investigate its textural properties in the following studies.

III.1.3 Oxidation of activated carbon with ozone

The AC-HTC-180-KOH and AC-HTC-240-KOH were modified using ozone; the ozone oxidation was carried out in a fixed bed glass reactor equipped with a stirrer and continuously fed with ozone flow of 55 mg/L for 2 hours, ozone was produced using an ozone generator and the reactor was loaded with 2 g of activated carbon. The recovered solid was dried at 105°C for 24h. The modified activated carbon will be labeled as AC-HTC-180-O3 and AC-HTC-240-O3.

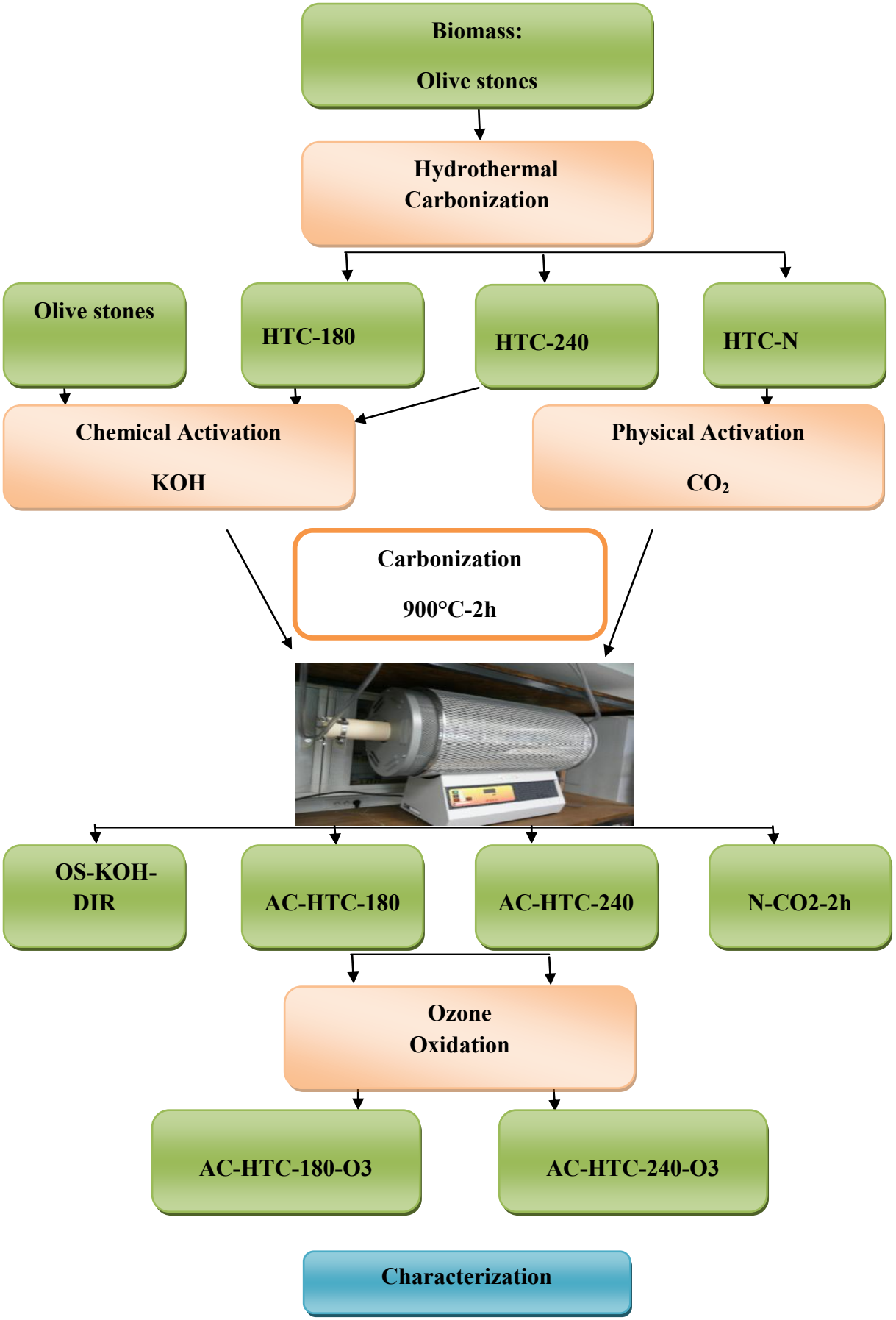

Figure 48: Experiments methodology

III.2 Characterization of activated carbon

III.2.1 Instrumentation of gas adsorption

The gas sorption analysis was accomplished by N_2 at -196 ºC and CO_2 adsorption at 0°C using Micromeritics ASAP 2020and ASAP 2420 automatic equipments pictured in Figure 49.a and Figure 49.b respectively. The measurements were performed using a volumetric method, it is called manometric, this technique is essentially involved the pressure variation during the adsorption to determine the volume of gas adsorbed, in fact the solid materials must be degassed under vacuum and at high temperature before analysis, the temperature should be carefully selected in order to avoid any destruction of the organic structure of materials, in this study carbon samples were degassed at 125 °C and for 48 h prior to any gas adsorption, The amount of gas adsorbed is calculated as the difference between the pressure estimated by the real gas equation of state and the measured pressure, the adsorbed amount is expressed as volume per unit of mass cm3/ g (S.T.P). The curve related the quantity of gas adsorbed to the relative pressure (P/P°) is called adsorption isotherm, then the isotherm data were analyzed using the Brunauer-Emmet-Teller (BET) and the Non-Local Density Functional Theory (NLDFT) models.

a) b)

Figure 49: A photograph of ASAP 2020 (a) and ASAP 2420 (b) automatic equipment

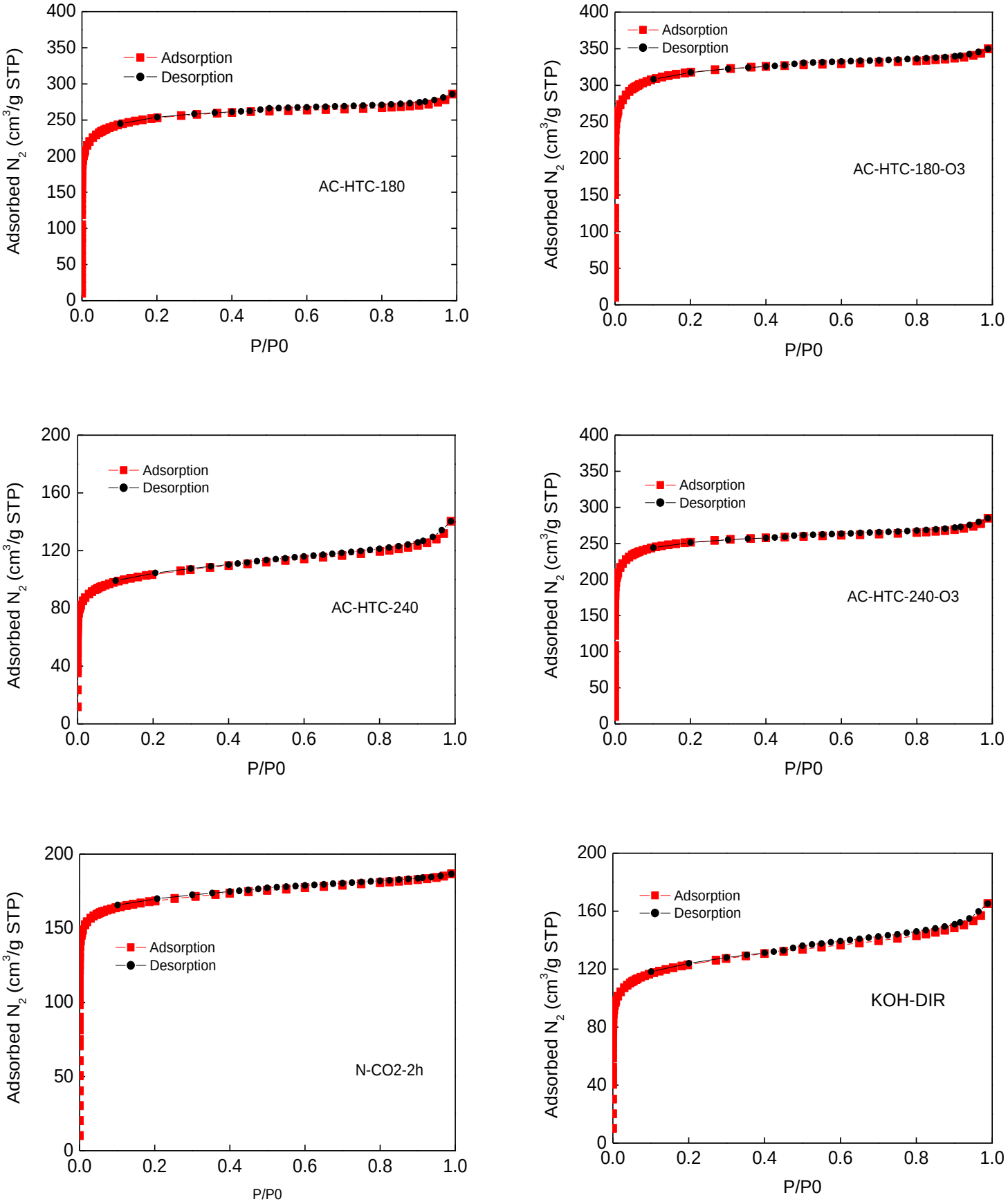

Figure 50: Nitrogen adsorption isotherms

According to the adsorption isotherms depicted in figures 50, the nitrogen adsorption had occurred at quiet low relative pressure, indicative of the presence of pores with extremely small size, some samples show a relatively high nitrogen uptake (around 350 cm^3/g STP), and actually it varied from activated carbon to another depending on hydrothermal, activation and post treatment conditions.

In addition, considerable information about surface area and porous structure of AC network could be provided by a close insight into the shape of adsorption isotherm. All AC-samples displayed steep type I isotherm excluding AC-HTC-240 and KOH-DIR they are both show an intermediate between type I and II which reflect the presence of combination of micropores and mesopores, the pore filing is mainly enhanced by the strong interaction energy within the pore walls at very low pressure, and the pore can accommodated only one layer of nitrogen molecule, then the gas adsorption almost maintain constant and only slight increase was observed at relative pressure over than 0.2, this finding is interpreted through the horizontal plateau parallel to P/P° axis which follow a concave shape. Previous studies showed that KOH was powerful in creating well-developed pores and highly homogenous micro porosities by activation of OS produces comparing to others activation agents such as $ZnCl_2$ and H_3PO_4 (Alslaibi et al. 2014; Hui and Zaini 2015)

As shown in figure 50, the AC-HTC-180 has much more nitrogen uptake than AC-HTC-240, indeed the adsorbed amount outstandingly increase from 106 cm^3 STP g^{-1} to 246 cm^3 STP g^{-1} as the hydrothermal temperature of hydrochar synthesis increase from 180°C to 240 °C, likewise this finding is similar to that of AC prepared by KOH chemical activation of hydrochar derived rye straw that because the resulted AC properties strongly depends on hydrothermal temperature, but in the case of rye straw the nitrogen uptake increase as HT temperature increase from 180°C to 240 °C and considerably decrease as the HT increase to 280 °C, this difference may be due to the structure of raw materials, in fact OS is much more rich in lignin (30%) than rye straw (19%), and as have been explained previously in chapter II, section II.2.2.3 through a deep investigation on the thermal behavior of HTC-180 and HTC-240, it has been found that DTG peak is shifted to more higher temperature characteristic of lignin compound, which fundamentally results micropores (Suhas et al. 2007; Parshetti et al. 2015) and voids created by the benzene- ring materials precipitated during lignin thermal treatment (Li et al. 2016) and generally during carbonization steps more gases are evolved transform micropore to mesopore, thereby resulting some volatile tars wouldn‘t immediately escape the carbon network and may remains in the final structure of materials and consequently blocked the pore channel (Parshetti et al. 2015).

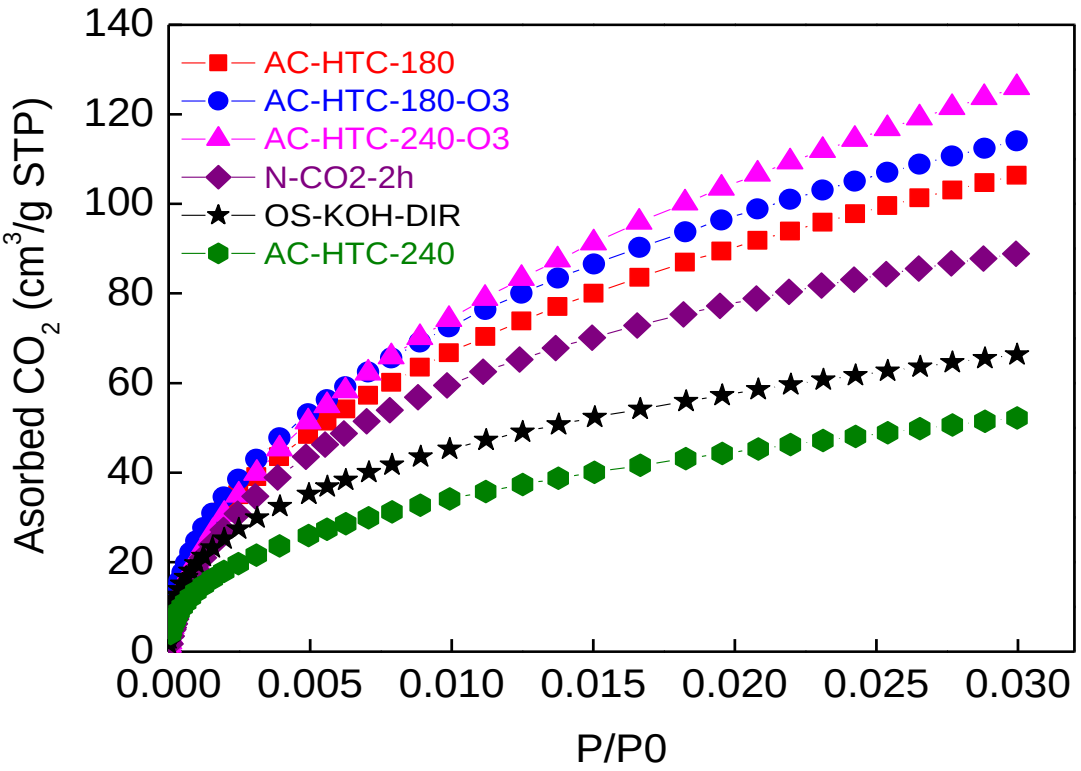

Figure 51: CO_2 adsorption isotherms

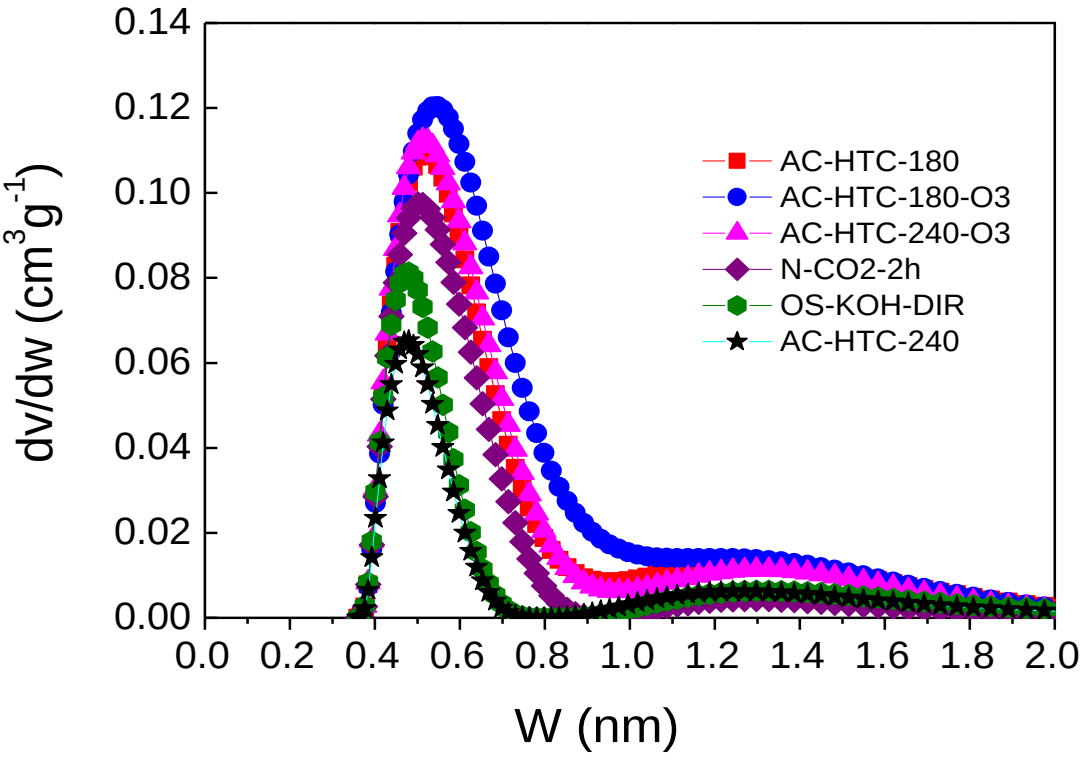

Figure 52: Pore size distribution using NLDFT method

The Olive stones directly activated with KOH (OS-KOH-DIR) were prepared for the sake of comparison with hydrochar derived AC, figure 50 shows that OS-KOH-DIR has less nitrogen uptake (156 cm^3 STP g^{-1}) than AC prepared from hydrochar at low temperature suggest less development of microporous structure. The adsorption isotherms of OS-KOH-DIR and AC-HTC-240 are characterized by slight increase in nitrogen uptake at high relative pressure ($P/P°=0.9$) which attributed to the smallest conchoidal cavities (Ferrero et al. 2015) and negligible hysteresis loop mainly due to the presence of small mesopores fractions.

The adsorption isotherm of hydrochar physically activated with CO_2 shows a sharper knee at low relative pressure and low nitrogen uptake than those obtained with AC-HTC-180.

The AC-HTC-240 isotherm is obviously transformed to type I that mean that the micropores fraction increase after post treatment of AC-HTC-240 by oxidation with ozone.

In order to get close insight into the narrow microporosity fraction, CO_2 gas has been proven to be a suitable candidate of such application, the CO_2 physisorption isotherm at 77 K are depicted in figure 51, all adsorption isotherm are type I, the adsorption results show a different trend than those previously obtained with N_2 gas, this result suggest that AC-HTC-180-O3 and AC-HTC-240-O3 produce prevalently narrow micropores. On other hand, AC-HTC-240 and OS-KOH-DIR has the lowest CO_2 uptake.

These speculations are validated by NLDFT pore size distributions PSDs given by figure 52, assessment of PSDs is of primordial importance in the characterization of solid with very narrow pores, in this research PSD was obtained by application of Saieus® software on the extent of adsorption isotherm of N_2 and CO_2 gases and using heterogeneous surface as a model. AC -HTC-240 has tendency to produce smallest and less sharp PSDs centered in 0.49, whereas the PSDs of AC-HTC-180 was shifted towards large pore width. A remarkable effect of the oxidation treatment on AC, the maximum is shifted from 0.52 nm to 0.54 nm in case of AC -HTC-180 and from 0.49 nm to 0.52 nm in case of AC-HTC-240 with much more sharper PSDs than materials without oxidation. Similar results have been found by (Chiang et al. 1995), a significant effect of ozonation treatment on narrow micropores and actually no obvious difference has been found on pores diameter higher than 2 nm, in the same study, the micropores size were increased to more than 0.8 nm for oxidized activated carbon with ozone which is greater than pore size diameters observed on AC without oxidation (between 0.6 and 0.7 nm). In addition, oxidation treatment seems to have a particular impact on activated carbon properties such as specific surface area and pores volume. The characterization results are sown in figures 53 and 55.

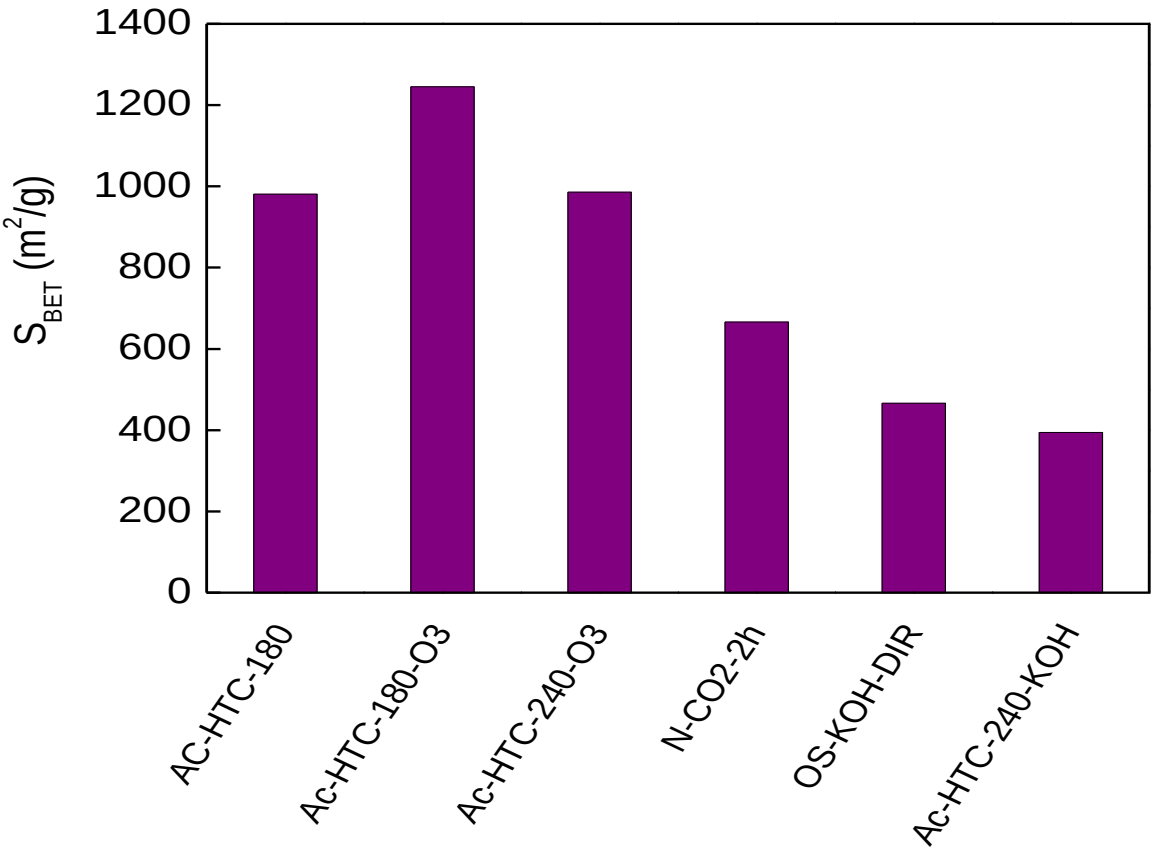

Figure 53: BET specific surface area

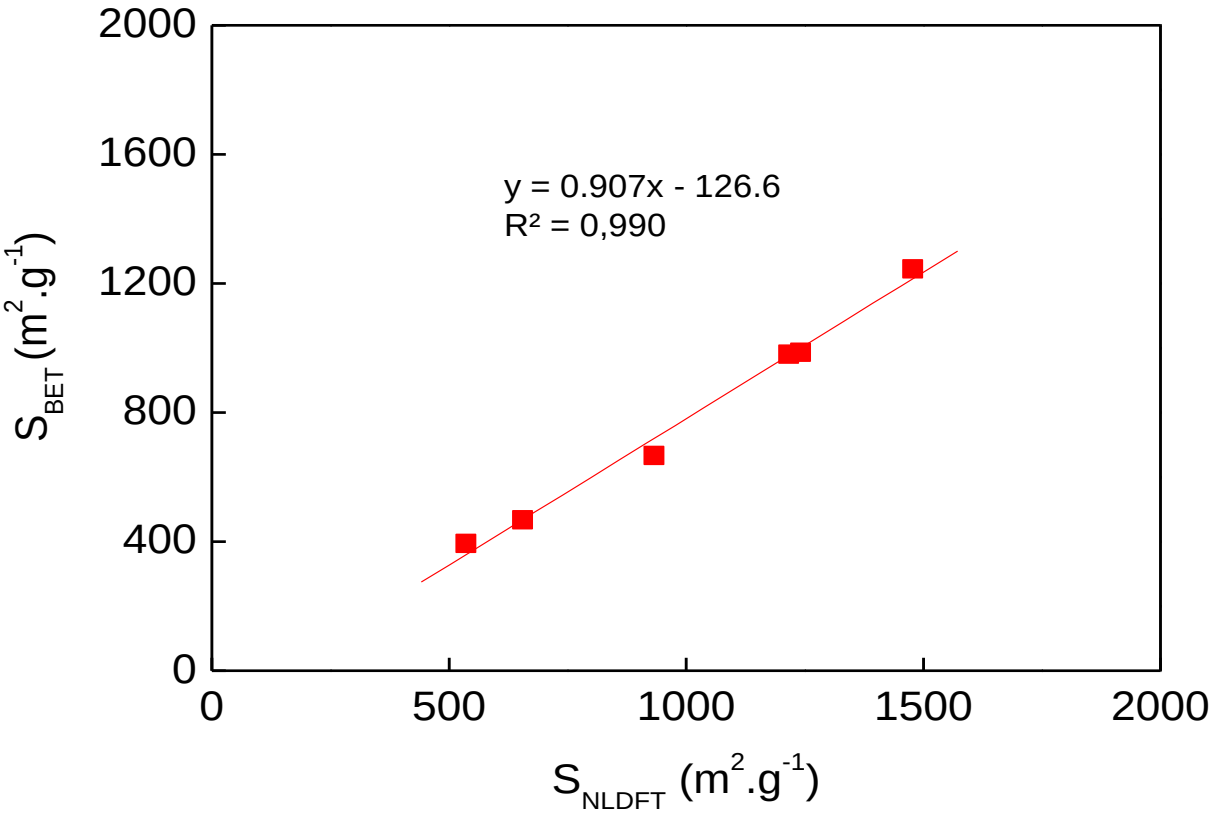

Figure 54: BET surface area as function of NLDFT surface area

The hydrothermal carbonization of olive stones improves the textural properties activated carbon prepared, this technique considerably ameliorates the specific surface area BET (Figure 53) of resulted AC, and the overwhelming majority of created pores are micropores, the AC-HTC-180 shows a relatively high surface area than AC-KOH-DIR, similar results of olive waste directly activated with KOH with optimized activation parameters (temperature =600°C and KOH/precursor ratio=2) were obtained by (Abdel-Ghani et al. 2016). AC-HTC-240 shows less S_{BET} surface area than AC-HTC-180, besides to the aforementioned reasons, a possible explanation for such result is that as this materials are mainly produced from the remained lignin on the hydrochar, which already has tendency to develop narrow micropore and then using KOH chemical agent might produce an important amount of K_2CO_3 and metallic potassium might remain in the final structure of AC even after rigorous washing which further block some pores and obviously a remarkable decrease in the surface area (Alslaibi et al. 2014) therefore for tuning the porous structure adjusting the hydrothermal temperature to material composition is a perfect option, but generally KOH activation agent is well known to develop high surface area, (Alslaibi et al. 2014) studied the synthesis of AC from olive stones and suggested that high development on AC textural properties (surface area and pores volume) is mainly due to the intercalation of potassium element on the network structure of carbon, similarly (Marsh et al. 1984) reported that the formation of microporosity is deduced to the effect of oxygen of the alkali which remove cross-linking and stabilizing carbon atoms in crystallites. Moreover, the AC physically activated (N-CO2-2h) shows a higher surface area (667 m^2g^{-1}) than that obtained by CO_2 activation of hydrochar prepared from OS at temperature 220°C and 20h (438 m^2g^{-1}) (Román et al. 2013), these results are completely coherent with this study and proved that adjusting hydrothermal temperature is a key option strongly affect AC textural properties.

The BET was plotted as function of NLDFT surface area in figure 53, a linear relationship was established with high coefficient correlation (R^2=0.99), both model give a close result in case of samples with boarder PSDs, but in case of AC-HTC-240 and AC-KOH-DIR which present pores with small size a remarkable difference were noticed, this results were expected and have been justified previously in chapter II, section II.2.3.2.

Actually, the largest pore size distribution, surface area and pore volume were given by oxidized AC, exceptional increase in surface area from (S_{NLDFT} = 536 m^2g^{-1} and S_{BET}= 400 m^2g^{-1}) to (S_{NLDFT} = 1242 m^2g^{-1} and S_{BET}= 987 m^2g^{-1}) and pores volume from 0.23 cm^3g^{-1} to 0.44 cm^3g^{-1} of the AC-KOH-240.

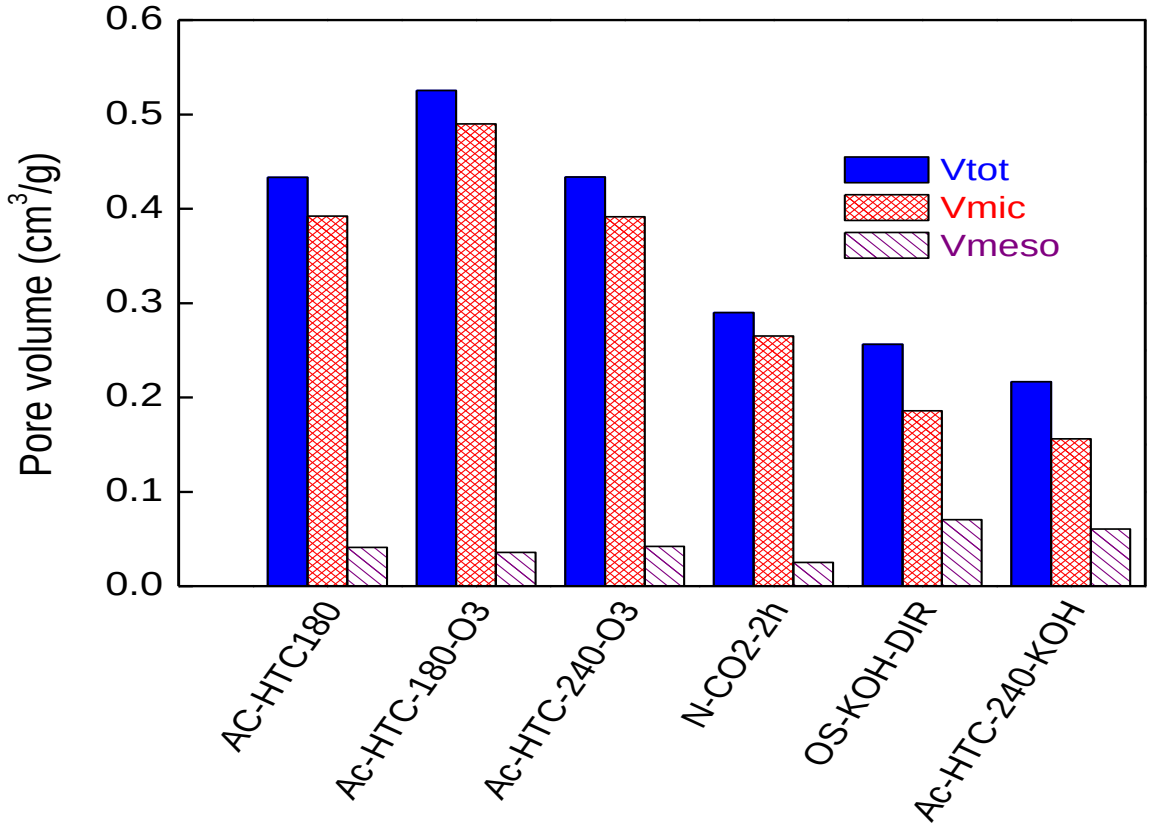

Figure 55: Micropore, mesopores and total pore volume Pore volume

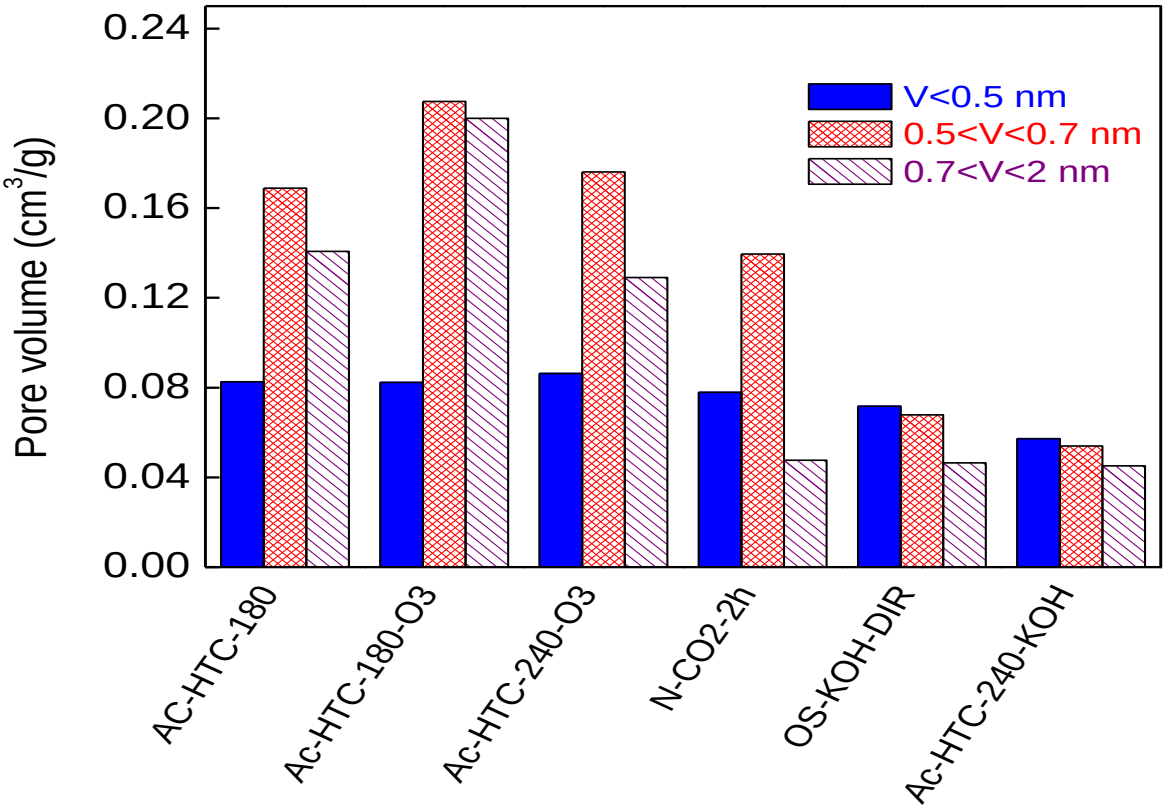

Figure 56: Volumes of the supermicropores (Vsupmic) and ultramicropores (Vumic)

Similar result obtain for AC-HTC-180, the surface area from (S_{NLDFT} = 1217 m^2g^{-1} and S_{BET}= 981 m^2g^{-1}) to (S_{NLDFT} = 1478 m^2g^{-1} and S_{BET}= 1245 m^2g^{-1}) and pore volume from 0.43 cm^3g^{-1} to 0.53 cm^3g^1 (figure 55). Oxidation of AC by ozone has been the subject of many scientific papers, usually activated carbon used as catalysts on the ozonation process to increase its efficiency (Shahamat et al. 2014) but it is possible as well to use ozone treatment in modification of AC surface (Lota et al. 2016). (Chiang et al. 1995) stated that when AC exposed to 25 mg/l ozone and maintained for thirty minutes, the BET surface area was increased from 783 m^2g^{-1} to 851 m^2g^{-1} and pores volume from 0.32 ccg^{-1} to 0.344cc g^{-1}, during this research two mechanisms have been observed on ozone oxidation of AC, one leads to an enlarge the pores diameter and the second one create new pores. On the other hand, oxidation treatment by ozone may has a negative effect on textural properties of AC by destroying its porous structure, (Valdés et al. 2002) found that surface area slightly increased after exposure time of 10 min and dramatically decreased (about 40%) after 2h of treatment at constant flow of 76 mg of O3/min and a similar behavior shown on micropore volume, in fact the damage of AC structure was deduced to the gasification of the carbon by ozone. (Deitz and Bitner 1972) proposed the following three reactions mechanism of AC and ozone:

$$C_xO_y(solid) + O_3 \rightarrow C_xO_{y+1}(solid) + O_2 \quad \text{(I)}$$

$$C_xO_y(solid) + O_3 \rightarrow C_{x-1}O_{y+1}(solid) + CO_2 \quad \text{(II)}$$

$$C_xO_y(solid) + O_3 \rightarrow C_{x-2}O_y(solid) + CO_2 + CO \quad \text{(III)}$$

A systematic investigation on the reactions behavior, (Deitz and Bitner 1972) found that during reaction (I) an increase on the oxygen content of AC without loss of weight leads to micropores plugging and subsequently reduction of surface area, in case of reactions (II) and (III), respectively, a minor weight loss without change in extent of surface and major weight loss and an oxidative etching process has been occurred, during reaction III an increase of surface area could be achieved which is the case of the current research. Generally, it could be concluded that the effect of ozone on AC depends on several parameters such as: nature of AC, oxidation time and ozone flow (Shahamat et al. 2014).

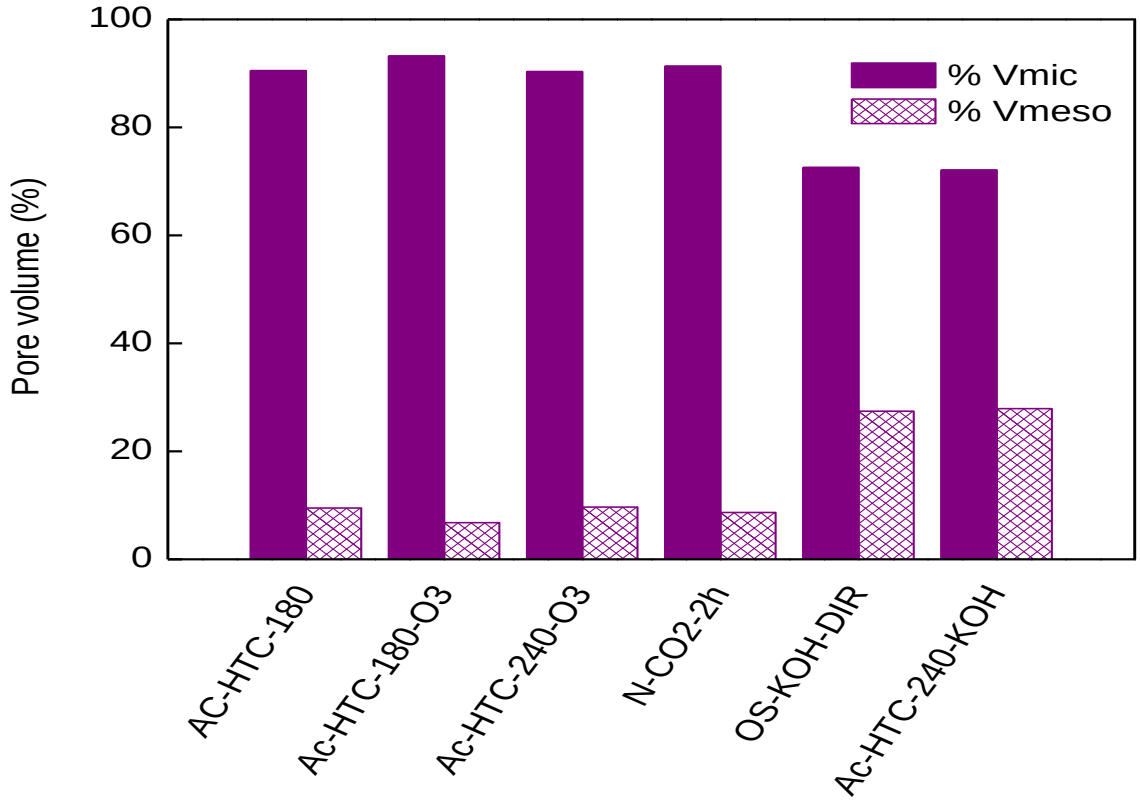

Figure 57: Mesopore and micropore fractions

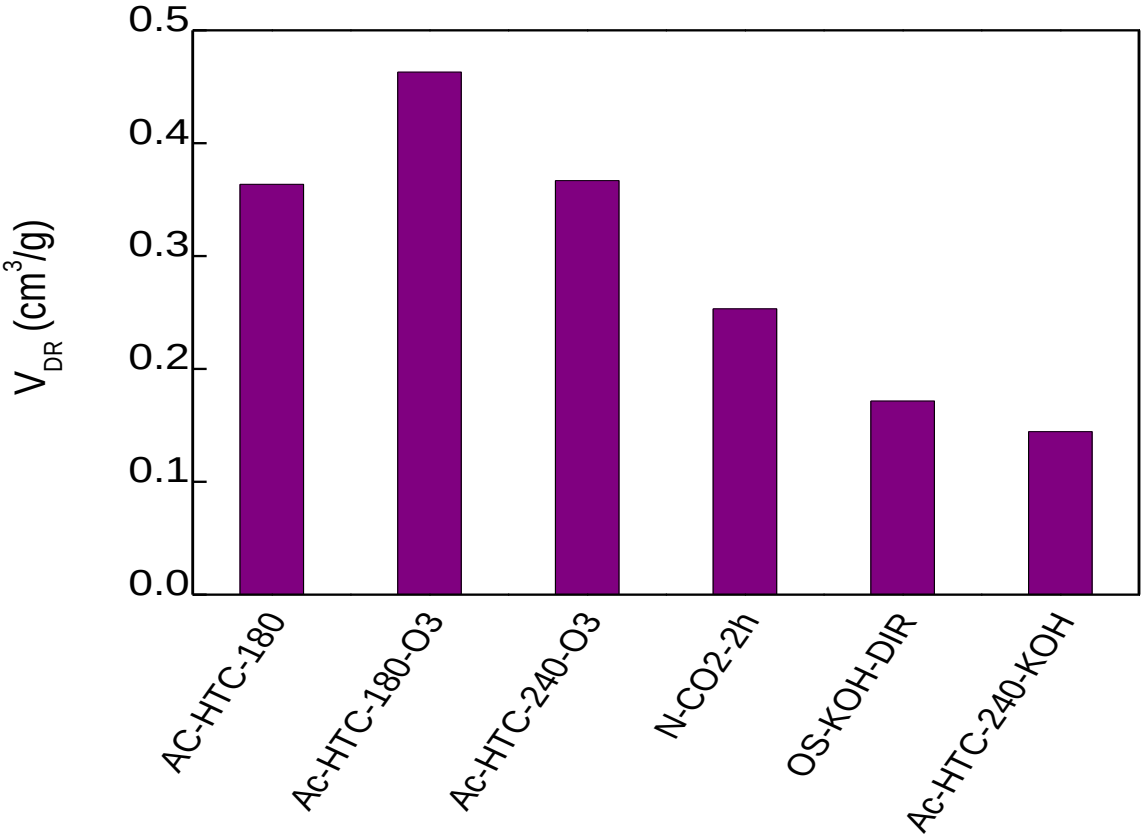

Figure 58: Microporous volumes according to Dubinin Radushkevich

More than 90% of the developed pores are micropores (figure 57), the predominating pores size are between 0.5 and 0.7 nm (figure 56), with the exception of AC-HTC-240 and OS-KOH-DIR, these two materials exhibit about 27% mesopores, the presence of mesopores is favorable and has an outstanding effect on the majority of technological applications such as (adsorption, catalysis, electrodes…) that because the surface of mesopores is more available for ion or molecules (Gong et al. 2014).

Figure 58 illustrates the micropores volume measured by the Dubinin-Radushkevich (DR) model, this phenomenological model is employed to characterize micropous carbon with a narrow PSD and also it is commonly used as a reference in pore volume determination. The highest V_{DR} is attributed to oxidized samples and AC-HTC-180, N-CO2-2h characterized by very low mesopores fraction that because the difference between V_t ($P/P°=0.99$) and V_{DR} is negligible (0.03 cm^3/g).

III.2.2 Surface chemistry analyses

III.2.2.1 Point of zero charge (pHpzc)

The point of zero charge is the point at which the external net surface charge of materials is zero, it is of paramount importance to determine the pHpzc of activated carbon especially in case of its further uses in applications related to adsorption and catalyst, this technique is established based on the assumption that protons, H+, and hydroxyl groups, OH−, are potential-determining ions. The pHpzc is commonly used to assess the effect of pH of surrounded solution on the activated carbon surface charge, at pH (solution) less than pHpzc the surface of solid surface is positively charged contrary for higher pH solution than phpzc it will be negatively charged or neutral when pH equal to pHpzc, generally pHpzc value of ACs varied from 2 to 10.5.

The pHpzc of prepared ACs in this work were measured according to the following batch equilibrium method (Rivera-Utrilla et al. 2001): the initial pH value of 50 ml of NaCl (0.01 M) solution were modified to 2, 4, 6, 8, 10 and 12 using HCl (0.1M) or NaOH (0.1M) then a 0.15 g of AC were added and the solution stirred for 48h. The final pH were measured using pH-meter of type CG841-SCHOTT (standard pH meter, Meter Lab) and the pHpzc were obtained by plotting [pHi-pHf] versus the pHi, the intersection of the resulted curve with the bisector present the pHpzc value. The results are shown in Figure 59 and table 10.

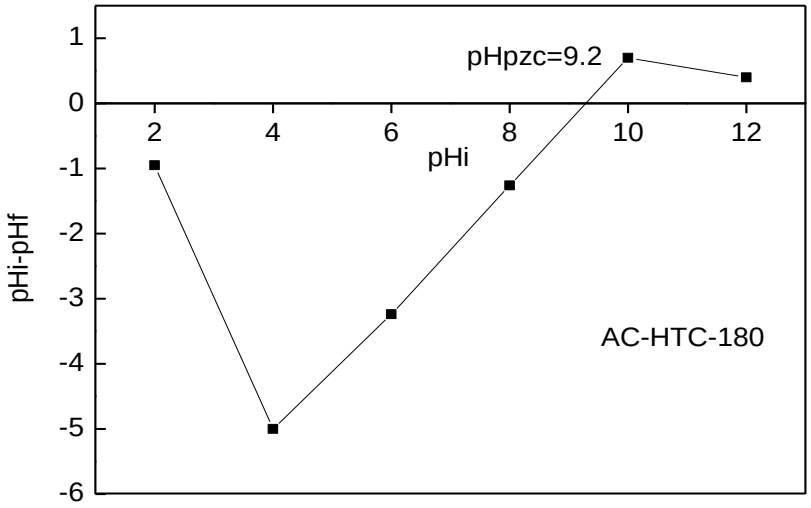
pHpzc=9.2
pHi
pHi-pHf
AC-HTC-180

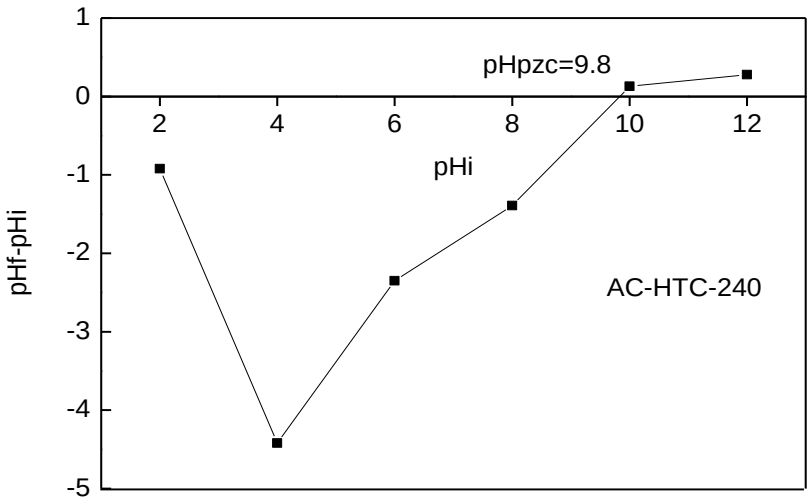
pHpzc=9.8
pHi
pHf-pHi
AC-HTC-240

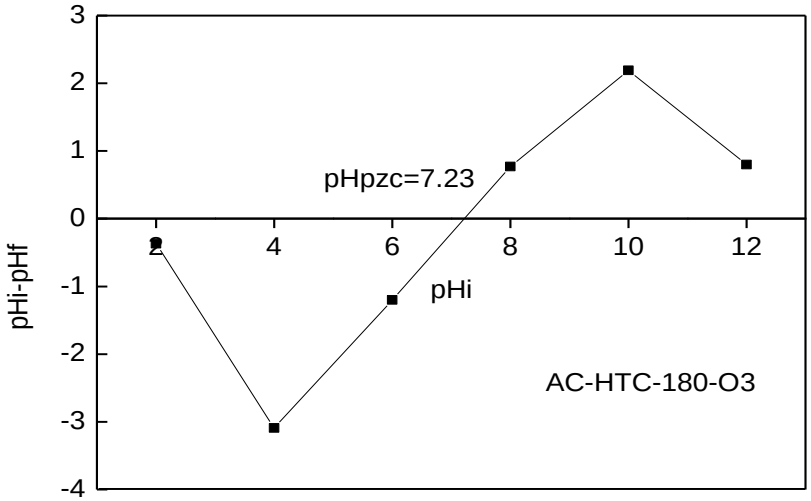
pHpzc=7.23
pHi
pHi-pHf
AC-HTC-180-O3

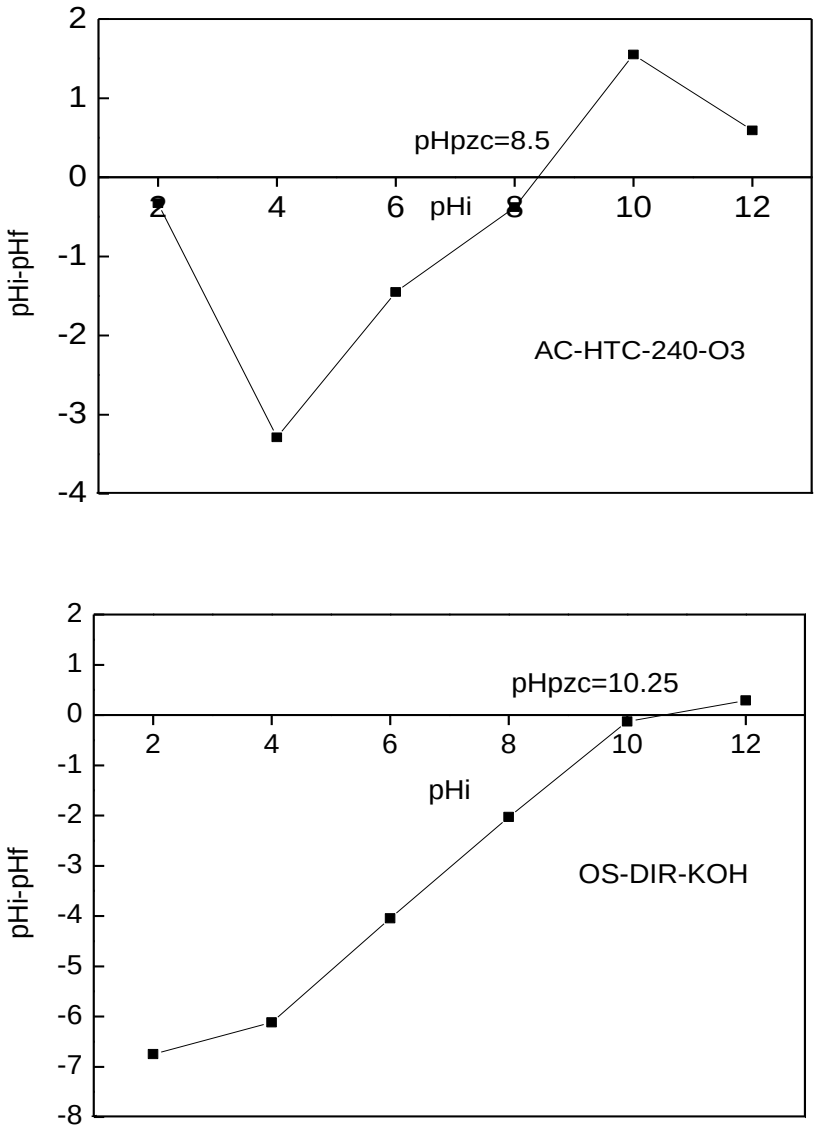

Figure 59: pHpzc of prepared activated carbon

The pHpzc of activated carbon depends strongly to the precursor origin and activation conditions**,** the pHpzc of hydrochar derived activated carbon and OS directly activated with KOH exhibit a high pH pzc values indicative of basic characters of materials, the OS-KOH-DIR shows a slight higher pHpzc value than AC-HTC-180 and AC-HTC-240 that may due to the nature of started materials (hydrochar) which usually shows a high acidic surface character (Román et al. 2012; Mestre et al. 2015; Jain et al. 2016), otherwise a slight increase of pH pzc of AC-HTC-240, these result are in agreement with the literature (Román et al. 2012) found that an increase of HT temperature leads to reduce the acidity of hydrochar.

As expected oxidation of ACs with ozone decreases the pH pzc of activated carbon, as shown in table 10 the pH pzc of AC-HTC-180-O3 is reduced from 9.2 to 7.23 and the surface

character changes from basic to neutral and for AC-HTC -240-O3 the pH pzc value is reduced to 8.5 and the surface become a weakly basic.

Table 10: pHpzc of chemically activated carbon

	AC-KOH-180	AC-KOH-240	AC-KOH-180-O3	AC-KOH-240-O3	OS-KOH-DIR
pH pzc	9.2	9.8	7.23	8.5	10.25

III.2.2.2 Boehm titration method

In order to investigate the surface chemistry character of the prepared ACs and to get a depths insight into the carbon surface functionalities, a Boehm titration method was performed (Boehm 1994, 2002). A 0.2 g of activated carbon were added to 50 ml solutions of 0.02 N sodium bicarbonate ($NaHCO_3$), sodium carbonate (Na_2CO_3), sodium hydroxide (NaOH) and hydrochloric acid (HCl), respectively. The mixture were shacked for 24 h and then filtered, a 5 ml of each solution were titrated with sodium hydroxide or hydrochloric acid, depending on the initial solution. This methodology presumes that $NaHCO_3$ neutralizes carboxylic group, Na_2CO_3 neutralizes carboxylic and lactones, NaOH neutralizes carboxylic, lactones and phenolic groups. HCl determine the number of surface basic site of activated carbon. The Boehm titration results are shown in table 11.

Table 11: Boehm titration results

	Carboxyl	**Lactone**	**Phenol**	**Basic**	**Acid**
AC-KOH-180	0.015	0	0.23	0.5	0.245
AC-KOH-240	0	0	0.09	0.4	0.09
AC-KOH-180-O3	0.12	0.03	0.03	**0.12**	0.18
AC-KOH-240-O3	0.0575	0.0125	0.18	0.37	0.25
OS-KOH-DIR	0	0	0	0.47	0

The results show that unmodified materials prepared by chemical activation have strong basic properties, the OS-KOH-DIR has the lowest acid group although this finding is in agreement with pHpzc result (pH pzc=10.25) but it is not completely convenient that because the basic content is only 0.47 meq/g, that could be strongly due to the release of a important amount of carbonates in basic solution (Mohamed et al. 2011). It is worthy to note those activated carbons prepared from hydrochar are rich in variety of acidic functional groups, AC-HTC-

180, according to (Jain et al. 2016) hydrothermal treatment enhance the formation of oxygenated functional groups on surface of hydrochar and the amount and type of functional groups are strongly dependent to HT treatment conditions (time and temperature) and also the type of started materials, thereby this study is consistent with the literature, as shown in table 11 the phenol groups is more pronounced in AC-HTC-180 this possibly due to the nature of olive stones which are rich in lignin and usually lignin under HT is converted to phenolic hydrochar (Jain et al. 2016), on the other hand the quantities of phenolic and carboxylic groups are enormously decreased in AC-HTC-240 that because an increase of hydrothermal temperature improves the decomposition of oxygen function groups into gas product, at this point it is worthy to highlight the potential of HT to tune the surface chemistry of ACs which upgrade its performance in various applications, the evolution of oxygen functional groups content as function of hydrothermal treatment temperature is depicted in figure 60.

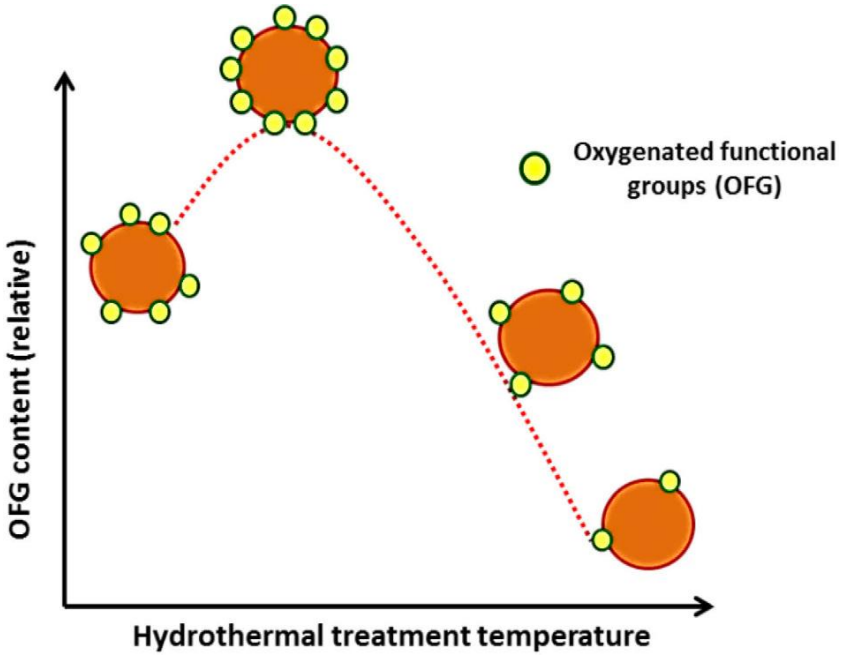

Figure 60: Changes of oxygen functional groups content as function of HT temperature (Jain et al. 2016)

In addition, an obvious effect of ozone treatment on the amount of both acidic and basic groups, an important increase of phenol content from 0.09 to 0.18 meq/g was shown on AC-HTC -240 whereas a significant increase of carboxylic content from 0.015 to 0.12 meq/g, this difference on ozone effect is actually due to the nature of activated carbon, also it could be noted that phenolic groups are reduced in AC-HTC-180-O3 that because its dehydration leads to the formation of lactones groups (Szymański et al. 2002), generally the ozone treatment reduce basic groups of both treated ACs . The same results have been reported by several authors (Chiang et al. 1995; Valdés et al. 2002; Jaramillo et al. 2009).

III.2.3 Water adsorption

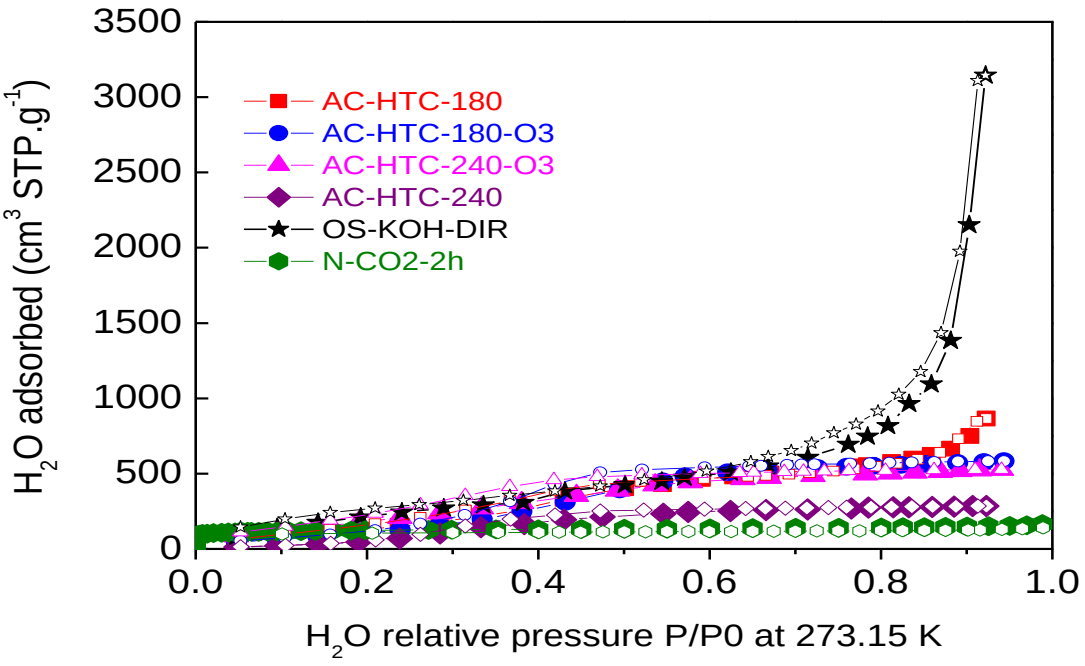

Figure 61: Water adsorption isotherm

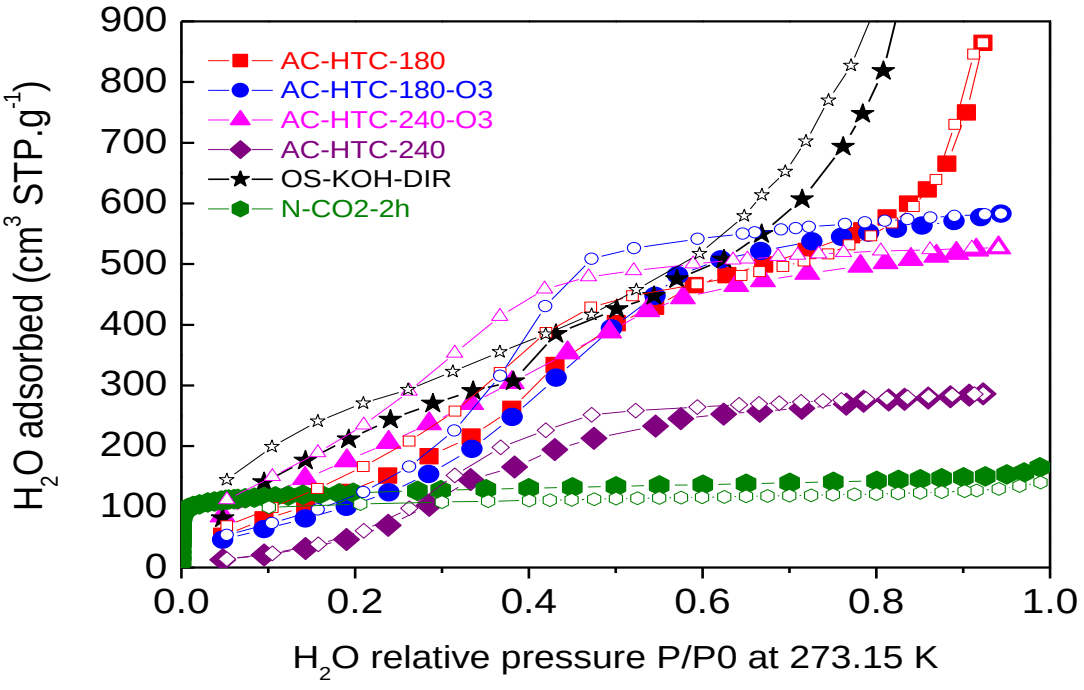

Figure 62: Zoom in of water adsorption isotherm

Figure 61 and 62 depict the adsorption water isotherms, the oxidized activated carbon with ozone exhibit type V isotherm and this type of isotherm showed to increase linearly with the

sum of oxygen functional group (Li et al. 2005), N-CO2-2h type I or OS-KOH-DIR and AC-HTC-180 exhibited adsorption isotherm type II (multilayer adsorption), an important water amount has been adsorbed even at low relative pressure, the adsorbed amount keep rising until relative pressure 0.5 and then the steady-state was almost reached and water uptake didn‘t vary for AC-HTC-180-O3 and AC-HTC-240-O3, otherwise OS-KOH-DIR and AC-HTC-180 show a high water uptake at relative pressure 0.8 and the adsorption didn‘t exhibit a saturation limit, this behavior could be possibly explained by the fact that molecules water looking locations where they can establish bond to the preadsorbed water molecules or to both water molecules and surface site (Brennan et al. 2002).

Generally water adsorption onto activated carbon is strongly depend to pore size distribution and surface functional groups (Sonwane et al. 1998; Li et al. 2005). Moreover, ACs prepared from KOH chemical activation showing a hydrophilic surface that because the voids created by removing K is substituted by OH- functional groups after water washing, this finding explained the hydrophilic character of activated carbon chemically activated comparing to N-CO2-2h, also according to the lowest affinity coefficient (figure 63) of N-CO2-2h it is obvious that it has less hydrophilic character than the other carbon materials.

In addition, AC-HTC-180 has a slightly higher water uptake than AC-KOH-180-O3, although this finding is not really in agreement with previous study of (Rivera-Utrilla et al. 2011) which is demonstrated that modification of ACs by ozonation making its surface more hydrophilic but oxidation treatment of AC-HTC-180 fixed more carboxylic acids (which is the hydrophilic polar oxygen groups) (Mestre et al. 2007) and simultaneously destroyed the basic site therefore the sum of functional groups decrease and the carbon surface becomes less hydrophilic, on the other hand this finding is convenient with study carried out by (Li et al. 2005) where he reported that water coefficient affinity linearly increases with the sum of oxygenated functional surface groups and basic sites.

Furthermore, all prepared carbon showed a hysteresis loop contrary to N-CO2-2h exhibited negligible hysteresis which is suggested that the adsorption followed pores filling mechanism rather than capillary condensation for type V and II.

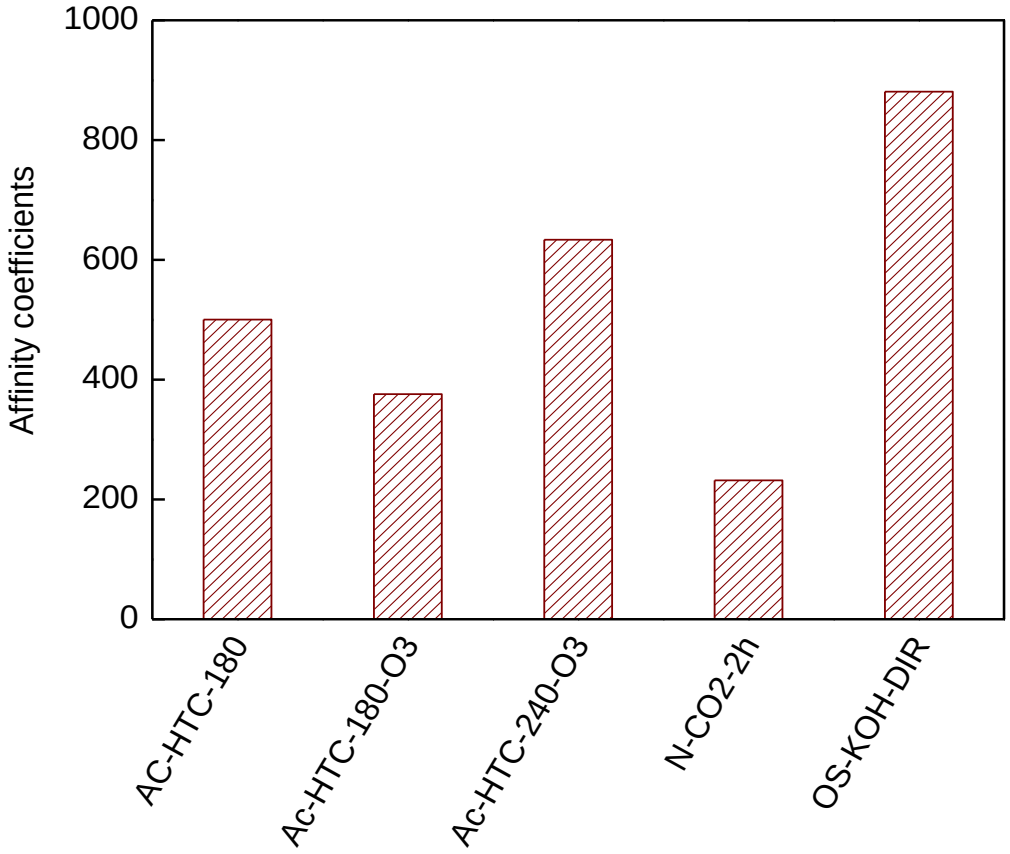

Figure 63: Water affinity coefficients

III.1 Summary

In the first section of this chapter, a various hydrochar were synthesized at different hydrothermal conditions HTC-180 (temperature 180°C and time6 h), HTC-240 (HT: temperature 240°C and time 6 h) and HTC-N (HT: temperature 180°C and time 6 h using ammonia 28%) and then used as started materials for activated carbon.

In the second part, HTC-180, HTC-240 and olive stones were selected to chemically activate with KOH and HTC-N were physically activated using CO_2. The activated carbon samples were characterized and the effects of HTC treatment on ACs were investigated. When hydrochar prepared at low HT severity (severity less than 5) were activated, the obtained AC had high surface areas, as high as 1215 m^2g^{-1} and narrow pores size distribution, in fact hydrochar synthesised at severity at higher than 6.5 are actually rich in lignin content of olive stone whose activation result fundamentally microporous carbon materials and usually release a high amount of gases during its pyrolysis which negatively affect the specific surface area. Moreover, increasing severity affect the surface chemistry of hydrochar and subsequently the ACs, this study shows that HTC is an effective technique to produce hydrophilic carbon

materials rich on oxygenated surface groups. To conclude HT process can strongly control the final physical and chemical properties of ACs, therefore HTC is potential methodology to produce tunable carbon materials and making them suitable candidates for various industrial applications such as adsorption, catalyst and storage.

Ozonation post-treatment of ACs significantly increases the specific surface area, the maximum obtained S_{NLDFT} was 1478 m^2g^{-1} and maximum of PSD was centred on 0.54 nm. In the next chapter, the ACs will be tested on adsorption of pharmaceuticals species and on hydrogengas.

Chapter IV: Application of HTC-Activated Carbon (Adsorption)

IV.1 Introduction

This chapter is divided into two parts, the first section being devoted to assess the efficiency of prepared activated carbon derived from hydrochar on one of the key environmental applications of carbon materials which is adsorption, two pharmaceuticals compounds (ibuprofen and metronidazole) had been chosen to study their adsorption onto AC-HTC-180 and AC-HTC-240, the kinetic data were modeled using Pseudo first order, pseudo second order and intraparticule diffusion models, in addition the obtained isotherm results were investigated in the Langmuir and Freundlich models. Both kinetic and isotherm studies had been performed at different temperatures range. The second part consists to study the adsorption of hydrogen onto the prepared activated carbon at 298K and 10 MPa.

IV.2 Adsorption experiments

Ibuprofen2-(4-Isobutylphenyl) propanoicacid) and metronidazole (2-Methyl-5 nitroimidazole-1-ethanol) were selected to evaluated the performance of AC-HTC-180 and AC-HTC-240 activated carbon samples. The kinetic experiments were carried out in a batch adsorption mode, a 25 mg of ACs with 50 ml of pharmaceuticals solution with varied concentration (50, 100 and 200 mg/l) of ibuprofen and (60, 90 and 120 mg/l) of metronidazole were shacked at a constant speed 300 rpm in 100 ml reagent flasks. The isotherm adsorption experiments were performed at different temperature 20, 30 and 50°C by adding 25 mg of ACs to initial concentration varied from 20 to 200 mg/l.

Ibuprofen and metronidazole were spectrophotometrically analyzed at wavelengths of 221 and 315 nm, respectively, using a Shimadzu UV-1700 Spectrophotometer and the adsorbed amount was calculated according to the following equation:

$$q_t = \frac{(C_0 - C)}{w} \times V \qquad \text{IV.1}$$

$$R(\%) = \frac{(C_0 - C)}{C_0} \times 100 \qquad \text{IV.2}$$

Where qt is the adsorbed amount of pharmaceutical compound (mg/g), V is the volume of solution (ml), C_0 is the initial concentration (mg/l) and C the concentration at time t and w is the weight of ACs.

The main characteristics of adsorbent and pharmaceuticals are shown in table 12 and figure 64, respectively.

Table 12: Characteristics of activated carbon used in the adsorption experiments

	AC-HTC-180	AC-HTC-240
Specific surface area (m^2g^{-1})	1217	537
Total pore volume (cm^3g^{-1})	0.43	0.22
Micropore volume (cm^3g^{-1})	0.39	0.16
Mesopore fraction (%)	9.5	27.9
pHpzc	9.2	9.8
Amount of basic groups ($meqg^{-1}$)	0.5	0.4
Amount of acid groups ($meqg^{-1}$)	0.245	0.09

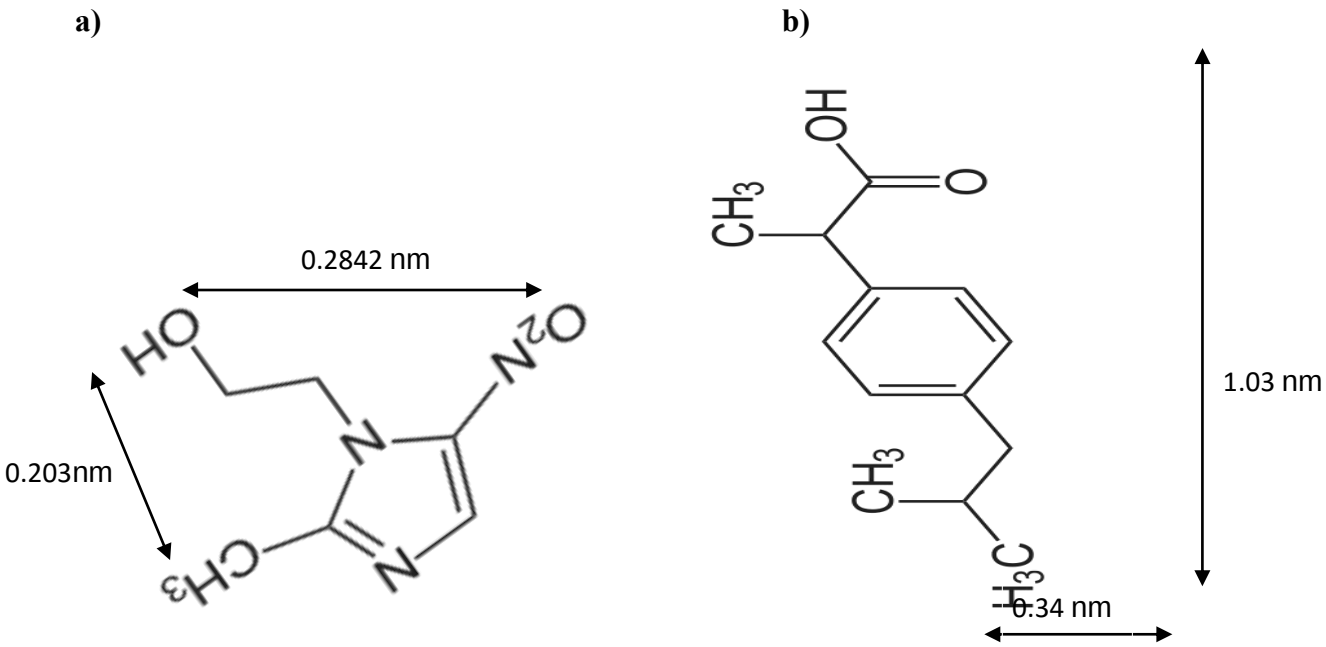

Figure 64: The optimized geometries of Ibuprofen (a) and metronidazole (b), calculated by ChemSketch software after 3D optimization

IV.2.1 Adsorption Kinetic

IV.2.1.1 Equilibrium time

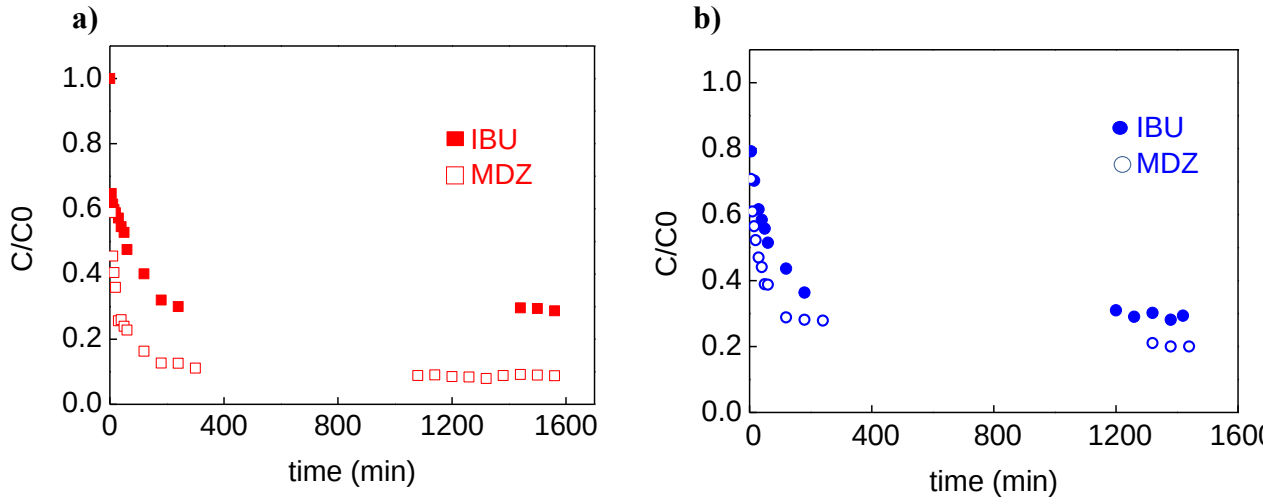

Figure 65: Adsorption kinetic tests for equilibrium time determination for the IBU (a) and MDZ (b)

The kinetic investigation is important to determine the equilibrium time and elucidate the adsorption mechanism. The necessary time to achieve the equilibrium of adsorption was determined by varying the contact time among the activated samples (AC-HTC-180 and AC-HTC-240) and pharmaceuticals solutions for up to 24 hours (figure 65). The removal percentage were increased only by 2% and 6% from 5h to 24 h for IBU adsorption and by 2.2 to 5% for MDZ in the same period of time onto AC-HTC-180 and AC-HTC-240 respectively, therefore it is considered that equilibrium has been reached at 5 hours.

IV.2.1.2 Effect of initial concentrations

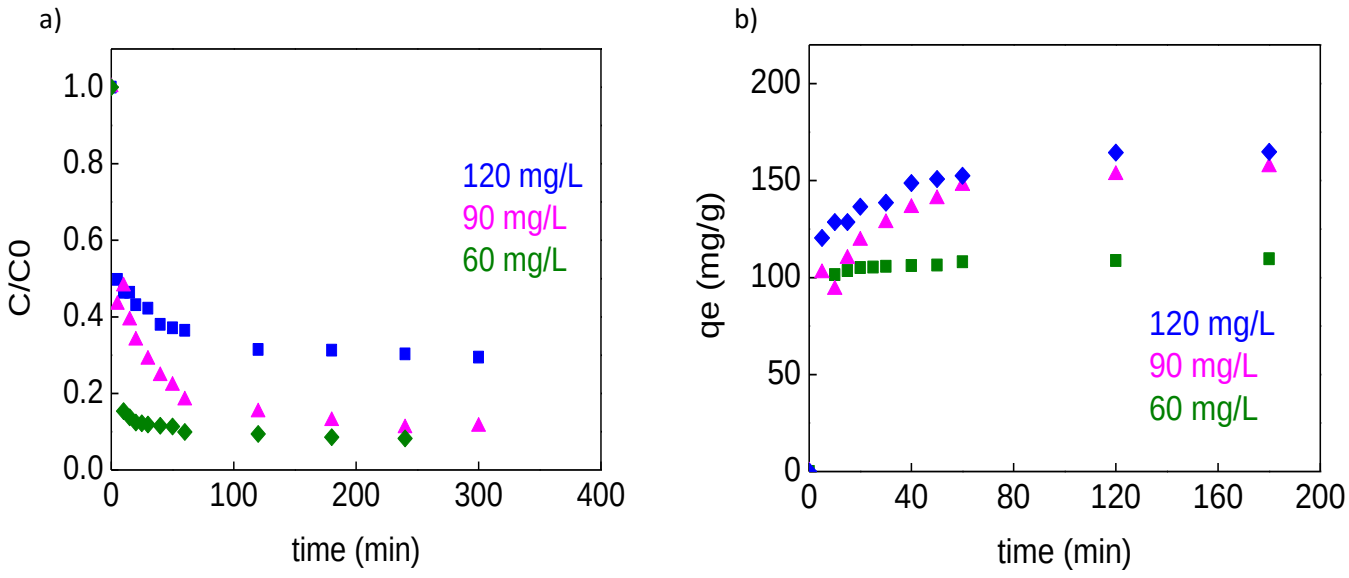

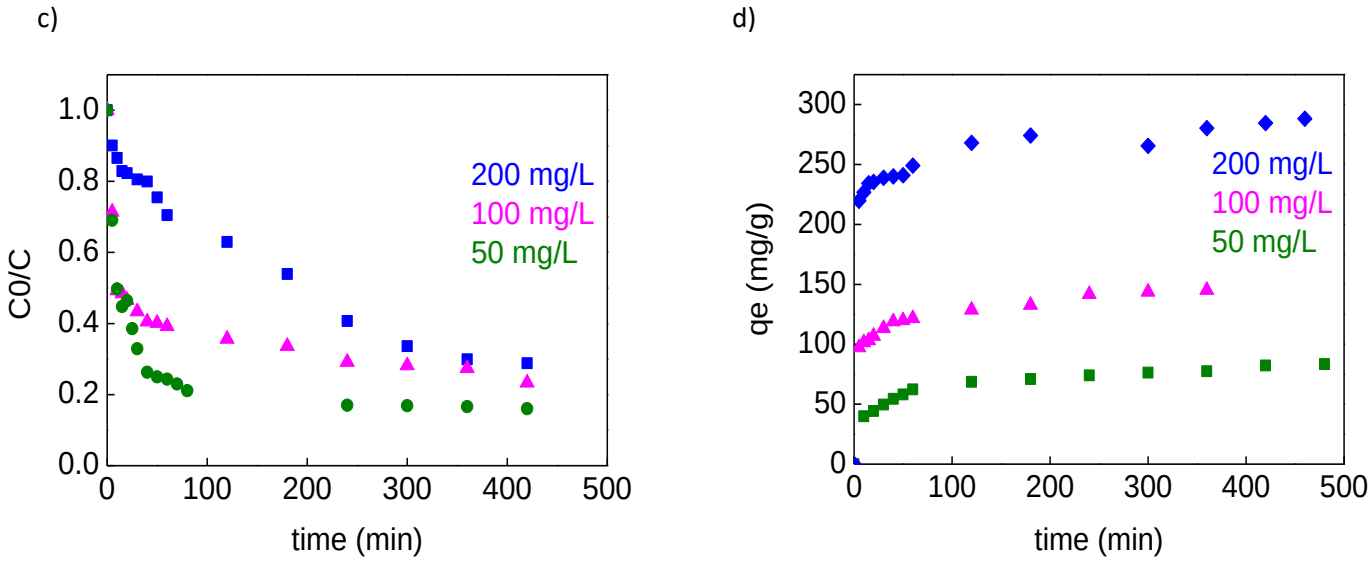

Figure 66: Kinetic of IBU and MDZ onto AC-HTC-180

The adsorption of medicines onto activated carbon was studied for different concentrations 50, 100 and 200 mg/L of IBU and 60, 90 and 120 mg/L of MDZ. The experiments were carried out under constant conditions using 0.25 g of AC and temperature 20 °C. As the initial concentration increases from 50mg to 200 mg/L and from 60 to 120 mg/L for IBU and MDZ, the adsorption capacity increase from 84 mg/g to 265,192 mg/g and from 113.6 mg/g to 169.27 mg/g in case of adsorption onto AC-HTC-180 (figure 66), these results demonstrate that the initial concentration C_0 promotes the adsorption uptake by adding a potential driving force to overcome the mass transfer resistance exist between the solid and aqueous phase (Tsai et al. 2004, 2006; Mestre et al. 2007), the maximum removal efficiency of IBU and MDZ onto AC-HTC-180 were 84 % and 92 % respectively.

The adsorption results onto AC-HTC-240 are shown in figure 67, the removal efficiency for the same drugs concentration described above were 97% and 71% for IBU and MNZ, the kinetic is rapid in the few first minute, similar to the pervious kinetic study onto AC-HTC-180, these kinetics behavior are expected because in the first few minute an important number of vacant surface site are accessible for adsorption during the first stage and then the vacant active site get occupied, the access to the pore started to be difficult because of the repulsive forces between the solute molecules on solid and in the bulk liquid phase. AC-HTC-180 showed a better removal efficiency of MDZ or AC-HTC-240 is better adsorbent for IBU, although this material present lowest physical properties comparing to AC-HTC-180.

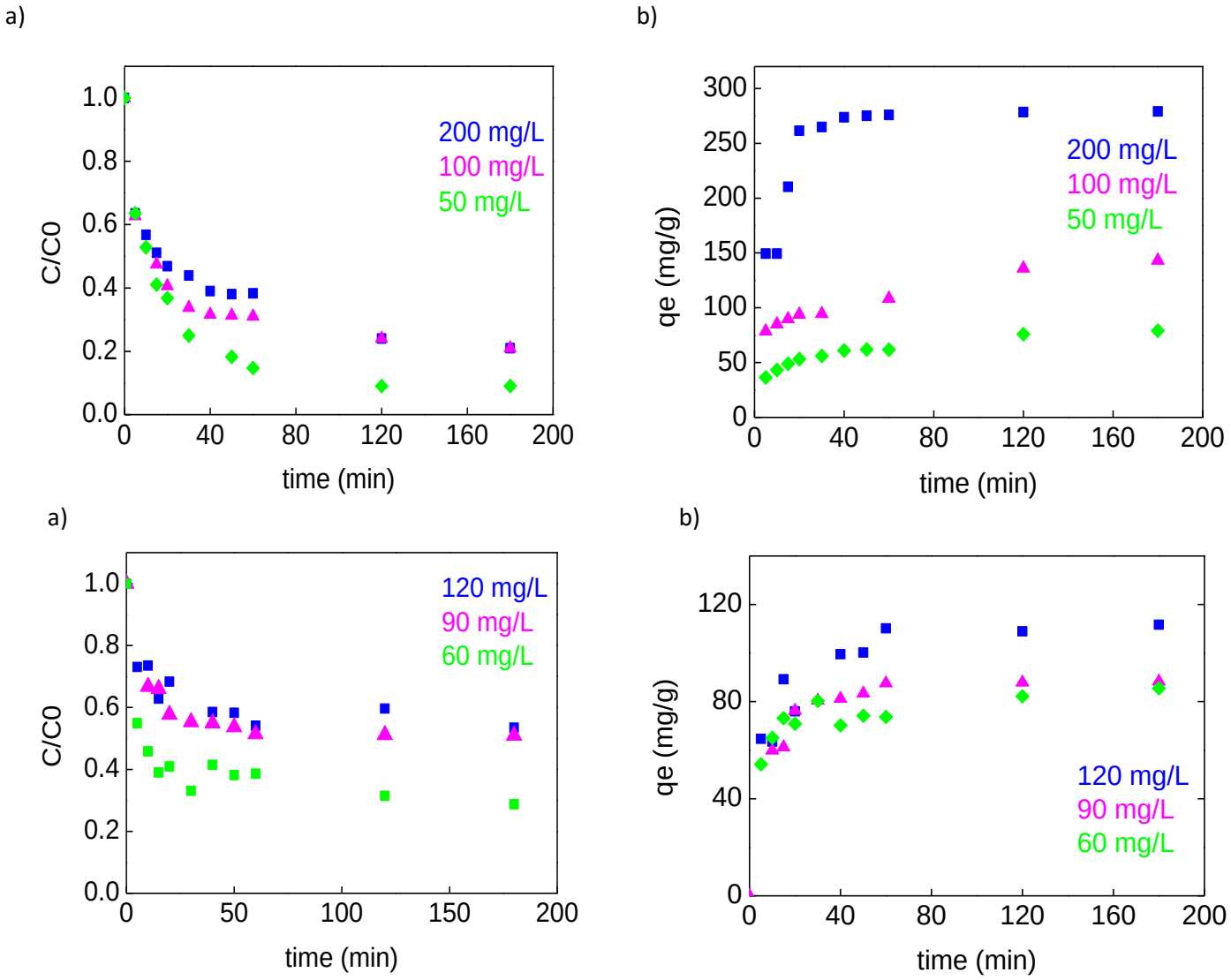

Figure 67: Kinetic IBU and MDZ onto AC-HTC-240-KOH

IV.2.1.3 Kinetic Models

The kinetic model is crucial to predict the mechanism of transport of molecule from liquid phase to the solid, to determine the key parameters monitoring the adsorption and to assess the performance of the adsorbent; the kinetic data were submitted to three models, pseudo-first order, pseudo-second order and intra-particular diffusion, which are commonly used to explain the adsorption behavior. Generally, adsorption mechanism is strongly depending on fluid-solid mass transport and on physicochemical properties of the adsorbent.

IV.2.1.3.1 Pseudo-first order and Pseudo-second order

The fitting of the pseudo first order, pseudo second order kinetic model and the experimental results are depicted in figure 68 and 69 where the first pseudo order data are shown as dash line, the pseudo second order data are displayed as solid lines and the experimental are

represented as full square symbol. The computed parameters from equation 4 and 5, K1 (min^{-1}), K(mg $g^{-1}min^{-1}$), $q_{e,cal}$ (mg g^{-1}) and regression coefficient (R^2) are presented in table 13. As shown in figures 68 and 69, the pseudo first order didn't show a good fit for the experiments adsorption data, also the regression coefficient is equal or less than 0.86 and in some case (0.52) that refers to unfavorable correlation, moreover it is well known in the literature that the pseudo first order model can describe only the adsorption in the first 40 min (Tran et al. 2017), therefore it can be concluded that the pseudo-first order is not adequate to fit the kinetic results of the varied initial concentration.

Table 13: kinetic parameters of pseudo first order and second order

		Pseudo first order			Pseudo second order		
	Concentration (mg/l)	K_1 (min^{-1})	$q_{e,cal}$ (mg g^{-1})	R^2	K (mg $g^{-1}min^{-1}$)	$q_{e,cal}$ (mg g^{-1})	R^2
IBU 180	200	0.007	72.67	0.96	0.00034	250	0.99
	100	0.009	62.05	0.86	0.0008	142.86	0.99
	50	0.002	40.97	0.96	0.0014	90,90	0.99
MDZ 180	120	0.005	44.7	0.86	0.0004	200	0.99
	90	0.008	45.97	0.89	0.00084	166.67	0.99
	60	0.004	9.31	0.86	0.0067	111.11	0.99
IBU 240	200	0.076	195.92	0.95	0.00047	333,33	0.99
	100	0.018	75.19	0.95	0.0006	146,67	0.99
	50	0.007	44.92	0.94	0.001	83,33	0.99
MDZ 240	120	0.012	63.75	0.83	0.0012	111.11	0.99
	90	0.002	45.15	0.52	0.0015	100	0.99
	60	0.019	33.65	0.98	0.002	90.90	0.99

The second order assumes that the rate of sorption follow second order reaction and the adsorbed molecule occupied two sorption site onto the adsorbent surface (Sepehr et al. 2016).

According to the fitting results, it is obviously that the adsorption of IBU and MDZ onto both activated carbon samples obeys to pseudo-second order model, as shown in the figure 68 and 69 the curves obtained by the pseudo second order data practically coincide with the experimental indicating a successful description for adsorption kinetic. In addition, the correlation coefficients values were as high as 0.99 meaning that the this model is the most appropriate way to fit the adsorption kinetic for all medicines used in this study, similar results have been reported for both drug by (Çalışkan and Göktürk 2010; Essandoh et al. 2015; Khazri et al. 2016; Banerjee et al. 2016). According to the data depicted in table 13 the pseudo order rate constant (K) decrease as the initial concentration increase, on the other hand in case of IBU adsorption onto AC-HTC-180, the value of K is slightly higher than that of AC-HTC-240 in the most of experience, this finding confirm that AC-HTC-240 is better adsorbent for IBU, although this material exhibits a poor textural porosity.

a)

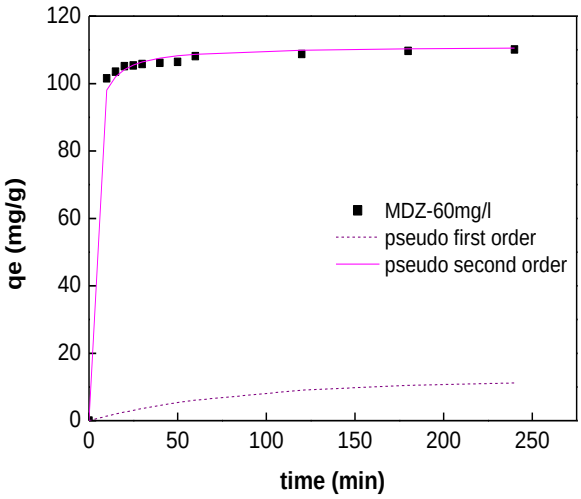

b)

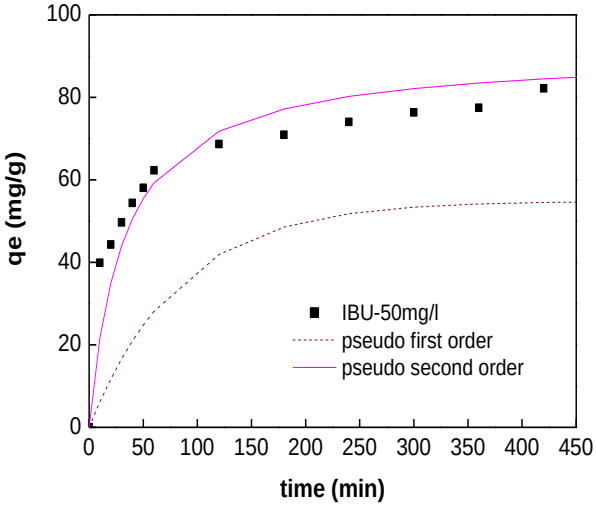

c)

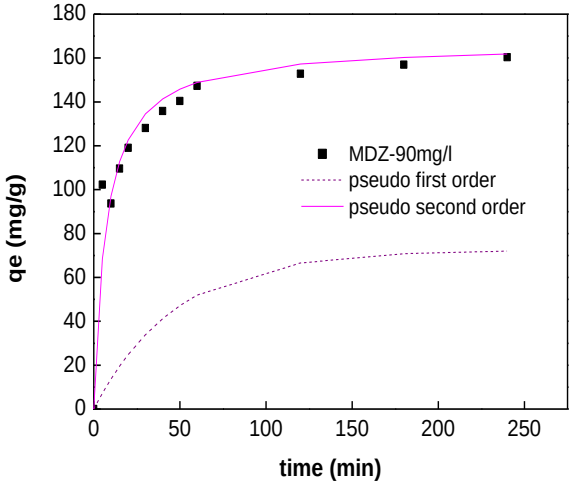

d)

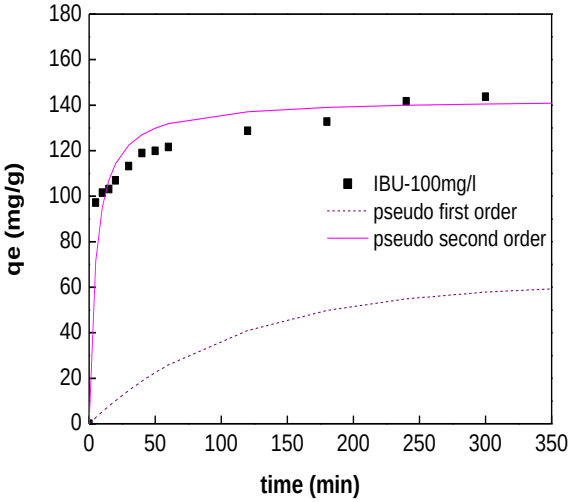

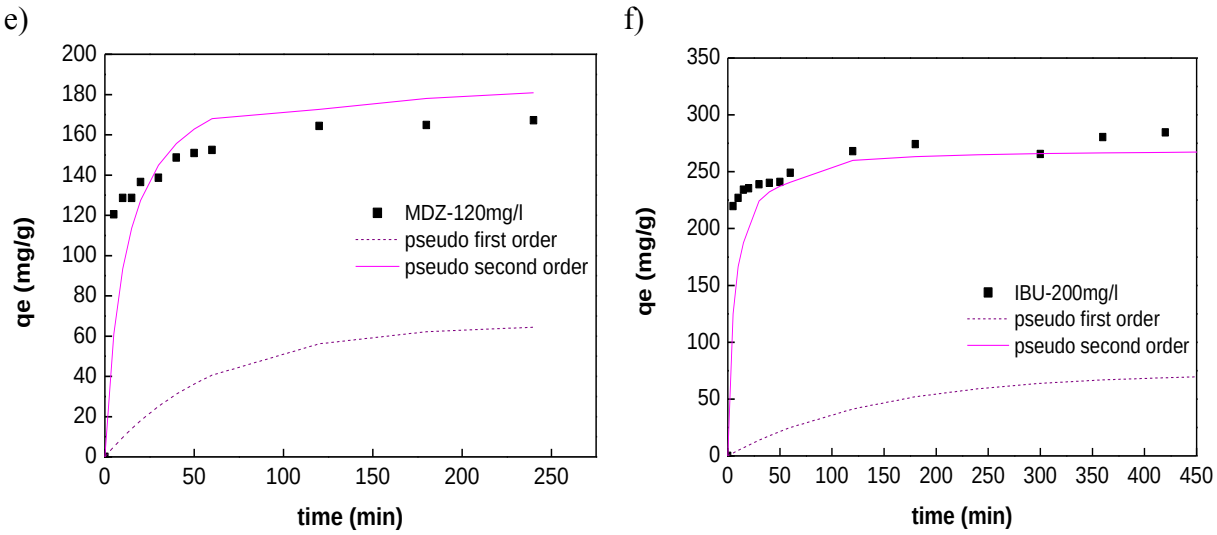

Figure 68: The first pseudo order model fitting of IBU and MDZ adsorption onto AC-HTC-180

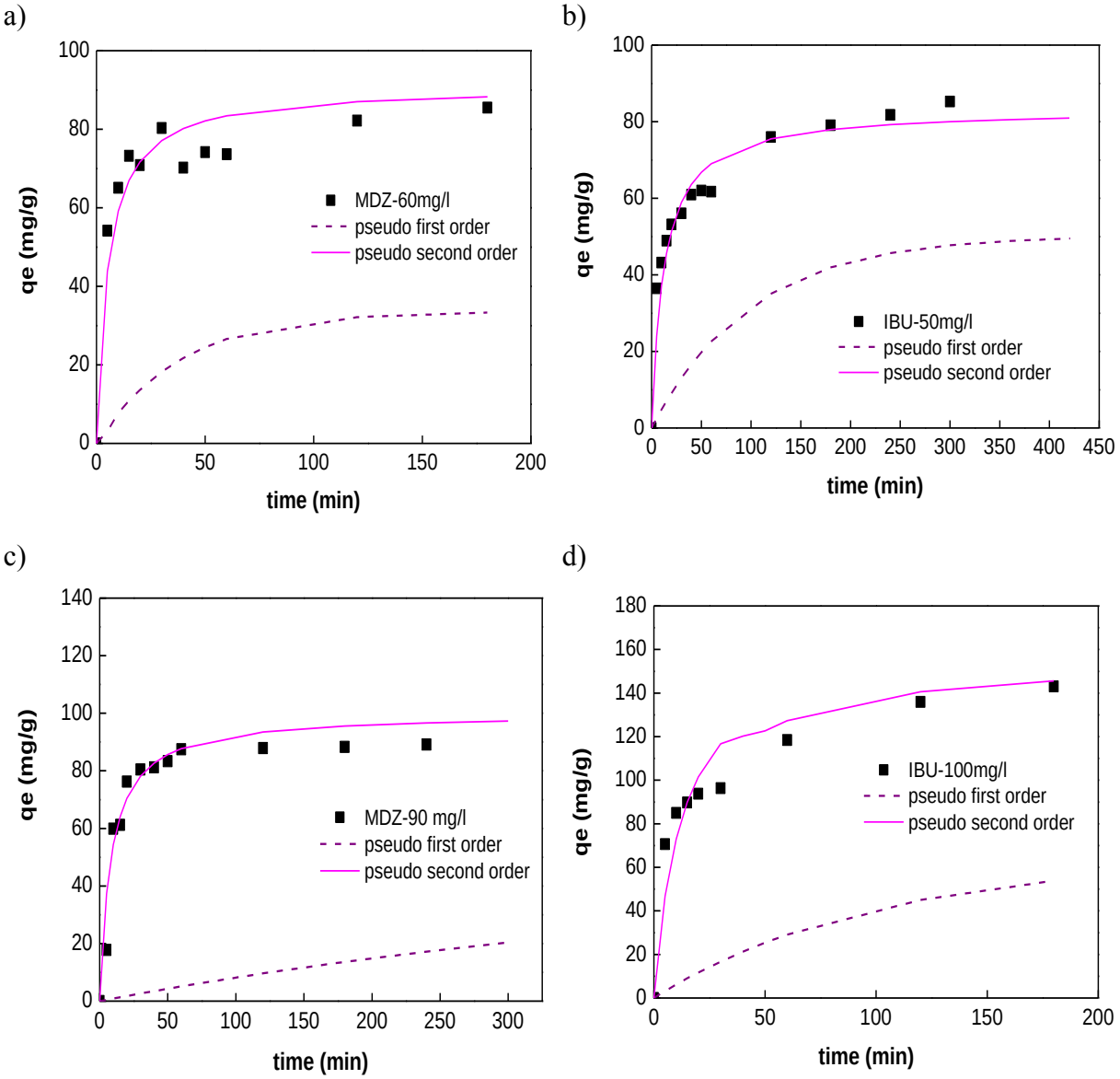

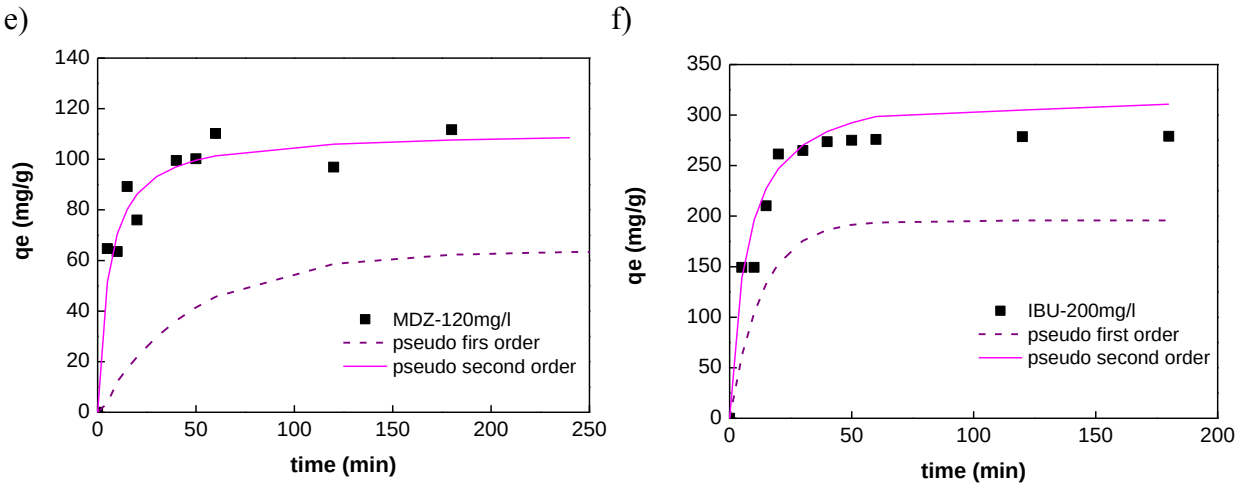

Figure 69: The first pseudo order model fitting the first pseudo order model fitting of IBU(b,d and f) and MDZ (a,c and d) adsorption onto AC-HTC-180

Similar observations in case of MDZ adsorption onto AC-HTC-240-KOH the value of K is mostly higher than AC-HTC-180 that means a more amount of AC-HTC-240 is needed to obtain the same results. According to this finding, it is possible to predict that the surface chemistry has a determinant effect on the adsorption capacity. Actually, the pHpzc of both ACs are higher than pH of solution of IBU (weak acid pH≈5), therefore both of ACs samples possessing excess of positive charge at the edge of its graphene layers, thus being notably advantageous to bound negatively charged organic molecules. But, according to Boehm titration results, AC-HTC-180 contains the highest amount of total acidic sites particularly high phenolic compounds, and the oxygen group in ACs draws the p-electron from of the aromatic rings, such behavior minimize the dispersive interactions between the p-electrons of the aromatic ring of IBU and graphene planes of carbon materials (Mansouri et al. 2015), therefore the repulsive electrostatic interactions between the surface groups of AC-HTC-180 and IBU molecules reduce the adsorption capacity. Moreover, theoretically IBU cannot be accommodated into both ACs ultramicropores due to its big size (length 1.03 nm and thickness (0.43nm), figure 64 a), but in previous research made by (Guedidi et al. 2013; Bahamon et al. 2017), it has been demonstrated that the benzene ring of the IBU can be enter longitudinally across its length, in addition AC-HTC-240 has a higher fraction of mesopores 27% (table 12), consequently IBU can be easily filled in the pore channels. Also it is important to mention that the hydrophilic character of AC-HTC-180 enhance the development of water clusters (forming on the oxygen group through H-bonding) at the entrance of pore that decrease the affinity and accessibility of IBU to the internal porous structure of ACs (Franz et al. 2000; Brennan et al. 2002).

IV.2.1.3.2 Intaparticule diffusion model

For the sake of the investigation of the diffusion mecanism, the experimental data were analyzed using the intraparticule diffusion model, the graphic results are depicted in figure 70 and the parmaters value in table 14. Actually, The adsorption process is affected by such factors as the characteristics adsorbate and the solution phase (concenration of adsorbate), the adsorbent(the pore geometriesand size), diffusion coefficient and the affinity between the adsorbent and the adsorbate are keys factors should be taken into considerationin the description of mechanism (Suresh et al. 2013). The intraparticule model can be defined by one, two or three steps. In case of one linear plot of qt versus $t^{0.5}$ then the adsorpion is assumed to be controlled by intra particle diffusion, it is possible that the plot exihbit three sections but this isnot the case of this study as seen in the figure 70 the data display two straigt linar plots, therefore the adsorption process is affected by two steps, otherwise the exernal surface adsorption is relatively quiet rapid as the first linar didn‘t appear in the graphs.

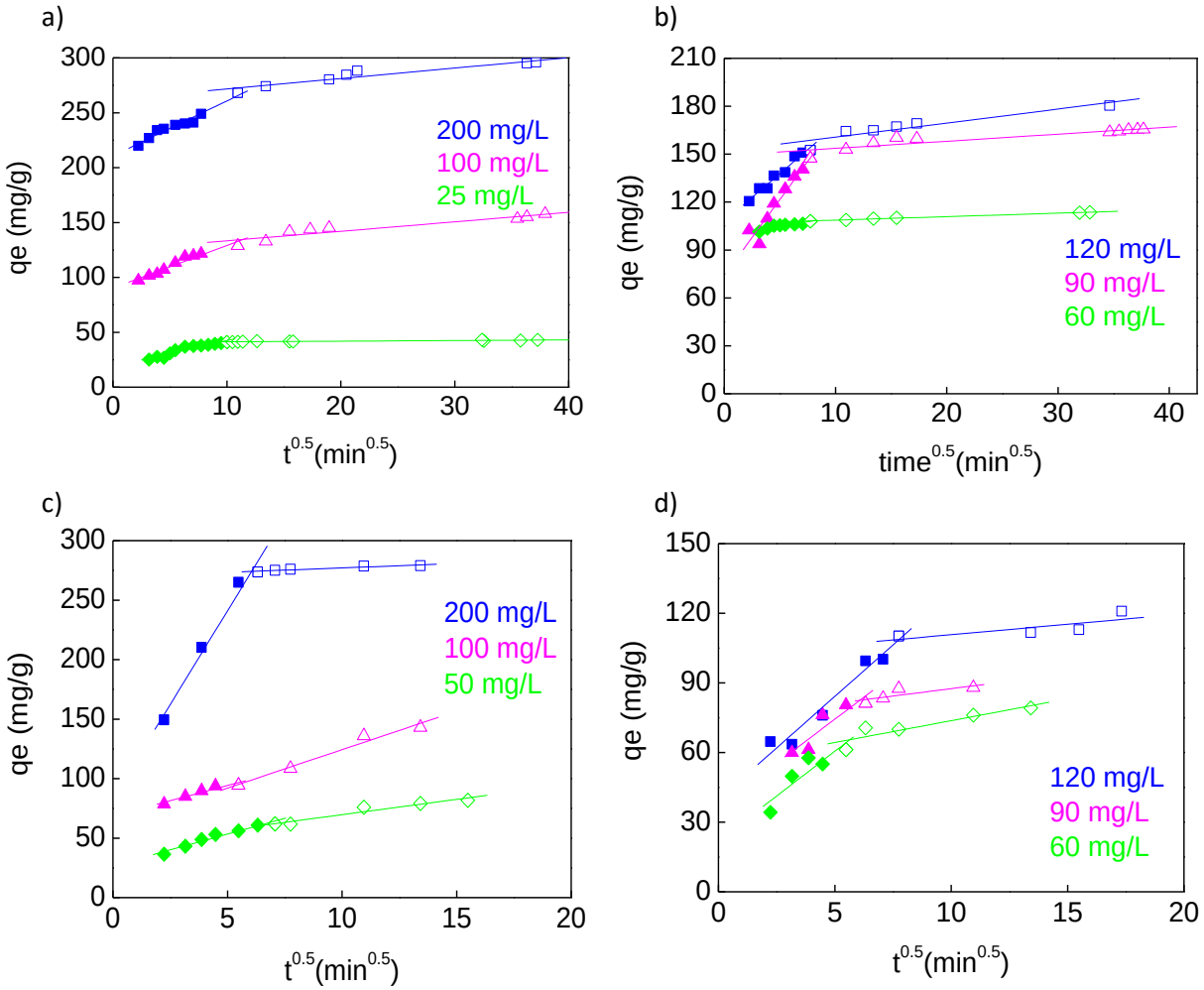

Figure 70: The intra-particle fitting of IBU and MDZ adsorption onto AC-HTC-180 and AC-HTC-180

All the intra-paarticule curves follow the same trend.The slope of the twosections are presented as a rate parameters (kp1,kp2) and are characteristics of the rate of adsorption in the region where intraparticule diffusion is rate controlling. The first section is attributed to the boundray layer effect and the second portion is reffered to the intra-particule diffusion (Abdel-Ghani et al. 2016). As shown in the figure 70 the first linear part didn‘t pass through the origin then it could be preddected that the adsorption of both medicins sepecies has a complex mecanism and the intra-particule diffusion is not the only decisive controlling step. The high correlation coefficient R^2 values reflect a strong relationship between qt and square adsorption time, the two parmaeters K_{d1} and K_{d2} were determined respecively from the first and second sections of the plots. In all adsorption experiment, the diffusion rate constants K_{d1} is higer than K_{d2} that could be explained by the high number of pore available to retain IBU and MNZ and after about 25 min almost in all case the pore probabely get bloked or the adsorbed molecule exert an steric hindrance on the solid surface.

The inercepts of the linear sections with y-axis provides the mesure of the boundary (or film layer) thickness –C". the boundary thickness values increase as the initial concentration increase, which reflect a greater effect of the external diffusion (or film diffusion) on the adsorption process.

Table 14: kinetic parameters of intraparticule diffusion model

	Inra-partcular Diffusion					
	First section			Second section		
Parameters	K_{p1} (mg/g/min^{½})	C (mg/g)	R^2	K_{p2} (mg/g/min^{½})	C (mg/g)	R^2
Concentration (mg/l)	IBU180					
200	5.005	210.74	0.98	0.95	262.24	0.95
100	3.88	90.24	0.97	0.86	124.69	0.94
50	2.36	18.88	0.96	0.058	40.72	0.89
	MDZ180					
120	5.99	107.88	0.98	0.88	151.85	0.92
90	9.52	74.02	0.96	0.44	149.18	0.91
60	1.17	98.95	0.93	0.216	106.54	0.99
	IBU240					
200	31.46	83.69	0.989	0.73	269.71	0.96
100	6.78	68.66	0.99	6.46	59.69	0.98
50	5.29	26.87	0.98	2.57	43.98	0.97
	MDZ240					
120	8.87	39.79	0.98	2.26	89.94	0.85
90	7.58	36.43	0.91	3.25	59.61	0.96
60	7.72	21.94	0.9	1.88	54.87	0.91

IV.2.1.4 Effect of temperature on Ibuprofen and Metronidazole adsorption

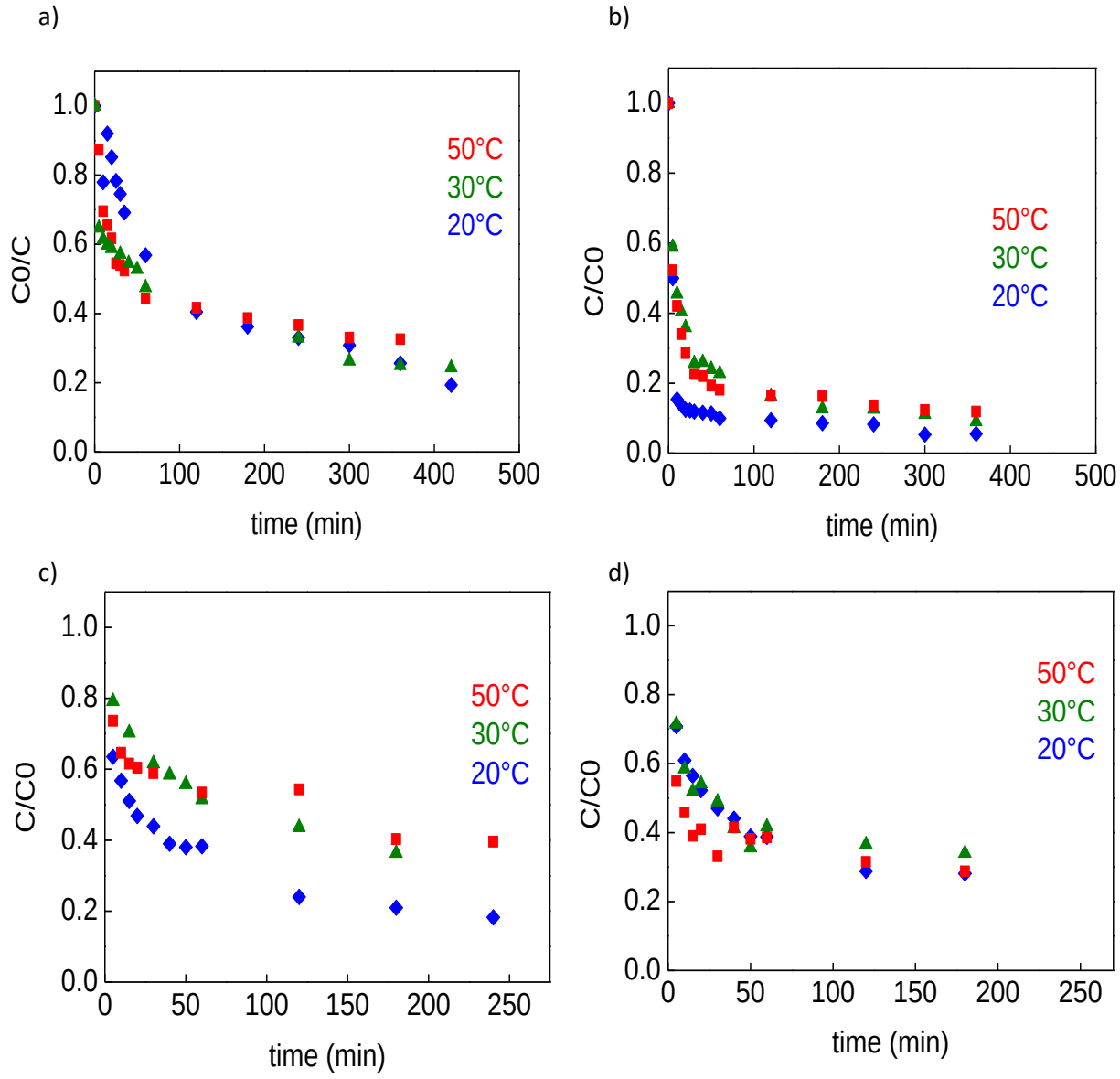

Figure 71: Adsorption isotherm of ibu (a,b) and MDZ (c,d) onto AC-HTC-180 and AC-HTC-240, respectively

The adsorption kinetics were carried out at temperatures 20, 30 and 50°C, while the volume of solution (50 ml) and carbon dose (25 mg) were kept unvaried, the initial concentration were 50 mg/L and 60 mg/l for ibuprofen and metronidazole, respectively. A remarkable decrease of both drugs concentration during the first 60 min, C/C0 ratio dramatically decreases from 0.79 to 0.40 and from 0.63 to 0.38 in case of IBU, and MDZ C/C0 ratio is decreases from 0.58 to 0.22 and from 0.71 to 0.39 for AC-HTC-180 and AC-HTC-240 respectively at 20°C. The maximum removal efficiencies were determined by AC-HTC-180 sample is 81% and 91% for IBU and MDZ. Generally temperature has an effect on the

adsorption process, but as shown in the figure for both molecules temperature didn‘t have a perceptible effect for almost all adsorption assays only AC-HTC- 240 made the exception in case of IBU at 20°C the result displayed in the figure 71 (c), which shows an increase in the adsorbed amount. These results are in agreement with those finding obtained by (Mestre et al. 2007; Essandoh et al. 2015) who found that ibuprofen adsorption is unaffected by temperature range between 25 and 40°C, the same result even noticed in case of other medicine adsorption onto activated carbon such as paracetamol (Villaescusa et al. 2011; Baccar et al. 2012).

IV.2.2 Adsorption Isotherm

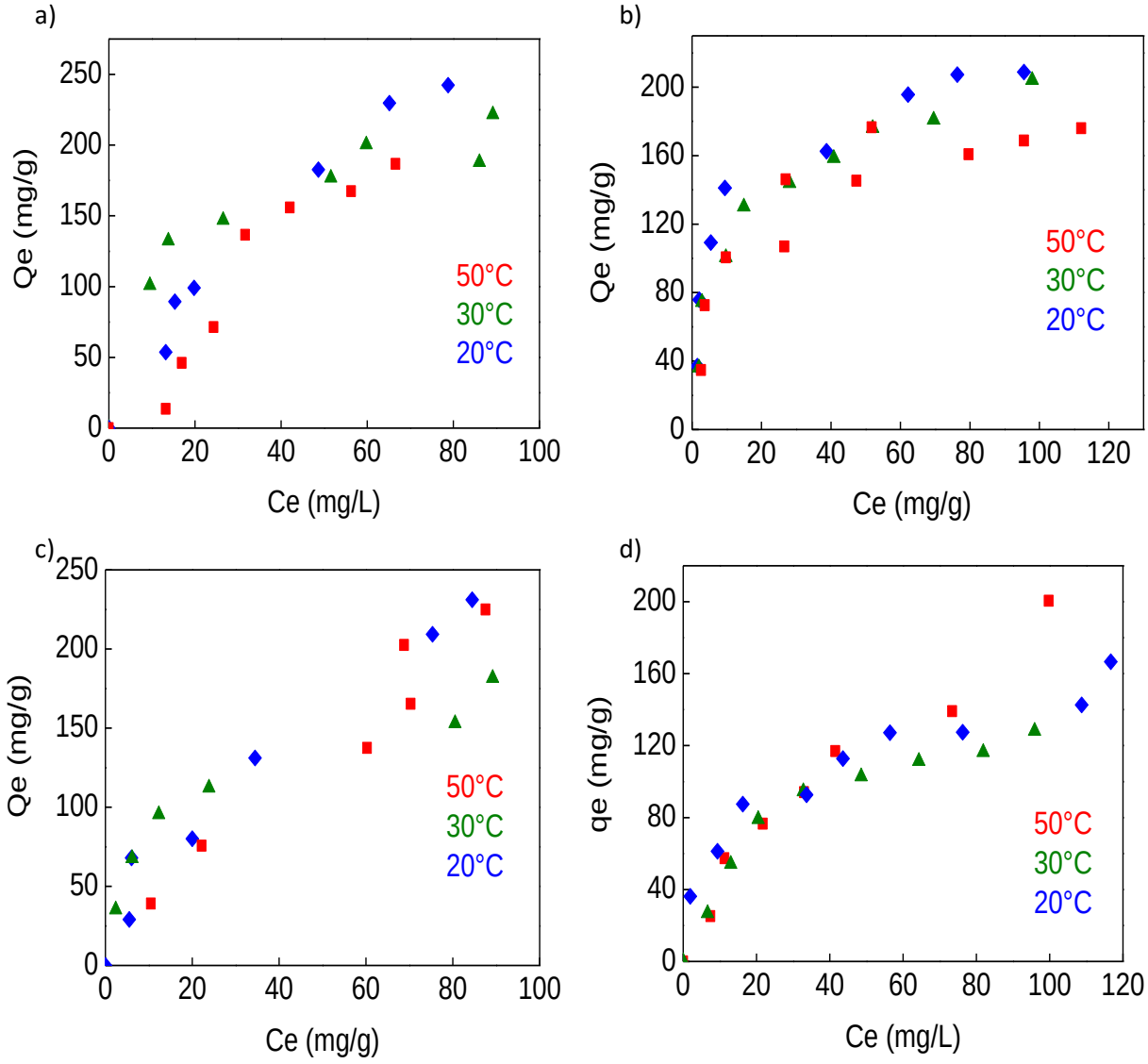

Figure 72: Adsorption isotherm of IBU (a,c) and MDZ(b,d) onto AC-HTC-180 and AC-HTC-240

The adsorption isotherms of IBU and MDZ onto AC-HTC-240 and AC-HTC-180 were studied at different temperatures 20, 30 and 50°C for 24 h. As seen in the Figure 72 the

temperature has not noticeable effect on the adsorption isotherms, this is in agreement with the previous kinetic and some of literature results, almost all of them belong to the L type according to the Giles classification. In case of adsorption into AC-HTC-180 the isotherms curves show a low concave curvatures this means that the adsorbed amount regularly increase therefore the saturation on surface didn‘t attain (L1-ype) and as the curves didn‘t show a plateau that means no limited sorption capacity and there is an important ability of deep removal of both IBU and MDZ medicines from aqueous solution (Bembnowska et al. 2003; Mestre et al. 2009). The adsorption onto AC-HTC-240 (figure 72 c and d) exhibits initial curvatures indicating that as the number of the filled site increase as the free solute molecules found difficulty to reach the vacant site available (Giles et al. 1960), during this first stage (Ce<60 mg/L for IBU and Ce<80 mg/L for MDZ) the adsorption is favorable correspond to monolayer adsorption and then the curve present an inflection point at high equilibrium concentrations due to change from plateau to an unfavorable shape because of the blockage of the pores, the monolayer followed by multilayer formation correspond to L3-type according to Giles classifications (Villaescusa et al. 2011).

IV.2.2.1 Isotherm Model

In order to have a deep knowledge about the adsorption mechanism, many equilibrium models have been developed relating the adsorbed amount to the concentration. Langmuir and Freundlich are the most commonly used models. The Langmuir model (theoretical) describes the monolayer adsorption, it represents the equilibrium distribution of the solute between the solid and liquid phase. Freundlich model (empirical) represents the multilayer adsorption with interaction between the adsorbed molecules on a heterogeneous surface. All experiments data of the IBU and MDZ adsorption onto AC-HTC-180 and AC-HTC-240 are displayed in figures73 and 74 respectively and the parameters results of are shown in table 15.

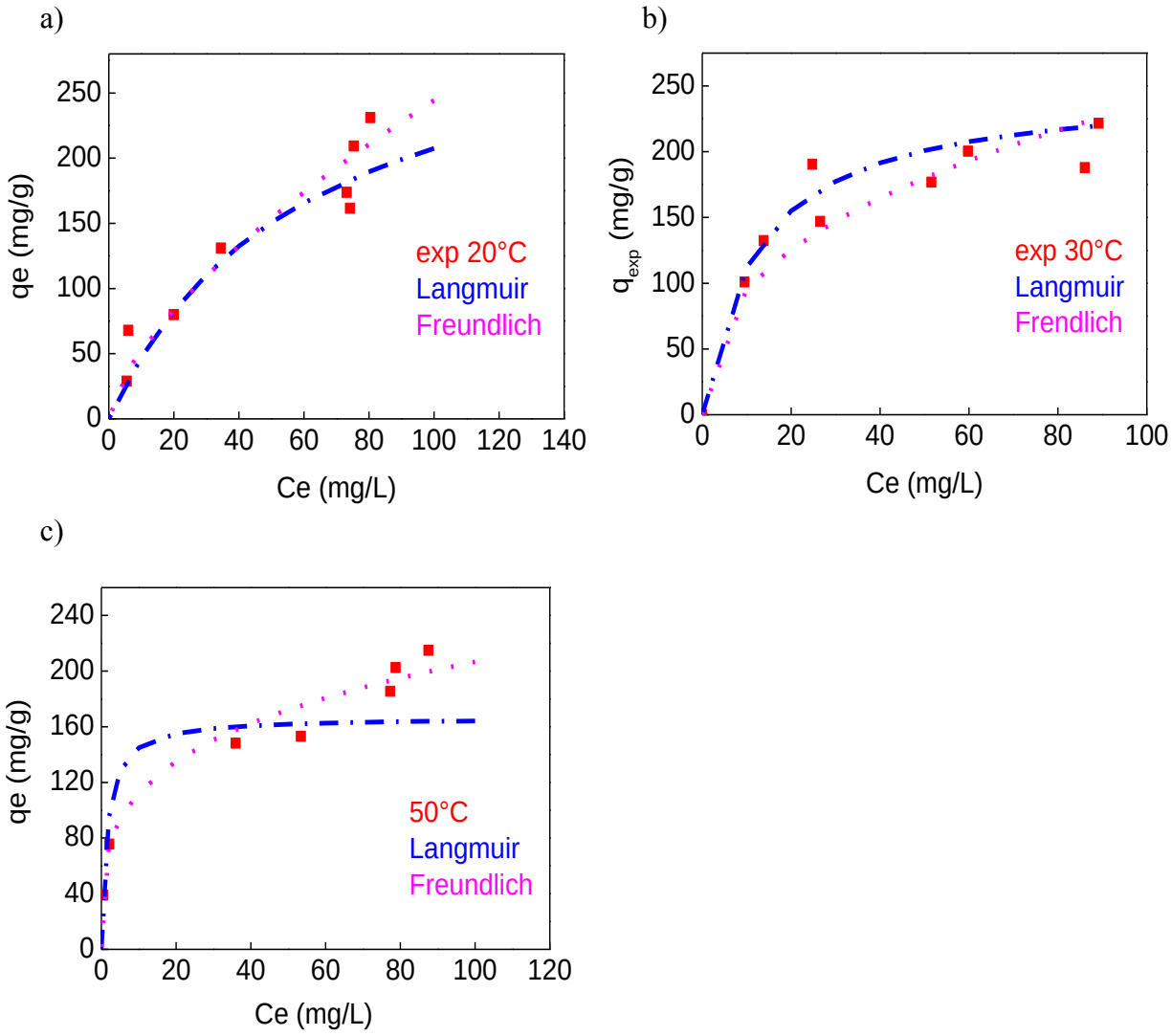

Figure 73: Experimental IBU adsorption isotherms at 20 °C (a), 30°C (b) and 50°C (c) onto AC-HTC- 180 presenting the fitting of Langmuir and Freundlich models to the experimental data

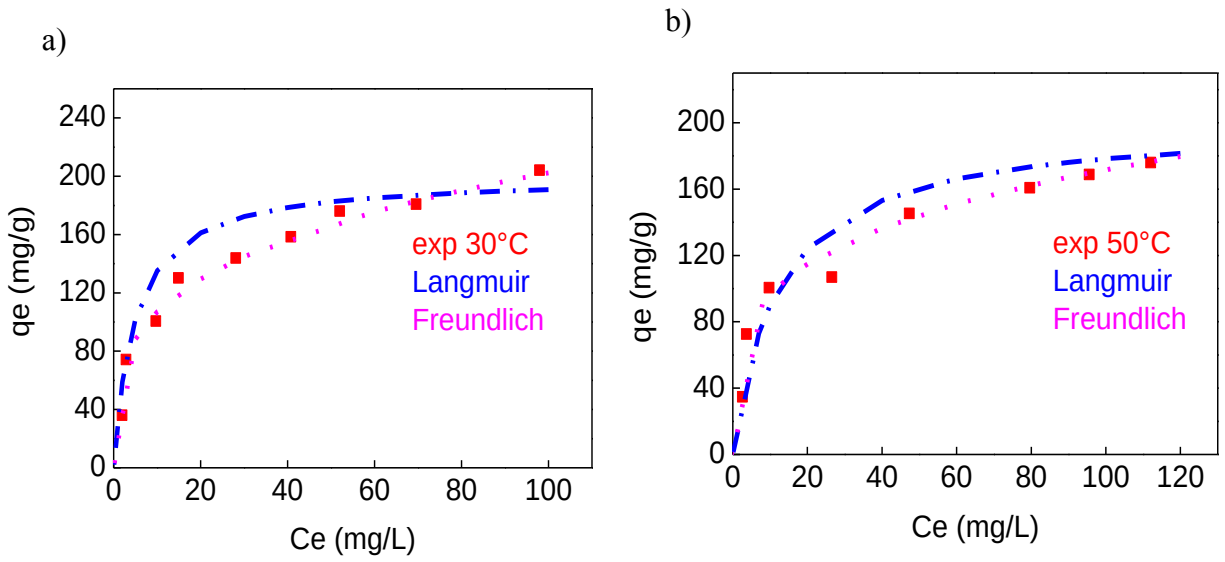

c)

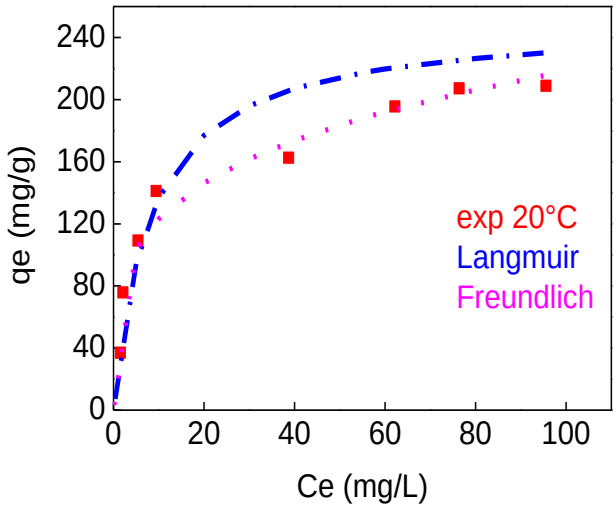

Figure 74: Experimental of MDZ adsorption isotherms at 20°C (a), 30°C (b) and 50°C (c) onto AC-HTC- 180 presenting the fitting of Langmuir and Freundlich models to the experimental data

Table 15: Langmuir and Freundlich isotherms parameters of IBU and MDZ adsorption onto AC-HTC- 180

		IUB-180			MDZ-180		
	Tempreture (°C)	20	30	50	20	30	50
Langmuir	qmax (mg/g)	500	250	500	250	200	200
	Kl (l/mg)	0.016	0.08	0.021	0.12	0.208	0.08
	R^2	0.89	0.87	0.94	0.95	0.9	0.98
Freundlich	K_f (l/mg)	18.17	45.65	20.93	65.56	56.49	54.27
	n_f	1.64	2.83	1.66	3.86	3.6	4
	R^2	0.93	0.99	0.94	0.98	0.98	0.99

Generally, high correlation coefficients of IBU and MDZ adsorption isotherms were obtained for both Langmuir and Freundlich models. It is important to determine the most adequate

correlation with experimental data to establish the adsorption system. But it would be difficult and not sufficient to make choice of model only based in the determination coefficients.

MDZ and IBU adsorption isotherms onto both activated carbon and the fitting of the two isotherm models are depicted along with the experimental values. It could be clearly observed that the fitting of Freundlich models and the experiments curves are perfectly coincident, therefore it is possible to deduce that Freundlich model is more suitable to describe the adsorption of MDZ onto AC-HTC-180 and AC-HTC-240. On the other hand, the dimensionless constant of Freundlich model ~~n~~", which is referred to the adsorption intensity or surface heterogeneity, it shows~~1~~/n" value varied from 0 to 1 for all adsorption experiments and that suggest a favorable adsorption.

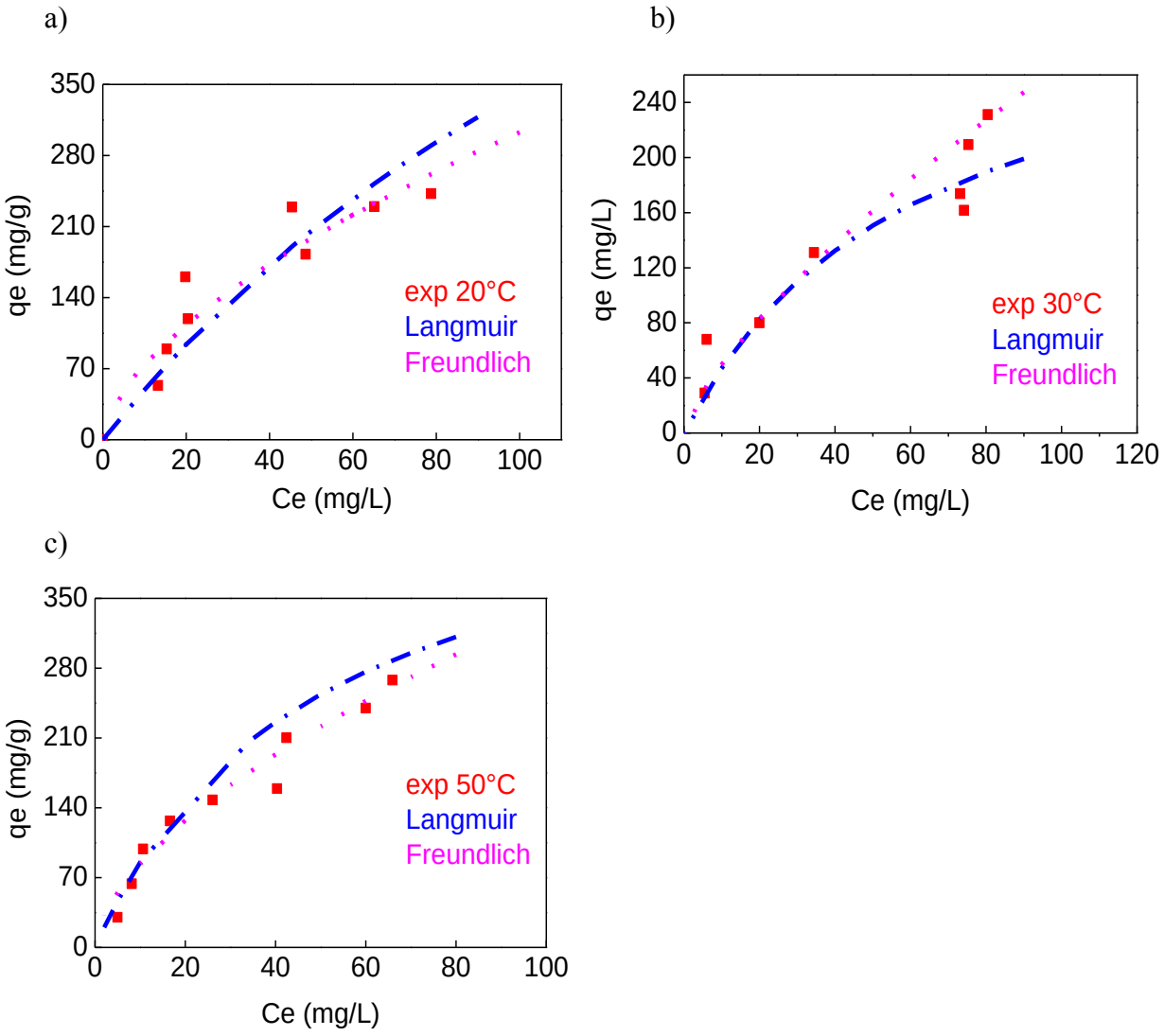

Figure 75: Experimental IBU adsorption isotherms at 20°C (a), 30°C (b) and 50°C (c) onto AC-HTC- 240 presenting the fitting of Langmuir and Freundlich models to the experimental data

The activated carbon prepared from hydrochar at low HT temperature (180°C), AC-HTC-KOH-180 shows high removal capacity of MDZ (208.86 mg/g at 20°C, 204mg/g at 30°C and 176.95 mg/g at 50°C) than AC-HTC- 240 (166.67 mg/g at 20°C, 152.49 mg/g at 30°C and 200mg/g at 50°C), actually, as has been discussed in the previous chapter (chapter 3),AC-HTC- 180 has a much higher pore volume (0.429 cm^3/g) and surface area (1209 m^2g^{-1}) which absolutely enhance the adsorption of the small sized molecules (MDZ), in fact the porosity of AC-HTC- 180 is not the only features of this ACs, also it possesses a high oxygen groups content mainly phenolic groups, which are strong electron activators that the delocalization of the π electron direct the electron toward the aromatic rings of carbon graphene planes, this improves the adsorption of aromatic compounds as metronidazole by enhancing the dispersion interactions and hydrogen bonds (Rivera-Utrilla et al. 2017).

The maximum removal of IBU onto AC-HTC-240 activated carbon samples at 20, 30 and 50°C were 242 mg/g, 221 mg/g and 268 mg/g and 231 mg/g, 227 mg/g and 218 mg/g for AC-HTC- 180.

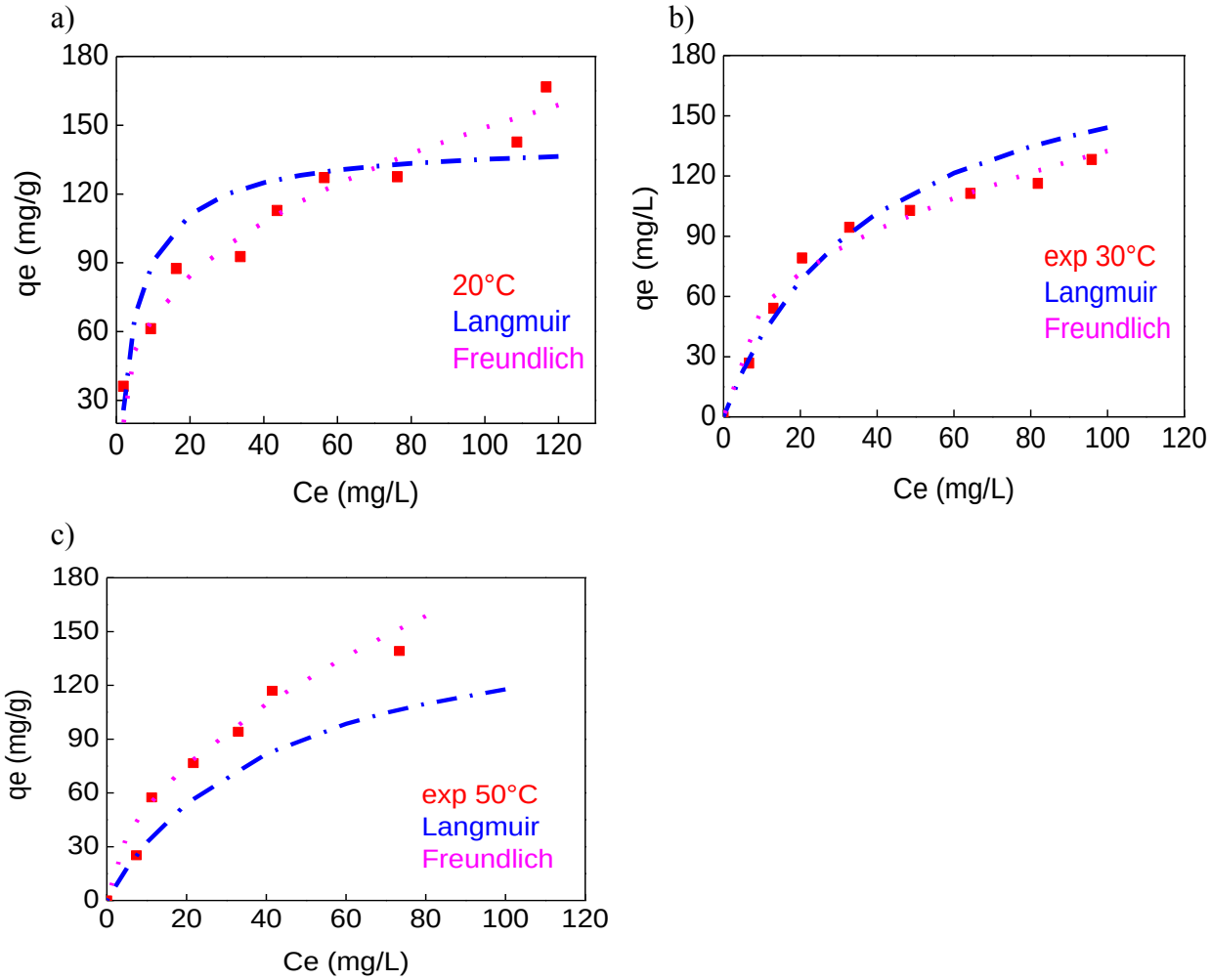

Figure 76: Experimental MDZ adsorption isotherms at 20°C (a), 30°C (b), 50°C (c) onto AC-HTC- 240 presenting the fitting of Langmuir and Freundlich models to the experimental data

Table 16: Langmuir and Freundlich isotherms parameters of IBU and MDZ adsorption onto AC-HTC- 240

		IUB-240			MDZ-240		
	Temperature (°C)	20	30	50	20	30	50
Langmuir	Qmax (mg/g)	500	166.67	200	142.86	200	200
	Kl (l/mg)	0.01	0.12	0.55	0.175	0.026	0.02
	R^2	0.95	0.875	0.965	0.805	0.98	0.96
Freundlich	K_f (l/mg)	11.32	26.87	61.56	29.31	33.481	15.29
	n_f	1.5	2.18	3.80	2.83	3.46	1.87
	R^2	0.98	0.969	0.987	0.983	0.984	0.975

IV.2.3 Effect of Activated carbon modification on IBU and MDZ adsorption

The equilibrium adsorption studies of AC-HTC-180, AC-HTC-180-O3 and AC-KOH-DIR are shown in figures 77 and 78. Both AC-HTC-180 and AC-HTC-180-O3 isotherms are of L1- type and AC-KOH-DIR is of L3-type according to the Giles classification (Giles et al. 1960).Actually, most of the pharmaceuticals species are described by L-type (Baccar et al. 2012), L1-type features by a fast adsorption uptake at low concentration that the curve increase steeply to reach a plateau indicating complete adsorption. L3-type characterize by a monolayer adsorption followed by a multilayer formation (Reddy et al. 2016), in fact the multilayer formation is mainly due to the blockage of pores of AC-KOH-DIR, this block could be explained by the water cluster formed in the entrance of pores especially these materials (AC-KOH-DIR) showed a high affinity to water therefore it has more interaction to the solvent than the solute. The maximum uptakes of all ACs are shown in table 17.

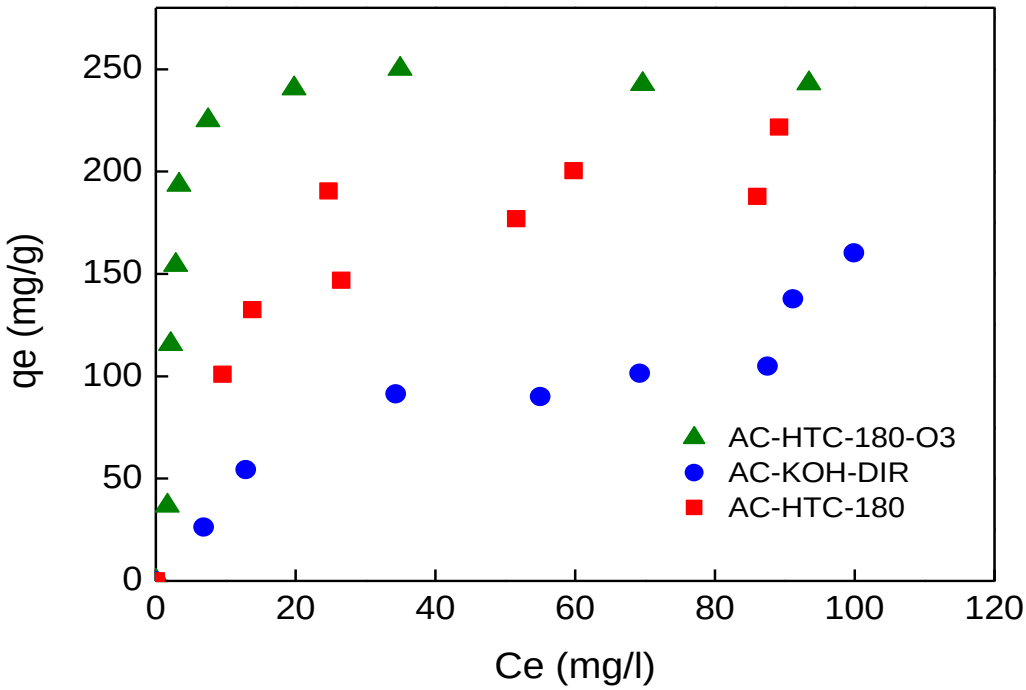

Figure 77: Adsorption isotherms of IBU

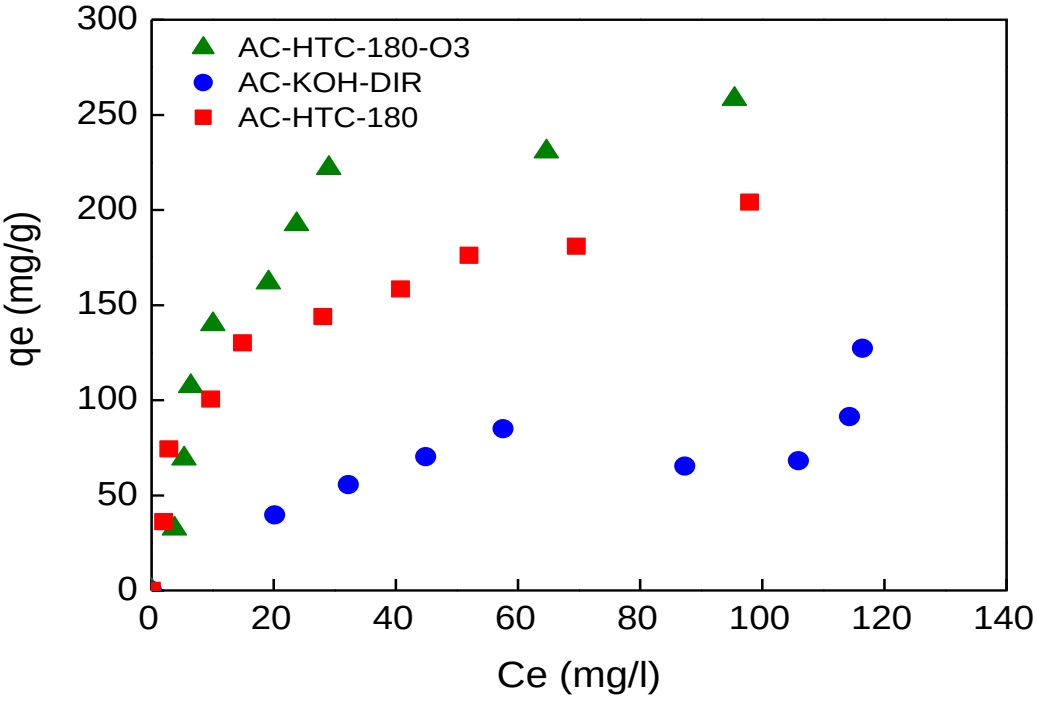

Figure 78: Adsorption isotherms of MDZ

Table 17: Summary of porous characteristics, and maximum medicines uptake

Samples	BET (m^2g^{-1})	Median pore width (nm)	qmax (mg/g) IBU	qmax (mg/g) MDZ
AC-HTC-180	981	0.52	265.19	169.27
AC-HTC-240	400	0.49	287.97	111.7
AC-HTC-180-O3	1245	0.55	243.06	258.32
AC-KOH-DIR	466	0.47	160.19	127.2

IV.2.4 Summary

This study proves that activated carbon prepared from hydrothermal carbonization of olive stones develop powerful features made them potential to remove different type of pharmaceuticals. The kinetics data follow the pseudo second order model and the Freundlich model showed to be perfect to describe the adsorption onto both activated carbon samples. Varying the temperature between 20-50°C does not have a remarkable effect on the adsorption process for both investigated medicines. It could be concluded that HTC-derived activated carbon has a powerful capability to be used in large scale water treatment applications.

IV.3 Hydrogen sorption measurements: experimental methods

The manometric equipment used for hydrogen adsorption has the same functionality as that used for nitrogen and carbon dioxide adsorption measurement, the apparatus was supplied by Micromeritics-Particulate Systems® (High Pressure Volumetric Analyzer II: HPVA II) and the experiments could be performed at high pressure (11 MPa). A photograph of the apparatus is depicted in figure 79.

Figure 79: HPVA II - High Pressure apparatus Analyzer

In each adsorption experiment a 1g of activated carbon samples were degassed at 125°C under vacuum for 6 hours at least, in order to remove all chemical species which may be remain on the surface of materials, before the adsorption test the weight of AC samples was measured and then was placed in a sample holder, next the chamber of 10 cm^3 contain the sample was rapidly evacuated so that to avoid any possible contamination and hydrogen is allowed to enter. The temperature was fixed at 298 K and the pressure for adsorption were 0.05, 0.15, 0.3, 0.6, 0.8, 1, 1.5, 2, 3, 4, 6, 7, 8, 9 and 10 MPa.

Usually the amount of hydrogen adsorbed given by software of manometric apparatus is actually the excess amount and not the absolute adsorbed amount. To overcome this limitation and assess the total adsorbed amount Gibbs defines the concept of –surface excess" and the absolute amount is expressed by the following equation:

$$n_{absolute} = n_{gas} + n_{excess} \qquad \text{IV.1}$$

Or $$n = \frac{PV}{ZRT}$$ IV.2

And based on the assumption that the density of adsorbed layer is close to the density of liquid, the excess volume could be approximately calculate as following:

$$V_{excess} = \frac{n_{excess} \times M_{H_2}}{\rho_{liq}}$$ IV.3

Then the absolute adsorbed amount is:

$$n_{absolute} = n_{exc} \times (1 + \frac{P \times M_{H_2}}{Z \times R \times \rho_{liq} \times T})$$ IV.4

Where

Z is the compressibility factor for corrected ideal gas equation

P is the pressure at given temperature and R is a gas constant.

And the isosteric heat of adsorption is determined by the Clausiuse-Clapeyron equation from the Microactive software:

$$-\frac{Qst}{R} = \frac{\partial \ln(P)}{\partial\left(1/T\right)}$$ IV.5

IV.4 Hydrogen adsorption performances

IV.4.1 Hydrogen adsorption isotherm

The adsorption isotherms experiments were performed using the following carbon materials hydrochar chemically activated (AC-HTC-180 and AC-HTC-240) and physically activated (N-CO2-2h), modified AC-HTC-240 (AC-HTC-240-O3) and for the sake of comparison OS directly activated with KOH (AC-OS-DIR) according to the traditional activation route were evaluated at 298 K and pressure 10 MPa. The adsorbed amount of hydrogen in w % per mass of AC is calculated according to the following equation:

$$wt(\%) = \frac{m_H}{m_{sample} + m_H} \times 100$$ IV.6

Where m_H is weight of adsorbed hydrogen and m_{sample} is weight of AC.

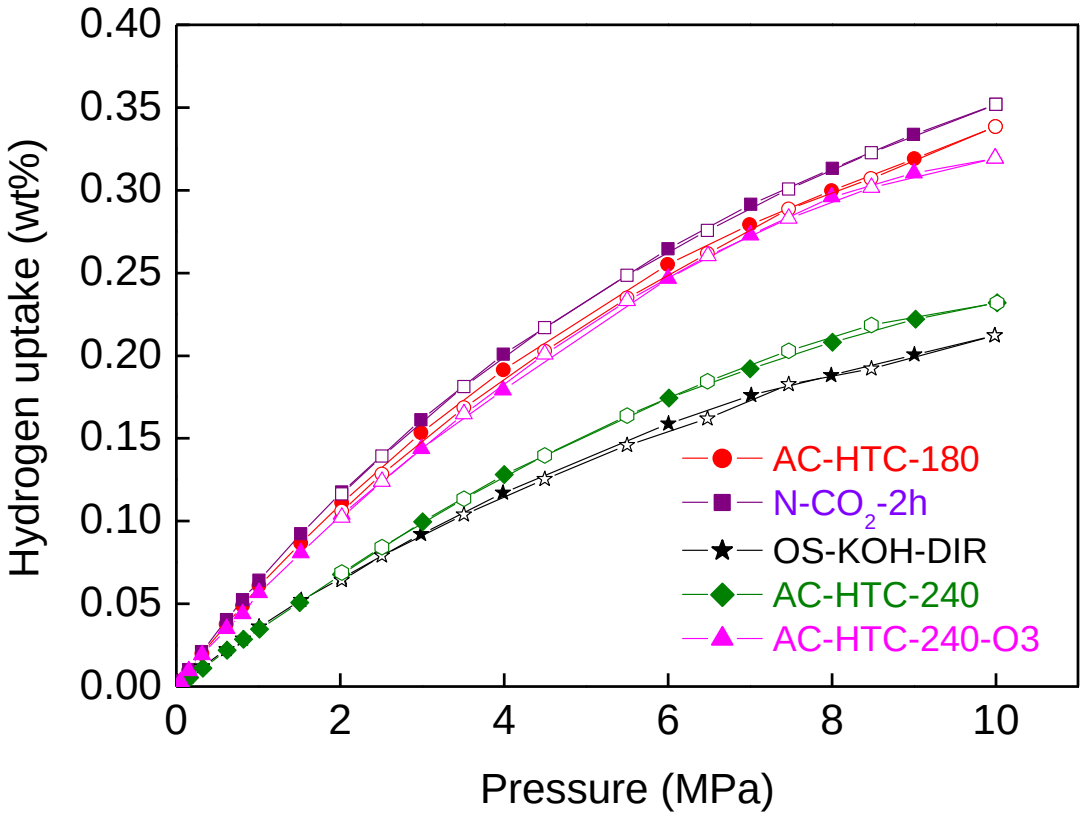

Figure 80: Hydrogen adsorption isoherm at 298 K

All the hydrogen adsorption isotherms shown in figure 80 exhibit similar type I isotherm according the IUPAC classification and practically all of them are reversible and without a significant hysteresis loop, regarding to the adsorbed amount of hydrogen kept increasing even at high pressure which is indicative of no saturation and a more adsorbed amount can be achieved at higher pressure, also the hysteresis can be drawn an idea about adsorption mechanism therefore its existence is competent evidence of a chemisorptions or condensation in mesopores which is not the case of this study consequently only physisorption of hydrogen occurred on the pores walls of solid (Yu 2016).

The remarkable difference between all isotherms curves is the adsorbed amount which significantly varied from activated carbon to another; it is decreases in the order:

N-CO_2-2h ≈ AC-HTC-180 〉 AC-HTC-240- O3 〉 AC-HTC-240 〉 OS-KOH-Dir

The highest adsorption capacities were obtained for N-CO_2-2h, AC-HTC-180 and AC-HTC-240-O3 with slight difference (table 18). The important hydrogen amount adsorbed on N-

CO_2-2h was 0.35 (wt %) although this sample didn't show the highest BET surface area (932 m^2g^{-1}) therefore the surface area is not the only feature which control the adsorption and a deep investigation on ACs properties and hydrogen uptake is extremely important. Generally hydrochar derived activated carbon shows higher adsorption efficiency than OS directly activated, and physical or chemical activation of hydrochar prepared at low temperature (180°C) seems potential precursor in hydrogen adsorption at the same time ozone modification of (AC-HTC-240) extremely improves the adsorbed amount, as shown in table 18 the hydrogen uptake raised from 0.23 to 032 wt%.

Table 18: Comparison of adsorption capacities of prepared ACs

Materials	S_{BET} ($m^2.g^{-1}$)	Vmicropore ($cm^3.g^{-1}$)	H2 up-take (wt %)
AC-HTC-180	1217	0.39	0.34
N-CO2	932	0.26	0.35
OS-KOH-DIR	655	0.19	0.21
AC-HTC-240	536	0.16	0.23
AC-HTC-240-O3	1242	0.39	0.32

IV.4.2 Effect of surface area in Hydrogen adsorption

The hydrogen uptake at 298 K is plotted as function of specific surface area shown in the figure 81, the specific surface area is a key factor may controlling the adsorption of hydrogen on carbon porous materials, a linear relationship is established between specific surface area and hydrogen uptake, with high correlation coefficient (R^2) equal to 0.67, indicating the interest to develop materials with relatively high surface area to improve the hydrogen adsorption capacities, as previously mentioned in table 18 the hydrogen adsorption capacities of AC-HTC-240 increase from 0.23 wt % to 0.32 wt % as its surface area enhanced from 536 m^2g^{-1} to 1242 m^2g^{-1} after oxidation treatment with ozone. These results are consistent with those obtained by (Akasaka et al. 2011) where the hydrogen adsorption capacity was around

0.3 wt% and the specific surface area was 780 m^2g^-1, the experiments were carried out at 298 K and using ACs fabricated from KOH activation of coffee bean wastes.

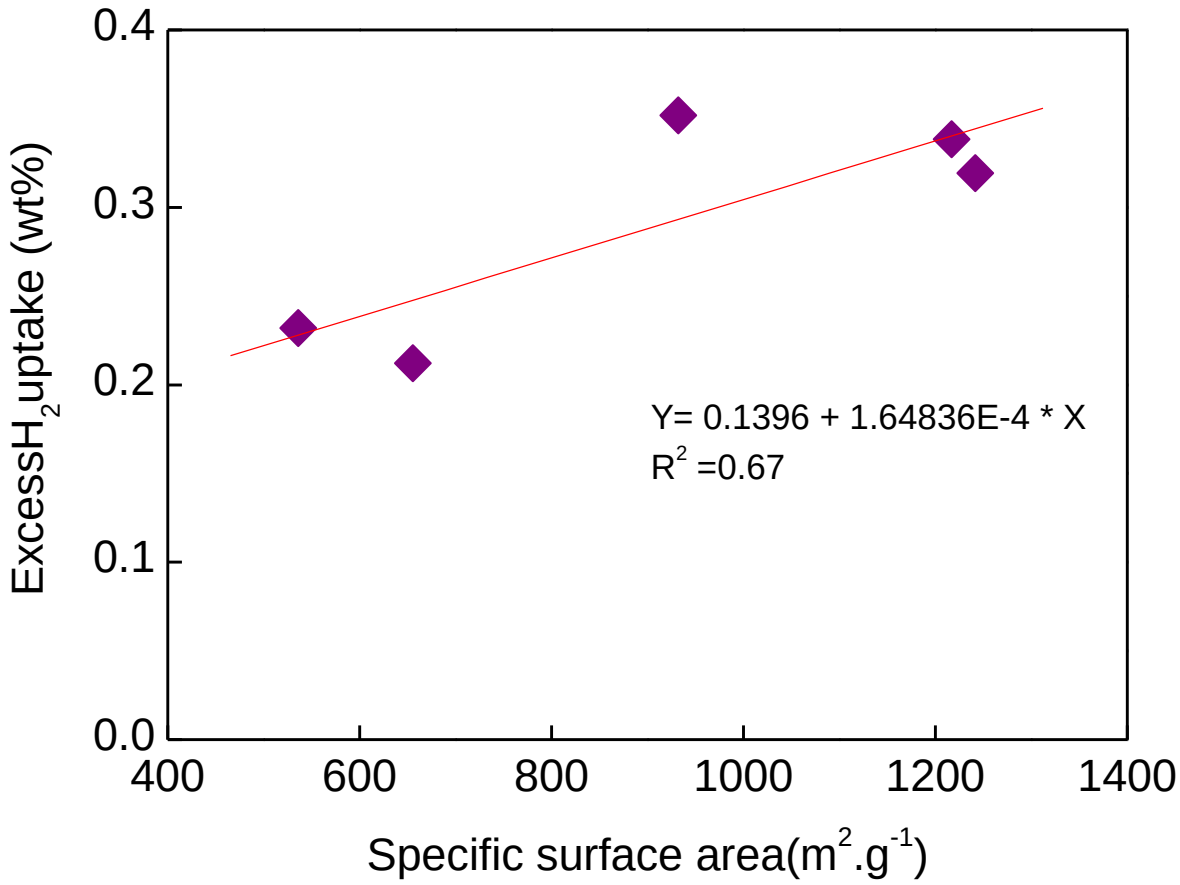

Figure 81: Excess hydrogen uptake as function of specific surface area

IV.4.3 Effect of micropores in Hydrogen adsorption

Generally, it is well known in the literature that higher hydrogen adsorption capacities usually ascribed to the ultramicropores size between 0.6 and 0.7 nm, that because this pore width is scarcely higher than the dynamic diameters of hydrogen (0.289 nm) (Zhao 2012; Yu 2016), therefore the interaction potential between hydrogen molecules and the surrounding pores walls is significantly important (Sun et al. 2011). Besides to the pore size, pore volume has a crucial role as well in hydrogen uptake. The pore volume increase from 0.19 cm^3 g^{-1} to 0.39 cm^3 g^{-1} in case of the excess hydrogen adsorption increased from 0.21 wt% to 0.34 wt% in case of ACs samples for AC-OS-DIR and AC-HTC-180 respectively. This finding is coherent with previous studies, (Ramesh et al. 2017) was pronounced that the hydrogen adsorption capacity was improved by about 70% as pore volume ranging from 0.19 cm^3 g^{-1} to 0.74 cm^3 g^{-1}, this same results have been obtained also in case of porous materials rather than carbon ,

metal-organic framework (MOF) shows an improvement of hydrogen uptake of 58% as pore size is reduced to 045-0.61 nm and pore volume increased by 33% (Somayajulu Rallapalli et al. 2013)

The excess of hydrogen uptake versus micropores volume (pore size between 0.5 and 0.7 nm) shows a linear trend and the obtained correlation coefficient (R^2) was higher than that obtained for excess hydrogen uptake as function of total pores volume obtained, as shown in figure 82 the determination coefficient is decreased from 0.803 to 0.47.

It is well reported in literature that micropores volume is a determined parameters in hydrogen adsorption, (Xia et al. 2014) determined a correlation coefficient as high as 0.9 to micropores volume and as high as 0.78 to total pores volume for hydrogen uptake at 298 K and 80 bar, similarly (Baranowski et al. 2008) determined a correlation coefficient higher than 0.8 to the micropores volume.

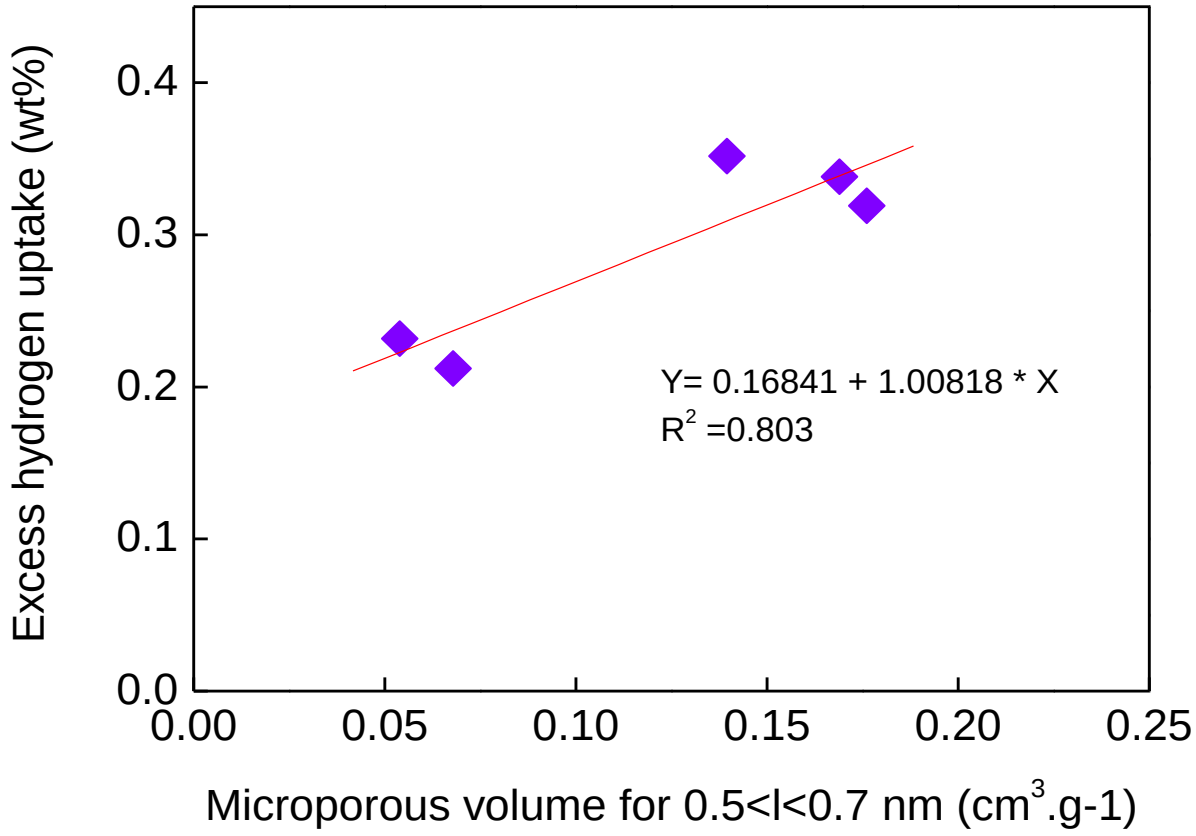

Figure 82: Excess of hydrogen uptake as function of ultramicropores

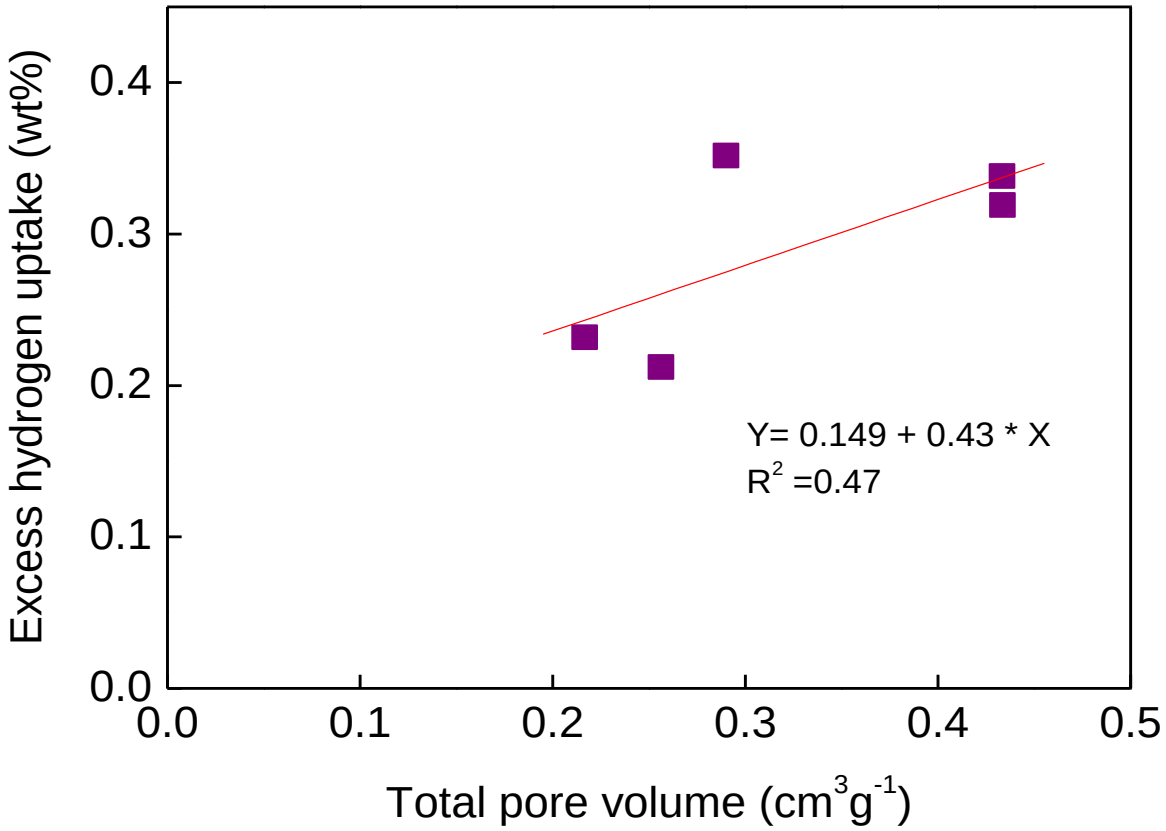

Figure 83: Excess hydrogen uptake as function of total pore volume

IV.4.4 Isosteric Heat of Adsorption

Isoseric heat of adsorption (q_{st}) is an indicator of the srength of the interractions between hydrogen molecules and carbon surface, it characerizes the differential change of energy that take place when an infinitesimal number of molecules are adsorbed at constant pressure and temperature (Peng and Morris 2010). The isosteric heat meseared in this study were higher than of those usally obtained in the litterature, in case of MOFs is between 4-9 KJ.mol^{-1}(Yu 2016), in the range of 4-6 KJ.mol^{-1} for graphite materials and sevilla et al found that it could be exceed 6 KJ.mol^{-1} for activated carbon prepared from hydrochar. The calculated isosteric heat of adsorption of AC-HTC-180, N-CO_2-2h and OS-KOH-DIR were beween 8 and 12 KJ.mol^{-1},these values are somewhat higher than those generally obtained in the litterature. Actually the isosteric heat depends strongly to micropores size and only narrow micropores may attribute the carbon high affinity to hydrogen molecules, the pore size of the materials of this study are between 0.48 nm and 0.53 nm this probably justify the high value of isosteric heat, an other hand a maximum of qst was reached at lower hydrogen uptake (Figure 84) and then gradually decreased as hydrogen adsorption capacities increase, the slight variation of

qst is due to the fact tat no saturation is achieved on the surface of materials (Schaefer et al. 2016).

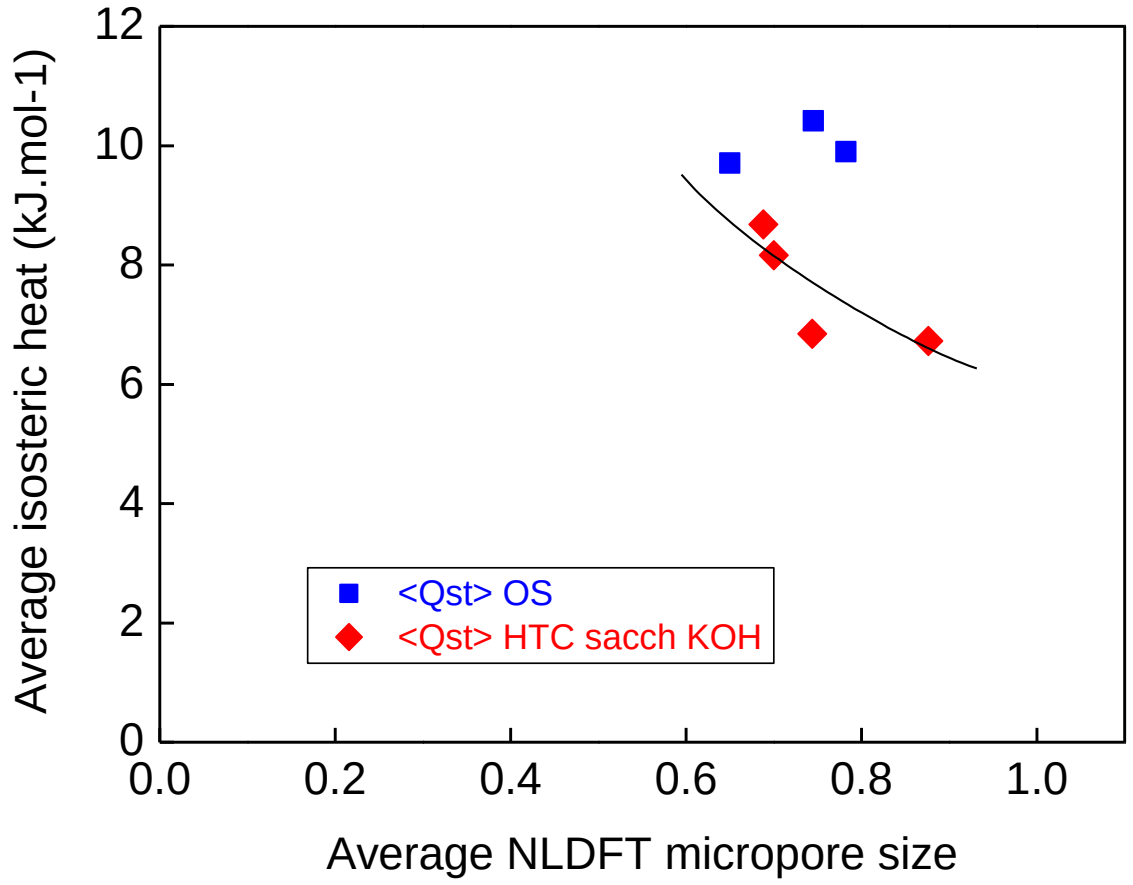

Figure 84: Average isosteric heat of AC derived olive stones and saccharose as function of NLDFT micropre size

Actually, chemical properties of ACs can strongly affect the hydrogen upake and the isosteric heat, the highest isosteric heat value is attributed to OS-KOH-DIR, taking into account the characterization results of boehm titration the inconvnient amount of basic group and previous study performed by (Enoki et al. 1990; Schaefer et al. 2016), it suggest that the obtained result of isosteric is due to the alkali metal (residual potassium ion) that still attached to the final sructure of activated carbon even after washing and therefore leads to high physisorption phenomenon.

In addition, it is worthy to note that the highest hydrogen uptake was achieved by N-CO2-2h desipite this material didn‘t display the highest surface area or pore volume, this propose that the effect of surface chemistry of materials is a prominent parameter. Therefore, a possible explanation of this finding is the nitrogen effect which may enhance the hydrogen uptake, recently (Zheng et al. 2010) reported that the doped heterogenous nitrogen atoms increase the

adsorption heat and subsquently ameliorate the hydrogen uptake, but unfortunately it could be not drawn an accruate idea about its effect in this study as we didn't prepare ACs from hydrochar without doped nitrogen for the comparaison.

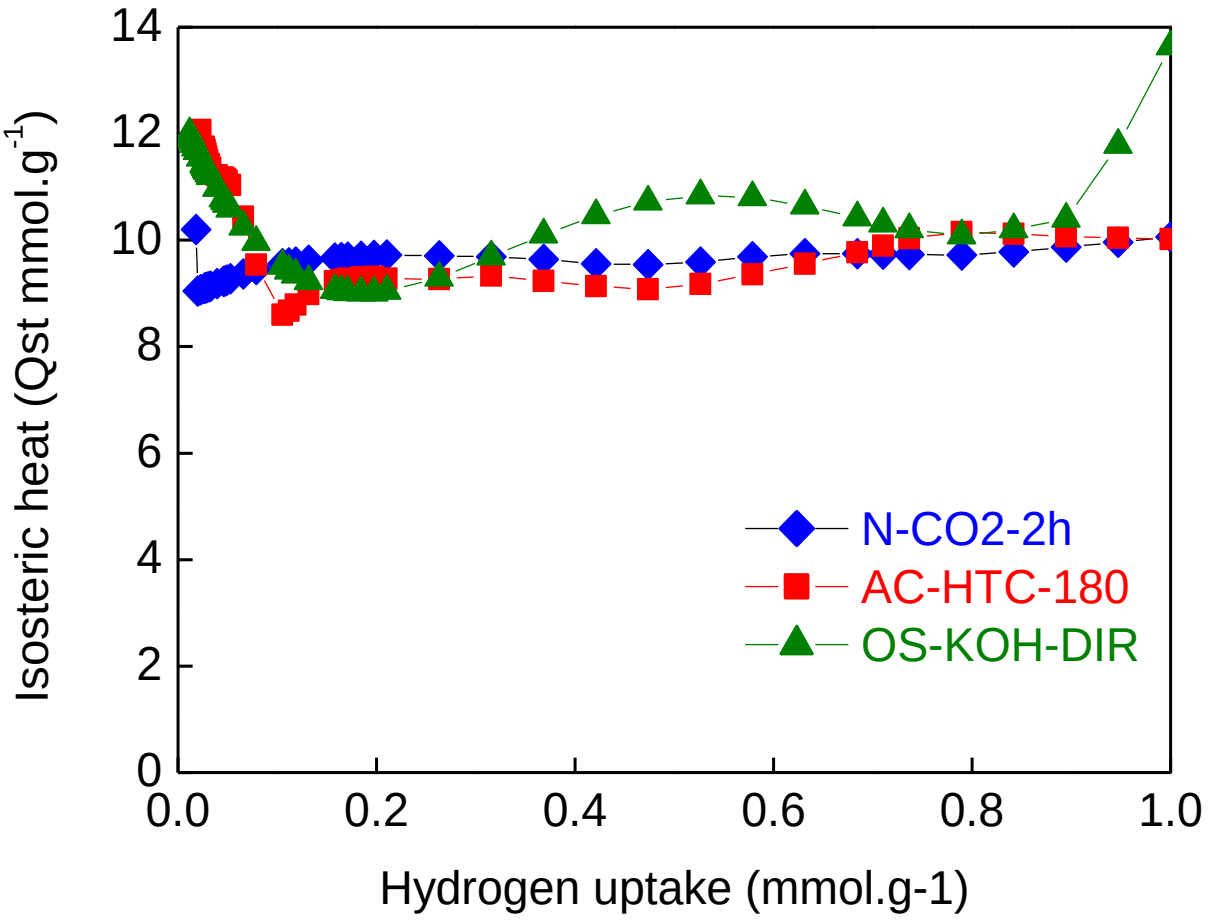

Figure 85: Isosteric heat as function of hydrogen uptake

IV.5 Modeling of Adsorption Isotherms: Langmuir Isotherm Model

The experimental adsorption isotherms data obtained by different prepared ACs samples were modeled by fitting to Langmuir model (equation IV.7) and Freundlich (equation IV.8). The numerical fitting parameters are displayed in table 19 and the experimental and the fitting curves to both adsorption models are depicted in figure 86.

$$w = \frac{w_m kp}{1 + kp} \qquad \text{IV.7}$$

$$w = k_p p^{1/n} \qquad \text{IV.8}$$

The Langmuir model is straightforward model which usually proposed to quantify the adsorbed amount or Freundlich model is more suitable to describe the adsorption qualitatively (Zhou et al. 2001). Both of models displayed a high correlation coefficient (R^2> 0.8), but Langmuir model gives well-fitting adsorption isotherms that because the theoretical data given by Langmuir simulation is practically confined with the experimental one (see figure 86), also at pressure less than 7 MPa Langmuir gave a good description for hydrogen adsorption but beyond this pressure a remarkable deviations appeared and Langmuir model no longer valid, in fact according to the characterization of the prepared activated carbon reported in chapter III, the materials didn‘t show a significant surface heterogeneity for both geometrical (different pore size distribution) and chemical (surface functional groups) therefore the adsorption is not mainly related to the heterogeneity of surface as Freundlich equation assumes. The estimated maximum hydrogen uptake obtained by Langmuir is deduced to AC-HTC-240, but this value probably is overestimated by Langmuir model that because of the relatively low correlation coefficient (R^2= 0.87). The fitted parameters corresponds to N-CO2-2h and AC-HTC-180 are quiet close only the value of K which is higher for N-CO-2h than AC-HTC-180 indicating a larger strength interaction and higher affinity of hydrogen to N-CO-2h.

Table 19: Langmuir and Freundlich isotherm parameters for the adsorption of hydrogen

Models	**Parameters**	**AC-HTC-180**	**N-CO2-2h**	**AC-KOH-DIR**	**ACHTC-240-KOH**	**Ac-HTC240-O3**
Langmuir	w_m	0.717	0.72	0.49	0.79	0.74
	K	0.089	0.096	0.077	0.045	0.08
	R^2	0.99	0.99	0.99	0.87	0.98
Freundlich	n	1.15	1.15	1.13	1.06	1.136
	Kp	0.0535	0.057	0.032	0.032	0.050
	R^2	0.99	0.99	0.99	0.99	0.99

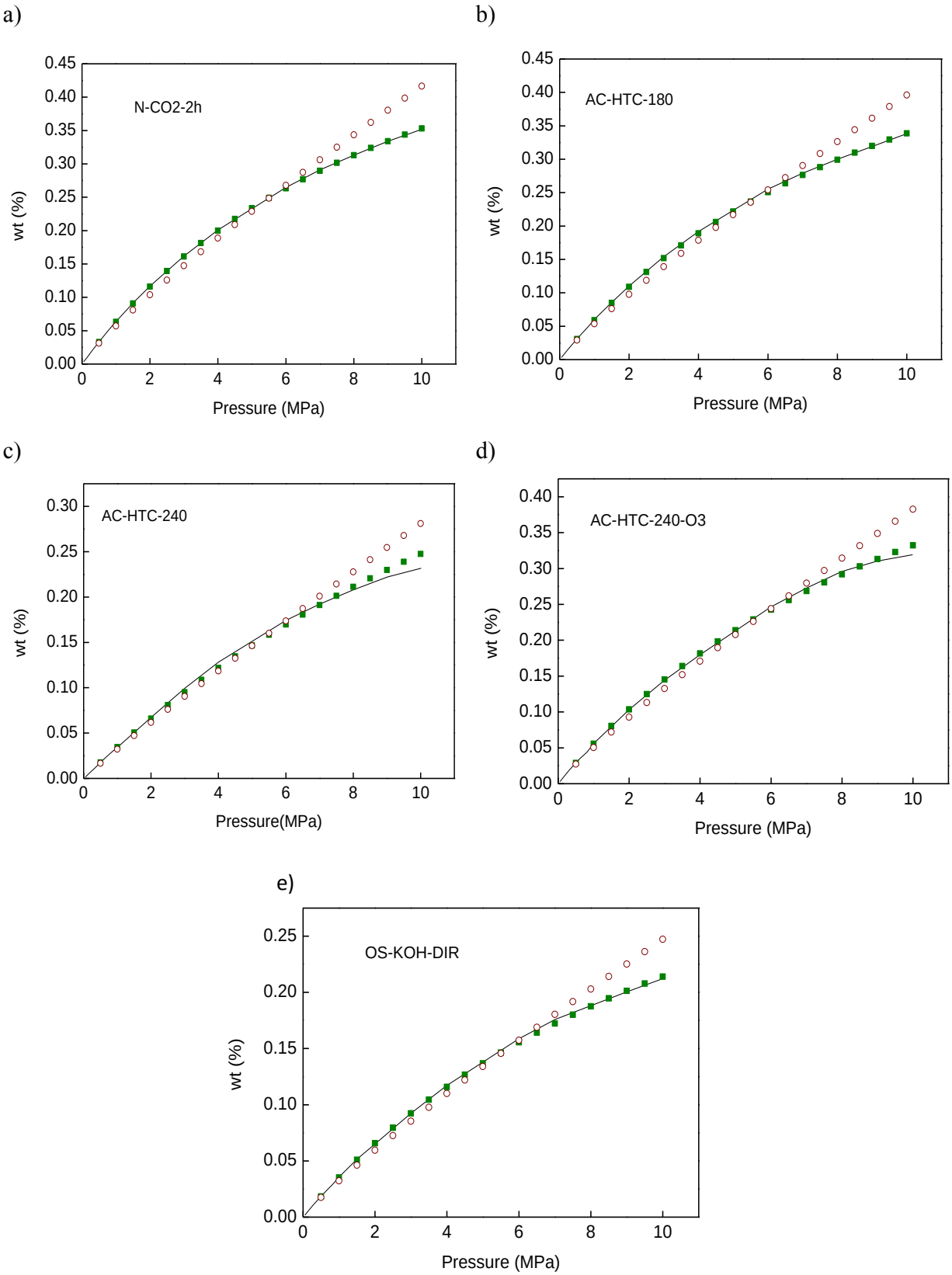

Figure 86: Experimental hydrogen adsorption isotherms presenting the fitting of Langmuir (empty cercal) and Freundlich (full square) models to the experimental data

IV.6 Summary

Hydrogen adsorption at 298K and 10 MPa onto activated carbon prepared from hydrochar and olive stones were performed, the experiments results show that the physical adsorption of hydrogen is strongly depend on micropores volume and surface area, but in this study it had been demonstrate that they are not the only parameters which monitor the adsorption process, the surface chemistry can remarkably increase hydrogen uptake even in case of low surface area and pore volume. The adsorption isotherm data were regressed with Freundlich and Langmuir models, the best fitted results were given by Freundlich model. Generally, hydrochar derived activated carbon is found to give better result than olive stones directly activated and these preliminary results could be extremely enhanced by a further optimization of both activation and post treatment condition

Conclusion

The underlying motivation for this thesis is to extract as much detail as possible about the hydrothermal carbonization of lignocellulosic biomass under different conditions (time and temperature). Hence, olive stones were chosen in terms of their availability and cheapness in the Mediterranean countries and in Tunisia in particularly. The analyses results of the recovered hydrochar were investigated using the severity factor; the preliminary results have shown that olive stones are sensitive to the HT treatment even at low severity conditions and a more accurate investigation on the thermo-gravimetric analyses through the deconvolution of the differential ATG curves using Gaussian functions with the Origin® software, the three main compounds of olive stones: hemicelluloses, cellulose and lignin were affected by HT process to different extent, hemicelluloses were completely hydrolyzed at severity as low as 4, actually hemicelluloses act as a protective barrier for cellulose, that once it hydrolyzed the cellulose compounds become more accessible and its degradation occurred at severity equal to 4.7, lignin start to react under low severity but as it is not really affected even in harsher conditions. In fact, the severity factor is useful to optimize the amount of some powerful organic compounds released in the aqueous phase such as furfural and 5-hydroxymethylfurfural (5-HMF). Modifying the HT medium by adding salts or acid helpful to catalyse reactions occurring under hydrothermal process, additionally changing HTC medium could be efficient to enhance the production of some organic compounds. Throughout this study, a various parameters should be taking into consideration in order to adjust hydrochar properties to each its future application, this methodology appears to be compulsory to make this technology strongly appealing. Actually, hydrochar have been used in numerous applications such soil conditioner, fuel and activated carbon precursor.

Activated carbon materials produced by HT carbonization of olive stones at low temperature (180°C) and high temperature (240°C) for 6h by both activation techniques: physical activation using CO_2 and chemical activation using potassium hydroxide as activation agent, the resulted carbon materials were subjected to different characterization techniques in order to assess its physical properties (porosities, pore volume…) and its chemical properties (surface functional groups, pHpzc). The activated carbon produced at low HT temperature and chemically activated characterized by a high porosity development and narrow pore size distribution centred an 0.52 nm, the micropores fraction was as high as 90%, his materials has a hydrophilic character and rich on surface functional group contrary to ACs prepared at high

HT temperature which exhibit lower porosity development and narrower pore size distribution but it contains a high fraction of mesopores about 27 % which is important for many applications like adsorption and catalyst. In fact, hydrothermal step affect deeply the final structure properties of ACs that the activated carbon prepared from hydrochar at 180°C, they are in reality synthesised from hydrochar rich in cellulose and lignin content or at 240 °C and 6h hydrochar are mainly composed of lignin. On the other hand, hydrochar produced in aqueous ammonia solution and physically activated using CO_2 showed a high porosities and narrow pores size distribution centred in 0.5 nm. Post treatment of activated carbon by ozone oxidation appears to be advantageous to improve its physical and chemical ACs properties. The resultant carbon materials AC-HTC-180 had high surface areas, as high as 1478 m^2g^{-1}, besides a great improvement in specific surface area (1242m^2g^-1) of AC-HTC-240. Generally the activated carbon prepared from hydrochar showed a higher porosities than those prepared directly from olive stones.

The utilization of ACs in different applications is somewhat different characterization route. In this study, ACs was used to remove pharmaceuticals. Ibuprofen and Metronidazole are two drugs commonly used and in many countries without medical certificate therefore it is frequently reject in waste water. Both activated carbons showed a good performance in ibuprofen and metronidazole adsorption. The equilibrium adsorption data of IBU and MDZ on AC-HTC-180 and AC-HTC-240 at various temperatures were well fitted by Freundlich isotherm and the kinetic adsorption data were well described by the pseudo second order. Generally, the surface chemistry of ACs was a key parameters which governing the adsorption onto both ACs.

The prepared materials were subjected to adsorption of hydrogen also; AC-HTC-180, N-CO2 and AC-HTC-240-O3 showed the most promising results. Although the hydrogen uptake was so far from DOE hydrogen system targets but we strongly believe that an optimization of the hydrothermal carbonization, activation and post treatment process, these results would be significantly improved.

Finally, there is a lot of work which has not achieved in this study due to time and equipments limitations. Hence, further works are needed to improve the materials properties and made it more suitable for various applications.

References

Abdel-Ghani NT, El-Chaghaby GA, ElGammal MH, Rawash E-SA (2016a) Optimizing the preparation conditions of activated carbons from olive cake using KOH activation. New Carbon Mater 31:492–500.

Abdel-Ghani NT, Rawash ESA, El-Chaghaby GA (2016b) Equilibrium and kinetic study for the adsorption of p-nitrophenol from wastewater using olive cake based activated carbon. Glob J Environ Sci Manag 2:11–18.

Ahmed MJ, Theydan SK (2013) Microporous activated carbon from Siris seed pods by microwave-induced KOH activation for metronidazole adsorption. J Anal Appl Pyrolysis 99:101–109.

Akasaka H, Takahata T, Toda I, et al (2011) Hydrogen storage ability of porous carbon material fabricated from coffee bean wastes. Int J Hydrog Energy 36:580–585.

Alatalo S-M, Repo E, Mäkilä E, et al (2013) Adsorption behavior of hydrothermally treated municipal sludge & pulp and paper industry sludge. Bioresour Technol 147:71–76. doi: 10.1016/j.biortech.2013.08.034

Alslaibi TM, Abustan I, Ahmad MA, Abu Foul A (2014) Preparation of activated carbon from olive stone waste: optimization study on the removal of Cu2+, Cd2+, Ni2+, Pb2+, Fe2+, and Zn2+ from aqueous solution using response surface methodology. J Dispers Sci Technol 35:913–925.

Anthonia EE, Philip HS, others (2015) An overview of the applications of furfural and its derivatives. Int J Adv Chem 3:42–47.

Baccar R, Sarrà M, Bouzid J, et al (2012) Removal of pharmaceutical compounds by activated carbon prepared from agricultural by-product. Chem Eng J 211–212:310–317. doi: 10.1016/j.cej.2012.09.099

Bahamon D, Carro L, Guri S, Vega LF (2017) Computational study of ibuprofen removal from water by adsorption in realistic activated carbons. J Colloid Interface Sci 498:323–334.

Bandosz TJ (2006) Activated Carbon Surfaces in Environmental Remediation. The City College of New York , Academic Press

Banerjee P, Das P, Zaman A, Das P (2016) Application of graphene oxide nanoplatelets for adsorption of Ibuprofen from aqueous solutions: Evaluation of process kinetics and thermodynamics. Process Saf Environ Prot 101:45–53. doi: 10.1016/j.psep.2016.01.021

Baranowski B, Zaginaichenko S, Schur D, et al (2008) Carbon nanomaterials in clean energy hydrogen systems. Springer Science & Business Media

Basso D (2016) Hydrothermal carbonization of waste biomass. Phd, University of Trento

Bembnowska A, Pe\lech R, Milchert E (2003) Adsorption from aqueous solutions of chlorinated organic compounds onto activated carbons. J Colloid Interface Sci 265:276–282.

Benavente V, Calabuig E, Fullana A (2015) Upgrading of moist agro-industrial wastes by hydrothermal carbonization. J Anal Appl Pyrolysis 113:89–98. doi: 10.1016/j.jaap.2014.11.004

Berge ND, Ro KS, Mao J, et al (2011) Hydrothermal Carbonization of Municipal Waste Streams. Environ Sci Technol 45:5696–5703. doi: 10.1021/es2004528

Blanco López M., Blanco C., Martínez-Alonso A, Tascón JM. (2002) Composition of gases released during olive stones pyrolysis. J Anal Appl Pyrolysis 65:313–322. doi: 10.1016/S0165-2370(02)00008-6

Bobleter O (1994) Hydrothermal degradation of polymers derived from plants. Prog Polym Sci 19:797–841. doi: 10.1016/0079-6700(94)90033-7

Boehm H. (2002) Surface oxides on carbon and their analysis: a critical assessment. Carbon 40:145–149. doi: 10.1016/S0008-6223(01)00165-8

Boehm HP (1994) Some aspects of the surface chemistry of carbon blacks and other carbons. Carbon 32:759–769. doi: 10.1016/0008-6223(94)90031-0

Borrero-López AM, Fierro V, Jeder A, et al (2016) High added-value products from the hydrothermal carbonisation of olive stones. Environ Sci Pollut Res 24:9895--98.

Braghiroli FL (2014) Polyphénols végétaux traités par voie humide : synthèse de carbones biosourcés hautement poreux et applications. Université de Lorraine

Brennan JK, Thomson KT, Gubbins KE (2002a) Adsorption of Water in Activated Carbons: Effects of Pore Blocking and Connectivity. Langmuir 18:5438–5447. doi: 10.1021/la0118560

Broch A, Jena U, Hoekman SK, Langford J (2013) Analysis of solid and aqueous phase products from hydrothermal carbonization of whole and lipid-extracted algae. Energies 7:62–79.

Burress JW (2009) Gas sorption in engineered carbon nanospaces. University of Missouri–Columbia

Çalışkan E, Göktürk S (2010) Adsorption Characteristics of Sulfamethoxazole and Metronidazole on Activated Carbon. Sep Sci Technol 45:244–255. doi: 10.1080/01496390903409419

Çeçen F, Aktas Ö (2011) Activated carbon for water and wastewater treatment: Integration of adsorption and biological treatment. John Wiley & Sons

Chaturvedi V, Verma P (2013) An overview of key pretreatment processes employed for bioconversion of lignocellulosic biomass into biofuels and value added products. 3 Biotech 3:415–431.

Chen H, Wang H, Xue Z, et al (2012) High hydrogen storage capacity of rice hull based porous carbon. Int J Hydrog Energy 37:18888–18894.

Cheng F, Liang J, Zhao J, et al (2008) Biomass waste-derived microporous carbons with controlled texture and enhanced hydrogen uptake. Chem Mater 20:1889–1895.

Chiang H-L, Chiang PC, You JH (1995) The influences of O3 reaction on physico-chemical characteristics of activated carbon for benzene adsorption. Toxicol Environ Chem 47:97–108.

coronella (2014) Research aims to help dairy farmers generate sustainable energy. https://fr.scribd.com/doc/266944153/coronella-lab. Accessed 18 Jun 2017

Correa CR, Voglhuber A, Oberlaender D, et al (2014) Hydrothermal Carbonization of Acrocomia Aculeata for the Production of Hydrochar and Activated Carbon. In: Conference on International Research on Food Security.

Danso-Boateng E, Holdich RG, Shama G, et al (2013) Kinetics of faecal biomass hydrothermal carbonisation for hydrochar production. Appl Energy 111:351–357. doi: 10.1016/j.apenergy.2013.04.090

De Jong W, Van Ommen JR (eds) (2014) Biomass as a Sustainable Energy Source for the Future: Fundamentals of Conversion Processes. John Wiley & Sons, Inc, Hoboken, NJ

Deitz VR, Bitner JL (1972) The reaction of ozone with adsorbent charcoal. Carbon 10:145–154.

Ding H, Bian G (2015) Adsorption of metronidazole in aqueous solution by Fe-modified sepiolite. Desalination Water Treat 55:1620–1628.

Do DD, Herrera L, Fan C, et al (2010) The role of accessibility in the characterization of porous solids and their adsorption properties. Adsorption 3.

Eddaoudi M (2005) Characterization of Porous Solids and Powders: Surface Area, Pore Size and Density. J Am Chem Soc 14117.

Elliott DC, Biller P, Ross AB, et al (2015) Hydrothermal liquefaction of biomass: Developments from batch to continuous process. Bioresour Technol 178:147–156. doi: 10.1016/j.biortech.2014.09.132

Elmouwahidi A, Bailón-García E, Pérez-Cadenas AF, et al (2017) Activated carbons from KOH and H 3 PO 4-activation of olive residues and its application as supercapacitor electrodes. Electrochimica Acta 229:219–228.

Elmouwahidi A, Zapata-Benabithe Z, Carrasco-Marín F, Moreno-Castilla C (2012) Activated carbons from KOH-activation of argan (Argania spinosa) seed shells as supercapacitor electrodes. Bioresour Technol 111:185–190.

Enoki T, Miyajima S, Sano M, Inokuchi H (1990) Hydrogen-alkali-metal-graphite ternary intercalation compounds. J Mater Res 5:435–466. doi: 10.1557/JMR.1990.0435

Essandoh M, Kunwar B, Pittman CU, et al (2015) Sorptive removal of salicylic acid and ibuprofen from aqueous solutions using pine wood fast pyrolysis biochar. Chem Eng J 265:219–227. doi: 10.1016/j.cej.2014.12.006

Falco C (2012) Sustainable biomass-derived hydrothermal carbons for energy applications.

Falco C, Baccile N, Titirici M-M (2011) Morphological and structural differences between glucose, cellulose and lignocellulosic biomass derived hydrothermal carbons. Green Chem 13:3273. doi: 10.1039/c1gc15742f

Ferrero GA, Fuertes AB, Sevilla M (2015) From Soybean residue to advanced supercapacitors. Sci Rep 5:16618.

Fierro V, Torné-Fernández V, Montané D, Celzard A (2005) Study of the decomposition of kraft lignin impregnated with orthophosphoric acid. Thermochim Acta 433:142–148. doi: 10.1016/j.tca.2005.02.026

Franz M, Arafat HA, Pinto NG (2000) Effect of chemical surface heterogeneity on the adsorption mechanism of dissolved aromatics on activated carbon. Carbon 38:1807–1819.

Funke A, Ziegler F (2010) Hydrothermal carbonization of biomass: a summary and discussion of chemical mechanisms for process engineering. Biofuels Bioprod Biorefining 4:160–177.

Garlapalli RK, Wirth B, Reza MT (2016) Pyrolysis of hydrochar from digestate: Effect of hydrothermal carbonization and pyrolysis temperatures on pyrochar formation. Bioresour Technol 220:168–174.

Gavish N, Promislow K (2016) Dependence of the dielectric constant of electrolyte solutions on ionic concentration - a microfield approach. Phys Rev E 94(1-1):012611. doi: 10.1103/PhysRevE.94.012611

Genzeb Belsie Nge (2014) Hydrothermal carbonization and investigation of biochar using IR spectroscopy. Instituto Superior Técnico

Giles CH, MacEwan TH, Nakhwa SN, Smith D (1960) 786. Studies in adsorption. Part XI. A system of classification of solution adsorption isotherms, and its use in diagnosis of adsorption mechanisms and in measurement of specific surface areas of solids. J Chem Soc Resumed 3973–3993.

Gómez MJ, Martínez Bueno MJ, Lacorte S, et al (2007) Pilot survey monitoring pharmaceuticals and related compounds in a sewage treatment plant located on the Mediterranean coast. Chemosphere 66:993–1002. doi: 10.1016/j.chemosphere.2006.07.051

Gong Y, Wang H, Wei Z, et al (2014) An efficient way to introduce hierarchical structure into biomass-based hydrothermal carbonaceous materials. ACS Sustain Chem Eng 2:2435–2441.

Guedidi H, Lakehal I, Reinert L, et al (2017) Removal of ionic liquids and ibuprofen by adsorption on a microporous activated carbon: Kinetics, isotherms, and pore sites. http://dx.doi.org/10.1016/j.arabjc.2017.04.006.

Guedidi H, Reinert L, Lévêque J-M, et al (2013) The effects of the surface oxidation of activated carbon, the solution pH and the temperature on adsorption of ibuprofen. Carbon 54:432–443.

Hao W (2014) Refining of hydrochars/hydrothermally carbonized biomass into activated carbons and their applications. Department of Materials and Environmental Chemistry (MMK), Stockholm University

Harmsen PFH, Huijgen W, Bermudez L, Bakker R (2010) Literature review of physical and chemical pretreatment processes for lignocellulosic biomass. Wageningen UR Food & Biobased Research

Hendriks A, Zeeman G (2009) Pretreatments to enhance the digestibility of lignocellulosic biomass. Bioresour Technol 100:10–18.

Huang C-C, Chen H-M, Chen C-H (2010) Hydrogen adsorption on modified activated carbon. Int J Hydrog Energy 35:2777–2780. doi: 10.1016/j.ijhydene.2009.05.016

Hui TS, Zaini MAA (2015) Potassium hydroxide activation of activated carbon: a commentary. Carbon Lett 16:275–280.

Ishibashi N, Yamamoto K, Wakisaka H, Kawahara Y (2014) Influence of the Hydrothermal Pre-treatments on the Adsorption Characteristics of Activated Carbons from Woods. J Polym Environ 22:267–271. doi: 10.1007/s10924-013-0623-x

Isikgor FH, Becer CR (2015) Lignocellulosic biomass: a sustainable platform for the production of bio-based chemicals and polymers. Polym Chem 6:4497–4559.

J. C (2012) Techniques Employed in the Physicochemical Characterization of Activated Carbons. In: Hernndez Montoya V (ed) Lignocellulosic Precursors Used in the Synthesis of Activated Carbon - Characterization Techniques and Applications in the Wastewater Treatment. ISBN: 978-953-51- 0197-0 InTech,

Jagiello J, Olivier JP (2013) Carbon slit pore model incorporating surface energetical heterogeneity and geometrical corrugation. Adsorption 19:777–783.

Jain A, Balasubramanian R, Srinivasan MP (2015) Production of high surface area mesoporous activated carbons from waste biomass using hydrogen peroxide-mediated hydrothermal treatment for adsorption applications. Chem Eng J 273:622–629. doi: 10.1016/j.cej.2015.03.111

Jain A, Balasubramanian R, Srinivasan MP (2016) Hydrothermal conversion of biomass waste to activated carbon with high porosity: A review. Chem Eng J 283:789–805. doi: 10.1016/j.cej.2015.08.014

Jaramillo J, Gómez-Serrano V, Álvarez PM (2009) Enhanced adsorption of metal ions onto functionalized granular activated carbons prepared from cherry stones. J Hazard Mater 161:670–676. doi: 10.1016/j.jhazmat.2008.04.009

Jin F (2014) Application of hydrothermal reactions to biomass conversion. Springer, Berlin Heidelberg

Jin H, Lee YS, Hong I (2007) Hydrogen adsorption characteristics of activated carbon. Catal Today 120:399–406. doi: 10.1016/j.cattod.2006.09.012

Jones OAH, Voulvoulis N, Lester JN (2001) Human Pharmaceuticals in the Aquatic Environment a Review. Environ Technol 22:1383–1394. doi: 10.1080/09593332208618186

Jung YH, Kim KH (2014) Pretreatment of biomass: processes and technologies. In: Elsevier Inc.

Kambo HS (2014) Energy Densification of Lignocellulosic Biomass via Hydrothermal Carbonization and Torrefaction. Thesis

Kanetake T, Sasaki M, Goto M (2007) Decomposition of a lignin model compound under hydrothermal conditions. Chem Eng Technol 30:1113–1122.

Khazri H, Ghorbel-Abid I, Kalfat R, Trabelsi-Ayadi M (2016) Removal of ibuprofen, naproxen and carbamazepine in aqueous solution onto natural clay: equilibrium, kinetics, and thermodynamic study. Appl Water Sci. doi: 10.1007/s13201-016-0414-3

Khelfa A (2009) Etude des étapes primaires de la dégradation thermique de la biomasse lignocellulosique. Metz. Thesis

Kopetzki D (2011) Exploring hydrothermal reactions: from prebiotic synthesis to green chemistry. Universität Potsdam Potsdam

Kral H, Rouquerol J, Sing KSW, Unger KK (1988) Characterization of Porous Solids. Elsevier

Kruse A, Dinjus E (2007) Hot compressed water as reaction medium and reactant: properties and synthesis reactions. J Supercrit Fluids 39:362–380.

Kumagai S, Hirajima T (2014) Effective Utilization of Moso-Bamboo (Phyllostachys heterocycla) with Hot-Compressed Water. In: Jin F (ed) Application of Hydrothermal Reactions to Biomass Conversion. Springer Berlin Heidelberg, Berlin, Heidelberg, pp 155–170

Kumar P, Barrett DM, Delwiche MJ, Stroeve P (2009) Methods for Pretreatment of Lignocellulosic Biomass for Efficient Hydrolysis and Biofuel Production. Ind Eng Chem Res 48:3713–3729. doi: 10.1021/ie801542g

Kümmerer K (2004) Pharmaceuticals in the Environment — Scope of the Book and Introduction. In: Kümmerer K (ed) Pharmaceuticals in the Environment. Springer Berlin Heidelberg, Berlin, Heidelberg, pp 3–11

Lee HV, Hamid SBA, Zain SK (2014) Conversion of lignocellulosic biomass to nanocellulose: structure and chemical process 2014,pp 20.

Leimkuehler EP (2010) Production, characterization, and applications of activated carbon. University of Missouri–Columbia

Li L, Quinlivan PA, Knappe DRU (2005) Predicting Adsorption Isotherms for Aqueous Organic Micropollutants from Activated Carbon and Pollutant Properties. Environ Sci Technol 39:3393–3400. doi: 10.1021/es048816d

Li P, Yang H, Wang X, et al (2016) Effects of acid and metal salt additives on product characteristics of biomass microwave pyrolysis. J Renew Sustain Energy 8:063103.

Lim KL, Kazemian H, Yaakob Z, Daud WRW (2010) Solid-state Materials and Methods for Hydrogen Storage: A Critical Review. Chem Eng Technol 33:213–226. doi: 10.1002/ceat.200900376

Lin AY-C, Yu T-H, Lin C-F (2008) Pharmaceutical contamination in residential, industrial, and agricultural waste streams: Risk to aqueous environments in Taiwan. Chemosphere 74:131–141. doi: 10.1016/j.chemosphere.2008.08.027

Liu Z, Zhang F-S, Wu J (2010) Characterization and application of chars produced from pinewood pyrolysis and hydrothermal treatment. Fuel 89:510–514. doi: 10.1016/j.fuel.2009.08.042

Lota G, Krawczyk P, Lota K, et al (2016) The application of activated carbon modified by ozone treatment for energy storage. J Solid State Electrochem 20:2857–2864.

Lynam JG, Coronella CJ, Yan W, et al (2011) Acetic acid and lithium chloride effects on hydrothermal carbonization of lignocellulosic biomass. Bioresour Technol 102:6192–6199. doi: 10.1016/j.biortech.2011.02.035

Lynam JG, Reza MT, Vasquez VR, Coronella CJ (2012a) Effect of salt addition on hydrothermal carbonization of lignocellulosic biomass. Fuel 99:271–273.

Mansouri H, Carmona RJ, Gomis-Berenguer A, et al (2015) Competitive adsorption of ibuprofen and amoxicillin mixtures from aqueous solution on activated carbons. J Colloid Interface Sci 449:252–260.

Marsh H, Yan DS, Ógrady TM, Wennerberg A (1984) Formation of active carbons from cokes using potassium hydroxide. Carbon 22:603–611.

McMillan WG, Teller E (1951) The Assumptions of the B.E.T. Theory. J Phys Chem 55:17–20. doi: 10.1021/j150484a003

Mestre AS, Pires J, Nogueira JM, et al (2009) Waste-derived activated carbons for removal of ibuprofen from solution: role of surface chemistry and pore structure. Bioresour Technol 100:1720–1726.

Mestre AS, Pires J, Nogueira JMF, Carvalho AP (2007) Activated carbons for the adsorption of ibuprofen. Carbon 45:1979–1988. doi: 10.1016/j.carbon.2007.06.005

Mestre AS, Tyszko E, Andrade MA, et al (2015) Sustainable activated carbons prepared from a sucrose-derived hydrochar: remarkable adsorbents for pharmaceutical compounds. RSC Adv 5:19696–19707. doi: 10.1039/C4RA14495C

Ming J, Wu Y, Liang G, et al (2013) Sodium salt effect on hydrothermal carbonization of biomass: a catalyst for carbon-based nanostructured materials for lithium-ion battery applications. Green Chem 15:2722–2726.

Mishima K, Matsuyama K Effects of Salts on the Decomposition Behavior of Cellulose in Subcritical Water, 14th International Conference on the Properties of Water and Steam in Kyoto.

Mohamed EF, Andriantsiferana C, Wilhelm AM, Delmas H (2011) Competitive adsorption of phenolic compounds from aqueous solution using sludge-based activated carbon. Environ Technol 32:1325–1336. doi: 10.1080/09593330.2010.536783

Mok WS, Antal Jr MJ (1993) Biomass fractionation by hot compressed liquid water. In: Advances in thermochemical biomass conversion. Springer, pp 1572–1582

Moussa M, Bader N, Querejeta N, et al (2017) Toward sustainable hydrogen storage and carbon dioxide capture in post-combustion conditions. J Environ Chem Eng 5:1628–1637.

Nefzaoui A (1991) Valorisation des sous-produits de l'olivier. Options Mediterranéennes 16:101–108.

Nowicki L, Ledakowicz S (2014) Comprehensive characterization of thermal decomposition of sewage sludge by TG–MS. J Anal Appl Pyrolysis 110:220–228. doi: 10.1016/j.jaap.2014.09.004

O. M (2011) The use of metronidazole and activated charcoal in the treatment of diarrhea caused by Escherichia coli 0157:H7 in an in vitro pharmacodynamic model. Afr J Pharm Pharmacol 5:1292–1296. doi: 10.5897/AJPP11.274

Overend RP, Chornet E, Gascoigne JA (1987) Fractionation of lignocellulosics by steam-aqueous pretreatments [and discussion]. Philos Trans R Soc Lond Math Phys Eng Sci 321:523–536.

Parmar A, Nema PK, Agarwal T, others (2014) Biochar production from agro-food industry residues: a sustainable approach for soil and environmental management. Curr Sci 107:1673–82.

Parshetti GK, Chowdhury S, Balasubramanian R (2015) Biomass derived low-cost microporous adsorbents for efficient CO 2 capture. Fuel 148:246–254.

Parshetti GK, Kent Hoekman S, Balasubramanian R (2013) Chemical, structural and combustion characteristics of carbonaceous products obtained by hydrothermal carbonization of palm empty fruit bunches. Bioresour Technol 135:683–689. doi: 10.1016/j.biortech.2012.09.042

Patwardhan PR, Satrio JA, Brown RC, Shanks BH (2010) Influence of inorganic salts on the primary pyrolysis products of cellulose. Bioresour Technol 101:4646–4655. doi: 10.1016/j.biortech.2010.01.112

Peng L, Morris JR (2010) Prediction of hydrogen adsorption properties in expanded graphite model and in nanoporous carbon. J Phys Chem C 114:15522–15529.

Peterson AA, Vogel F, Lachance RP, et al (2008) Thermochemical biofuel production in hydrothermal media: a review of sub-and supercritical water technologies. Energy Environ Sci 1:32–65.

Radovic LR (2004) Chemistry & physics of carbon. CRC Press

Rajalakshmi N, Sarada BY, Dhathathreyan KS (2015) Porous Carbon Nanomaterial from Corncob as Hydrogen Storage Material. Adv Porous Mater 2:165–170. doi: 10.1166/apm.2014.1068

Ramesh T, Rajalakshmi N, Dhathathreyan KS (2017) Synthesis and characterization of activated carbon from jute fibers for hydrogen storage. Renew Energy Environ Sustain 2:4.

Reddy TV, Chauhan S, Chakraborty S (2016) Adsorption isotherm and kinetics analysis of hexavalent chromium and mercury on mustard oil cake. Environ Eng Res 22:95–107.

Regmi P, Moscoso JLG, Kumar S, et al (2012) Removal of copper and cadmium from aqueous solution using switchgrass biochar produced via hydrothermal carbonization process. J Environ Manage 109:61–69.

Reinoso FR, Heintz EA, Marsh H (1997) Introduction to carbon technologies. Servicio de Publicaciones

Reza MT (2011) Hydrothermal carbonization of lignocellulosic biomass. University of Nevada, Reno. Thesis

Reza MT, Andert J, Wirth B, et al (2014) Hydrothermal carbonization of biomass for energy and crop production 1: 2300-3553.

Rivera-Utrilla J, Bautista-Toledo I, Ferro-García MA, Moreno-Castilla C (2001) Activated carbon surface modifications by adsorption of bacteria and their effect on aqueous lead adsorption: Adsorption of *E coli* on activated carbons. J Chem Technol Biotechnol 76:1209–1215. doi: 10.1002/jctb.506

Rivera-Utrilla J, Sánchez-Polo M, Gómez-Serrano V, et al (2011) Activated carbon modifications to enhance its water treatment applications. An overview. J Hazard Mater 187:1–23. doi: 10.1016/j.jhazmat.2011.01.033

Rivera-Utrilla J, Sánchez-Polo M, Ocampo-Pérez R (2017) Removal of Antibiotics from Water by Adsorption/Biosorption on Adsorbents from Different Raw Materials. In: Bonilla-Petriciolet A, Mendoza-Castillo DI, Reynel-Ávila HE (eds) Adsorption Processes for Water Treatment and Purification. Springer International Publishing, Cham, pp 139–204

Rodríguez G, Lama A, Rodríguez R, et al (2008) Olive stone an attractive source of bioactive and valuable compounds. Bioresour Technol 99:5261–5269. doi: 10.1016/j.biortech.2007.11.027

Rodriguez-Reinoso F, Garrido J, Martin-Martinez JM, et al (1989) The combined use of different approaches in the characterization of microporous carbons. Carbon 27:23–32.

Román S, Nabais JMV, Laginhas C, et al (2012) Hydrothermal carbonization as an effective way of densifying the energy content of biomass. Fuel Process Technol 103:78–83. doi: 10.1016/j.fuproc.2011.11.009

Román S, Valente Nabais JM, Ledesma B, et al (2013) Production of low-cost adsorbents with tunable surface chemistry by conjunction of hydrothermal carbonization and activation processes. Microporous Mesoporous Mater 165:127–133. doi: 10.1016/j.micromeso.2012.08.006

Romero-Anaya AJ, Molina A, Garcia P, et al (2011) Phosphoric acid activation of recalcitrant biomass originated in ethanol production from banana plants. Biomass Bioenergy 35:1196–1204. doi: 10.1016/j.biombioe.2010.12.007

Sangchoom W, Mokaya R (2015) Valorization of Lignin Waste: Carbons from Hydrothermal Carbonization of Renewable Lignin as Superior Sorbents for CO_2 and Hydrogen Storage. ACS Sustain Chem Eng 3:1658–1667. doi: 10.1021/acssuschemeng.5b00351

Schaefer S, Fierro V, Izquierdo MT, Celzard A (2016) Assessment of hydrogen storage in activated carbons produced from hydrothermally treated organic materials. Int J Hydrog Energy 41:12146–12156. doi: 10.1016/j.ijhydene.2016.05.086

Sepehr MN, Al-Musawi TJ, Ghahramani E, et al (2016) Adsorption performance of magnesium/aluminum layered double hydroxide nanoparticles for metronidazole from aqueous solution. Arab J Chem. doi: 10.1016/j.arabjc.2016.07.003

Sevilla M, Fuertes AB (2009) The production of carbon materials by hydrothermal carbonization of cellulose. Carbon 47:2281–2289. doi: 10.1016/j.carbon.2009.04.026

Sevilla M, Fuertes AB, Mokaya R (2011) High density hydrogen storage in superactivated carbons from hydrothermally carbonized renewable organic materials. Energy Environ Sci 4:1400–1410.

Shafeeyan MS, Daud WMAW, Houshmand A, Shamiri A (2010) A review on surface modification of activated carbon for carbon dioxide adsorption. J Anal Appl Pyrolysis 89:143–151. doi: 10.1016/j.jaap.2010.07.006

Shahamat YD, Farzadkia M, Nasseri S, et al (2014) Magnetic heterogeneous catalytic ozonation: a new removal method for phenol in industrial wastewater. J Environ Health Sci Eng 12:50.

Shen W, Li Z, Liu Y (2008) Surface chemical functional groups modification of porous carbon. Recent Pat Chem Eng 1:27–40.

Shi Y, Zhang X, Liu G (2015) Activated carbons derived from hydrothermally carbonized sucrose: remarkable adsorbents for adsorptive desulfurization. ACS Sustain Chem Eng 3:2237–2246.

Silvestre-Albero J, Silvestre-Albero A, Rodríguez-Reinoso F, Thommes M (2012) Physical characterization of activated carbons with narrow microporosity by nitrogen (77.4 K), carbon dioxide (273K) and argon (87.3 K) adsorption in combination with immersion calorimetry. Carbon 50:3128–3133.

Sing KSW (1982) Reporting physisorption data for gas/solid systems with special reference to the determination of surface area and porosity (Provisional). Pure Appl Chem 54:2201–2218.

Somayajulu Rallapalli PB, Raj MC, Patil DV, et al (2013) Activated carbon @ MIL-101(Cr): a potential metal-organic framework composite material for hydrogen storage: A potential MOF composite material for hydrogen storage. Int J Energy Res 37:746–753. doi: 10.1002/er.1933

Sonwane CG, Bhatia SK, Calos N (1998) Experimental and Theoretical Investigations of Adsorption Hysteresis and Criticality in MCM-41: Studies with O $_2$, Ar, and CO $_2$ý. Ind Eng Chem Res 37:2271–2283. doi: 10.1021/ie970883b

Suhas, Carrott PJM, Ribeiro Carrott MML (2007) Lignin – from natural adsorbent to activated carbon: A review. Bioresour Technol 98:2301–2312. doi: 10.1016/j.biortech.2006.08.008

Sun Y, Webley PA (2010) Preparation of activated carbons from corncob with large specific surface area by a variety of chemical activators and their application in gas storage. Chem Eng J 162:883–892.

Sun Y, Yang G, Wang Y-S, Zhang J-P (2011) Production of activated carbon by K2CO3 activation treatment of furfural production waste and its application in gas storage. Environ Prog Sustain Energy 30:648–657.

Suresh S, Srivastava VC, Mishra IM (2013) Studies of adsorption kinetics and regeneration of aniline, phenol, 4-chlorophenol and 4-nitrophenol by activated carbon. Chem Ind Chem Eng Q 19:195–212. doi: 10.2298/CICEQ111225054S

Szymański GS, Karpiński Z, Biniak S, Świątkowski A (2002) The effect of the gradual thermal decomposition of surface oxygen species on the chemical and catalytic properties of oxidized activated carbon. Carbon 40:2627–2639. doi: 10.1016/S0008-6223(02)00188-4

Thomas KM (2009) Adsorption and desorption of hydrogen on metal–organic framework materials for storage applications: comparison with other nanoporous materials. Dalton Trans 1487–1505.

Titirici M-M (2013) Sustainable carbon materials from hydrothermal processes. John Wiley & Sons

Titirici M-M, White RJ, Brun N, et al (2015) Sustainable carbon materials. Chem Soc Rev 44:250–290. doi: 10.1039/C4CS00232F

Titirici M-M, White RJ, Falco C, Sevilla M (2012) Black perspectives for a green future: hydrothermal carbons for environment protection and energy storage. Energy Environ Sci 5:6796–6822.

Toufiq Reza M, Freitas A, Yang X, et al (2016) Hydrothermal carbonization (HTC) of cow manure: Carbon and nitrogen distributions in HTC products. Environ Prog Sustain Energy 35:1002–1011. doi: 10.1002/ep.12312

Tran HN, You S-J, Hosseini-Bandegharaei A, Chao H-P (2017) Mistakes and inconsistencies regarding adsorption of contaminants from aqueous solutions: A critical review. Water Research 120: 88-116.

Tsai WT, Chang CY, Ing CH, Chang CF (2004) Adsorption of acid dyes from aqueous solution on activated bleaching earth. J Colloid Interface Sci 275:72–78.

Tsai W-T, Lai C-W, Su T-Y (2006) Adsorption of bisphenol-A from aqueous solution onto minerals and carbon adsorbents. J Hazard Mater 134:169–175.

Ubago-Pérez R, Carrasco-Marín F, Fairén-Jiménez D, Moreno-Castilla C (2006) Granular and monolithic activated carbons from KOH-activation of olive stones. Microporous Mesoporous Mater 92:64–70.

Valdés H, Sánchez-Polo M, Rivera-Utrilla J, Zaror CA (2002) Effect of ozone treatment on surface properties of activated carbon. Langmuir 18:2111–2116.

Vanoye L, Fanselow M, Holbrey JD, et al (2009) Kinetic model for the hydrolysis of lignocellulosic biomass in the ionic liquid, 1-ethyl-3-methyl-imidazolium chloride. Green Chem 11:390–396.

Villaescusa I, Fiol N, Poch J, et al (2011) Mechanism of paracetamol removal by vegetable wastes: The contribution of π–π interactions, hydrogen bonding and hydrophobic effect. Desalination 270:135–142. doi: 10.1016/j.desal.2010.11.037

Wang Q, Li H, Chen L, Huang X (2001) Monodispersed hard carbon spherules with uniform nanopores. Carbon 39:2211–2214. doi: 10.1016/S0008-6223(01)00040-9

Wang W-L, Ren X-Y, Li L-F, et al (2015) Catalytic effect of metal chlorides on analytical pyrolysis of alkali lignin. Fuel Process Technol 134:345–351. doi: 10.1016/j.fuproc.2015.02.015

Wang Y, Yao G, Jin F (2014) Hydrothermal Conversion of Cellulose into Organic Acids with a CuO Oxidant. In: Jin F (ed) Application of Hydrothermal Reactions to Biomass Conversion. Springer Berlin Heidelberg, Berlin, Heidelberg, pp 31–59

Wiedner K, Naisse C, Rumpel C, et al (2013) Chemical modification of biomass residues during hydrothermal carbonization – What makes the difference, temperature or feedstock? Org Geochem 54:91–100. doi: 10.1016/j.orggeochem.2012.10.006

Xia K, Hu J, Jiang J (2014) Enhanced room-temperature hydrogen storage in super-activated carbons: The role of porosity development by activation. Appl Surf Sci 315:261–267.

Xiao Y, Dong H, Long C, et al (2014) Melaleuca bark based porous carbons for hydrogen storage. Int J Hydrog Energy 39:11661–11667.

Xing W, Liu C, Zhou Z, et al (2012) Superior CO2 uptake of N-doped activated carbon through hydrogen-bonding interaction. Energy Environ Sci 5:7323. doi: 10.1039/c2ee21653a

Yan L, Yu J, Houston J, et al (2017) Biomass Derived Porous Nitrogen doped Carbon for Electrochemical Devices. Green Chem 2: 84-99

Yang L, Liu Y, Ruan R, et al (2011) Advances in production of 5-hydroxymethylfurfural from starch. Mod Chem Ind 1:014.

Yu Z (2016) Equilibrium and kinetics studies of hydrogen storage onto hybrid activated carbon-metal organic framework adsorbents produced by mild syntheses. Nantes, Ecole des Mines. Thesis

Zhang B, Huang H-J, Ramaswamy S (2008) Reaction kinetics of the hydrothermal treatment of lignin. Appl Biochem Biotechnol 147:119–131.

Zhao W (2012) Synthèse et caractérisation de matériaux carbonés microporeux pour le stokage de l'hydrogène. Université de Lorraine. Thesis

Zheng Z, Gao Q, Jiang J (2010) High hydrogen uptake capacity of mesoporous nitrogen-doped carbons activated using potassium hydroxide. Carbon 48:2968–2973.

Zhou L, Zhang J, Zhou Y (2001) A Simple Isotherm Equation for Modeling the Adsorption Equilibria on Porous Solids over Wide Temperature Ranges ý. Langmuir 17:5503–5507. doi: 10.1021/la010005p

Zieâlisld M, Wojeieszak R, Monteverdi S, Bettahar MM Role of nickel on the hydrogen storage on activated carbon. Catalysis 6: 777-783